



Federal Ministry
of Education
and Research

UNIVERSITE D'ABOMEY - CALAVI (UAC)

INSTITUT NATIONAL DE L'EAU



WASCAL
West African Science Service Center on Climate
Change and Adapted Land Use

Registered under N°:127-18/UAC/VR-AARU/SA

A DISSERTATION

Submitted

In partial fulfillment of the requirements for the degree of

DOCTOR of Philosophy (PhD) of the University of Abomey-Calavi (Benin Republic)

In the framework of the

Graduate Research Program on Climate Change and Water Resources (GRP-CCWR)

By

KOFFI Kouakou Valentin

Public defense on: 12/27/2017

=====

**HYDROGEOCHEMISTRY AND IMPACTS OF CLIMATE CHANGE ON
GROUNDWATER RECHARGE: CASE STUDY OF THE CRYSTALLINE BASEMENT
AQUIFER OF NORTHERN GHANA**

=====

Supervisors:

Emmanuel Obuobie (PhD), Senior Research Scientist, Water Research Institute, Ghana

Stefan Wohnlich, Full Professor, Ruhr-Universität Bochum, Germany

Daouda Mama, Full Professor, University of Abomey Calavi, Benin

=====

JURY

AGBOSSOU Euloge,	Full Professor, University of Abomey-Calavi, Bénin,	President
KOUAME Kan Jean,	Associate Professor, University Féix Houphoët-Boigny, Cote d'Ivoire,	Reviewer
GNAZOU D. T. Masamaéya,	Associate Professor, University of Lomé, Togo,	Reviewer
BOUKARI Moussa,	Full Professor, University of Abomey-Calavi, Bénin,	Reviewer
AFOUDA Abel,	Associate Professor, University of Abomey-Calavi, Bénin,	Examiner
MAMA Daouda,	Full Professor, University of Abomey-Calavi, Bénin,	Director

DECLARATION

I, Kouakou Valentin KOFFI, declare that this PhD dissertation entitled “**Hydrogeochemistry and Impacts of Climate Change on Groundwater Recharge: Case Study of the Crystalline Basement Aquifer of Northern Ghana**” is my own research work and contains no material that has been submitted previously, in whole or in part, for the award of any other academic degree to any other University. Every possible effort is made to acknowledge contributions from others, whenever and whoever involved, in different forms including proper citation within the body of the dissertation, in the reference section of the dissertation, and formal acknowledgement under the appropriate section.

Kouakou Valentin KOFFI

27.12.2017 Abomey-Calavi, BENIN

DEDICATION

To:

My late grandfather KONAN Kouassi for dedicating his life for my education.

ACKNOWLEDGEMENTS

I am really thankful to the Almighty God for his grace and mercy on my life. He has never let me down; he made my PhD work possible.

This PhD work was realized in the framework of the West African Science Service Center on Climate Change and Adapted Land use (WASCAL) and funded by the German Ministry of Education and Research (BMBF) in collaboration with the Benin Ministry of High Education and Scientific Research (MESRS). I was provided a five-month scholarship by the German Academic Exchange Service (DAAD) for my second stay at the Ruhr University Bochum (RUB) in Germany that helps me to work with the hydrogeology team and to complete my laboratory analysis. I am grateful to the BMBF, the MESRS and the DAAD.

I am greatly thankful to Prof. Daouda Mama for accepting to supervise this work. His support, his guidance and his availability helped me to greatly improve the quality of this work.

I am really grateful to Dr. Emanuel Obuobie for his dedication that made this work feasible. Dr Obuobie's work was not limited in supervising this thesis but he also spent a lot of time to support me in collecting data that were valuable for this thesis.

I want to sincerely thank Prof. Dr. Stefan Wohnlich, who promptly accepted to supervise this thesis even though he was not involved in the design of the research at the beginning. He provided a workspace, facilities for the chemical analysis at the laboratory of the Department of Applied Geology, Ruhr University of Bochum (RUB) and support need. His guidance and comments greatly helped me to accomplish this work.

I am grateful to Prof. Abel Afouda and the staff members of the GRP Water Resources and Climate Change who provided me every facilities and support that were available within their means and gave me the opportunity to achieve this PhD project.

I would like to thank Dr. Andre Banning for his outstanding comments on the hydrogeochemistry chapter of the thesis that greatly improves this work. As second manager of the laboratory he made all the facilities available for the analysis.

Thanks are due to Prof. Dr. Bernd Diekkrüger who helped me in designing the project of this thesis. His comments greatly helped me to improve the proposal of this work.

I would also like to thank Dr. Bossa and Dr. Yira Yacouba for their support in the installation of the piezometers during my field work.

I would like to thank Mr Enoch Asare, Head of Groundwater Resources at the Water Resources Commission of Ghana for providing a valuable data for the work.

I am also grateful to my friend Dr. Kouadio Kouakou for helping me in analysing the climate data.

Many thanks are also due to Mr Aaron Bundi Aduna, WASCAL basin coordinator in Ghana and Mr Guug Samuel for their support during my field work and my stay in Bolgatenga.

I would like to thank Dr. Dominik Wisser who helped me in finding a second supervisor and supported my application to the DAAD short-term scholarship who allowed me to stay in Germany during five months to work with the research team of the Hydrogeology group at the Department of Applied Geology, Ruhr University of Bochum (RUB).

I am grateful to my colleagues of the GRP Water Resources and Climate Change who created a collaborative working environment among PhD students. Especially, I appreciated the support of Dr. Djigbo Félicien Badou and Dr. Jean Hounkpè during my stays in Benin.

My sincere grateful goes to my fellows PhD students and staffs of the Hydrogeology group at the Department of Applied Geology, Ruhr University of Bochum (RUB) who were always available to help me. Special thanks to Dr. Björn Droste, Christoph Knuth and Nikolaus Richard who supported me in analysing the sample at the laboratory.

I really fall short in word to thank to my friend Sidy Ouattara who freely made his room available for me during my second stay in Bochum.

My deepest gratitude goes to Mr Ouffouet Koffi and his wife Mrs Ouffouet for their support since my first year at the university up to now that allowed me to start and complete this project.

My sincere gratitude goes to Dr. Kouamé Bossombra Nadege for her endless love, support, encouragement and continued prayers.

Last but not the least I would like to thank everybody who contributed to the success of this work.

ABSTRACT

Northern Ghana is mostly underlain by a crystalline rock aquifer. Like in many arid and semi-arid areas, surface water is largely unavailable in the prolonged dry season. Therefore groundwater appears to be a good alternative source for domestic and agricultural water supply. However, crystalline basement rocks are characterised by a poor water storage and low water yield. The water quality is also usually poor due to elevated content in some minerals like fluoride. Further, climate change may worsen the situation groundwater since recharge is fairly related to rainfall in the area. Therefore this work was done to provide decision support for the sustainable development and management of groundwater resources in Northern Ghana.

The current work first studied the water quality of both surface and groundwater in a part of the crystalline basement aquifer of Northern Ghana which covers 25000 km² and used five different methods to estimate present day recharge, namely the baseflow (BF) recession analysis, the Chloride Mass Balance (CMB) method, the Water Table Fluctuation (WTF) method, the model based method using the distributed WetSpss model and the simple water balance method.

The study revealed that groundwater chemistry is mainly controlled by cation exchange and silicate weathering processes and Ca-Mg-HCO₃ is the major water type, regardless of aquifer geology.

The recession curve analysis results in recharge ranging from 29 mm to 68 mm representing 3% and 9% of annual rainfall in 2004 and 2005, respectively; with average value of 49 mm (5%) for the period 2003-2008. The estimated annual baseflow based on the six methods ranged from 19.1 mm to 69.8 mm or from 2% to 7% of the annual rainfall.

Groundwater recharge estimated by the WTF and CMB methods ranges from 68 mm (6%) to 163 mm (17%) with a mean value of 10% and from 21 mm (2.1%) to 191 mm (19.3%) with average value of 81 mm (8.1%), respectively.

The recharge estimated by the WetSpss model, for the period lasting from 2003 to 2008, ranged from 519 mm to 756 mm, representing 68% and 70% of the annual rainfall during 2005 and 2007, respectively. The Average recharge estimated using the simple water balance method for the period 1976-2005 fell within the range of 283 mm (26.3%) to 330 mm (29.2%) with average of 300 mm (28%).

Compared to the recharge rate of 300 mm during the baseline period (1976-2005), the ensemble mean recharge is projected to increase in periods 2011-2040, 2041-2070 and 2071-2100 by a rate ranging from 23% to 44%, from 29% to 55% and from 33% to 55%, respectively.

This work suggested the use of dynamical downscaling methods for comparison purpose and the coupling of the WetSpss model with groundwater flow model in order to improve the results.

Keywords: hydrogeochemistry- climate change- groundwater recharge- crystalline basement aquifer-Northern Ghana

SYNTHESE DE LA THESE

Résumé

Le Nord du Ghana repose majoritairement sur le socle cristallin. Dans cette zone caractérisée par un climat semi-aride, les eaux de surface sont largement indisponibles pendant la longue saison sèche. Par conséquent, les eaux souterraines semblent être la seule alternative pour l'approvisionnement en eau domestique et agricole. Cependant, les roches cristallines du socle sont caractérisées par une faible capacité de stockage d'eau. La qualité de l'eau est souvent mauvaise en raison de la teneur élevée en certains minéraux comme le fluor. De plus, le changement climatique pourrait aggraver la situation. Ce travail a donc été réalisé afin de proposer des outils d'aide à la décision pour une gestion durable des ressources en eau dans les régions Nord du Ghana.

La zone d'étude qui est le socle cristallin du Nord du Ghana couvre une superficie d'environ 25000 km². Le présent travail a d'abord étudié la qualité des eaux de surface et souterraines dans le bassin versant de Veve qui est situé à l'Est de la zone d'étude. La recharge a été estimée en utilisant cinq différentes méthodes, à savoir la méthode de Fluctuation du Niveau Piézométrique de la nappe (FNP), la méthode du Bilan de Masse des Chlorures (BMC), la méthode de l'analyse de la récession de l'écoulement de base, la modélisation basée sur le modèle WetSpass et une méthode simplifiée de bilan de masse.

L'analyse des eaux de surface et souterraines échantillonnées montre que la chimie des eaux souterraines est principalement contrôlée par l'échange de cations et le processus d'altération du silicate. La majorité des échantillons appartient au faciès Ca-Mg-HCO₃, indépendamment de la géologie de l'aquifère.

L'analyse de la récession a estimé une recharge variant entre 29 mm et 68 mm représentant respectivement 3% et 9% des pluviométries annuelles des années 2004 et 2005 avec une moyenne de 49 mm (5%). Les six méthodes d'estimation d'écoulement ont permis d'obtenir un écoulement de base variant entre 19.1 et 69.8 mm.

La recharge des eaux souterraines estimée par les méthodes FNP et BMC varie respectivement de 68 mm (6%) à 163 mm (17%) avec une valeur moyenne de 109 mm (10%) et de 21 mm (2,12%) à 191 mm (19,3%) avec une valeur moyenne de 81 mm (8,14%).

Le modèle WetSpass dans la simulation du ruissellement total a été jugée satisfaisante, mais le modèle a surestimé la recharge qui varie entre 519 mm (55%) et 756 mm (70%). La recharge estimée à l'aide de la méthode de bilan hydrique simplifiée pour la période 1976-2005 varie de 283 mm (26,3%) à 330 mm (29,2%) avec une valeur moyenne de 300 mm (28%).

Par rapport à la recharge de la période de référence (1976-2005) qui a été estimée à 300 mm, la recharge future devrait augmenter pendant les périodes 2011-2040, 2041-2070 et 2071-2100 à un taux variant respectivement de 23% à 44%, de 29% à 55% et de 33% à 55%.

Le travail recommande l'utilisation de méthodes de désagrégation dynamique des projections climatiques est vivement recommandée pour des fins de comparaison et le couplage de WetSpass avec un modèle hydrogéologique afin d'améliorer les résultats du modèle WetSpass.

Mots-clés : hydrogéochimie- impact du changement climatique- recharge- socle cristallin- Nord du Ghana.

Introduction

L'eau est un élément essentiel pour le développement économique et social. Les eaux de surface qui sont facilement accessibles sont sujettes à une pollution grandissante et à une variation temporelle et saisonnière significative de leur quantité. Contrairement aux eaux de surface les eaux souterraines ont l'avantage d'être moins exposées à la pollution, d'être disponible à proximité des points de demande et d'avoir une quantité qui varie peu en fonction des saisons. Bien qu'il soit souvent possible de traiter les eaux en y éliminant les polluants ceci nécessite de lourds investissements. Ces avantages que présentent les eaux souterraines, conjugués à la croissance démographique galopante ont accru l'usage des ressources souterraines dans le monde au dépend des eaux de surface. Dans les régions du nord du Ghana caractérisées par un climat semi-aride et dont la zone rurale est singulièrement caractérisée par des habitations éloignées les unes des autres, l'exploitation des eaux souterraines apparait comme le moyen le mieux adapté pour un développement économique et social durable. Mais l'exploitation des eaux souterraines peut être entravée par la faible capacité de stockage du socle cristallin constituant l'aquifère de cette zone. Bien que moins exposées à la pollution, les eaux souterraines peuvent être sujettes à des problèmes de qualité liés à la composition chimique de la roche encaissante. Le changement climatique pourrait aussi bien augmenter la pression grandissante sur les ressources en eau souterraine que réduire de façon considérable la recharge. Dès lors, il devient important d'étudier l'impact du changement climatique sur la recharge qui est le seul moyen du renouvellement des ressources en eau souterraine. Ceci nécessite la connaissance de la recharge actuelle qui sera utilisée comme référence. Compte tenu de l'incertitude liée aux projections climatiques les études visant à l'analyse des impacts du changement climatique doivent se baser sur plusieurs projections climatiques. Dans la zone d'étude et ses environs, quelques études ont essayé d'estimer la recharge mais seulement l'une d'entre elles a étudié l'impact du changement climatique en se basant sur une seule projection, montrant la nécessité d'une étude se basant sur plusieurs projections. L'objectif principal de cette thèse est de fournir une aide à la décision pour le développement durable et la gestion des ressources en eaux souterraines du Nord du Ghana en utilisant plusieurs techniques pour estimer la recharge des eaux souterraines à différentes échelles spatiales et temporelles, les impacts du changement climatique sur la recharge.

Zone d'étude

La zone d'étude est située dans la partie nord du Ghana, dans le bassin de la Volta. Elle s'étend sur trois régions administratives, à savoir les régions « Upper-West », « Upper-East » et du « Nord » (Figure 1). La géologie de cette zone est majoritairement constituée du socle cristallin. L'épaisseur du régolithe peut atteindre 40m voire plus. Elle se situe entre 9° 00 N -11° 00 N et 3°00 W - 0°68 W et occupe une superficie d'environ 25882 km². Un climat semi-aride prévaut dans cette zone. La pluviométrie annuelle de la zone d'étude, basée sur 51 ans (1961-2009) des stations climatiques de Bole, Wa, Navrongo et Wa, varie respectivement de 762 mm à 1820 mm avec une moyenne de 1100 mm, de 523 mm à 1543 mm avec une moyenne de 1046 mm et de 671 mm à 1365 mm avec une moyenne de 988 mm. La région a des saisons humides et sèches distinctes. La saison humide commence en avril /mai et prend fin en octobre, avec un pic en août pour les parties ouest et nord de la zone et en septembre pour la partie sud. Les précipitations annuelles et l'évapotranspiration potentielle annuelle (ETP) suivent un gradient Nord- Sud, mais dans des directions opposées. Les précipitations diminuent du sud au nord tandis que l'ETP diminue du nord au sud. Les précipitations annuelles représentent respectivement 40% et 80% de l'ETP annuel dans les parties Nord (Navrongo) et Sud. Dans la zone d'étude, les températures moyennes les plus élevées sont obtenues dans les mois de mars et d'avril, tandis que les plus basses sont observées pendant la période de juillet à septembre durant laquelle les pluviométries mensuelles sont plus élevées que l'ETP mensuelle.

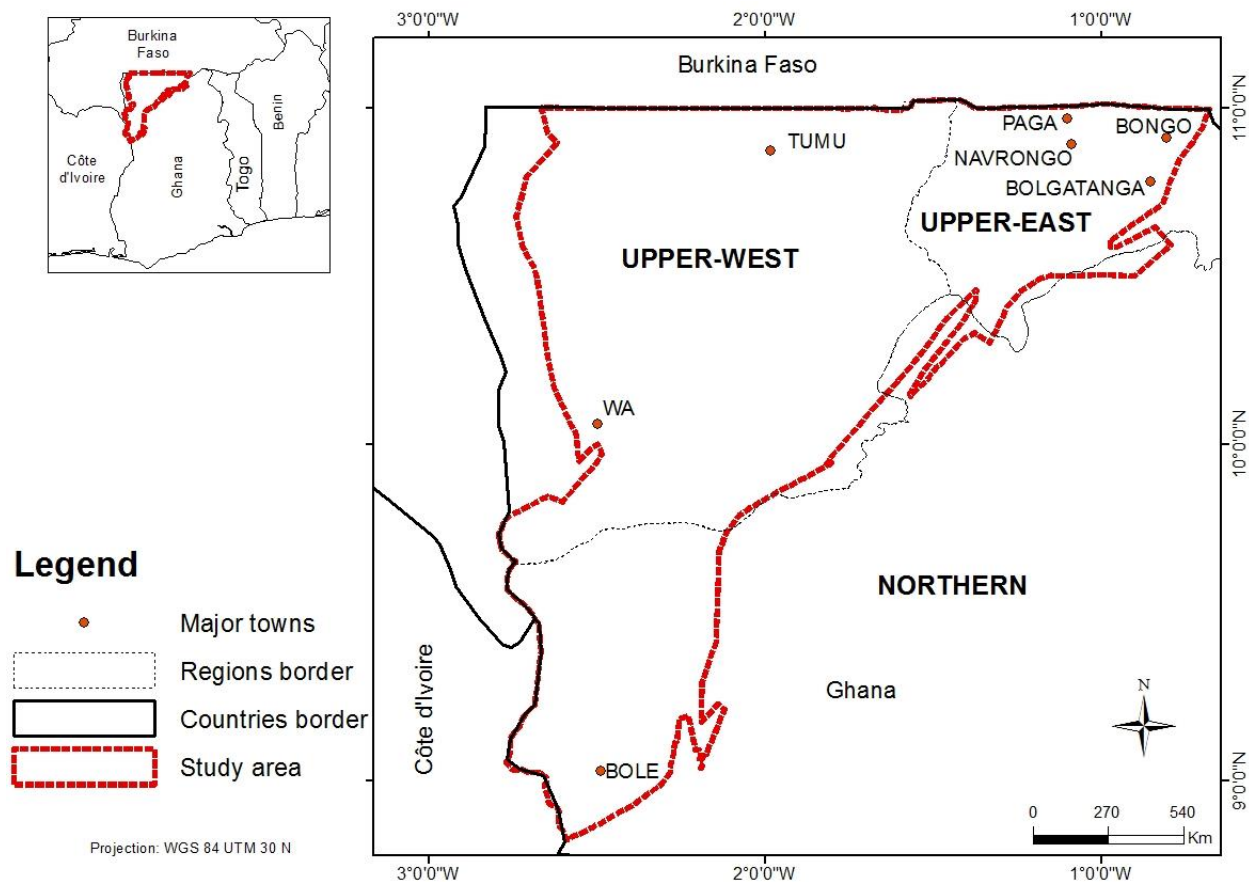


Figure 1 : Présentation de la zone d'étude

Matériel et méthodes

Ce travail dont l'objectif principal est d'étudier l'impact du changement climatique sur la recharge dans le socle cristallin du nord du Ghana s'est tout d'abord évertué à analyser la qualité des eaux dans la zone d'étude. Ensuite, cinq méthodes ont été utilisées pour la recharge actuelle de la nappe. Finalement, l'impact du changement climatique a été analysé en se basant sur la moyenne de douze projections résultant de la combinaison entre trois modèles climatiques globaux, deux modèles régionaux et de deux scénarios. Ce travail aidera dans les prises de décisions et les mises en place de gestion des ressources en eau dans la région nord du Ghana.

Dans le cadre de la caractérisation hydrogéochimique, soixante et un (61) échantillons d'eau souterraine et quatre (4) échantillons d'eau de surface ont été collectés et analysés. Les analyses ont permis de déterminer la teneur en éléments chimiques suivants : Calcium (Ca^{2+}), Magnésium (Mg^{2+}), Sodium (Na^+), Potassium (K^+), Bicarbonate (HCO_3^-), Chlore (Cl^-), Sulfate (SO_4^{2-}), Fer

total (Fe), phosphate (PO_4^{3-}), Ammonium (NH_4^+), nitrate (NO_3^-), nitrite (NO_2^-), Manganèse (Mn_{tot}), la dureté totale (CaCO_3). Les Solides Totaux Dissous (TDS), le pH, la conductivité électrique, la turbidité, la couleur, la salinité et l'oxygène dissous ont été également déterminés. Les analyses des isotopes stables, notamment le deutérium et l'oxygène 18, ont quant à elles porté sur cinquante-six (56) échantillons d'eau souterraine et cinq (5) échantillons d'eau de surface.

Les cinq différentes méthodes utilisées pour l'estimation de la recharge sont : la méthode de Fluctuation du Niveau Piézométrique de la nappe (FNP), la méthode du Bilan de Masse des Chlorures (BMC), la méthode de la récession de l'écoulement de base, la modélisation basée sur le modèle WetSpass et une méthode simplifiée de bilan de masse.

Les données primaires de cette étude ont été collectées pendant les années 2014 et 2015. Les données climatiques d'observation ont été collectées auprès des services météorologiques du Burkina Faso et du Ghana. Les données historiques et projections climatiques des différents modèles et scénarios ont été gratuitement téléchargées sur la plateforme de CORDEX. Quant à la carte d'utilisation et de couverture des terres, utilisée pour décrire la zone d'étude et comme entrée du modèle WetSpass, elle a été téléchargée à partir de la base de données du projet GLOWA Volta.

Afin d'estimer la recharge des eaux souterraines par la méthode WTF, les données piézométriques issues de dix (10) piézomètres situés dans la zone d'étude ont été recueillies auprès de la Commission des ressources en eau du Ghana. Sept puits supplémentaires ont été suivis dans le cadre de cette étude pour recueillir des données piézométriques de juin 2014 à décembre 2016. Afin de supprimer l'effet barométrique sur la fluctuation du niveau des eaux souterraines dans ces sept piézomètres, la pression atmosphérique a été mesurée dans l'un des sept puits.

Pour l'estimation de la recharge par le biais de la méthode de BMC des échantillons d'eau souterraine et de pluie ont été collectés pendant les saisons pluvieuses des années 2014 et 2015 à différents endroits de la zone d'étude.

Résultats et discussion

L'objectif de la caractérisation hydrogéochimique, qui a porté sur les eaux du bassin versant de Veau, était d'identifier les processus géochimiques influençant la qualité de l'eau et l'usage des eaux de surface et souterraines à des fins agricoles et domestiques dans la région. Les résultats ont montré que l'échange de cations et l'altération des silicates sont les processus dominants qui contrôlent la composition chimique de l'eau souterraine dans la zone d'étude. L'indice de genèse météorique montre que la majorité des échantillons sont issus d'une percolation peu profonde d'eau météorique. Les valeurs de TDS suggèrent que toutes les eaux souterraines échantillonnées sont fraîches. Les résultats obtenus à partir des 65 échantillons d'eau montrent également que le type d'eau dans la zone d'étude est principalement Ca-Mg-HCO₃. Selon les observations et les calculs effectués dans cette étude, les eaux souterraines de la région sont en grande partie adaptées à l'irrigation et peuvent être utilisées à des fins agricoles. Aucune pollution due aux activités anthropiques n'a été détectée. Les eaux de surface se révèlent également aptes à l'irrigation. L'Analyse en Composante Principale (ACP) s'est révélée être un bon outil puisqu'il a donné 6 facteurs importants à partir de l'ensemble de données de 13 paramètres. L'ACP a également suggéré que les échantillons d'eau souterraine proviennent d'une recharge récente. La méthode de Classification Ascendante Hiérarchique (CAH) a permis de classer les échantillons d'eau en 3 classes qui se sont révélées être liées au niveau de la minéralisation des échantillons mais pas aux formations géologiques. Les échantillons de la classe C1 ont une minéralisation relativement plus faible tandis que la classe C2 est composée de ceux de la plus haute minéralisation et la classe C3 est le groupe de transition entre ces deux premiers groupes.

Cette étude a l'avantage, contrairement aux précédentes, d'aborder réellement les processus hydrogéochimiques qui influencent la qualité de l'eau de cette zone. Les analyses basées sur le ratio d'isotopes stables des eaux de surface et des eaux souterraines ont révélé que la recharge de la nappe dans la zone se fait essentiellement par la recharge locale concentrée après accumulation des écoulements des eaux de pluie. Afin de déterminer la source de la recharge de l'aquifère dans la zone d'étude (fortes pluies, pluies légères ou les deux à la fois...), il est recommandé d'étudier les ratios $\delta^2\text{H}$ et $\delta^{18}\text{O}$ dans les eaux de pluie des différents événements pluvieux et les eaux souterraines pendant au moins une saison pluvieuse.

L'estimation de la recharge par la séparation de l'hydrogramme de la rivière Sissili (un sous-bassin de la Volta Blanche) à son exutoire de Wiasi a été réalisée en utilisant la méthode d'analyse de la courbe de récession et les filtres de séparation de débit de base. Une tentative a été faite pour tester la performance des filtres de débit de base durant la saison sèche et la période de récession en considérant que pendant ces périodes le débit du cours d'eau est uniquement constitué de l'écoulement de base. Six filtres et deux outils de détermination des périodes de récession et de la recharge ont été utilisés à cet effet. Les filtres utilisés sont : le filtre BFLOW, Minimum Local et celui dénommé filtre d'Eckhardt sont incorporés dans un outil hébergé en ligne appelé WHAT, tandis que Aquapak, AdUKIH, EcohydRology sont exécutés localement sur une machine. Les deux outils de détermination des périodes de récessions et de la recharge basée sur la récession sont des programmes Visual Basic. Les résultats des analyses suggèrent que la recharge varie de 3% à 9% des précipitations annuelles, avec une valeur moyenne de 5%. Les résultats ont également montré que le filtre «BFLOW» a donné les meilleures performances pour estimer le débit de base sur la période 2003-2008.

Les estimations de recharge basées sur la récession et les méthodes de séparation d'écoulement de base sont considérées comme des valeurs de recharge potentielles et doivent être validées avec des estimations réelles des méthodes de recharge telles que les traceurs, la fluctuation du niveau piézométrique de la nappe phréatique et le bilan des chlorures. La valeur moyenne de l'indice de brillance (ou de changement) mensuelle de Richards-Backer de la rivière Sissili à l'exutoire de Wiasi suggère qu'elle est une rivière stable.

L'utilisation de la méthode dite Fluctuation du Niveau Piézométrique (FNP) a permis d'estimer la recharge à partir de l'hydrogramme de onze (11) piézomètres. La recharge de la nappe d'eau souterraine du socle cristallin du nord du Ghana a été estimée entre 68 mm (6%) et 163 mm (17%), avec une recharge moyenne de 109 mm (10%). La variabilité spatiale et temporelle de la recharge et la réponse du niveau piézométrique de la nappe aux précipitations dans la zone d'étude a été attribuée à la variabilité spatiale et temporelle des précipitations et à l'hétérogénéité des propriétés de l'aquifère dans la zone d'étude. En outre, la recharge estimée à partir des piézomètres dont les rendements spécifiques ont été estimés à partir d'une analyse en laboratoire concorde avec celle estimée par la méthode BMC. Par conséquent, il est suggéré d'utiliser cette méthode pour déterminer le rendement spécifique et/ou le combiner avec des essais de pompage

de longue durée en utilisant un piézomètre d'observation pour améliorer la détermination des valeurs de rendement spécifiques et donc la recharge des eaux souterraines. Les résultats de cette étude pourraient être améliorés en augmentant le nombre de piézomètres dans la zone d'étude.

La recharge estimée par la méthode du Bilan de Masse des Chlorures (BMC) corrobore les résultats d'études antérieures effectuées dans des zones situées à l'intérieur ou à proximité de la zone de la présente étude. La recharge a été jugée très variable dans la zone d'étude. La recharge estimée par la méthode du bilan de masse de chlorure varie de 21 mm à 191 mm, soit 2,1% à 19,3% des précipitations annuelles moyennes. La recharge moyenne en surface est de 81 mm, ce qui représente 8,14% de la pluviométrie annuelle moyenne. Contrairement à la formation géologique, le type de sol semble être l'un des facteurs qui contrôlent la recharge des eaux souterraines dans la zone d'étude. Comme il n'est pas possible de relier les classes de sol définies par la FAO à la texture du sol, il est recommandé de (collecter le sol) d'identifier la texture du sol et la conductivité hydraulique à Saturation du sol dans les sites où les échantillons d'eau souterraine ont été collectés afin de déterminer dans quelle mesure la texture du sol contrôle la recharge de l'eau souterraine dans la zone. Ce travail suggère également l'utilisation d'une méthode de haute précision telle que le chromatogramme ionique pour la détermination de la teneur en chlore dans les eaux de pluie.

Bien que la performance du modèle basée sur les critères de performance tels que le Nash et le coefficient de détermination ait été jugée satisfaisante, il a été constaté que la recharge estimée par le modèle, qui varie entre 55% et 70%, est largement supérieure à celles estimées par d'autres travaux qui ont utilisés le modèle WetSpss et d'autres modèles dans la région. Donc le modèle n'a pas pu être utilisé pour l'estimation des recharges futures afin de déterminer l'impact du changement climatique sur la recharge. Par conséquent, une méthode simplifiée de bilan hydrologique a été utilisée.

Cette méthode de bilan hydrologique a permis d'estimer une recharge variant entre 282 mm et 330 mm par an, soit 26.3% à 29.2% de la pluviométrie annuelle moyenne durant la période 1976-2005.

L'étude de l'impact du changement climatique sur la recharge utilisant l'approche de bilan hydrologique simple s'est basée sur douze scénarios climatiques. L'analyse d'ensemble de

l'impact du changement climatique sur la recharge suggère une augmentation de la recharge à court, moyen et long terme. En outre, tous les scénarios projettent une augmentation de la température future. En utilisant le test de tendance de Mann-Kendall, une tendance positive a été détectée dans toutes les projections de température faites par tous les scénarios. En ce qui concerne les précipitations, une augmentation a également été suggérée par huit sur les douze scénarios; tandis que les quatre autres suggèrent une diminution des précipitations futures. De plus, contrairement à la température, la tendance des précipitations est mitigée car l'analyse des tendances ne suggère aucune tendance pour certains scénarios, alors que des tendances positives et négatives ont été détectées pour d'autres.

Conclusion

Ce travail a été fait pour estimer l'impact du changement climatique sur la recharge des eaux souterraines dans la zone d'étude. La recharge actuelle estimée par l'analyse de l'écoulement de base, la méthode du Bilan de Masse des Chlorures, la méthode de Fluctuation du Niveau Piézométrique et une méthode de bilan hydrique simplifiée fluctue entre 19.07 mm et 330 mm soit respectivement entre 2% et 29% de la pluviométrie annuelle. Les résultats de ce présent travail se sont avérés être en accord avec les travaux précédents dans et autour de la zone d'étude. La recharge devrait augmenter respectivement de 34% à 38%, 33% à 51%, 38% à 51% à court, moyen et long terme par rapport à la recharge durant la période de référence qui a été estimée à 300 mm.

Une étude plus approfondie, prenant en compte les métaux lourds, d'autres substances traces inorganiques et organiques ainsi que des paramètres microbiologiques est nécessaire pour la caractérisation complète de l'hydrogéochimie des eaux souterraines et leur aptitude aux différents usages. Il est vivement conseillé de prendre en compte l'effet saisonnier en effectuant plusieurs campagnes d'échantillonnage pendant les différentes saisons.

Il est également recommandé de densifier le réseau hydrométrique en installant de nouveaux hydromètres automatiques de haute précision afin d'améliorer la précision des modèles de bilan hydrique dans la zone. Ce présent travail s'étant basé sur une méthode désagrégation statistique, l'utilisation de méthodes de désagrégation dynamique des projections climatiques est vivement recommandée pour des fins de comparaison. La performance du modèle WetSpass peut être liée

au mécanisme du modèle et à la qualité des différentes données d'entrée. Mais comme il a été calibré et validé en utilisant les données de débit observé, sa performance pourrait être aussi influencée par la qualité de ces données de débit observé. Par conséquent, il est recommandé d'entreprendre une étude pour laquelle le calibrage et validation seront basés sur le couplage du modèle WetSpass avec un modèle hydrogéologique tel que MODFLOW.

TABLE OF CONTENTS

DECLARATION	I
DEDICATION	II
ACKNOWLEDGEMENTS	III
ABSTRACT	V
SYNTHESE DE LA THESE	VI
TABLE OF CONTENTS.....	XVI
LIST OF TABLES	XX
LIST OF FIGURES	XXII
ACRONYMS	XXV
Chapter 1 – GENERAL INTRODUCTION	1
1.1. Introduction	1
1.2. Statement of the research problem	4
1.3. Literature review	6
1.3.1. Groundwater quality and hygeochemical processes.....	6
1.3.2. Estimation of groundwater recharge.....	6
1.3.3. Impact of climate change on groundwater recharge.....	7
1.4. Research questions	7
1.5. Research Objective.....	8
1.4. Hypothesis	8
1.5. Novelty	8
1.6. Scope of the thesis.....	9
1.7. Expected results and benefits	10
1.8. Organization of the Thesis	10
Chapter 2 - DESCRIPTION OF THE STUDY AREA	11
2.1. Location.....	11
2.2. Climate	12
2.3. Land use and Land cover	15
2.4. Geology and Hydrogeology	15

2.4.1. Regional geology.....	15
2.4.2. Geology of Ghana.....	17
2.4.3. Hydrogeology of the study area.....	17
2.5. Demography, environmental, social and economic activities.....	18
Chapter 3 - DATA, MATERIALS AND METHODS	19
3.1. Introduction	19
3.2. Data	19
3.2.1. Climate data.....	19
3.2.2. Topographic data	20
3.2.3. Streamflow data.....	20
3.2.4. Land use and land cover data	22
3.2.5. Hydrogeological data.....	22
3.2.6. Geological data	23
3.2.7. Soil data.....	23
3.2.8. Hydrogeochemical data	24
3.2.9. Leaf area index data.....	28
3.3. Materials.....	28
3.4. Methods.....	29
3.4.1. Hydrogeochemistry.....	29
3.4.2. Estimation of groundwater recharge in the Sissili Basin using streamflow hydrograph analysis.....	42
3.4.3. Estimation of groundwater recharge using Water Table Fluctuation method.	51
3.4.4. Estimation of groundwater recharge using Chloride Mass Balance method	53
3.4.5. Estimation of groundwater recharge using WetSpas model	54
3.4.6. Estimating recharge using a simple water balance method	61
3.4.7. Study of the impact of climate change.....	63
3.5. Conclusion.....	66

Chapter 4 HYDROGEOCHEMISTRY AND GROUNDWATER RECHARGE PROCESS	67
4.1. Introduction	67
4.2. General Hydrogeochemistry	72
4.2.1. Chloro-Alkaline Indices	72
4.2.2. Weathering process	73
4.2.3. Saturation index	77
4.3. Drinking water quality	79
4.3.1. Total Dissolved Solids (TDS) and turbidity	80
4.3.2. Total Hardness	80
4.3.3. Major Ions	81
4.4. Usability of the water for irrigation.....	83
4.4.1. Sodium Absorption Ratio (SAR).....	83
4.4.2. Sodium percentage.....	84
4.4.3. Residual Sodium Carbonate (RSC)	86
4.4.4. Magnesium Hazard (MH).....	86
4.4.5. Permeability index (PI).....	87
4.5. Statistical analyses.....	88
4.5.1. Principal Component Analysis (PCA).....	89
4.5.2. Correlation between parameters	89
4.5.3. Extraction of Components	92
4.5.4. Agglomerative hierarchical clustering (AHC).....	95
4.6. Stable isotopes.....	98
4.7. Conclusion.....	99
Chapter 5 -ESTIMATION OF GROUNDWATER RECHARGE.....	101
5.1. Introduction	101
5.2. Recharge estimation using streamflow hydrograph analysis	102
5.2.1. Recession analysis	102

5.2.2.	Recharge estimated by recession analysis	103
5.2.3.	Baseflow Separation	104
5.3.	Recharge estimation using Water Table Fluctuation method	111
5.3.1.	Groundwater level response to Rainfall.....	111
5.3.2.	Estimation of specific yield	115
5.3.3.	Groundwater recharge estimation.....	116
5.4.	Recharge estimation using the Chloride Mass Balance method	117
5.4.1.	Chloride in Rain.....	117
5.4.2.	Chloride in groundwater	119
5.4.3.	Recharge estimation.....	120
5.5.	Recharge estimated by the WetSpass model.....	123
5.6.	Conclusion.....	126
Chapter 6 - IMPACT OF CLIMATE CHANGE ON GROUNDWATER RECHARGE.....		127
6.1.	Introduction	127
6.2.	Recharge estimated using the simple water balance method	127
6.3.	Statistical downscaling.....	131
6.3.1.	Comparison between models outputs and observation data	131
6.3.2.	Future climate projection	131
6.4.	Impact of climate change on groundwater recharge	136
6.5.	Conclusion.....	138
Chapter 7 - GENERAL CONCLUSION AND PERSPECTIVES		139
7.1.	Conclusion.....	139
7.2.	Perspectives.....	141
REFERENCES		143
APPENDICE.....		176
Appendix A: Published article and communication		176
Appendix 2: Chemical analysis		177
Appendix 3 : Specific yield in the literature		180
Appendix 4: Climate projection.....		181

LIST OF TABLES

Table 3-1: Instruments and methods used for the analysis	30
Table 3-2: Methods used to analyse the data	31
Table 3-3: Classification of irrigation water quality based on Na%	37
Table 3-4: Guildford's rule of thumb for interpreting correlation coefficient.....	40
Table 4-1 Geological units, number of samples and predominant hydrochemical facies in the Vea catchment	70
Table 4-2 Statistics of physico-chemical and hydrochemical parameters of groundwater sampled in Vea Catchment, Northeast Ghana.....	71
Table 4-3: Summary of mineral saturation indices of the sampled water	78
Table 4-4: Total hardness as CaCO ₃ for groundwater in the Vea area, Northeast Ghana	81
Table 4-5: Normality test of the variables based on 4 methods.....	88
Table 4-6: Bartlett's sphericity test	89
Table 4-7: Correlation matrix of the hydrochemical parameters.....	90
Table 4-8: Composition of Igneous Rocks and their Breakdown (Worrall 2013).....	91
Table 4-9: Eigenvalue, variability and cumulative (%) of each of the extracted components.	93
Table 4-10: Factor loadings after varimax rotation	94
Table 5-1: Performance evaluation of the different recession methods in the study area	102
Table 5-2: Annual recharge in percentage	104
Table 5-3: Performance of baseflow methods during dry and recession periods in the Sisili basin at Wiasi, Ghana.....	111
Table 5-4: Range of groundwater table fluctuation in the monitoring wells.....	113
Table 5-5: Specific yield used in estimation of groundwater recharge in crystalline basement aquifers of northern Ghana.	115
Table 5-6: Estimated recharge by the Water Table Fluctuation method compared with recharge results from Chloride Mass Balance method.....	117
Table 5-7: Average Chloride content in rain for the rainy seasons of 2014 and 2015 in the study area.....	119
Table 5-8: Summary of recharge estimated using CMB method by previous works in the regions or in area with crystalline basement aquifer.	121
Table 5-9: Estimated groundwater recharge with respect to geological formation	122

Table 5-10: Groundwater recharge with respect to FAO soil types	123
Table 5-11: Performance evaluation criteria of the model.	124
Table 5-12: Estimated recharge by WetSpas in the study area	125
Table 6-1: Correlation between the FAO Penman-Monteith and two types of the Hargreaves methods.	129
Table 6-2: Comparison between uncorrected and corrected data showing the performance of the Bias Correction Method for the station of Navrongo	131
Table 6-3: Increase in future temperature compared to the observed mean temperature of the baseline period	133
Table 6-4: Trend analysis of mean temperature in the baseline and the future periods across the study area.	134
Table 6-5: Projected change in annual rainfall relative to the baseline (%).	135
Table 6-6: Trend analysis of the annual rainfall in the baseline and future periods in the area.	136
Table 6-7: Range of projected change in groundwater recharge relative to the baseline (%)	138

LIST OF FIGURES

Figure 2-1: Map of Northern Ghana showing the location of the study area	11
Figure 2-2: Lamb index of annual rainfall (1961-2009) in the study area using data from the stations of Bole, Wa and Navrongo.	13
Figure 2-3: Comparison between monthly rainfall, potential evapotranspiration and mean temperature in the study area.	14
Figure 2-4: Main geological units of West Africa (Spudis 2005).	16
Figure 2-5: Geological map of the study area (source: Glowa Volta).	18
Figure 3-1: Location of the study area of the streamflow analysis.....	21
Figure 3-2: Land use map of the study area of the streamflow analysis.....	22
Figure 3-3: Map of northern Ghana showing the monitoring wells	23
Figure 3-4: Location of sampling wells and rain samplers.....	25
Figure 3-5: Location of Ghana in western Africa (upper left map), location of the Veua Catchment in Ghana (upper right map), and geology and water sampling points of the study area (lower map). M&UG: migmatite and undifferentiated granite.	27
Figure 3-6: Flow chart of the AdUKIH computer code for baseflow separation (Aksoy et al. 2008)	47
Figure 3-7: Estimation of groundwater level rise using hypothetical data	52
Figure 3-8: Schematic representation of water balance for a non-homogenous land cover grid cell (Batelaan and De Smedt 2001; Abdollahi et al. 2017)	55
Figure 4-1: Box-plots of the chloro-alkaline indices of groundwater samples from different lithologies (Figure 3-5) in the study area. The red crosses indicate average values; black horizontal line indicates median values.	73
Figure 4-2: Relation between Ca+Mg and SO ₄ +HCO ₃	74
Figure 4-3: Plot of Sodium versus chloride	74
Figure 4-4: Stability field diagrams of the partial system MgO–Na ₂ O–Al ₂ O ₃ –SiO ₂ –H ₂ O of the chemical composition of groundwater samples.	75
Figure 4-5: Relation between Ca+Mg-SO ₄ -HCO ₃ and Na-Cl	76
Figure 4-6: Gibbs' diagrams for cations (A) and anions (B) indicating rock-water interaction ...	77
Figure 4-7: DSI/CSI of Groundwater in Veua Catchment, Northeast Ghana.....	79
Figure 4-8: Ca/Mg ratio rock dissolution of groundwater in the Veua area, Northeast Ghana.....	79

Figure 4-9: Piper diagram of the analysed groundwater samples (triangle) with respect to Geological formation and surface water samples	82
Figure 4-10: Wilcox Log diagram of groundwater in the Veua area, Northeast Ghana.....	84
Figure 4-11: Rating of groundwater samples based on electrical conductivity and percent sodium in Veua area, Northeast Ghana	85
Figure 4-12: Classification of irrigation water in Veua (northeast Ghana), based on permeability index.....	87
Figure 4-13 Screen plot of principal components showing change on slope after	93
Figure 4-14: Plot of the variables on the plan F1-F2 (A) and plan F1-F3 (B) summarising correlation between variables and factors in the one hand and between parameters in the other hand.....	95
Figure 4-15: Dendrogram for the groundwater samples, showing the division into three clusters.	96
Figure 4-16: Distribution of the different clusters in the Veua catchment, Northern Ghana	97
Figure 4-17: Stiff plot of major anions of the three clusters.....	97
Figure 4-18: Plot of deuterium with respect to Oxygen 18	99
Figure 5-1: Power regression MRC of the Sisili river, tributary to the White Volta River, 2003-2007, Northern Ghana.....	103
Figure 5-2: Annual recharge and rainfall amount.....	104
Figure 5-3: Comparison of discharge with rainfall for quality control.....	105
Figure 5-4: Comparison of monthly flashiness index and the monthly weighted average rainfall	106
Figure 5-5: Variation of monthly average baseflow and flashiness indexes for the period 2003-2008. Box-plots represent the average monthly BFI, solid blue line represents FI, blue crosses represent outliers and discontinued red line represents monthly rainfall.	107
Figure 5-6: Range of annual Baseflow Index (BFI) estimated by the different methods.....	108
Figure 5-7: Variation annual Baseflow Index (BFI) with respect to the different filter methods	108
Figure 5-8: Interannual variability of baseflow index of the Sisili River at Wiasi, Northern Ghana. Box-plots represent the average monthly BFI, solid orange line represents annual rainfall, red asterisks represent outliers and discontinued blue line represents monthly FI.....	109

Figure 5-9: Range of baseflow estimated by baseflow tools for the period 2003-2008. The red asterisks and the dots represent outliers and mean values, respectively.....	110
Figure 5-10: Comparison of baseflow and annual rainfall amount. Boxplots represent range baseflow estimated by the different methods, asterisks represent outliers and orange line represents annual rainfall.	110
Figure 5-11: A plot of groundwater hydrograph and rainfall at Bonia (rainfall based on data from Navrongo station), showing seasonal variation of water level in response to the rainfall.....	113
Figure 5-12: Variation of groundwater level at Gowrie in the rainy season (Apr - Sep). Encircled rises are attributed to recharge from irrigation water.....	114
Figure 5-13: A plot of groundwater hydrograph for a well at Wa. The nature of decline of the groundwater levels is an indication of overexploitation of the resources.....	114
Figure 5-14: Comparison between chloride content obtained at the laboratories of WRI and RUB	118
Figure 5-15: Comparison between chloride content in groundwater analysed at WRI and RUB laboratories.....	120
Figure 5-16: Comparison between simulated and observed total flow for the calibration (A) and validation (B) of the model.	125
Figure 6-1: Monthly PET by the FAO Penman-Monteith versus: A) Hargreaves (HG) method, B) Modified Hargreaves (MDG) method, for the station of Tamale.	128
Figure 6-2: Average monthly potential evapotranspiration estimated by the FAO Penman-Monteith (PM), the Hargreaves (HG) method and the Modified Hargreaves (MDG) method for the period 1970-2009 for Tamale station.....	129
Figure 6-3: Mean annual recharge (%) during the baseline period (1976-2005)	130
Figure 6-4: Estimated temperature by the twelve scenarios for the baseline and future periods in the study area	133
Figure 6-5: Estimated rainfall by the twelve scenarios for the baseline and future periods in the study area.	135
Figure 6-6: Projected change in groundwater recharge relative to the baseline period.....	138

ACRONYMS

AHC	Agglomerative Hierarchical Clustering
BFI	Baseflow index
CAI	Chloro-Alkaline Index
CMB	Chloride Mass Balance Method
CORDEX	Coordinated Regional climate Downscaling Experiment
CSIRO	Commonwealth Scientific and Industrial Research Organization
DEM	Digital Elevation Database
DGH	Direction Générale des l’Hydraulique
DO	Dissolved oxygen
EC	Electrical conductivity
ECHAM4	European Centre HAMburg, 4th Generation
FAO	Food and Agriculture Organization
FI	Flashiness index
GCM	Global Climate Models
GMA	Ghana Meteorological Agency
GSA	Ghana Standard Authority
HAP	Hydrological Assessment Project of the Northern Regions of Ghana
$\delta^2\text{H}$	Isotope ratio of hydrogen-2
IDW	Inverse Distance Weighting
IPCC	Intergovernmental Panel on Climate Change
IPCC	Intergovernmental Panel on Climate Change
LAI	Leaf Area Index
LARS-WG	Long Ashton Research Station Weather Generator
LMWL	Local Meteoric Water Line

LSC	large-scale circulation
MGI	Meteoritic genesis index
MH	Magnesium Hazard
MHG	Modified Hargreaves
MODIS	Moderate-Resolution Imaging Spectroradiometer
MRC	Master Recession Curve
NSE	Nash-Sutcliffe model Efficiency
NTU	Nephelometric Turbidity Units
$\delta^{18}\text{O}$	Isotope ratio of oxygen-18
OGCM	Oceanic Global Climate Models
PCA	Principal Component Analysis
PET	Potential Evapotranspiration
PI	Permeability index
PM	Penman-Monteith
R^2	Coefficient of determination
RCM	Regional Climate Model
RCP	Representative Concentration Pathway
RCP	Concentration Pathways
RD-HR	Recursive Digital filter for Hard Rock aquifer
RD-P	Recursive Digital filter for Porous aquifer
RMSE	Root Mean Square Error
RSC	Residual Sodium Carbonate
RUB	Ruhr University Bochum
SAR	Sodium adsorption ratio
SI	Saturation index

SWAT	Soil and Water Assessment Tool
Sy	Specific yield
TDS	Total dissolved solids
TH	Total Hardness
TSS	Total Suspended Solids
UNEP	United Nations Environment Programme
UNESCO	United Nations Educational, Scientific and Cultural Organization
UNICEF	United Nations International Children's Emergency Fund
USGS	United States Geological Survey
WHAT	Web-based Hydrograph Analysis Tool
WHO	World Health Organization
WMWL	World Meteoric Water Line
WWAP	World Water Assessment Programme
WTF	Water Table Fluctuation

Chapter 1 – GENERAL INTRODUCTION

1.1. Introduction

The global hydrosphere consists of a series of reservoirs interconnected by water cycling in various phases. The earth's water, divided into fresh water and salt water, is held by the oceans; ice sheets and glaciers; terrestrial water (rivers, soil moisture, lakes and ground water); the biosphere (water in plants and animals); and the atmosphere. Fresh water is the one containing no significant amounts of salts, such as in rivers and lakes. Salt water is water of the seas, distinguished by high salinity (McGraw-Hill, 2003). The oceans, with a mean depth of 3.8 km, hold 97% of all the earth's water. Approximately 70% of the total fresh water is locked up in ice sheets and glaciers, while almost all of the remainder is ground water. Rivers and lakes hold only 0.3% of all fresh water and the atmosphere a mere 0.04% (Barry and Chorley 2004).

In Africa, majority of the population do not have access to safe drinking water. Although the target for safe drinking water for 2015 was met in 2010, a study by WHO/UNICEF Joint Water Supply and Sanitation Monitoring Programme reveals that in 2015, 663 million people had no access to water worldwide (WHO/UNICEF 2015). This report stresses that about half of those people who had no access to water were from sub-Saharan Africa. Worldwide, water scarcity is projected to increase from 47% in 2000 to 65% in 2025, even though by 2010 the actual number of people using improved drinking water sources had increased by 11% since 1990 (UNEP 2013).

Sub-Saharan Africa has been found to have the largest number of countries facing water-stress compared to the other regions (Msangi 2014). In that region (sub-Saharan Africa) it is expected that about 230 million of people will be affected by water scarcity by 2025 (UNEP 2008). Due to climate change, in some arid and semi-arid regions water scarcity is expected to displace between 24 and 700 million people (WWAP 2009). In its fifth assessment report, IPCC (2014) stressed that temperature over Africa is increasing faster than the global average. The IPCC also reported that in West-Africa increase in temperature under RCP4.5 and RCP8.5 may range between 3°C and 6°C by the end of the 21st century above the 20th century baseline. In Ghana, a

work by Stanturf et al. (2011) highlighted that over the whole country temperature has increased by about 1°C since 1960. Margulis et al. (2010) stressed that the highest increase in temperature over the period 2010-2050 in Ghana will occur in three northern regions; namely the Northern, the Upper-West and the Upper-East regions. All the temperature projections suggest an increase in temperature and are reliable, but rainfall signal and magnitude are uncertain (Chaturvedi et al. 2012; Alexander and Arblaster 2017). In this concern, confidence in projected rainfall over Africa was qualified as low to medium by the IPCC (2013).

About 94% of the world's population growth, which has increased by almost 1.5 billion people since 1990, has occurred in developing regions. Worldwide, Sub-saharan Africa has seen the greatest proportional population growth of about 59%. In many countries located in this part of the world an increase in population that has limited access to improved drinking water has been observed. This is due to both population growth and rapid urbanization in countries (WHO/UNICEF 2011).

One of the strategies to fix this issue is to enhancing groundwater extraction, because of its less sensitivity to climate change, compared to surface water. Groundwater is water that occurs below the surface of the ground, as opposed to that at the surface. It is also defined as water that occurs below the surface in soil or rocks that are saturated, either in cavities and pores (through which it can flow) or below the water table. Groundwater has an erosive action in permeable rocks, such as limestone, in which it can form underground rivers and caves (Daintith and Martin 2005).

The main sources of groundwater are meteoric and marine. Besides these sources, we have other minor source, namely connate water. That one is water which located in the pores of a sedimentary rock ever since it was deposited. The term "connate" comes from a Latin phrase meaning "born with" (Younger 2007).

Groundwater is widely used for potable water supply of the population and cattle-breeding farms, industrial water supply, irrigation, balneological use and for energy production (geothermal water). Some mineral can also be extracted from groundwater (e.g., iodine, bromine). Because of the pollution of surface water the use of groundwater in domestic and drinking water supply has greatly increase making it as main resource in some countries (Zektser and Everett 2004). This increase in global groundwater exploitation due to the greater benefits from it started during the twentieth century (Van der Gun 2012). Groundwater, as a source of

domestic and potable water supply, has some advantages over surface one. Except the uncertainties related to underground aspect of its flows, their exploitation offers some advantages as a better protection from pollution and evaporation, a relatively constant temperature, the short distance between the source and the use, and the little variability of its response to the demand over time. The extrema of this response is shifted from one to six months in relation to pluviometric extrema. Groundwater resources, due to availability of regulating capacity, are not subjected to multiannual and seasonal fluctuations (Dassargues 1991; Zektser and Everett 2004). In some northern and arid zones, where surface water flows freeze up or dry up in some periods of a year, groundwater is the only water supply source. In many cases, it is possible to abstract groundwater in the direct vicinity of a consumer.

By 2020, between 75 million and 250 million people are expected to be exposed to increased water stress due to climate change. This will adversely affect livelihoods and aggravate water-related problems if coupled with increased demand (IPCC 2007).

On the one hand, the increasing of groundwater supply with the population growth, lead to a proactive management of groundwater supplies (Cherkauer 2004). On the other hand, the less sensitivity of groundwater to climate change compared to surface water increases the interest of scientists and policy makers in groundwater. According to (IPCC 2007), climate change refers to any change in climate over time, whether due to natural variability or as a result of human activity. In addition to this phenomenon, the significant impact of land use change on groundwater has been pointed out by several studies and is not subjected to any doubt anymore (e.g., Scanlon et al. 2005; Pan et al. 2011; Gebere et al. 2016).

“Climate change affects groundwater recharge and discharge rates, as well as groundwater quality. Since knowledge of current recharge and levels in both developed and developing countries is poor, research efforts are underway to help us better understand the future impact of climate change on groundwater”(UNESCO 2011). But a good assessment of the future recharge requires the use of accurate methods to determine the actual current recharge and ensemble analysis by using several scenarios.

This study, which comes within this scope, aims to contribute to the improvement of knowledge about groundwater process, current and future groundwater recharge, and the integrated management of water resources in Northern Ghana.

1.2. Statement of the research problem

Over the World, more than 1.5 billion people depend mainly on groundwater as their source of drinking water (UNESCO 2011). Groundwater is the main source of water in most rural areas. Many countries use the resource to sustain agriculture, industry, streams, lakes, wetlands, and ecosystems (UNESCO 2011). The use of groundwater is expected to increase because of the effect of climate change on water resources. In fact, climate change will affect groundwater, but because of its characteristic buffer capacity, groundwater is more resilient to the effects of climate change than surface water. This buffer capacity which is one of the major strengths of groundwater systems, allows long dry periods to be bridged and generally reduces the risk of temporary water shortages (Van der Gun 2012). In Africa, where groundwater is the major source of drinking water, its use for irrigation is forecast to increase substantially to combat growing food insecurity (MacDonald et al. 2012). In the Volta river basin, the study by Oguntunde et al. (2017) projected an increase in both frequency and magnitude of drought due to climate change. This will result in an increase in irrigation water demand.

In 1998, 52% of the rural population in Ghana was dependent on groundwater tapped by boreholes with hand pumps and open wells with and without pumps (Gyau-Boakye 2001). As pointed out by Martin & Van De Giesen (2005), 19 of the 23 towns on the Burkinabe side of the Volta River basin and 11 of the 20 towns on the Ghanaian side, depend exclusively on groundwater for domestic water supply.

The northern part of Ghana is characterized by a semi-arid climate, with a prolonged dry season of about 7 months and a shorter wet season of 5 months. All the rivers and streams dry up in the dry season except for the main channel of the White Volta which is sustained by flow releases from the Bagre dam located few kilometres upstream of the region. As a result, surface water supplies in the region are unreliable and insufficient to meet the water demands for socio-economic development in many places in the basin, thereby making groundwater sources the preferred and most cost-effective means of supplying water to the largely rural and dispersed population in the basin (Obuobie 2008). In addition to the domestic water supply, groundwater sources are relied on for dry season irrigation of vegetables as well as for watering of cattle and other livestock in the region. However, aquifers in northern Ghana are dominantly the hard rock type (Crystalline basement rock). This aquifer has no primary porosity and may not be able to

sustain the increasing demand on the resource. Further, climate change may worsen the situation as recharge is dependent on rainfall in northern Ghana and research findings suggest an increase in temperature and a decrease in rainfall in the area (Asante and Amuakwa-Mensah 2014). Several studies have shown that the impact of climate change is essential, and without proactive measures, the resources will not be able to stand-up to such constraints (Kasei 2010).

As the uses of water strictly depend on its quality, the use of groundwater in the crystalline basement of Northern Ghana is negated by the poor quality of the resource in some locations where groundwaters with high fluoride concentrations have been found. High fluoride concentrations above WHO limit of 1.5 mg/L are related to health implications of mottled teeth, dental and skeletal fluorosis. Furthermore, in the rural areas, groundwater and surface water are used in domestic water supply without any proper treatment.

In addition, estimation and understanding of groundwater recharge, understanding the processes controlling groundwater recharge and quality are the cornerstone of sustainable integrated groundwater and land use management, and are necessary in formulating an effective groundwater protection policy. Together with natural groundwater discharge and artificial extraction, groundwater recharge is the most important water budget component of a groundwater system. Recharge is needed to determine one of the important groundwater resources sustainability indicators. The ratio of the total groundwater abstraction to groundwater recharge is particularly useful for policy makers due to its simplicity and the scale at which it is applied. It helps them make better-informed decisions regarding land use and water management since protection of natural recharge areas is paramount to the sustainability of the groundwater resource (Xu and Beekman 2003; Girman et al. 2007; Kresic 2009).

Therefore, a study of water quality, process controlling groundwater quality and the impact of climate change on groundwater recharge in the area are of crucial importance for sustainable development and management of water resources in the crystalline basement aquifer of Northern Ghana.

1.3. Literature review

1.3.1. Groundwater quality and hydrogeochemical processes

Water is the source of life but its quality can be a real threat for environment and especially for human life. Interest on water quality has really increased because the declining water quality has become a global issues and the uses of water strictly depend on its quality. This has increase interest on study of the quality of water. In Ghana, study of water is for great importance as in many areas poor water groundwater quality related to high concentraton of minerals like arsenic and fluoride was found in many areas. Arsenic has is a toxin and carcinogen while fluride High fluoride concentrations above WHO limit of 1.5 mg/L are related to health implications of mottled teeth, dental and skeletal fluorosis. In the crystalline basement aquifer of Northern Ghana the main quality problem is releted to the high content of fluoride that was found to be associated with microcline-rich granitoids (Smedley et al. 1995; Apambire et al. 1997; Firemping et al. 2013).

Some studies related to groundwater quality have been carried out in the Northern Ghana (e.g. Smedley et al. 1995; Anku et al. 2009; Loh et al. 2012; Tay 2012). The works of Anku et al. (2009) and Loh et al. (2012) focused on groundwater quality in the crystalline basement aquifer of Northern Ghana but they used a small data compared to size of the study area and the sampled locations are not well distributed. Loh et al. (2012) did not take into account the quality of water for domestic use. Apambire et al. (1997), on the other hand, focused mostly on the genesis of elevated fluoride concentrations in groundwater.

1.3.2. Estimation of groundwater recharge

Recharge is the entry of water into the saturated zone. It is the means by which groundwater storage is replenished, and is thus also one of the principal causes of rises in water table levels. For the most part, recharge occurs from above, by means of downward migration of moisture through an overlying (Younger 2007). Numerous studies have been focused on groundwater recharge in the Volta Basin, especially in Northern Ghana, over the past three decades. Notably, Bannerman and Ayibotele (1984), Friesen et al. (2005), Martin (2006), Sandwidi (2007), Carrier (2008), Ofosu-Addo et al. (2008) and Obuobie (2008) who focus their studies in the Upper East and Upper West Regions of Ghana, Volta Basin, Atankwidi river Basin (275 km²) in Ghana, the

Kompienga Dam Basin (5911 km²) in Burkina Faso, the upper half of Ghana (97,704 km²), the White Volta in Ghana (48,800 km²) and the White Volta Basin of Ghana (106,000 km²), respectively. Obuobie used three methods at different scale and concluded that the long-term average recharge estimated by the chloride mass balance in the Upper-East Region was 8 % of the long-term mean annual rainfall of 990, while the simulated mean recharge by the SWAT model was 59.0 mm, which represented about 7 % of the mean annual rainfall (824 mm). Using the Water Table Fluctuation method the same author found recharge representing 8 % of the annual rainfall (870 mm) in 2006, and 92.0 mm in 2007, which represented 7 % of the annual rainfall of 1294 mm. In the Atankwidi river basin located in the crystalline basement aquifer of Northern Ghana, Martin (2006) used three methods to estimate groundwater and suggested that the long-term average recharge estimated by the chloride mass balance method represented 6% of the annual rainfall of 990 mm.

1.3.3. Impact of climate change on groundwater recharge

Since groundwater recharge is the mean by which groundwater resources are renewed the impact of climate on groundwater resources mostly focus on studying the impact on groundwater recharge. Review of works related to impact of climate change on groundwater resources and the summary of methodologies used can be found in the work by Kumar (2012). In Ghana, although some work related to the impact of climate change have been done, only the work by Obuobie (2008) in White Volta basin studied the impact of climate change by using one scenario. This work found that the shallow groundwater recharge is expected to increase by about 29 % in the period 2030-2039 compared to recharge of the baseline period 1991-2000 which was estimated to 59.0 mm by using the SWAT model.

1.4. Research questions

Questions to be answered by this work are the following:

1. What are the processes influencing groundwater quality in the crystalline basement aquifer of Northern Ghana?
2. What is the spatial and the temporal variability of groundwater recharge in Northern Ghana?
3. To what extent does climate change impact groundwater recharge in Northern Ghana?

1.5. Research Objective

The main objective of this thesis is to study groundwater quality and recharge, and to assess the impacts of climate change on recharge.

Specific objectives:

1. Investigate the processes influencing groundwater quality in the crystalline basement aquifer of Northern Ghana;
2. Estimate groundwater recharge at different temporal and spatial scales (local- and basin-scale estimates) in the crystalline basement aquifer of Northern Ghana; and
3. Evaluate the impact of climate change on the groundwater recharge in the crystalline basement aquifer of Northern Ghana.

1.4. Hypotheses

This research was based on the following hypotheses: *(i)* groundwater quality is governed by silicate weathering and cation exchange and groundwater water is suitable for irrigation and drinking water purposes, *(ii)* and climate change will reduce groundwater recharge in the crystalline basement aquifer of Northern Ghana.

1.5. Novelty

Although some studies estimating groundwater recharge have been done in the area, none has use more than three different methods. Among these studies, only one studied the impact of climate change, but the study was based on scenario only. This study is the first work using five different methods to estimate groundwater recharge in the study area. This study estimating the impact of climate on ensemble basis is the first study using twelve data sets resulting from the combination of two Regional Climate Models and three Global Climate Models under two climate scenarios to determine the impact of climate change in the area. Further, this is the first study to really address the hydrogeochemical processes influencing this area's water quality.

1.6. Scope of the thesis

This work was done under the WASCAL project funded by the German Ministry for Education and Research (BMBF). The question behind this work is to have a clear picture of the quality of groundwater resources, the processes influencing this quality and the impact of climate change on groundwater. It helps to know the role that groundwater resources can play in the crystalline basement aquifer today and in future climate change context.

For the purpose of the study, the crystalline basement aquifer of Northern Ghana, where people mostly rely on groundwater resources, was selected. This aquifer type covers the major part (54%) of the total land area of Ghana. Very few studies related to groundwater recharge have been done in the area and only the work by Obuobie (2008) studied the impact of climate by using only one scenario. There is a high uncertainty in using a singular scenario in climate impact study as well as using one method only to estimate groundwater recharge. Understanding of hydrogeochemical processes and knowledge of the water quality helps to know the usability of the water and the recharge processes that are relevant to draw a better water and land management plan. Studies related to hydrogeochemistry use a small data set or data collected from areas that are not well distributed in area. They did not consider the different geological formations in their analyses.

To fill this gap, this work focused the hydrogeochemical study in a part of the basement aquifer where the major geological formations were represented. There were a huge number of boreholes in the area and they are well distributed. The sampled wells were selected by taking into account the geological formations. The water quality and the hydrogeochemical processes controlling this quality were analysed. Secondly, five different methods are used to estimate groundwater recharge. Finally, the impact of climate change based on an ensemble analysis of the combination of three Global Climate Models, two Regional Climate Models and two scenarios resulting in twelve data sets. The estimation of the future recharge is based on a method that does not take into account the geology of the area.

1.7. Expected results and benefits

At the end of this work, expected results are listed as follow:

1. The processes influencing groundwater quality in the crystalline basement aquifer of Northern Ghana will be known;
2. The range of groundwater recharge at different temporal and spatial scales (local- and basin-scale estimates) in the crystalline basement aquifer of Northern Ghana will be known; and
3. The impact of climate change on the groundwater recharge in the crystalline basement aquifer of Northern Ghana will be known.

1.8. Organization of the Thesis

The thesis is organized into seven chapters. The first chapter is the general introduction. The second presents the study area by discussing the geological units, the climate, the land use and the land cover. The third chapter presents the data, the materials and the methods used in this work; while the fourth one discusses the different hydrogeochemical processes that influence the quality of water in the study area and the usability of both surface and groundwater for irrigation and drinking purposes. The fifth chapter focuses on groundwater recharge and baseflow analysis. The impacts of climate change on the groundwater recharge is estimated in the sixth chapter, while seventh chapter summarizes all the findings and presents recommendations for improvement and further research works.

Chapter 2 - DESCRIPTION OF THE STUDY AREA

2.1. Location

The study area is located in the northern part of Ghana, within the Volta basin. It encompasses three administrative regions, namely the Upper-West, Upper-East and Northern regions (Figure 2-1). It lies between $9^{\circ} 00' N - 11^{\circ} 00' N$ and $3^{\circ} 00' W - 0^{\circ} 68' W$ and occupies a surface area of about 25882 km^2 .

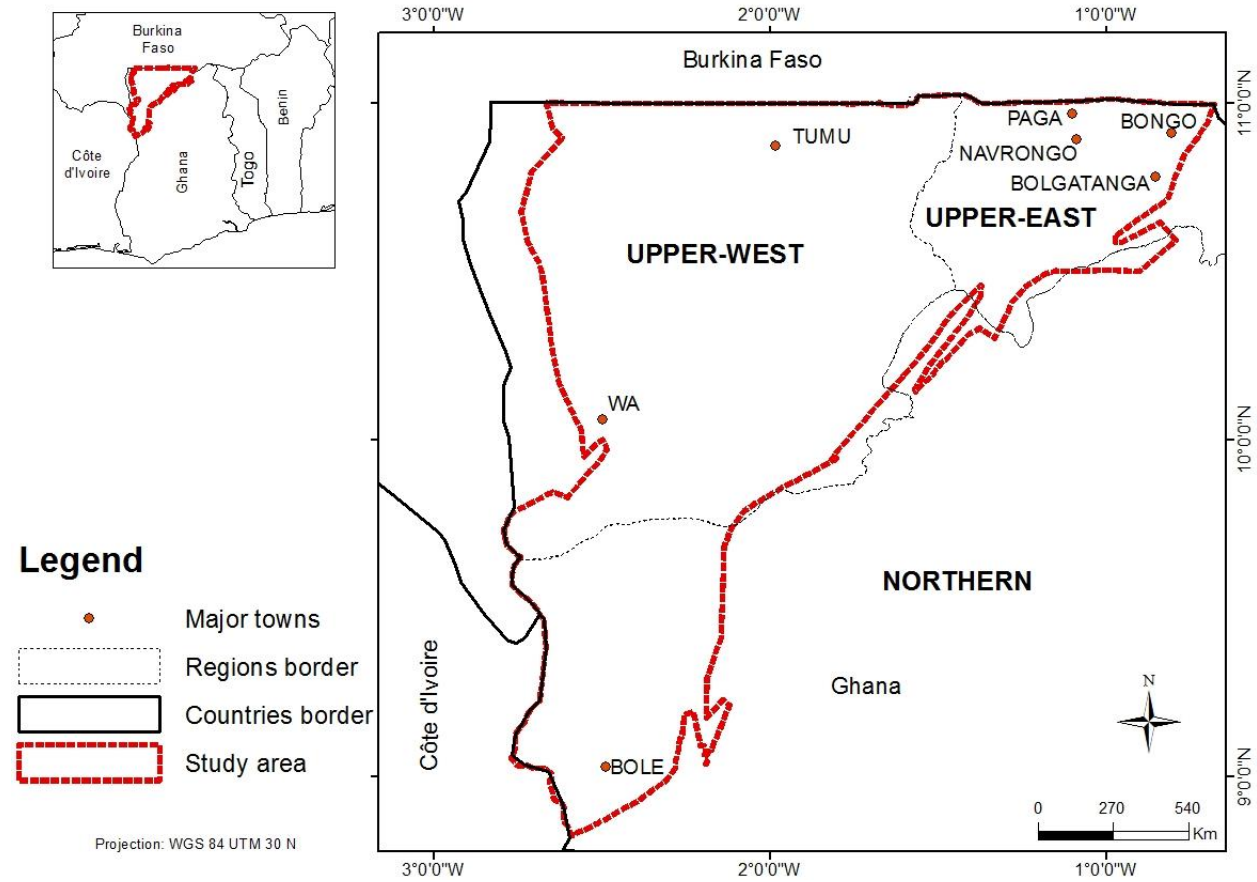


Figure 2-1: Map of Northern Ghana showing the location of the study area

2.2. Climate

The annual rainfall of the study area, based on 51 years (1961-2009) data from Bole, Wa Navrongo and Wa climate stations, ranges from 762 mm to 1820 mm with average of 1100 mm, from 523 mm to 1543 mm with average of 1046 mm and from 671 mm to 1365 mm with average of 988 mm at Bole, Wa and Navrongo, respectively (Figure 2-2). The area has distinct wet and dry seasons. The wet season starts in April/May and ends in October, with the peak in August for the central and northern part of the area and in September for the southern part (Figure 2-3). Based on the work of Oguntunde and Abiodun (2013), the year can also be divided into four seasons. The period January-March is termed as dry season while July-September is wet season. The periods April-June and October-December are identified as dry-wet and wet-dry transition seasons, respectively. Highest Potential Evapotranspiration (PET) occurs in February, while the lowest is obtained in August. Mean annual PET is 1353 mm, 2074 mm, 2427 mm in the southern (Bole area), western (Wa area) and Northern (Navrongo area), respectively. The dry season starts in October/November and ends in April. Figure 2-2 shows the rainfall patterns for the period 1961-2009 based on the Lamb index. The annual rainfall amount is higher in the southern part than in the northern part of the area as depicted by Figure 2-3, following the gradient that is mostly observed in West-Africa. PET is higher than rainfall during eight months (October-May) in the northern (Navrongo) and western part (Wa) of the study area and during six months (November-April) in the southern part. Annual rainfall follows a unimodal pattern in the area but it tends to a bimodal in the southern part as shown in Figure 2-3. Both annual rainfall and PET follow a South-North gradient. Rainfall decreases from south to north while PET decreases in opposite direction from north to south. Annual rainfall represents 40% and 80% of annual PET in the northern (Navrongo) and the southern parts, respectively. In the study area the highest mean temperature occurs in March and in April, while the lowest occurs in the period July-September.

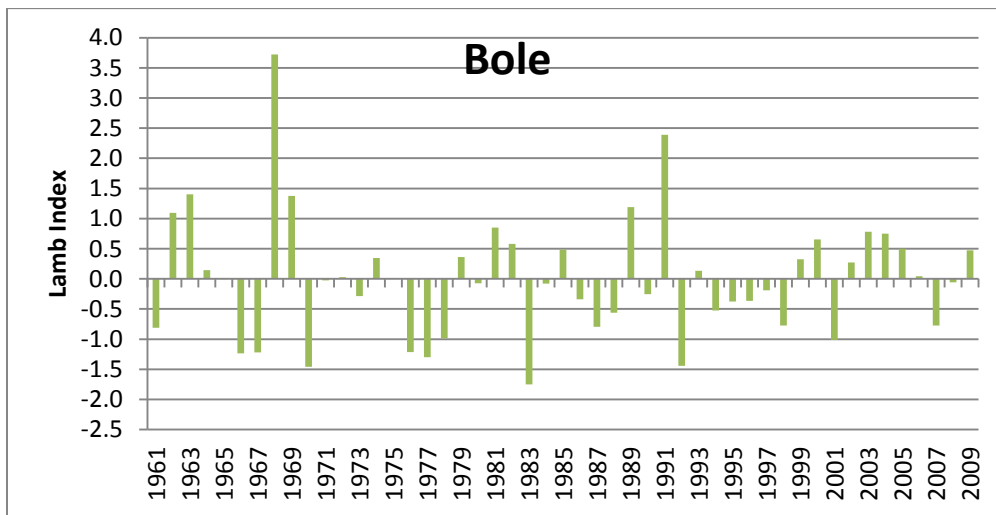
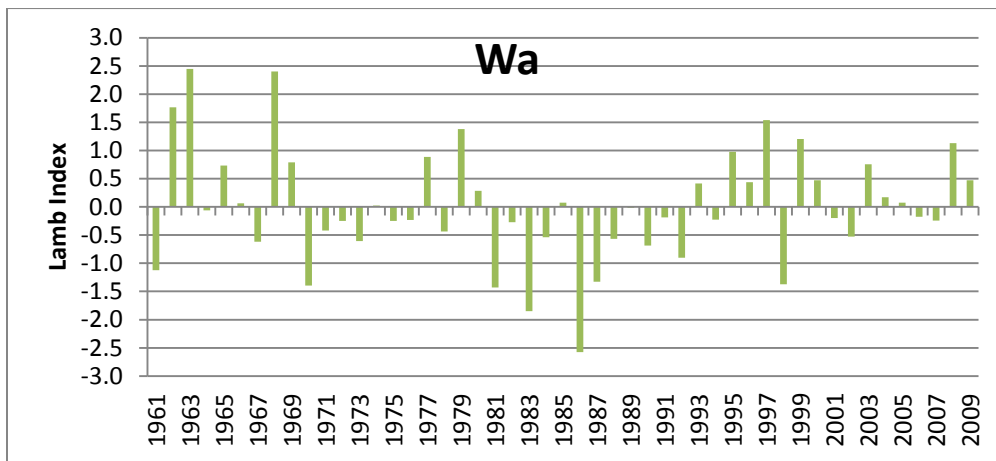
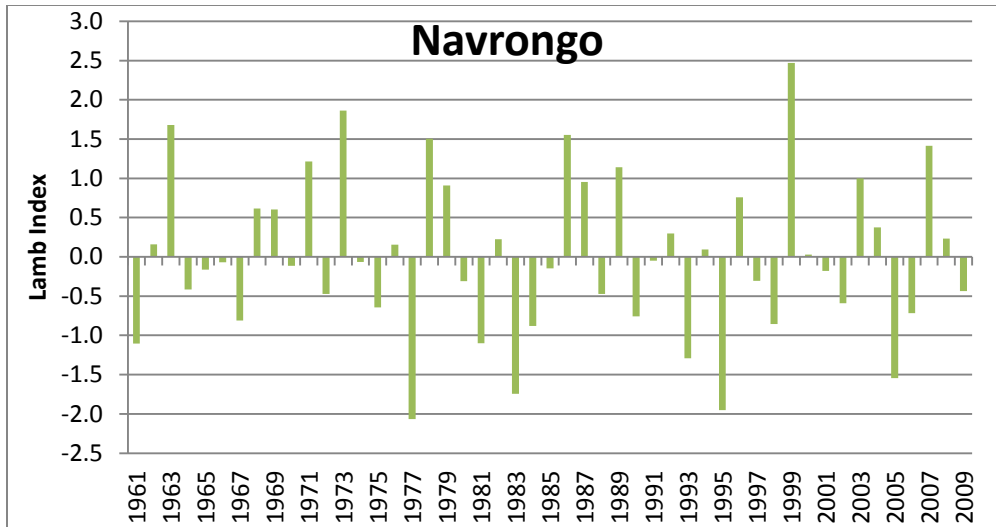


Figure 2-2: Lamb index of annual rainfall (1961-2009) in the study area using data from the stations of Bole, Wa and Navrongo.

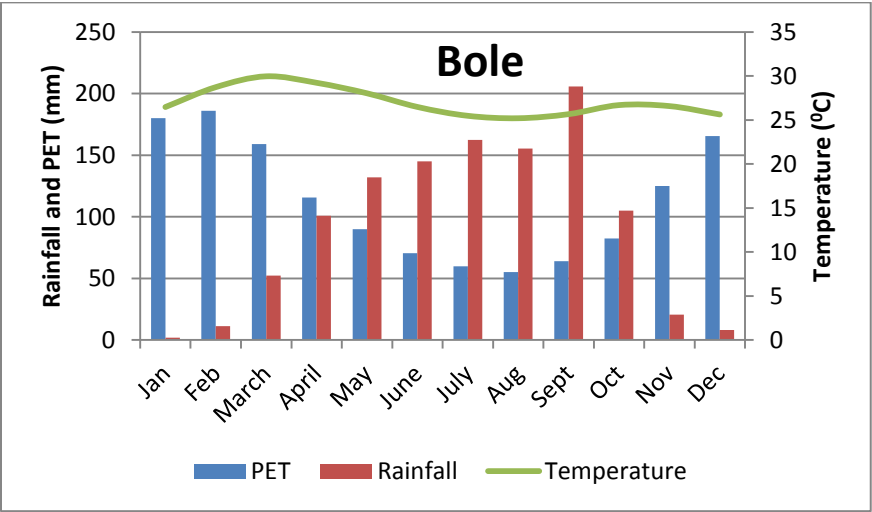
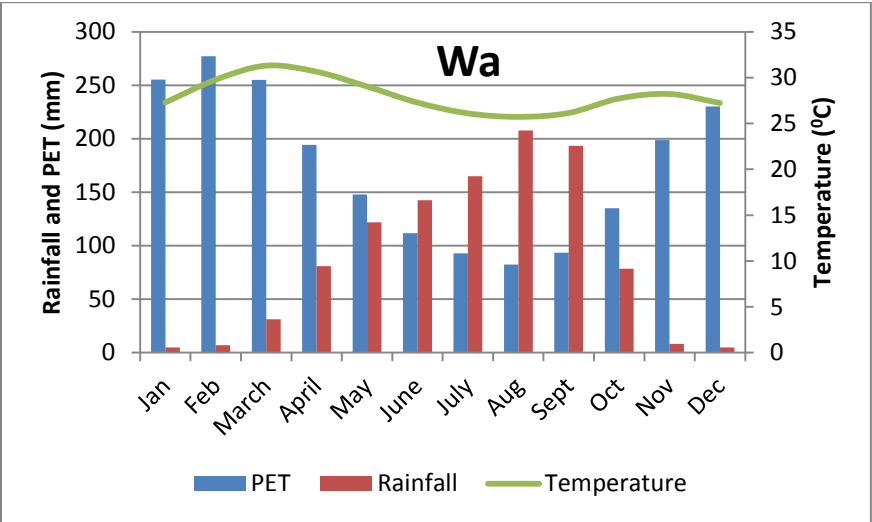
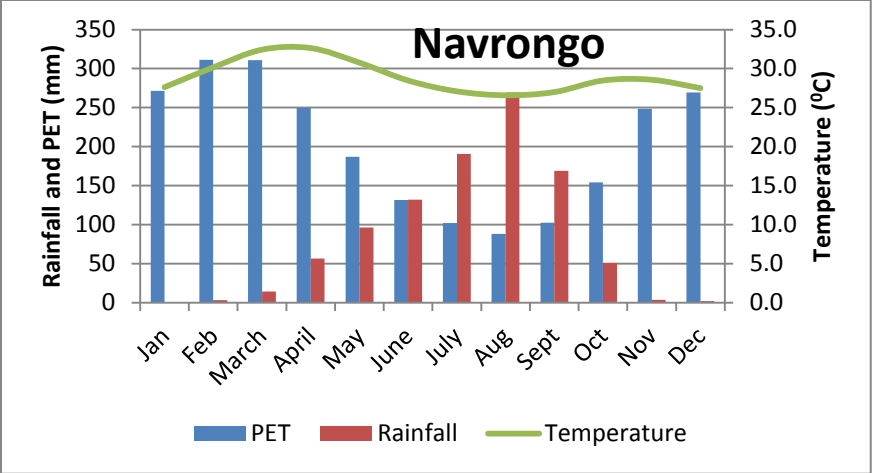


Figure 2-3: Comparison between monthly rainfall, potential evapotranspiration and mean temperature in the study area.

2.3. Land use and Land cover

The study area falls in the Sudan savannah and the Guinea savannah zones. There are three major land uses in the study area : cultivated savannah woodland (open and closed), savannah woodland (open and closed), grassland with/without scattered trees and shrubs (Carrier 2008). Vegetation of the area consists of grass with scattered drought resistant trees such as the shea, the baobab, dawadawa, acacias and neem that form the guinea savannah woodland vegetation belt; and the area has a gentle slope (Loh et al. 2012). Compound farms and bush farms are the two types of farms found in the study area. The compound farms are located around the immediate vicinity of the house, while the bush farms are located out of the village (Bagamsah 2005). Slopes are generally gentle in the study area (Anku et al. 2009).

2.4. Geology and Hydrogeology

2.4.1. Regional geology

The West African geology consists of a vast Precambrian craton (formed since about 1600 Ma) surrounded by mobile zones that experienced major tectonic events in the Upper Precambrian and Paleozoic, resulting in the formation of chains such as the Pan-African chains of the Rokelides, Pharusides and Dahomeyides; the Caledonian Hercynian Mauritanide chain; the Hercynian chain of the Moroccan Meseta; the Anti-Atlas chains; and the Ougarta chains (Dakoure 2003). The western part of the craton consists of the Guinea Rise, also called the Man shield, which occupies the southern half of the West African craton. The Pan African belt of the Rokelides on the boundary of this part is associated with marginal tectonic events due to the reactivation of the Archaean rocks. The North of the craton is occupied by the sediments of the great Taoudeni Basin formed from the Infracambrian to the Lower Palaeozoic, which is obscured in the east by continental Tertiary to Quaternary deposits and in the west by the Mauritanide belt, which forms the eastern boundary of the Mesozoic-Tertiary sediment of the Senegal Basin. The southwest, falling in the Bove Basin, is occupied by Lower Palaeozoic sediments which interrupt the continuity of the Rokelide belt with the Mauritanide belt. In the southwestern and eastern parts of Taoudeni Basin and Bove Basin, respectively, Mesozoic dolerite sills occur. In the eastern part, the craton underlies Infracambrian to Lower Palaeozoic sediments of the Volta Basin and the Pan African rocks of the Togo-Benin-Nigeria swell which are joined to each other

by the intensely thrustfaulted rocks of the Togo belt. The Mesozoic Tertiary Iullmedden Basin, which separated to the block of the narrow Cretaceous Bida Basin and Benue Trough by the Togo-Benin-Nigeria swell, is limited in the north by the Pan African rocks in the Adrar des Iforas and the Air, and the Pan African rocks of the Gourma lie on its western boundary. The Chad Basin located at the extreme east is mainly occupied by Quaternary sediments. Some granite intrusions of Palaeozoic to Jurassic and Tertiary ages occur in Niger, Nigeria and Cameroun. Smaller narrower basins of Cretaceous age located along the southern coast of West Africa are filled with sediments (Spudis 2005). The main geological units of West Africa are presented by Figure 2-4.

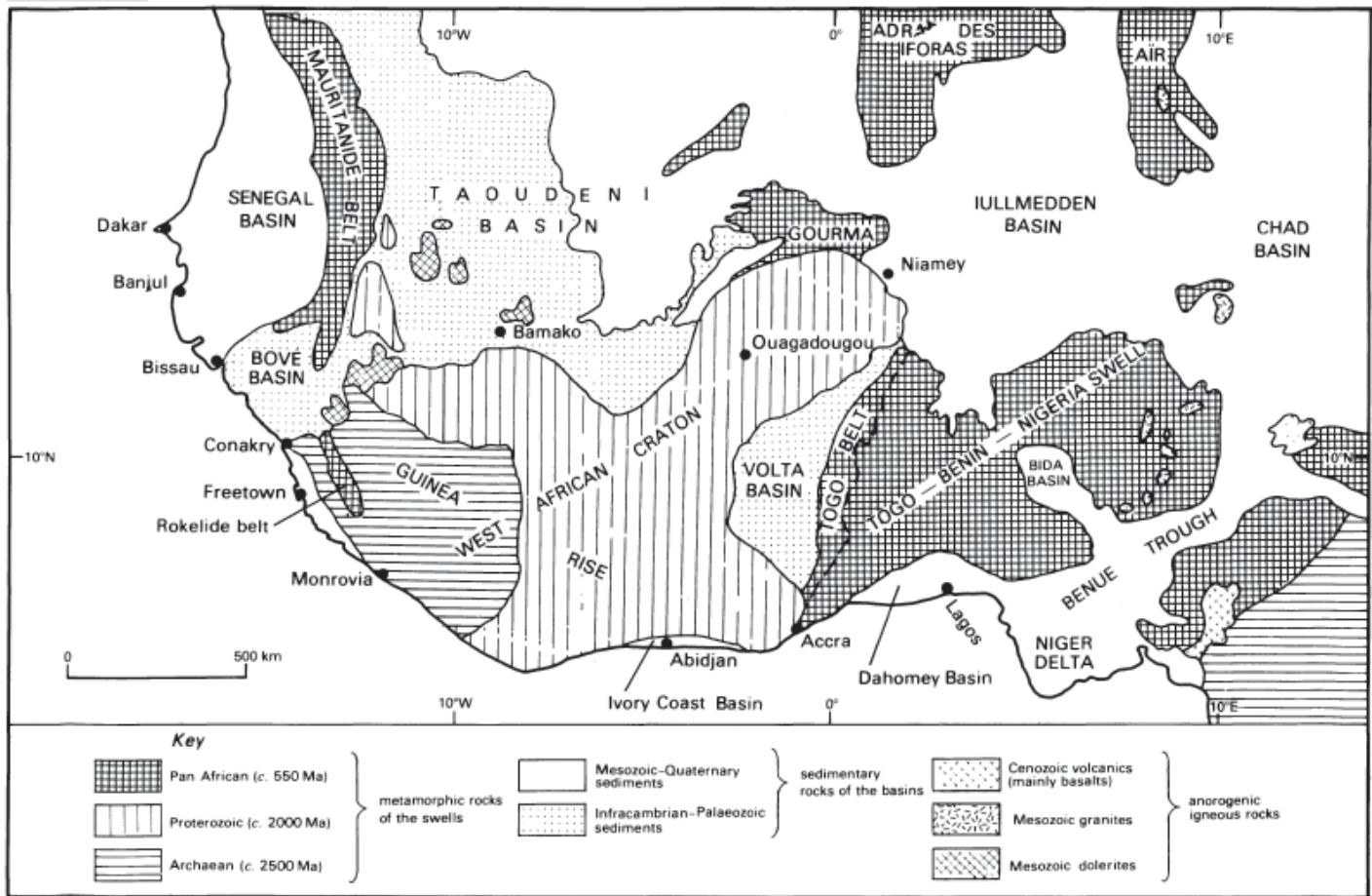


Figure 2-4: Main geological units of West Africa (Spudis 2005).

2.4.2. Geology of Ghana

Geological formations in Ghana can be classified into 3 main groups, namely Paleoproterozoic rocks, gneisses and supracrustal rocks. Paleoproterozoic rocks predominate in the southwestern and northwestern parts of the country whereas gneisses and supracrustal rocks of mostly Neoproterozoic age occur in the southeast and the east of the country. Flat-lying shelf/marine sediments of very late Precambrian to Paleozoic age are found in the central and northeastern parts of the country. Cenozoic sediments occur in a small strip along the coast. Kortatsi (1994) stated that as the Basement Complex and the consolidated sedimentary formation cover 54 % and 45 % of the country respectively, they are the two main geological provinces in Ghana. This work also highlighted that the Basement Complex consist mainly of gneiss, phyllites, schists, migmatites, granite-gneiss and quartzites that are grouped into Birimian, granite, Togo, Dahomeyan and Tarkwaian rock formations; while the consolidated sedimentary formation found in the Volta basin consist mainly of sandstones, shale, arkose, mudstone, sandy and pebbly beds and limestones. Rocks of these two geological provinces have little or no primary porosity.

2.4.3. Hydrogeology of the study area

As presented in Figure 2-5 the study area is mostly underlain by the Precambrian basement rocks of the West Africa craton. The basement rocks in area studied are classified into four groups, namely, the Cape Coast granites, Dixcove granites, undifferentiated granites, and rocks of the Birimian Supergroup (Leube et al. 1990).

Groundwater quality problem in the study is mostly related to high-fluoride and high-nitrate concentrations (Anku et al. 2009). The water table depth varies from ground level in the rainy season to about 15 m in the dry season. Groundwater in recent years has become a premium source of portable water supply for most communities in Ghana and mostly for regions encompassed by the study area (Obuobie 2008). Shallow groundwater is used smallholding irrigation and for watering of cattle during the dry season, thereby contributing to food security and the economy (Obuobie 2008; Namara et al. 2011).

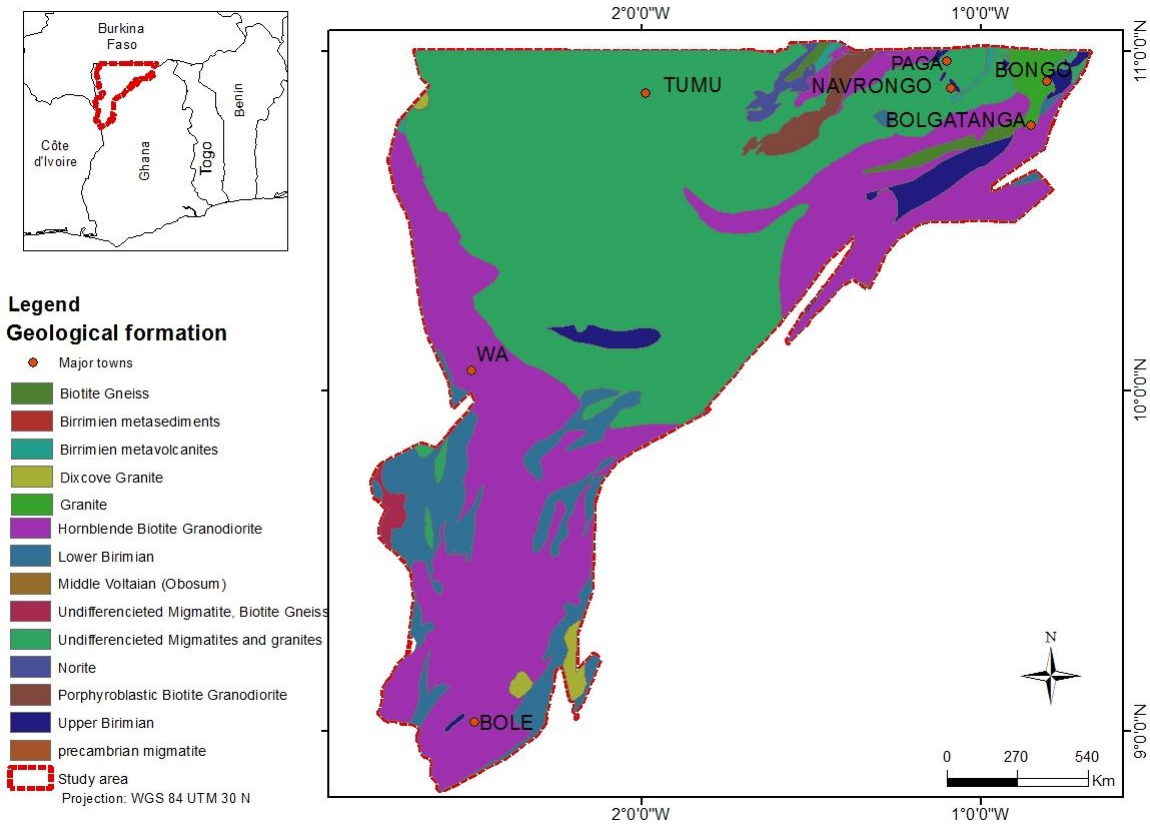


Figure 2-5: Geological map of the study area (source: Glowa Volta).

2.5. Demography, environmental, social and economic activities

In 2010 the population size of the three northern regions covered by the study area was estimated to be about 7409687 (Ghana Statistical Service 2012). The same report of the Ghana Statistical Service (2012) showed that majority of the population in the area is living in rural areas and agriculture is the main economic activity. Rainfed agriculture predominates in the area and the cultivated crops in the area are guinea corn, maize, millet, rice, soya beans, groundnuts, cotton, yam, cowpea, and sorghum. Population density was estimated to be 35.0, 118.4 and 38.0 persons per square kilometre for the Northern Region, Upper-East Region and Upper-West Regions, respectively (Ghana Statistical Service 2012). In the area where people are organized under chiefs at the lineage and settlement levels and there are three main religions, namely Christianity, Islam and African traditional religions. Muslims predominate in the Northern Region and represented 60% of the population, while Christianity leads with 41.7% and 44.5% in the Upper-East Region and Upper-West Region, respectively (Ghana Statistical Service 2012).

Chapter 3 - DATA, MATERIALS AND METHODS

3.1. Introduction

Data collected in the framework of this study were collected from different sources and can be classified into primary and secondary data. Primary data were collected during the two-year field work while secondary data were collected from different public and private services or freely downloaded from some websites. Different materials and methods were used to collect and analyse the data in order to achieve the goals of this work.

3.2. Data

3.2.1. Climate data

Climate data collected during this work were precipitation, temperature, wind speed and potential evapotranspiration. Daily and monthly climate data including wind speed, rainfall and potential evapotranspiration for the period 1960-2012, with some missing data, were collected from the Ghana Meteorological Agency (GMET) and the National Meteorological Service of Burkina Faso.

Daily precipitation, daily maximum and minimum temperatures data were also provided by the Coordinated Regional Climate Downscaling Experiment (CORDEX) initiative and were obtained from the ESGF archives (<http://esgf.org/>). These data consist of historical data lasting from 1950 to 2005 and projected climate data, for the period 2006-2100, from two Regional Climate Models (RCM) nested in three Global Climate Models (GCM) based on scenarios RCP4.5 and RCP8.5. Data provided by CORDEX only used for the study of the impact of climate change in [chapter 6](#).

3.2.1.1. Precipitation data

Daily and monthly rainfall data were collected from the Ghana Meteorological Agency (GMET) and the National Meteorological Service of Burkina Faso. Historical and projected data of daily precipitation were freely provided by CORDEX. The precipitation data were used in most of the chapters. These rainfall data were used as inputs of the Wetspass model. They were also used in estimating potential evapotranspiration based on the modified Hargreaves method (Droogers and Allen 2002) and in downscaling data from the RCMs' data.

3.2.1.2. Temperature data

Like the precipitation data, daily and monthly minimum and maximum temperature data were collected from the Ghana Meteorological Agency (GMET) and the National Meteorological Service of Burkina Faso for various climate stations located in and around the study area. Historical and projected data of daily minimum and maximum temperature were freely provided by CORDEX. Like the rainfall data, the temperature data were used as input of the WetSpas model. They were also used in various tasks ranging from climate downscaling to the estimation of potential evapotranspiration based on the original Hargreaves (Hargreaves et al. 1985) and modified Hargreaves (Droogers and Allen 2002) methods.

3.2.1.3. Wind speed data

Daily and monthly mean wind speed data collected from Ghana Meteorological Agency (GMA) and the National Meteorological Service of Burkina Faso for various climate stations located in and around the study area. These data were used as input of the WetSpas model in order to estimate groundwater recharge.

3.2.1.4. Evapotranspiration data

Daily and monthly potential evapotranspiration data estimated using the the FAO- Penman-Montieth method (Allen et al. 1998) were collected from Ghana Meteorological Agency (GMA) and the National Meteorological Service of Burkina Faso for various climate stations located in and around the study area. The evapotranspiration data were used in several chapters in this work. They were particularly used in discussing the climate of the study area and as input of the WetSpas model.

3.2.2. Topographic data

The digital elevation model data processed from the shuttle radar topographic mission with 90 m resolution were downloaded from USGS Earth Resources Observation and Science (EROS) center database. They were used as input of the WetSpas model.

3.2.3. Streamflow data

River discharge data of the Sissili River at the station of Wiasi, located in the northern part of Ghana, for the period lasting from March 2003 to December 2008 with missing records from April 2007 to June 2007, used for the calibration of the WetSpas model were collected from

Hydrological Services Department of Ghana. They were used to estimate baseflow and groundwater recharge ([chapter 5](#)) and to calibrate and validate the WetSpss model.

The drained land area of the Wiasi station is about 12517 km² and is presented by Figure 3-3. This area is shared by Ghana and Burkina-Faso and it is underlain by a crystalline basement covered by a regolith layer that reaches 40 m (Carrier 2008). The average slope is 1.4%. The dominant land use type is forest (covering 40% of the study area), followed by woodland (26%) croplands (20%) (Figure 3-2). The cropland is more concentrated in the northern part of the catchment. The elevation in the catchment ranges from 126 – 402 m above mean sea level. The concentration time of the catchment, approximated by the formula of Linsley et al. (1982) is about 10.5 days. Major towns in and around the watershed are Koudougou, Gao, Po and Leo in BurkinaFaso, and Navrongo and Tumu in Ghana.

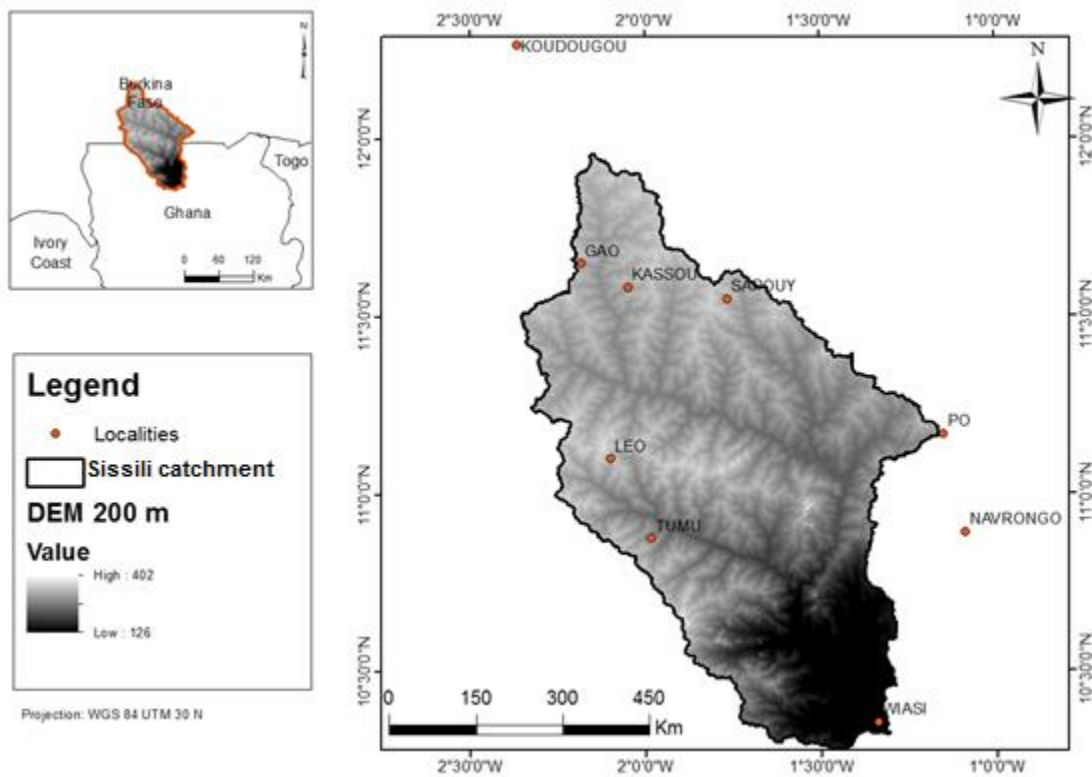


Figure 3-1: Location of the study area of the streamflow analysis

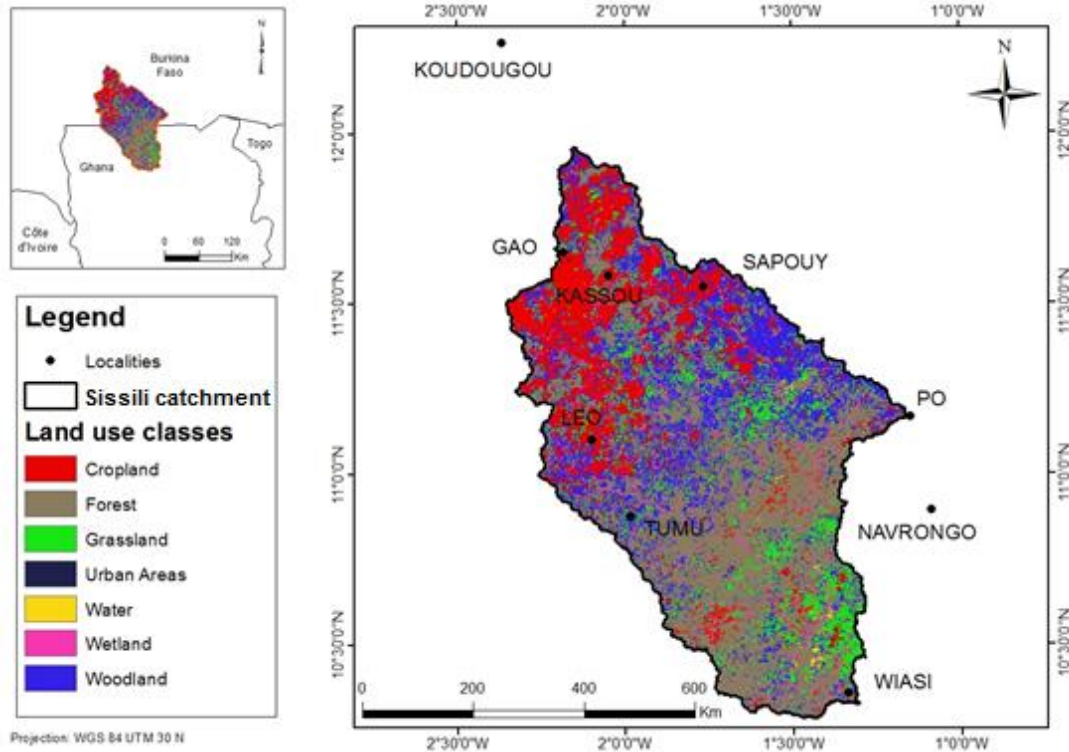


Figure 3-2: Land use map of the study area of the streamflow analysis

3.2.4. Land use and land cover data

Land use/ cover map of the study area for the year 2000 with a resolution of 250 m was downloaded from the Glowa Volta database. These data were used in describing the study area and as input of the WetSpass model.

3.2.5. Hydrogeological data

In order to estimate groundwater recharge by WTF method, available water level data from ten (10) monitoring wells located in the study area were collected from the Water Resources Commission of Ghana. Additional seven wells were monitored as part of this study to collect water level data from June 2014 to December 2016. In order to remove barometric effect on groundwater level rise, data on atmospheric pressure were collected at one of the seven well locations to correct the water level data collected from the seven wells. Distance between all the monitoring wells and the location where the atmospheric pressure was measured is less than 30 km and thus was deemed suitable to use for the seven wells. Locations of the monitored wells

are presented by Figure 3-3. Drilling logs of existed monitored wells were collected from Water Research Institute of Ghana.

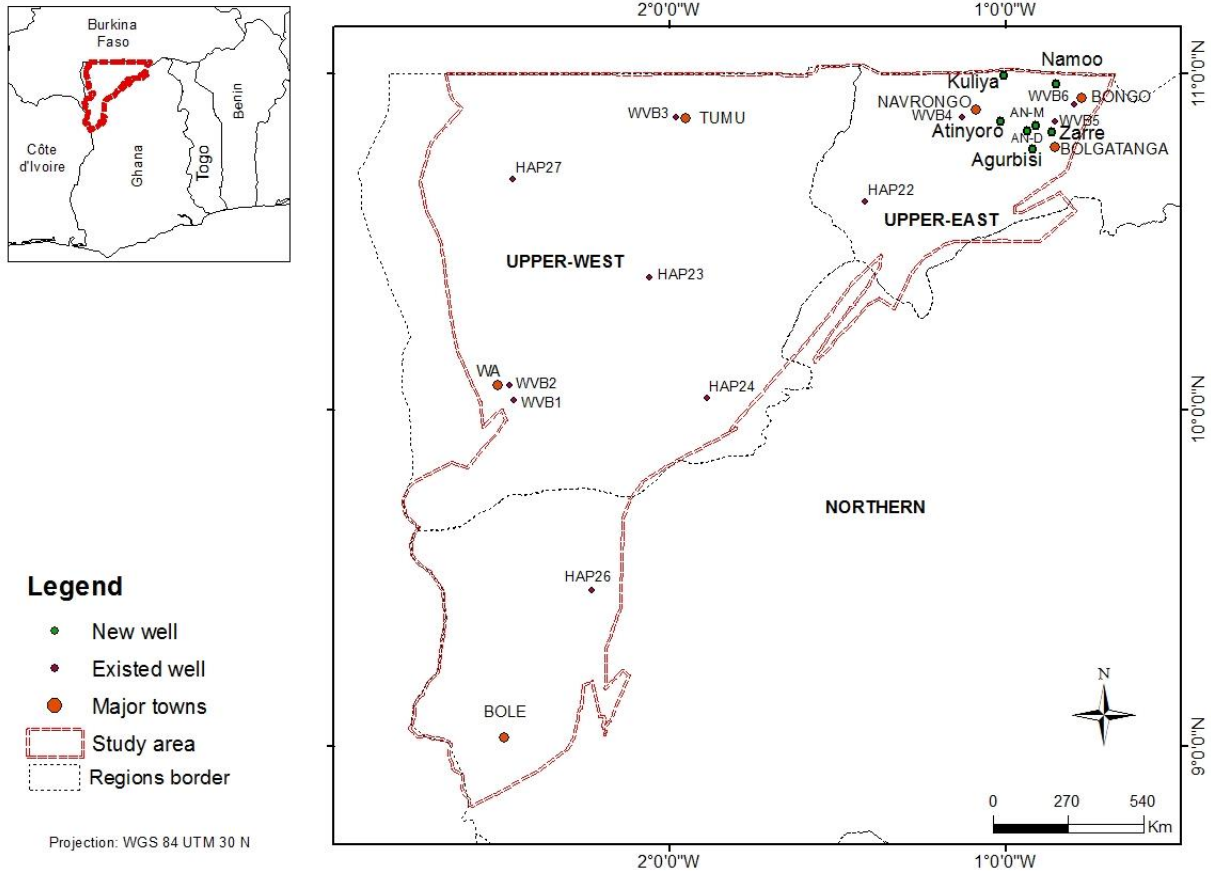


Figure 3-3: Map of northern Ghana showing the monitoring wells

3.2.6. Geological data

The geological map was downloaded from Glowa Volta database. It was used to describe the study area and in characterising hydrogeochemical processes. It was further used in discussing the groundwater recharge rate estimated by the different methods.

3.2.7. Soil data

The soil data were obtained from two sources, namely the Glowa Volta database and the harmonized world soil database (Batjes 2009). The data collected from the Glowa Volta database were used to discuss hydrogeochemical data in Chapter 4 and in chapter 5, while those processed from the harmonized world soil database (Batjes 2009) were used as input of the WetSpas model.

3.2.8. Hydrogeochemical data

The data were obtained from the hydrogeochemical analysis of the rain water, surface water and groundwater samples collected during the field work for the estimation of groundwater recharge using the Chloride Mass Balance (CMB method) and the hydrogeochemical characterisation of groundwater and surface water. The hydrogeochemical data used for the CMB method were composed only by chloride content in rain water and groundwater, while the data used for hydrogeochemical characterisation consist of wide range of parameters including chloride in groundwater and surface water.

3.2.8.1. Chloride data in rain water and groundwater

Chloride data in rain water and groundwater were obtained from the chemical analysis groundwater and rain water samples collected during the rainy seasons of 2014 and 2015. In 2014 samples were collected during the whole season from May to October whereas in 2015 it was done from the beginning of August to October (as August and September are the months receiving the highest amount of rainfall). Rain samples were collected at 21 locations scattered over the study area. In 2014 the samples were collected every two weeks while in 2015 rain samples were collected on daily basis and groundwater samples were collected at the end of September and early October to get samples representative of the recharge during the whole rainy season. Locations where both rain and groundwater samples were collected are presented in Figure 3-4. The samples were analysed at the laboratories of Water Research Institute in Ghana and Ruhr University Bochum (RUB) in Germany.

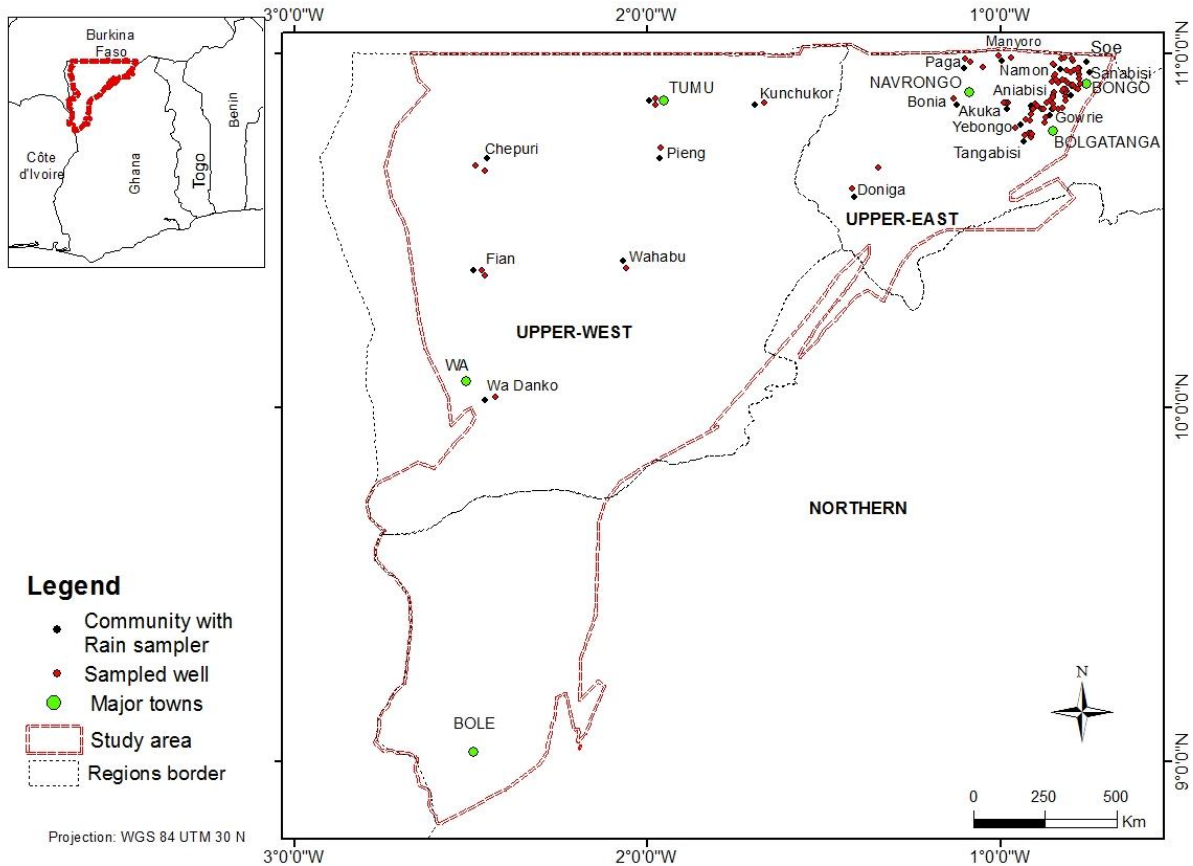


Figure 3-4: Location of sampling wells and rain samplers

3.2.8.2. Data used for the hydrogeochemical characterisation

Data of parameters such as pH, electrical conductivity (EC), temperature, salinity, dissolved oxygen (DO), and total dissolved solids (TDS) were measured *in situ*, whereas hydrochemical parameters such as Calcium (Ca^{2+}), Magnesium (Mg^{2+}), Sodium (Na^+), potassium (K^+), bicarbonate (HCO_3^-), chloride (Cl^-), sulphate (SO_4^{2-}), total iron (Fe), phosphate (PO_4^{3-}), ammonium (NH_4^+), nitrate (NO_3^-), nitrite (NO_2^-), manganese (Mn_{tot}), turbidity, colour, the total hardness (as CaCO_3) and total dissolved solids (TSS) were obtained from the analysis of a total of 65 samples (61 groundwater samples and four surface water samples) at the laboratory of Water Research Institute in Accra (cf. methodology in Table 3-1). The sampling points are presented in Figure 3-5. This geochemical data can be found in [Appendix 2](#).

Two of the surface water samples were collected from Gurugu dam and Veve dam. The Veve dam is the largest dam in the catchment and used for both irrigation and drinking purposes. The two

other surface water samples were taken from rivers (Naaba Kolga and Gurugu rivers). The groundwater samples were collected from boreholes and hand-dug wells equipped with pumps. These wells are the main sources of water supply for the inhabitants. The sampling was carried out at the end of the rainy season (from 25th September to 5th October 2015). The wells used in this study were selected in such a way that they represented the different geological formations, soils and land use types in the study area.

The study was conducted in the Veua catchment, which is a sub-catchment of the White Volta basin in Ghana and located between latitudes 10.43°N and 11°N, and longitude 0.45° and 1°W. Administratively, the Veua catchment is located in the upper east region of Ghana, where the population was estimated to be 1,046,545 in 2010, with a growth rate of about 1.2 percent and population density of 118 persons per km² (Ghana Statistical Service 2012). The total drainage area of the Veua catchment is approximately 305 km². The mean slope and the mean altitude are 0.2% and 196.5 m, respectively. Van der Sommen and Geirnaert (1988) noted that about 75% the annual rainfall occurs between July and September. The rainy season starts in May and ends in October. The climate is semi-arid and it is characterized by high temperatures with a long-term mean annual rainfall of about 990 mm. The soil types in the basin are haplic lixisol, ferric lixisols, eutric leptosol, lithic leptosol, gleyic lixisols, eutric fluvisols, eutric fluvisol and haplic luvisols with three main land use classes which are semi-natural (Grass, shrubs, trees or a mixture), artificial (bare areas, laterite and tarred roads, buildings, hamlets, rocks, etc.) and cropland (all crop types).

The Geological formations in the Veua catchment are: granite, hornblende biotite granodiorite (Hornblende B Granodiorite), biotite gneiss, upper birimian, and migmatite and undifferentiated granite (M&UG) covering 49%, 28%, 18%, 5% and 1% of the catchment area, respectively (Figure 3-5). The Upper Birimian consists of lava flows and dyke rocks of basaltic and andesitic composition. The Geological Survey Department of Ghana classified these rocks into basic volcanic subseries (metabasalt, metadolerite, amphibolite intrusions, and greenschists and actinolite-chlorite-greenschists), acid volcanic subseries (meta-rhyolites, quartz-feldspar porphyry, felsites, and quartz-chlorite schists) and sedimentary-volcanic subseries (meta-tuffaceous greywacke, quartzites and schistose conglomerate, and grit) (Kesse 1985). Rocks in area formed in the paleoproterozoic era between 2195 Ma and 2072 Ma (Oberthür et al. 1998; Attoh et al. 2006; Hirdes et al. 2007).

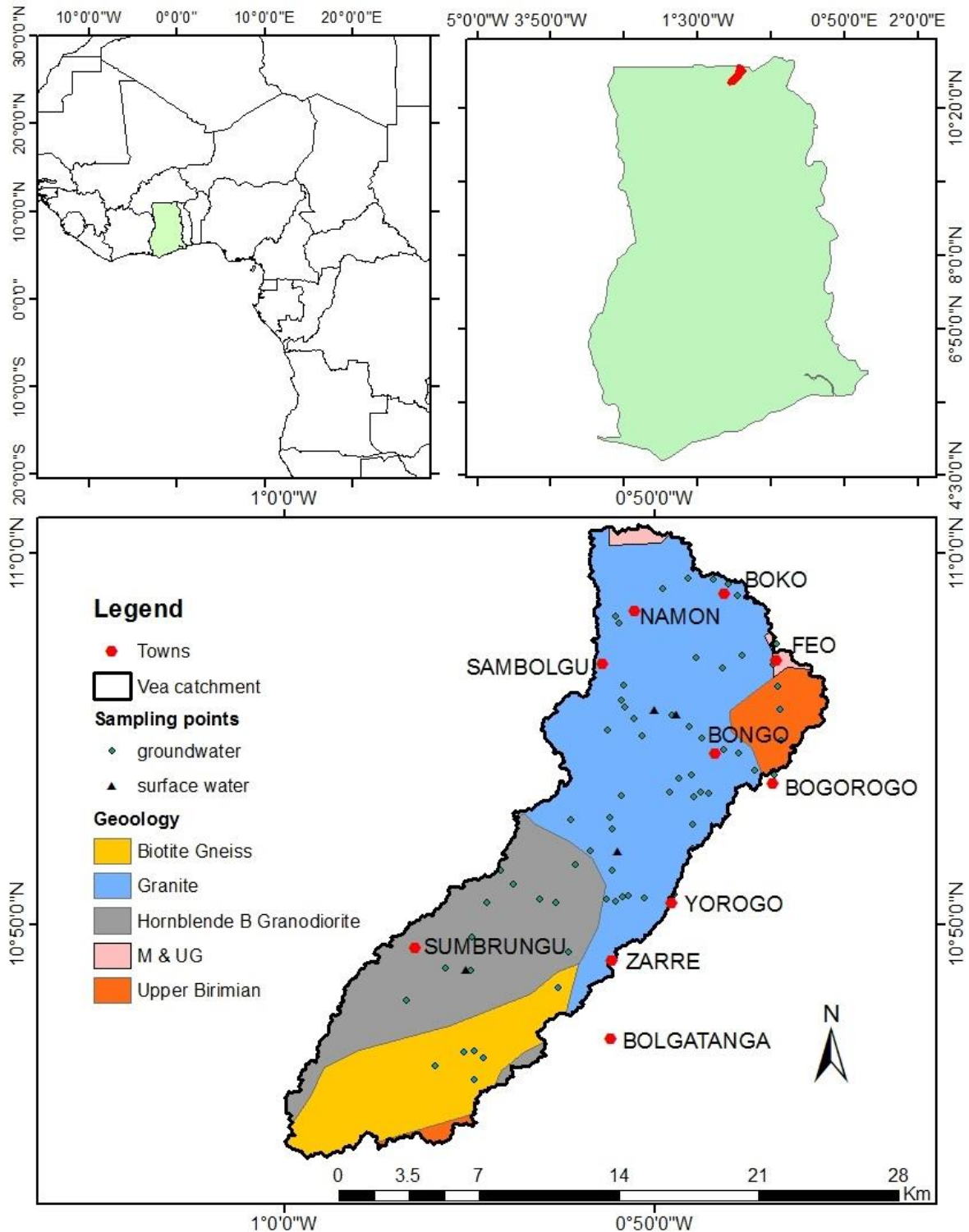


Figure 3-5: Location of Ghana in western Africa (upper left map), location of the Veia Catchment in Ghana (upper right map), and geology and water sampling points of the study area (lower map). M&UG: migmatite and undifferentiated granite.

3.2.9. Leaf area index data

LAI data with 1km resolution derived from MODIS land surface reflectance was downloaded from <ftp://ftp.glcg.umd.edu/glcg/GLASS/LAI/MODIS/1km/> (Liang and Xiao 2012). It was used as input of the WetSpass model.

3.3. Materials

The materials used in this study are:

- **Coolers containing ice blocks**, used to store the samples in order to keep the temperature of the samples low and constant.
- **Computer**, used to run all the models used in this study.
- **Multiparameter meter PELI 1520**, used to achieve *in situ* measurement of pH, electrical conductivity, temperature and salinity.
- **YSI ProODO[®]**, used to measure dissolved oxygen of surface water and groundwater in the field.
- **Dionex ion chromatography system**, used to analyse chloride in rain water and groundwater.
- **Containers for a water samples**, used to collect rainwater and groundwater samples from the field area to the laboratory for analysis (chapters 4 and 5).
- **Computer program Diagrammes - version 6.5** (Simler 2015), used to assess the results from the chemical analysis (chapter 4).
- **ArcGIS**, used to draw all the maps and to prepare the input data of the WetSpass model.
- **Excel spreadsheet**, used to prepare some input data for WetSpass model and the computer program Diagrammes the models, to draw some graphs and table.
- **Visual Basic Spreadsheet Macros**, used for Recession Curve Analysis (Posavec et al. 2006) and estimation of groundwater recharge (Posavec et al. 2009) (chapter 5).
- **Aquapak tool** (Nathan et al. 2007), a digital filter used to separate streamflow components (chapter 5).

- **EcohydRology** Fuka et al. (2013), a R package used to separate streamflow components (chapter 5).
- **R**, used to run the EcohydRology package (chapter 5).
- **MATLAB software**, used to run the statistical downscaling code (chapter 6).
- **WHAT** (Lim *et al.* 2005), online tool used to separate streamflow components (chapter 5).
- **GPS**, used to measure the geographical position of the data point.
- **WetSpass model**, used to simulate groundwater balance (chapter 6).
- **Rain water collectors**, used to collect rainwater for chloride analysis.
- **Water level meter**, this was used to measure the water level for boreholes and piezometers
- **Data loggers**, used to record groundwater level in the piezometers.

3.4. Methods

3.4.1. Hydrogeochemistry

For the hydrogeochemical study, 65 samples (61 groundwater samples and four surface water samples) were collected in different locations using pre-cleaned sterilized poly propylene plastic bottles with necessary precautions. In the field, the samples were stored in a cooler containing ice blocks in order to keep the temperature of the samples low and constant. At the laboratory, the samples were stored at 4 °C in a refrigerator for about a week before they were analyzed.

The results from the chemical analysis of water samples carried out in the laboratory were assessed using different methods to determine the water types and quality in the study area as well as the processes influencing the water chemistry. The assessment included determining: the ion balance; Sodium adsorption ratio (SAR); Total hardness; calcite, dolomite, anhydrite and aragonite saturation indices; and the use of a Piper diagram for inferring hydro-geochemical facies. This was carried out using the computer program Diagrammes - version 6.5 (Simler 2015). Table 3-2 gives an overview of the methods used to analyse the data.

Table 3-1: Instruments and methods used for the analysis

Parameter	Instruments and method used
pH	PELI 1520
Electrical conductivity	PELI 1520
Temperature	PELI 1520
Salinity	PELI 1520
Dissolved Oxygen	YSI ProODO [®]
Turbidity	Nephelometric Method
Colour (Apparent)	Visual Comparison Method
Total Suspended Solids	Gravimetric Method
Total Dissolved Solids	Gravimetric Method
Ammonia – nitrogen	Direct Nesslerization Method
Nitrate – nitrogen	Hydrazine Reduction Method
Phosphate – phosphorous	Stannous Chloride Method
Nitrite – nitrogen	Diazotization Method
Sulphate	Turbidimetric Method
Total Hardness	EDTA Titrimetric Method
Calcium	EDTA Titrimetric Method
Magnesium	Calculation Method
Chloride	Argentometric Method
Alkalinity	Strong Acid Titration Method
Total Iron	Atomic Absorption Spectrophotometer
Manganese	Atomic Absorption Spectrophotometer

Table 3-2: Methods used to analyse the data

Methods	References
Boxplot	Helsel and Hirsch (1992); Williamson et al. (1989)
stability diagrams	Pitkänen et al. (2004); Singaraja et al. (2014)
Saturation index	Lloyd and Heathcote (1985)
chloro-alkaline indices	Versluys (1916) ; Versluys (1931); Schoeller (1965)
weathering and ion exchange plots	Cerling et al. (1989); Fisher and Mullican (1997); Datta and Tyagi (1996)
Piper diagram	Piper (1944), Saka et al. (2013)
Gibbs diagram	Gibbs (1970); Kumar et al. (2014)
Sodium percentage and Wilcox diagrams	Wilcox and others (1948); Wilcox (1955)
Sodium adsorption ratio	Cobbina et al. (2012); Tomar et al. (2012)
Residual Sodium Carbonate	Aghazadeh et al. (2010); Yidana (2010)
Magnesium Hazard	Szabolcs and Darab (1964); (Singh et al. 2011)
Permeability index	Doneen (1964); Ishaku et al. (2011)

3.4.1.1. General Hydrogeology

Chloro-Alkaline indices

Along its path and its residence in the aquifer, groundwater interacts with rock which affects its quality (Zaidi et al. 2015). Versluys (1916), Versluys (1931) and Schoeller (1965) proposed ion exchange indices to better describe and understand these interactions. In this study, we used the

Chloro-Alkaline Indices (CAI-I and CAI-II) proposed by (Schoeller 1965) and depicted in Eq. 3-1 and Eq. 3-2 :

$$CAI - I = \frac{Cl - (Na + K)}{Cl} \text{ (meq/L)} \quad \text{Eq. 3-1}$$

$$CAI - II = \frac{Cl - (Na + K)}{SO_4 + HCO_3 + CO_3 + NO_3} \text{ (meq/L)} \quad \text{Eq. 3-2}$$

In the above equations, all the ion concentrations are expressed in meq/L.

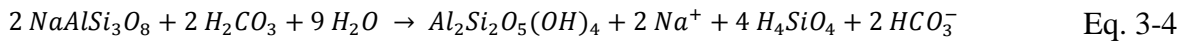
A positive CAI implies that Na^+ and K^+ ions of the water are replaced by Ca^{2+} and Mg^{2+} by contact with aquifer rocks or sediments, indicating reverse ion exchange. A negative CAI means that Ca^{2+} and Mg^{2+} of the water are exchanged against K^+ and Na^+ of surrounding formations (ion exchange). If CAI is equal to zero, it means there is equilibrium between the chemical composition of the water and that of the aquifer rocks, i.e. there is no exchange between water and rocks. In this study, the chloro-alkaline indices were analyzed only for groundwater samples.

Weathering process

The chemical composition of groundwater is mainly determined by the composition of the rock it is abstracted from, but other geochemical processes also play a key role in determining the amount of the chemical constituents in the groundwater (Razowska-Jaworek 2014). Weathering of rocks has been found to be one of the processes controlling the geochemical cycling of elements (Berg 1932). Middelburg et al. (1988) stated that the rate and nature of chemical weathering which vary widely are controlled by many variables, including parent-rock type, topography, climate and biological activity. In order to comprehend the weathering process taking place in the study area, different methods were used: a plot of $Ca^{2+} + Mg^{2+}$ versus $SO_4^{2-} + HCO_3^-$; the use of stability field diagrams of the partial system $MgO-Na_2O-Al_2O_3-SiO_2-H_2O$; determining the relationship between $Ca^{2+} + Mg^{2+}$ - $SO_4^{2-} + HCO_3^-$ and $Na^+ - Cl^-$; the use of a plot of

sodium vs. chloride; the use of the relationship between $Ca^{2+}+Mg^{2+} - SO_4^{2-}+HCO_3^-$ and Na^+-Cl^- , Ca^{2+}/Mg^{2+} ratio rock dissolution.

The plot of $Ca^{2+}+Mg^{2+}$ versus $SO_4^{2-}+HCO_3^-$ will be close to the $y=x$ line if the dissolution of calcite, dolomite and gypsum are the dominant reactions in a system. Ion exchange tends to shift the points to the right due to an excess of $SO_4^{2-}+HCO_3^-$ over $Ca^{2+}+Mg^{2+}$ whilst reverse ion exchange shifts the points to the left (Cerling et al. 1989; Fisher and Mullican 1997). In this scatter plot, the points above the equiline result from carbonate weathering (Eq. 3-3), whereas those below the equiline depict a silicate weathering (Eq. 3-4). Those along the equiline represent water whose chemistry results from both carbonate and silicate weathering (Datta and Tyagi, 1996).



(Albite)

(Kaolinite)

Saturation index

The saturation index (SI) defines the saturation state of minerals in the water. It can provide significant information on the various hydrogeochemical processes controlling the groundwater chemistry (Belkhiri et al. 2010; Kumar et al. 2015). Deutsch and Siegel (1997) stated that it is possible to predict the minerals that are responsible for controlling water quality from groundwater data without collecting the samples of the solid phase and analysing the mineralogy. When the $SI < 0$, the minerals will be dissolved and the water is said to be undersaturated with respect to the mineral. It may describe a short residence time or a lack of the considered mineral in the aquifer from which the water is discharging (Kortatsi 2006). On the other hand, when groundwater is supersaturated with respect to a mineral, the SI is > 0 , which means that the mineral will be precipitated. When SI is just equal to 0, it indicates that the water is saturated with respect to the mineral. However, due to uncertainty related to the minerals concentration, water with SI values comprised between -0.5 to 0.5 could be considered as saturated with respect to the mineral in question (Plummer et al. 1976). In this study, SI of calcite, dolomite, gypsum,

anhydrite and aragonite were calculated with Diagrammes software for groundwater samples using Eq. 3-5 (Lloyd and Heathcote, 1985):

$$SI = \log \left(\frac{IAP}{K_s(T)} \right) \quad \text{Eq. 3-5}$$

where IAP is the ion activity product of the solution, and $K_s(T)$ is the equilibrium constant of the reaction considered at temperature T.

The SI was determined in order to estimate the extent to which the groundwater has equilibrated with these minerals and also to investigate the thermodynamic controls on the composition of the water. It can help in determining the rocks in contact with the water during its movement.

The meteoric genesis index (MGI) (Eq. 3-6) that helps in determining whether groundwater source is of deep meteoric water aquifers ($MGI < 1$) or shallow meteoric water percolation type ($MGI > 1$) (Soltan 1998) was also calculated.

$$MGI = \frac{K^+ + Na^+ - Cl^-}{SO_4^{2-}} \quad \text{Eq. 3-6}$$

where elements are expressed in meq/L.

3.4.1.2. Drinking water quality

Assessment of the quality of water for drinking was based on the water quality guidelines of the World Health Organization -WHO (WHO, 2011) and the Ghana Water Standards - GWS (Ghana Standards Authority, 2013). The GWS was developed from the WHO guidelines. Table 4-2 (see page 68) only results regarding to TDS, turbidity, pH, Total Hardness, major ions are discussed in detail in this study. For the estimation of the means and standard deviations, parameter with values below detection limit were replaced by the detection limit value times 0.55 as suggested by Sanford et al. (1993).

TDS and turbidity

TDS is an indicator of the mineralisation of water. About 95 % of it is represented by major ions in natural water (Clark 2015). According to WHO (2011) the palatability of water with a TDS level of less than 600 mg/L is considered to be good and becomes significantly and increasingly unpalatable when TDS is greater than 1000 mg/L. Because of excessive scaling in water pipes,

heaters, boilers and household appliances, high levels of TDS may also be objectionable to consumers. However, no health-based guideline value regarding TDS has been proposed in the WHO guidelines.

Total Hardness (TH)

Total hardness accounts mainly for the magnesium and calcium contents naturally found in water. No health-based guideline value is proposed for hardness in drinking-water by WHO (2011). However, as hardness has an impact on water supply distribution systems, it is important to know the values. Usually, water with hardness above 200 mg/L tends to cause scale deposition in the treatment works, distribution system and pipework and tanks within buildings, depending on the interaction of other factors, such as pH and alkalinity. Water with a hardness of less than 100 mg/L (soft water) may have more corrosive effects for water pipes (Sawyer and McCarty 1967; WHO 2011).

Major ions

To facilitate interpretation of water chemistry data many hydrochemical diagrams are used. The Piper diagram, a trilinear diagram, aiming to describe water chemistry was first designed by (Hill 1940) and refined by (Piper 1944). In the Piper diagram, major ions are first grouped into anion and cations and the percentage of each ion based in the total milliequivalent of its group is calculated. Then, the ions are plotted in the two base triangles as cation and anions. Finally, the respective cation and anion locations for a sample are projected into the diamond field, which represents the total ion relationship and determined the water type. This method is not very convenient when plotting a large volume of data (Chadha 1999). A new diagram introduced by (Durov 1948) and developed by Burdon and Mazloun (1958) and Lloyd and Heathcote (1985) is also used. Some of the shortcomings of the trilinear diagrams of the type developed by Hill and Piper are removed in the diagram developed by Durov (1948), but, like the Piper diagram, suitable and free software are not common.

The Piper diagram was used in this study as samples are clearly plotted, allowing a clear distinction of the water types. It was done by using “Diagram”, a friendly and free software designed by (Simler 2015). Major ions play also a key role in the water quality study as they are the most abundant chemical ions in the water. Ions commonly considered in this group are Ca^{2+} , Mg^{2+} , Na^+ , K^+ , HCO_3^- , Cl^- , SO_4^{2-} , NO_3^- . The assessment of the water quality based on these ions

was done by comparing the contents of these ions to those of the guideline mentioned at the beginning of this section namely the WHO water quality guideline (WHO, 2011) and the Ghana Water Standard (GSA 2013).

3.4.1.3. Usability of the water for irrigation

Irrigation water can induce some hydrochemical changes by the presence of high concentrations of a particular salt or due to the presence of toxic constituents in groundwater (Alam 2014). These changes can lead to adverse impacts on plants and crop growth. Sodium is well known as one of the groundwater constituents that impair the groundwater quality for irrigation purposes. Karanth (1987) found that the Na percentage exceeding more than 50% of the total cations present in groundwater leads to reverse ion exchange reactions, causing deflocculation and reducing the fertility and permeability of the soils. But this reverse ion exchange issue is reduced if the amount of calcium plus magnesium is higher than the sodium. Therefore, the concentration of constituents in irrigation water can have a harmful effect on soil, plant growth and yield (Rusan et al. 2007).

Sodium percentage, Sodium Adsorption Ratio (SAR) and Residual Sodium Carbonate (RSC) are widely used to determine the suitability of water for irrigation purposes. In this study, the Sodium Adsorption Ratio (SAR), Sodium percentage, the Residual Sodium Carbonate (RSC), Magnesium Hazard (MH) and the permeability index were calculated to determine the usability of the water for irrigation.

Sodium Adsorption Ratio (SAR)

The SAR as described in Eq. 3-7 is used to determine whether the sodium content in the irrigation water will trigger reverse ion exchange or not. The higher the SAR, the less suitable the water for irrigation. In fact, irrigation water with excess sodium can significantly reduce crop productivity by affecting soil structure, soil aeration, flow rate, permeability, infiltration etc (Cobbina et al. 2012).

$$SAR = \frac{Na}{\sqrt{\frac{Ca+Mg}{2}}} \quad (\text{meq/L}) \quad \text{Eq. 3-7}$$

where elements are expressed in meq/L.

Sodium percentage

Sodium content is also expressed in terms of percentage sodium calculated using Eq. 3-8 (Wilcox 1955).

$$Na\% = \frac{(Na+K) \times 100}{Ca+Mg+Na+K} \quad (\text{meq/L}) \quad \text{Eq. 3-8}$$

The different classes of water based on sodium percentage are summarized in Table 3-3.

Table 3-3: Classification of irrigation water quality based on Na%

Range	Categories
<20	Excellent
20-40	Good
40-60	Permissible
60-80	Doubtful
>80	Unsuitable

The plot of sodium percentage with respect to EC in the Wilcox diagram is also used in rating irrigation water quality. In this study, this diagram was used.

Residual Sodium Carbonate (RSC)

The RSC index, firstly proposed by Eaton et al. (1935), determines the hazardous effect of carbonate and bicarbonate on the quality of water for agricultural purpose (Aghazadeh et al. 2010). RSC is the difference between the bicarbonate ions and those of calcium and magnesium and it is expressed in meq/L as shown by Eq. 3-9. When the RSC value is lower than 1.25 meq/L, the water is considered to be of good quality, while if the RSC value exceeds 2.5 meq/L, the water is considered harmful. When RSC is between 1.25 and 2.5 meq/L the water is termed marginal and it could be used with precautions such as good irrigation management techniques and soil salinity monitored by laboratory analysis (Richards 1954).

$$RSC = (HCO_3^- + CO_3^{2-}) - (Ca^{2+} + Mg^{2+}) \quad (\text{meq/L}) \quad \text{Eq. 3-9}$$

The use of RSC requires the content of HCO_3^- , CO_3^{2-} , Ca^{2+} , and Mg^{2+} . In this study, the content of CO_3 was not analysed but because the pH of the samples ranges from 6.83 to 8.5, CO_3 content is negligible compared with HCO_3^- (Chapman 1996), so $\text{HCO}_3^- + \text{CO}_3^{2-} = \text{HCO}_3^-$.

Magnesium Hazard

The residual Mg/Ca ratio (Nazzal et al. 2014) and the method established by (Szabolcs and Darab 1964) can be used to estimate the magnesium hazard (MH) for irrigation. In this study, we used the latter which is depicted in Eq. 3-10:

$$MH = \frac{Mg}{Mg+Ca} \times 100 \text{ (meq/L)} \quad \text{Eq. 3-10}$$

Permeability index

Because the permeability of soil is influenced by sodium, calcium, and magnesium and bicarbonate contents in soil as well as by long-term use of irrigation water, (Doneen 1964) established a permeability index, used as an irrigation water quality indicator, following formula of Eq. 3-11. In this study, the suitability of groundwater for irrigation based on PI indicator was determined. This criterion categorized water in three classes. Class I and Class II are categorized as good for irrigation, while Class III water is unsuitable for irrigation.

$$PI = \frac{Na + \sqrt{HCO_3}}{Ca + Mg + Na} \text{ (meq/L)} \quad \text{Eq. 3-11}$$

3.4.1.4. Statistical analyses

Analysis, interpretation and representation of results of a large number data are prone to difficulties that need to be solved. To that end some statistical methods such as multivariate methods are used. Among them, the Principal Component Analysis (PCA) and the Agglomerative Hierarchical Clustering (AHC) found to be useful in environmental studies in general and particularly in hydrogeochemical studies have been used widely (Kim et al. 2005;

Belkhiry et al. 2010; Fan et al. 2010). In this study both methods were implemented to identify processes controlling groundwater geochemistry and to classify groundwater samples of the study area.

The original dataset subject to the analyses consist of 61 groundwater samples (the five surface water samples were not considered for the statistical analysis) and 22 parameters. But before applying the multivariate methods to the dataset, certain parameters were excluded due to diverse reasons. It concerns parameters with additive characteristics such as total hardness (TH), alkalinity, TDS, salinity; parameters with an elevated number of samples below the detection limit such as Mn^+ , NH_4^+ , NO_2^- , TSS; SO_4^{2-} and parameters that show small regional variation such as temperature. Sample bongo 3 was also excluded from the analysis as its TDS is well above the other samples. Finally, the statistical analyses were applied to a hydrogeochemical dataset that consists of 60 groundwater samples and 13 parameters. These parameters include salinity (sal), EC, TDS, DO, Color (Col), Ca^{2+} , Mg^{2+} , Na^+ , K^+ , HCO_3^- , Cl^- , PO_4^{3-} , Fe_{tot} , Nitrate and pH. Before starting a normality test was done and variable that did not follow a normal distribution were log-transformed and standardized to avoid misclassifications related to the different orders of magnitude of both parameter value and the variance of the parameters being analysed and though leading to faulty interpretations (Güler and Thyne 2004; Yidana 2010).

Principal component analysis

Principal component analysis is a technique that identifies patterns in data and then presents them based on their similarities and differences. Mainly, it aims at summarizing a multivariate dataset by reducing the statistical noise in the data, exposing the outlier, and then arranging the components in descending order as accurately as possible with as few principal components (PCs) as possible. These principal components which form a new set of variables are linear combination of the original variables and they are uncorrelated with one another (Helsel and Hirsch 1992; Pitkänen et al. 2004). The first component which always explains the largest variance contains the most obvious information of the data matrix. There are no right criteria in the choice of PCs to be included; however, there are some very good guidelines. Reyment and Jvreskog (1996) and Joreskog et al. (1976) suggested that a useful principal component analysis should explain at least 75% and as high as 99% of variances of the original variables. Other criteria are that, each PC should have eigenvalues greater than one (Kaiser 1960). In other

words, PCs containing a greater variance than the original standardized variables are kept (Davis 1986). In fact, each variable of the original dataset contributes to a variance of 1. So, a factor that accounts for a variance less than 1 explains less information than every single variable of the original. As the aim of the PCA is to reduce the number of variables to allow an easy interpretation, these factors with variance less than 1 could not be retained. The next step is the rotation of the remaining principal axes in order to maximize the variance on the new axes. The method used was the Varimax normalized rotation that has been widely used (e.g. Helena et al. 2000; Cloutier et al. 2008; Mustapha and Aris 2012; Kura et al. 2013) and recommended by Kaiser (1960). This method moves each axes to positions such that projections from each variable onto the axes are either near the extremities or near the origin allowing the selected factors (or PCs) to explain approximately the same amount of information as do the much larger set of original observations (Davis 1986; Shrestha and Kazama 2007). Prior to the PCs selection, Pearson correlation matrix was used to determine the relationship between variables. The correlation coefficients were classified (Table 3-4) based on Guildford’s rule of thumb for interpreting the Pearson product moment correlation (Guilford 1942).

Table 3-4: Guildford’s rule of thumb for interpreting correlation coefficient

r-value	Interpretation
0.00 to 0.29	Negligible or little correlation
0.30 to 0.49	Low correlation
0.50 to 0.69	Moderate or marked correlation
0.70 to 0.89	High correlation
0.90 to 1.00	Very high correlation

Before starting the Principal Component Analysis, it was ensured that the variables follow a normal distribution as this analysis assumes normality of the dataset. Any variable that did not follow a normal distribution was log-transformed and standardized. This was followed by a test to verify the existence of any significant correlation between variables in the data set that

necessitated a Principal Component analysis. In this study the Bartlett's sphericity test and Kaiser-Mayer-Olkin (KMO) measure of sampling adequacy were used. The Bartlett's sphericity test gives an indication of the appropriateness to continuing with PCA. The Bartlett's Test measure indicates if there is correlation between variables in a dataset that can be analysed. With regard to the KMO, a PCA is performed only if the KMO value is greater or equal to 0.5 (Mustapha and Aris 2012).

Hierarchical Cluster Analysis (HCA)

The cluster analysis is a statistical method that classifies samples or variables into a group based on their similarity to each other and their dissimilarity to other groups (Kura et al. 2013). The HCA is one of the most cluster methods used in the hydrogeochemical data classification. It has been widely used in diverse environmental conditions and at different scales (e.g. Cloutier et al. 2008; Loh et al. 2012; Kura et al. 2013; Damtew 2015). Cloutier et al. (2008) used the HCA to identify groundwater recharge sources and the importance of the geological formations on minor and trace elements in the Paleozoic Basses-Laurentides sedimentary rock aquifer system in Quebec. This method was also found to be a useful tool in determining the spatial groundwater salinity groups in south-eastern Ghana (Yidana 2010).

For this work, the Euclidean distance was chosen as the distance measure, or similarity measurement, between sampling sites.

3.4.1.5. Stable isotope $\delta^2\text{H}$ and $\delta^{18}\text{O}$ in groundwater and surface water in the study area

Isotopes are atoms of the same element that have different numbers of neutrons. They can be classified into two main groups, namely stable isotope and unstable isotope (Hoefs 2009). Isotopes have been successfully used to study the history of the climate (e.g. Dansgaard et al. 1993; Edwards 1993; MacDonald and Edwards 1993; Linsley 1996). They have been found to be a useful tool on studying evaporation rate over both water body and land surface. Furthermore, studies have shown the usefulness of isotopes in groundwater management and especially in groundwater dating, recharge sources and recharge process. The most common way of analysing data of $\delta^2\text{H}$ and $\delta^{18}\text{O}$ of groundwater is to plot $\delta^2\text{H}$ with respect to $\delta^{18}\text{O}$ and compare this plot with both WMWL and LMWL. Plots below this line denote a recharge from evaporated meteoric water. This method helps in determining groundwater sources and recharge

process governing groundwater chemistry. The notation δ expressed as follow is used in this work (Eq. 3-12) :

$$\delta = \left(\frac{R_{sample} - R_{stand}}{R_{stand}} \right) * 1000 \quad \text{Eq. 3-12}$$

where R_{sample} stands for the isotopic ratio of the sample, and R_{stand} is the isotopic ratio of the standard VSMOW (Vienna Standard Mean Ocean Water) (Gonfiantini 1978). Positive value means that the sample to be enriched in the heavy isotope species, while negative value denotes depletion in the heavy isotope species relative to the standard.

In order to understand the recharge origin and process in the study area isotope content in surface and groundwater was analysed. 61 samples (56 groundwater samples and 5 surface water samples) were analysed for $\delta^{18}\text{O}$ and $\delta^2\text{H}$. Determination of oxygen ($^{18}\text{O}/^{16}\text{O}$) and deuterium ($^2\text{H}/^1\text{H}$) from water samples was performed by laser adsorption (PICARRO L2130-i $\delta\text{D}/\delta^{18}\text{O}$ Ultra High-Precision). Per sample, 10 individual measurements were calibrated by international standards (SLAP, SMOW, GISP) and evaluated for potential effects on drift- and memory. General analytical uncertainties related to the worldwide isotope VSMOV-standard (Vienna Standard Mean Ocean Water) are about $\pm 0,1\%$ and $\pm 0,3\%$ for $\delta^{18}\text{O}$ and $\delta^2\text{H}$, respectively. For the interpretation of the results the samples were plotted in the graph $\delta^2\text{H}$ with respect to $\delta^{18}\text{O}$. The Global Meteoric Water Line (GMWL, $\delta^2\text{H} = 8 \delta^{18}\text{O} + 10$) found by Craig (1961) was used as reference because lack of isotope data of rain fall. However, for comparison the LMWL based on the finding of Martin (2006) was drawn. Groundwater samples were classified into two groups based on the altitude. Altitudes lower than 200 m were considered as low while those higher than or equal to 200 m were considered as high.

3.4.2. Estimation of groundwater recharge in the Sissili Basin using streamflow hydrograph analysis

Streamflow can be separated into two main components, namely, direct flow and baseflow. Such separation is good for planning and management of water resources (Aksoy et al. 2008).

Separation of baseflow from direct flow has been used to assess groundwater recharge and discharge, flood assessment, contaminant generation study (Merritt et al. 2003), assessments of groundwater recharge and discharge (Arnold et al. 2000; Lee et al. 2006; Gebert et al. 2007), flood hydrograph analysis (Graszkiewicz et al. 2011), and land use and climate changes on water resources (Cooper et al. 1995; Dams et al. 2008).

Baseflow is the withdrawal of groundwater after the end of groundwater recharge. Many expressions have been used to define baseflow based on the purpose of use. Some common expressions used are groundwater flow, low flow, percolation flow, under-run, seepage flow, and sustained flow (Hall 1968). Hall (1968) defined it as the component of flow originating from groundwater storage or other delayed source. It is also defined as groundwater recession or groundwater discharge (Meyboom 1961). Similar to most of the water balance components, baseflow depends on the catchment characteristics such as land use and land cover, geology, soil, topography, climate, and temperature (Wittenberg 2006; Price 2011). Singh (1968) emphasized that it is also time and spatial dependent. Sometime, it is assumed to be equal to groundwater recharge (Cherkauer and Ansari 2005). This approximation is feasible in area where underflow, evapotranspiration from riparian vegetation, and other losses of ground water from the watershed can be neglected (Risser et al. 2005) and it is based on two main assumptions. The first one is that, baseflow equals groundwater discharge and the second is that groundwater discharge is approximately equal to recharge. Because baseflow is less than the actual amount of water that recharges the aquifer, terms such as “effective recharge” (Daniel 1996), “base recharge” (Szilagyi et al. 2003), or “observable recharge” (Holtschlag 1997) have been used to refer to this approximated recharge. Baseflow has shown to be a good parameter in calibrating and validating hydrological model (e.g. Ferket et al. 2010). However, estimating baseflow can be difficult. Several techniques have been designed to study the baseflow recession. These techniques use different approaches some of which are manual, automated, and chemical or field based (Meyboom 1961; Arnold and Allen 1999; Burns 2002; Lim et al. 2005; Aksoy et al. 2008). Each technique has certain advantages and drawbacks that depend on the characteristics of the catchment. Chemical approaches offer the most effective means of estimating baseflow but are expensive. The manual methods used as an alternative approach to estimate baseflow are time consuming (Sinclair and Pitz 1999) and can lead to inconsistent results. The automated methods are based on mathematical equations, less time consuming, and are useful in comparing baseflow

of different catchments. The recent past two decades have witnessed a tremendous development and use of these methods. One of the challenges related to the use of filters to separate baseflow is the definition of the filter's parameters values which put uncertainty on the separated baseflow. The number of these filter's parameters ranges from one to five. To validate the separated baseflow, the best practice is to compare the results of the filtered baseflow with those estimated by field measurement such as tracer or geochemistry or groundwater levels (e.g. Gonzales et al. 2009; Stewart 2015) that are somehow time consuming and costly. According to Su et al. (2016), validation of baseflow determined using baseflow filters are rarely done as they are limited by data scarcity in many catchments and they are also subjected to uncertainties due to complexity of hill slope hydrochemistry and spatial heterogeneity. Although one can decide to collect tracer data or groundwater level data to validate present-time baseflow estimated by filter methods, it is not possible to validate past baseflow when the required data was not already collected. Further, there is no option to validate past baseflow estimated by filter methods with new geochemistry or groundwater data that was not collected in the past. In fact, baseflow recession changes over time (Bart and Hope 2014; Thomas et al. 2015), implying that present-time baseflow recession characteristics may differ from those of the past. In this regard, many alternative solutions have been proposed. Furey and Gupta (2001) proposed two criteria to evaluate the performance of a baseflow filter. But these criteria are relevant for filters that are applied without any constraints, allowing baseflow to exceed total streamflow or to be negative.

3.4.2.1. Recharge estimation using hydrograph recession analysis

Recession analysis

A Visual Basic Spreadsheet Macro for Recession Curve Analysis designed by Posavec et al. (2006) was used to find recession period in the streamflow dataset. A detail description of the spreadsheet can be found in the aforementioned publication. This program uses the matching strip method and offers five regression models thus more advantageous when compared to the other methods that use the well-known and widely used exponential equation. The five models available in the spreadsheet are: linear ($y = ax + b$), logarithmic ($y = a \ln(x) + b$), second-order polynomial ($x = ay^2 + by + c$), power ($y = bx^a$), and exponential ($y = be^{ax}$). Where y represents discharge and x represents time.

After using the five models to analyse the recession, the model that gave the highest coefficient of determination (R^2) was retained as the most appropriate and the resulting Master Recession Curve (MRC) of that model was selected as the best for describing the recession of the baseflow in the catchment.

Recharge estimation

The groundwater recharge was estimated based on an adapted Meyboom's method implemented in a visual basic spreadsheet macro designed by Posavec et al. (2009). The use of the program requires streamflow data that defines recession periods preceding (recession 1) and following (recession 2) groundwater recharge. The program fits exponential regression model available in Microsoft Excel to baseflow recessions 1 and 2, and uses regression equations to calculate recharge volume that occur between these recessions. Recession periods provided for the estimation of recharge are those determined by the recession analysis. The program uses a step by step approach to estimate individual recharge amounts for different recharge periods. For instance, if there are n recharge periods the program has to be run n times. Details of the spreadsheet can be found in Posavec et al. (2009).

3.4.2.2. Baseflow separation

AdUKIH method

The AdUKIH is a smoothed minima baseflow separation tool for perennial and intermittent stream designed by Aksoy *et al.*(2008). It is a generalized version of the very known and widely used smoothed minima baseflow separation method developed by the United Kingdom Institute of Hydrology that separates baseflow for perennial stream only (Institute of Hydrology 1980). In arid and semi-arid environment such as Northern Ghana, baseflow originate mainly from groundwater discharge.

The AdUKIH method described by Aksoy *et al.* (2008) can be summarized as follow:

- Divide the daily flow data into non-overlapping blocks of n days.
- Mark the minima of each of these blocks, and call them Q_1, Q_2, \dots, Q_i and consider them in turns of three (Q_1, Q_2, Q_3), (Q_2, Q_3, Q_4, \dots), (Q_{i-1}, Q_i, Q_{i+1}). Let us consider Eq. 3-13 and Eq. 3-14:

$$0.9Q_i \leq \min(Q_{i-1}, Q_{i+1}) \quad \text{Eq. 3-13}$$

$$0.9Q_i < \min(Q_{i-1}, Q_{i+1}) \quad \text{Eq. 3-14}$$

Eq. 3-13 is used in case of intermittent stream whereas Eq. 3-14 is used for perennial stream. In each case, if the corresponding condition is verified then the central value is a turning point for the baseflow line. Continue this procedure until the whole time series has been analysed.

- Join the turning points by straight lines to form the baseflow hydrograph. If, on any day, the baseflow estimated by this line exceeds the total flow on that day, the baseflow is set equal to the total flow.
- Estimate the volume of water generated by baseflow beneath the baseflow hydrograph (V_{base}) between the first and last turning points. The volume is found by summing the individual trapezium areas, i.e. by multiplying the time between turning points by the average discharge of the turning points.
- Estimate the volume of water beneath the recorded hydrograph (V_{total}) between the first and last turning points. The volume is calculated by summing the average daily flow values between the first and the last turning points.
- The baseflow index (BFI) is then $V_{\text{base}}/V_{\text{total}}$.

A schematic representation of the procedure for estimating the baseflow with the AdUKIH code is presented in Figure 3-6.

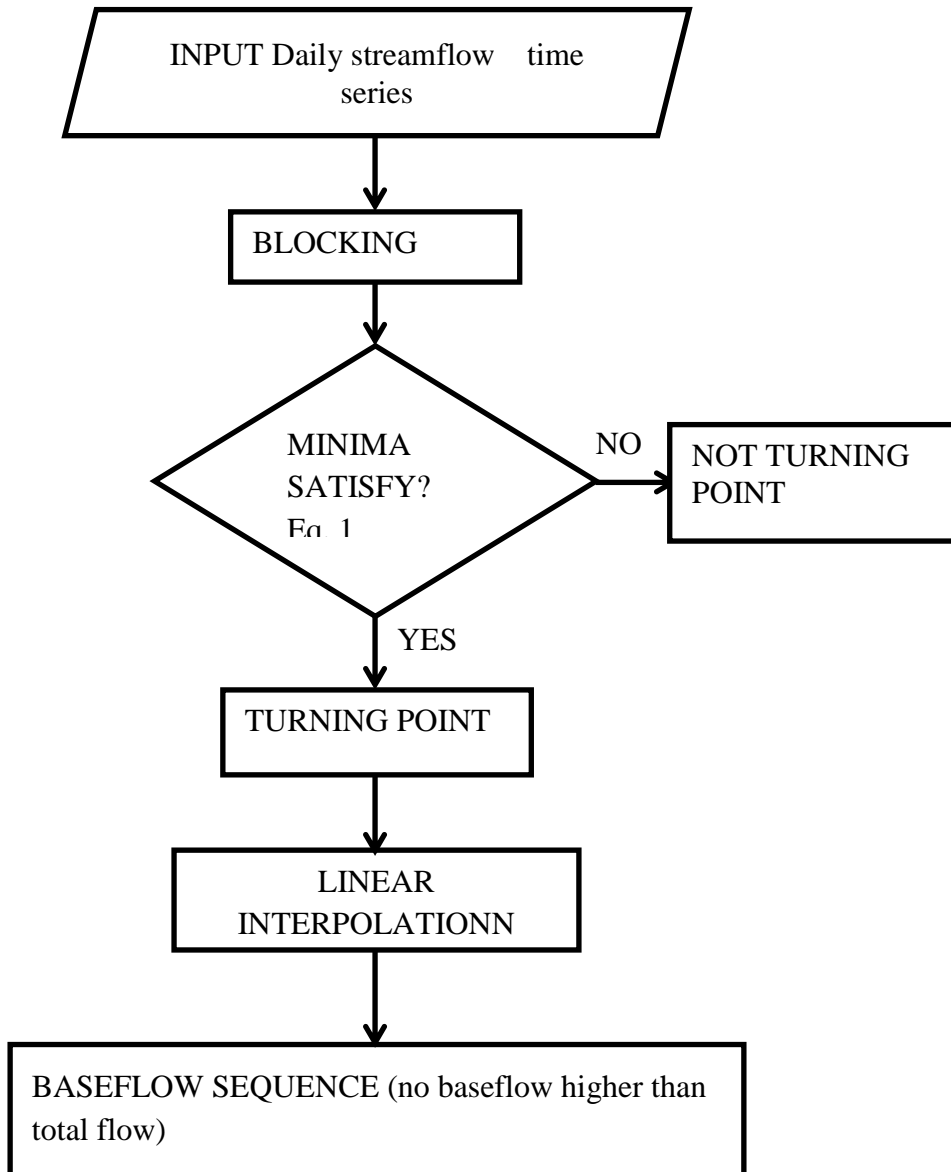


Figure 3-6: Flow chart of the AdUKIH computer code for baseflow separation (Aksoy et al. 2008)

WHAT and Aquapak tools

WHAT is an acronym of Web-based Hydrograph Analysis Tool developed by Lim *et al.*(2005) to separate hydrograph components using 3 methods, namely: BFLOW, Eckhardt digital filters, and local minimum method. It has been used in many studies (Lim et al. 2005, 2010, Lee et al. 2014a, b). A statistical component has been incorporated to give useful information for flow frequency analysis and time series analysis.

The BFLOW is the digital filter method firstly introduced by Lyne and Hollick (1979) and it has been used in several studies (e.g., Lyne and Hollick 1979; Nathan and McMahon 1990; Arnold and Allen 1999; Lee et al. 2014a; Singh et al. 2015). This method is presented in presented in Eq. 3-15. As for the Eckhardt (Eckhardt 2005) digital filter presented in Eq. 3-16, it is a general form of a digital filter based on digital filter parameter and maximum value of long term ratio of baseflow to total streamflow (BFI_{max}).

$$q_t = \alpha \times q_{t-1} + \frac{(1 + \alpha)}{2} \times (Q_t - Q_{t-1}) \quad \text{Eq. 3-15}$$

$$b_t = \frac{(1 - BFI_{max}) \times \alpha + b_{t-1} + (1 - \alpha) \times BFI_{max} \times Q_t}{1 - \alpha \times BFI_{max}} \quad \text{Eq. 3-16}$$

where b_t is the filtered baseflow at the t time step;

b_{t-1} is the filtered baseflow at the t-1 time step;

BFI_{max} is the maximum value of long term ratio of baseflow to total streamflow;

α is the filter parameter;

and Q_t is the total streamflow at the time step t .

Compared with previous digital filters, BFI_{max} is the new variable added by Eckhardt (2005). To reduce the subjective influence of using BFI_{max} on baseflow separation, representative BFI_{max} values were estimated for different hydrological and hydrogeological situations by comparing the baseflow from conventional separation methods with those of the Eckhardt digital filter method. Eckhardt (2005) proposed the use of BFI_{max} values of 0.80 for perennial streams with porous aquifers, 0.50 for ephemeral streams with porous aquifers, and 0.25 for perennial streams with hard rock aquifers.

The Aquapak tool designed by Nathan et al. (2007) is a digital filter uses the same Lyne and Hollick (1979) method used by BFLOW and presented earlier in Eq. 3-15.

EcohydRology baseflow filter

The EcohydRology is a R package designed by Fuka et al. (2013). The baseflow function allows separation of baseflow from stream flow data series. It is based on the recursive digital filter of Lyne and Hollick (1979). It requires a 1 column data frame with number of rows equal to the

length of the streamflow data series and return a 2 column data frame in which the first column contains baseflow, while the second contains quickflow, both in the same units as the input. As the tool is flexible, to perform the baseflow separation one has to specify values of the filter parameter and the number of passes which is the number of times one wants the filter to pass over the data.

For this work, a filter parameter of 0.925 was used based on the suggestion of Nathan and McMahon (1990). As the time step of the stream flow data is daily, a pass value of 3 was used as recommended in many baseflow separation studies (e.g. Ladson et al. 2013).

Efficiency test

In sciences and especially in hydrological science, the results of models are often evaluated to get an indication of the performance or efficiency of the model in mimicking local conditions. The Nash–Sutcliffe model efficiency coefficient-NSE designed by Nash and Sutcliffe (1970) has been found to be a good efficiency indicator. In this study, a modified form of NSE criterion (Eq. 3-17) was used to identify the method that best separates baseflow from the streamflow in the study area. As measured baseflow data was not available for the study area, two approaches were used in the efficiency analysis. The first one consisted of comparing separated baseflow with streamflow during dry season in which all the streamflow is mainly (or exclusively) composed of baseflow. The second approach is the comparison of separated baseflow against flow during period identified as recession period by the recession analysis tool (Posavec et al. 2006).

$$\mathbf{Modified\ NSE} = \mathbf{1} - \frac{\sum_{t=1}^T (q_t - bf_t)^2}{\sum_{t=1}^T (q_t - q_0)^2} \quad \text{Eq. 3-17}$$

q_t : observed flow during recession period

q_0 = mean of observed flow during recession period

bf = filtered baseflow

The NSE can range from $-\infty$ to 1. An NSE of 1 means that the model outputs match perfectly the observed data, while, an NSE of 0 indicates that the model predictions are as accurate as the mean of the observed data. A negative efficiency suggests that the mean of the observed data is a better predictor than the model. In that case, the residual variance (the numerator in the expression above), is larger than the data variance (the denominator) and the results are described as unacceptable (Moriasi et al. 2007). The NSE is sensitive to extreme values and large outliers in the dataset can cause a sub-optimal result.

Flashiness index

Baker et al. (2004) highlighted that the term “flashy”, in the context of streamflow, does not have a set of definition while it is applied to a set of characteristics. However, they stated that the flashiness describes how fast and frequent a streamflow changes in short time. "Flashy" streams have rapid rates of change whereas "stable" streams have slow rates of change (Poff et al. 1997). The flashiness index has been used in various studies. It has been used by several authors in determining the streamflow regime and the impact of land use/cover change on the hydrological cycle (e.g., Baker et al. 2004; Dow 2007)). Using data from 30 study watersheds, Deelstra et al. (2014) found a good correlation coefficient of 0.67 between BFI and FI; and FI decreases when BFI increases, suggesting that a smaller BFI corresponds to a greater value of FI and vice versa. It is a useful tool in analysing the impact of land use change on hydrological. The new flashiness index (FI) designed by Baker et al. (2004) and depicted Eq. 3-18 was used. Compared to several flow regime indices it has lower interannual variability (Baker et al. 2004).

$$\mathbf{R - B Index} = \frac{\sum_{i=1}^n 0.5(|q_{i+1}-q_i|+|q_i-q_{i-1}|)}{\sum_{i=1}^n q_i} \quad \text{Eq. 3-18}$$

Where q_i is daily flow at time step i , while q_{i-1} and q_{i+1} are flows of time steps preceding and following this time step, respectively.

The FI index has a dimensionless value and it ranges from 0 to 2 (maximum theoretical value). A value of FI equal to 0 means no change in discharge over the considered period.

3.4.3. Estimation of groundwater recharge using Water Table Fluctuation method.

The water table fluctuation (WTF) method estimates actual recharge, which is more reliable, compared to the potential recharge given by other methods. This method has been widely used to estimate groundwater recharge over a wide range of climates (Hall and Risser 1993; Healy and Cook 2002; Scanlon et al. 2002). In the Volta basin it has been used by some authors (Martin 2006; Sandwidi 2007; Obuobie 2008; Yidana et al. 2016). The value of specific yield and data of continuous change in groundwater level are the prerequisites of the use of the WTF method (Healy and Cook 2002). The WTF should work best for wells in areas with shallow unconfined aquifers that show a relatively rapid water-level rise in relation to the rate that water moves away from the water table (Scanlon et al. 2002; USGS 2013).

There are no assumptions underlying this method regarding movement of water through the unsaturated zone and, therefore, the presence of preferential flow paths in an area does not restrict its use. The WTF method can be used in studies covering a few square meters as well as in those covering hundreds or thousands of square meters. It can also be used to calculate net change in saturated-zone storage over any time interval (e.g. days, months, or years). The assumption of the WTF is that the rise of groundwater table is mainly due to groundwater recharge from rainfall (Crosbie et al. 2005). Therefore, all other components of the groundwater budget are neglected. This approach is a gross simplification of a very complex phenomenon, namely, movement of water to and from the water table (Healy & Cook, 2002; Scanlon et al., 2002). The groundwater recharge rate (R) can be estimated by applying this mathematical equation:

$$R = S_y \times \frac{dh}{dt} \approx S_y \times \frac{\Delta H}{\Delta t} \quad \text{Eq. 3-19}$$

Where S_y is specific yield of the groundwater aquifer material, h is the height of the water table and t is time (Healy and Cook 2002).

Application of the method WTF involves two steps: (1) estimating the water-level rise $DH(t_j)$ and (2) Estimating specific yield S_y . According to Meinzer (1923), “The specific yield (S_y) of a rock or soil, with respect to water, is the ratio of the volume of water which, after being saturated, it will yield by gravity to its own volume”.

Although there are many methods in estimating the specific yield, this estimation is not an easy task. A detail presentation of methods used to determine the specific yield was done by Johnson

(1967). These methods are classified into field and laboratory methods. The specific yield value can be calculated from the porosity and specific retention as below (Healy and Cook, 2002):

$$S_y = f - S_r \quad \text{Eq. 3-20}$$

Where f is porosity and S_r is specific retention (the volume of water retained by the rock per unit volume of rock).

Specific yield is treated as a storage term, independent of time that in theory accounts for the instantaneous release of water from storage. In reality, the release of water is not instantaneous. Rather, the release can take an exceptionally long time, especially for fine-grained sediments. Childs (1960) pointed out that S_y is not constant but varies as a function of depth to the water table.

For this work, specific yield of two wells at Aniabisi (AN-M and AN-D) was estimated by the method of sample saturation and drainage. This method consists of draining columns of saturated materials by gravity and determining both the volume of material drained and the volume of water yielded. The specific yield is then estimated by dividing the volume of water yield by the volume of the saturated material. For other wells, the specific yield was determined based on the study of Sinha and Sharma (1988) (Appendix 3). Their work proposes a range of specific yield for different aquifer material. For granite material the range of 0.02 to 0.04 was suggested. For this current work the mean value (i.e. 0.03) was used. The estimation of the variation of groundwater level (DH) was done manually as presented in Figure 3-7.

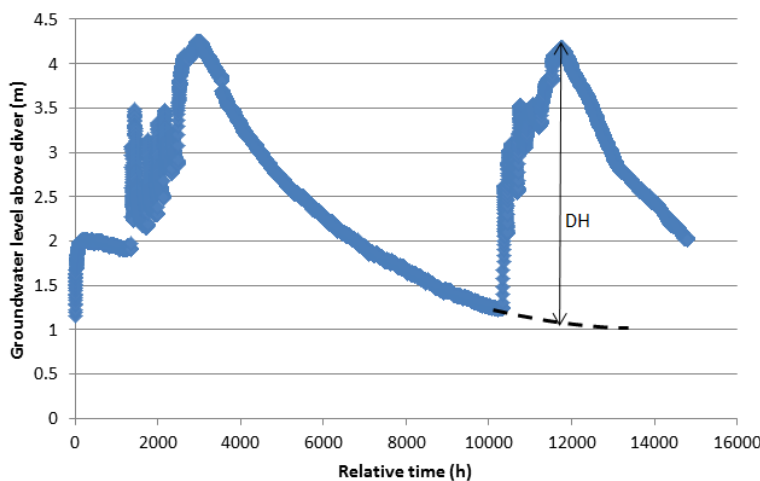


Figure 3-7: Estimation of groundwater level rise using hypothetical data

3.4.4. Estimation of groundwater recharge using Chloride Mass Balance method

The chloride mass balance (CMB) method has been used widely for recharge estimation especially in semi-arid and arid regions. It is easy to apply and inexpensive (Sumioka and Bauer 2003; Martin 2006; USGS 2013).

There are two approaches of the CMB method. The first CMB approach estimates recharge based on chloride contents of the unsaturated zone-pore water while the second uses chloride content in groundwater. Contrary to the second approach, the first one does not capture recharge resulting from preferential flow paths. Other drawback of the first approach is that the pore water profiles can show high spatial variability due to soil heterogeneities (Edmunds et al. 2002). Both approaches use average chloride concentration of precipitation over a period of time.

In the Volta Basin, the first approach (the unsaturated zone chloride approach) has been used by Carrier (2008) and Yidana et al. (2016) in the upper half of Ghana (97 704 km²) and a sub-catchments of the White Volta in Northern Ghana, respectively. Elsewhere in West Africa, this approach was used by Edmunds et al. (2002), Gaye and Edmunds (1996), Bromley et al. (1997) and Diouf et al. (2013) in Northern Nigeria, Northwestern Senegal, Southern Niger, and the Thiaroye sandy aquifer in Senegal, respectively. The second one, used in this study, has been used in the Volta Basin by Martin (2005), Sandwidi (2007), Obuobie (2008) and Addai et al. (2015) to estimate the groundwater recharge in the Atankwidi river Basin (275 km²) in Ghana, the Komienga Dam Basin (5911 km²) in Burkina Faso, the White Volta Basin of Ghana, and Nasia catchment, respectively. In other places of Africa, Brunner et al. (2004) and Demlie et al. (2007) have used the same method for recharge estimation in Botswana and the Akaki catchment of central Ethiopia.

This CMB approach was first used in a study by (Eriksson and Khunakasem 1969) to estimate recharge rates on the Coastal Plain of Israel. The chloride-tracer method provides an estimate of recharge by use of a mass-balance equation. The premise of the method is that, the chloride concentration of wet and dry deposition times the quantity of precipitation equals the chloride concentration of recharge times the quantity of recharge. Overland runoff is often assumed to be negligible; if not, its quantity and chloride concentration can be measured and these terms added to the equation. Long-term recharge can be estimated if the other terms are known. Significant error is inherent in the estimate of chloride concentration precipitation (including dry deposition)

and in the assumption that other sources of chloride, such as road salt, are insignificant (Sumioka and Bauer 2003; USGS 2013).

Assuming a steady-state condition with advection strongly dominating diffusion; and neglecting the mass of chloride from dry atmospheric deposition, a mass balance of chloride in precipitation, surface runoff and groundwater is obtained. The balance can be represented mathematically in Eq. 3-21 (McNamara, 2005; Sumioka and Bauer, 2004):

$$PC_p = RC_{gw} + QC_r \quad \text{Eq. 3-21}$$

where: P is annual precipitation (mm); C_p is concentration of chloride in precipitation (mg/l); R is annual groundwater recharge (mm); C_{gw} is concentration of chloride in groundwater (mg/l); Q is annual surface runoff (mm); and C_r is concentration of chloride in surface runoff (mg/l).

When surface runoff is neglected because of the lack of data for the area studied, the terms in equation can be re-arranged to calculate the groundwater recharge as:

$$R = \frac{PC_p}{C_{gw}} \quad \text{Eq. 3-22}$$

The CMB method is based on the assumptions that: (i) there is no storage of chloride in the unsaturated zone; (ii) precipitation and dry atmospheric deposition are the only sources of chloride in groundwater and surface runoff; (iii) measured chloride concentrations are at depths high enough such that, seasonal variations in concentration are small; and (iv) the concentration of chloride in surface runoff is the same as that in precipitation (Sumioka and Bauer 2003; McNamara 2005; Healy 2010).

3.4.5. Estimation of groundwater recharge using WetSpass model

WetSpass stands for Water and Energy Transfer between Soil, Plants and Atmosphere under quasi-Steady State (Batelaan and De Smedt 2001). It was built based on the concepts of WetSpa (Batelaan et al. 1996; Wang et al. 1996). This model has been used in several works to estimate groundwater recharge in different climatic conditions (e.g., Aish et al. 2010; Teklebirhan et al. 2012; Armanuos et al. 2016; Shrestha et al. 2016). In West-Africa and precisely in the Black Volta basin, a new version- WetSpass-M model has been used with good performed (Abdollahi

et al. 2017). WetSpas-M, where M stands for Monthly, runs at monthly time step. The model can run alone or coupled with a groundwater flow model such as MODFLOW (Shrestha et al. 2016). The methodology on the application of the WetSpas-M model has been described in sections below.

WetSpas-M is a physically based model for the estimation of long-term average spatial patterns of groundwater recharge, surface runoff and evapotranspiration employing physical and empirical relationships. The model performs water balance calculations on monthly basis, compared to the original WetSpas model that works on seasonal time step. It splits precipitation into four components, namely: interception, surface runoff, evapotranspiration and recharge as captured in the water balance schematics in Figure 3-8. The model considers precipitation as the starting point in computing the water balance.

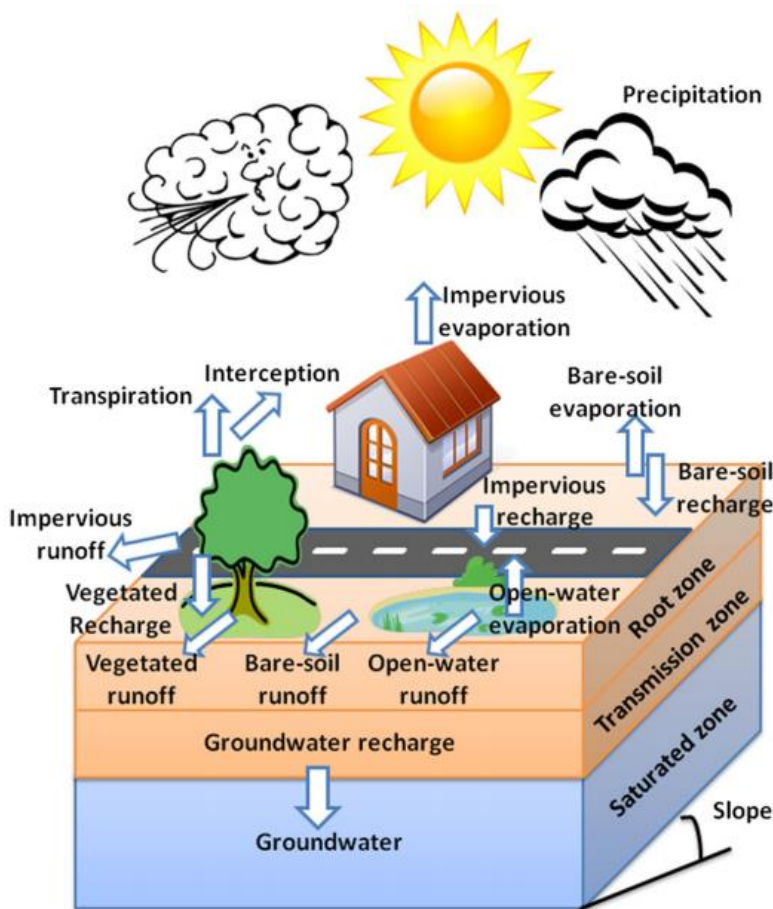


Figure 3-8: Schematic representation of water balance for a non-homogenous land cover grid cell (Batelaan and De Smedt 2001; Abdollahi et al. 2017)

The monthly water balance for a vegetated area depends on the monthly precipitation, interception fraction, surface runoff, actual transpiration, and groundwater recharge and can be expressed mathematically as:

$$P = I + S_v + T_v + R_v \quad \text{Eq. 3-23}$$

where P , I , S_v , T_v and R_v are precipitation, interception fraction, surface runoff, actual transpiration and groundwater recharge, respectively.

3.4.5.1. Interception

The monthly interception is calculated as a fraction of precipitation and depends on land-use/land-cover (Eq. 3-24):

$$I_m = I_R P_m \quad \text{Eq. 3-24}$$

where P_m is the interception [mm/month], I_m is the monthly precipitation and I_R [mm/month] is interception ratio and is computed using Eq. 3-25 suggested by de Groen and Savenije (2006):

$$I_R = \frac{I_m}{P_m} = 1 - \exp\left(\frac{-I_D d_p}{P_m}\right) \quad \text{Eq. 3-25}$$

where d_p is the number of rainy days [d/month] and I_D , expressed by Eq. 3-26, is the daily interception threshold which depends on land-use (Sutanto et al. 2012):

$$I_D = aLAI \left(1 - \frac{1}{1 + \frac{P_m [1 - \exp(-0.463LAI)]}{aLAI}} \right) \quad \text{Eq. 3-26}$$

where a is an interception parameter obtained by calibration, although Sutanto et al. (2012) suggested a value of 4.5mm. LAI is the leaf area index.

3.4.5.2. Surface runoff

The monthly surface runoff SR_m (mm/month) is estimated using a rational method applied using two coefficients:

$$SR_m = C_h C_{sr} (P_m - I_m) \quad \text{Eq. 3-27}$$

where C_{sr} and C_h are actual runoff coefficient (–) and coefficient (–) representing soil moisture conditions, respectively. C_h ranges from 0 to 1 and is computed following Eq. 3-28 :

$$C_h = \left(\frac{\theta_s}{\theta_{sat}} \right)^b \quad \text{Eq. 3-28}$$

where θ_s is the cell soil moisture content (m³/m³), θ_{sat} is the soil porosity (m³/m³) and b (–) represents the effect of rainfall intensity. For area lacking soil moisture data, C_h can be estimated using Eq. 3-29.

$$C_h = \begin{cases} \frac{P_m}{LP(P_m^\alpha + ET_m^\alpha)^{\frac{1}{\alpha}}} & \text{if } ET_m > P_m \\ 1 & \text{if } ET_m \leq P_m \end{cases} \quad \text{Eq. 3-29}$$

where ET_m is the potential evapotranspiration (mm/month) and LP is a calibration parameter (–). LP has a default value of 0.65 in WetSpass. It is used to avoid overestimation of surface runoff in places like semi-arid and arid areas where soil moisture is low and (potential) evapotranspiration is high (Abdollahi et al. 2017). It is found by calibration. Regarding the exponent α , Pistocchi et al. (2008) suggested a value of 1.5 at monthly scale. Regarding the potential runoff coefficient per grid cell, it is calculated based on two coefficients, namely, runoff coefficient for permeable areas (C_{per}) and runoff coefficient for the impervious part (C_{Imp}). The C_{per} is obtained from a weighted sum of land use, soil, and slope factors representing the first, second, and third term in the right-hand side in equation Eq. 3-30, respectively:

$$C_{per} = w1 \left(\frac{0.02}{n} \right) + w2 \left(\frac{\theta_w}{1 - \theta_w} \right) + w3 \left(\frac{S}{10 + S} \right) \quad \text{Eq. 3-30}$$

where n is the Manning's roughness coefficient which is dependent on the land use, θ_w is the volumetric soil water content at wilting point and S is the land surface slope in percentage. A value of 0.35% is set as a minimum slope in order to avoid underestimation of the runoff coefficient in flat areas. The sum w_1 , w_2 and w_3 has to be always equal to 1 as presented by Eq. 3-31 :

$$w_1 + w_2 + w_3 = 1 \quad \text{Eq. 3-31}$$

The weighted potential runoff coefficient (C_{wp}) for a given grid cell is calculated as follow (Eq. 3-32):

$$C_{wp} = \left(1 - \frac{A_{Imp}}{100}\right) C_{per} + \frac{A_{Imp}}{100} C_{Imp} \quad \text{Eq. 3-32}$$

where C_{Imp} is the runoff coefficient of the impervious area. A_{Imp} is the percentage of impervious surface per grid cell. In order to transform the potential runoff to the actual runoff coefficient the following equation is used (Abdollahi et al. 2017):

$$C_{sr} = \frac{C_{wp} \bar{P}_{24}}{C_{wp} \bar{P}_{24} - RCD \times C_{wp} + RCD} \quad \text{Eq. 3-33}$$

\bar{P}_{24} is the average daily rainfall in a month (mm/day), and RCD is the regional consecutive dryness level (mm). The value of RCD ranges between 1 and 10. A value of 1 corresponds to very heavy or torrential rainfall and more than 10 consecutive rainy days per month, while a value of 10 correspond to low regional intensity rainfall and less than 2 consecutive rainy days per month. In case rainfall is less than RCD , no adjustment is needed. In other words, C_{sr} is equal to C_{wp} .

Regarding monthly surface storage, runoff from the current month contributes to the volumetric runoff of the following month ($m^3/month$). Therefore runoff of a given month ($Q_{(t)}$) is estimated as presented in Eq. 3-34:

$$Q_{(t)} = xQ_{(t-1)} + 0.001(1 - x)ASR_m \quad \text{Eq. 3-34}$$

where x (-) is delay factor that ranges from 0 to 1, A is area (m^2) and $Q_{(t-1)}$ is volumetric runoff of the previous month ($m^3/month$) contributing to the current month.

3.4.5.3. Evapotranspiration

WetSpas-M estimates actual evapotranspiration as a function of potential evaporation (ETP) at a monthly timescale and vegetation coefficients. This vegetation coefficient is calculated using the Penman equation (Eq. 3-35):

$$C = \frac{1 + \frac{\gamma}{\Delta}}{1 + \frac{\gamma}{\Delta} \left(1 + \frac{r_c}{r_a}\right)} \quad \text{Eq. 3-35}$$

where γ is psychrometric constant (kPa^0C), Δ is slope of the first derivative of the saturated vapor pressure curve (slope of saturation vapor pressure at the prevailing air temperature) [$ML^{-1}T^{-2}C^{-1}$], r_c canopy resistance ($s\ m^{-1}$) and r_a is aerodynamic resistance ($s\ m^{-1}$) computed with Eq. 3-36:

$$r_a = \frac{1}{K^2 U_a Z_a} \left(\ln \left(\frac{Z_a - Z_d}{Z_0} \right) \right)^2 \quad \text{Eq. 3-36}$$

where K is the Von Karman constant (0.4) [-], U_a is the wind speed ($m.s^{-1}$) at measurement level $Z_a = 2m$, d is the zero-plane displacement length (m) and Z_0 is the roughness length for the vegetation or soil (m). For vegetated groundwater discharge areas, there is no soil or water availability limitation and the reference transpiration (T_{rv}) is estimated as follow (Eq. 3-37):

$$T_{rv} = c \times ETP \quad \text{Eq. 3-37}$$

But in vegetated areas where the groundwater level is below the root zone, the actual transpiration is modified (Eq. 3-38):

$$T_v = (1 - a_1^{w/T_{rv}}) T_{rv} \quad \text{Eq. 3-38}$$

where a_1 is a calibrated parameter related to the sand content of the soil type and w is the available water for transpiration (Eq. 3-39):

$$w = P_m + (\theta_{fc} - \theta_{pwp}) R_d \quad \text{Eq. 3-39}$$

where R_d is the rooting depth, $\theta_{fc} - \theta_{pwp}$ is the plant available water content per time step. Actual evapotranspiration for the vegetated area (ET_v) is obtained by summing up interception and actual transpiration. Finally, the total actual monthly evapotranspiration per grid cell [ET_m (mm/month)] is given by Eq. 3-40 :

$$ET_m = a_v ET_v + a_s ET_s + a_o ET_o + a_i ET_i \quad \text{Eq. 3-40}$$

ET_v , ET_s , ET_o , ET_i are actual evapotranspiration from vegetated, bare-soil, open-water and impervious area, respectively, while a_v , a_s , a_o , and a_i represent vegetated, bare-soil, open-water and impervious area components, respectively. The model considers precipitation as the starting point in computing the water balance (Batelaan and De Smedt 2001; Abdollahi et al. 2017).

3.4.54. Recharge

The groundwater recharge is calculated as a residual term of the water balance as expressed in Eq. 3-41:

$$R_m = P_m - SR_m - ET_m \quad \text{Eq. 3-41}$$

where R_m , P_m , SR_m and ET_m , all expressed in mm/month, are monthly recharge, precipitation, surface runoff and actual evapotranspiration, respectively.

Based on the fact that recharge is a slow process, monthly base-flow for each cell is calculated by taking into account the storage of the previous month and the recharge in the considered month:

$$Q_{b(t)} = \beta Q_{b(t-1)} + 0.001 N_m (1 - \beta) \phi R_m \quad \text{Eq. 3-42}$$

where β is a storage parameter (–) taking value between 0 and 1, $Q_{b(t-1)}$ is the base-flow from the previous month (m^3/month), N_m is number of days per month and ϕ (m^2/day) is the recharge contribution parameter to current base-flow. For grid cell area A (m^2) with recession index k (day) it is estimated as follow:

$$\phi = \frac{1.15A}{k} \quad \text{Eq. 3-43}$$

The inputs of the model are: topography, soil texture, wind speed, groundwater depth and potential evapotranspiration, number of rainy days, wind and temperature), slope. The LAI data is optional. Where it is not available, it is automatically generated by the model based on the DEM provided to the model.

A detail description of the model and the methodology can be found in the work by (Abdollahi et al. 2017).

3.4.6. Estimating recharge using a simple water balance method

Based on works done in two lithological units, namely sandstone and weathered rock, Martin and Van De Giesen (2005) applied linear regression method to determine the relationship between groundwater recharge and annual rainfall in these lithological units and derived groundwater recharge rate in the Volta Basin. This linear regression equation was used by Forkuor et al. (2013) to estimate groundwater recharge when determining the potential areas of groundwater development for agriculture in northern Ghana. Using a constant value of surface base on previous work done in the Volta Basin, Anayah et al. (2013) found that the method presented in Eq. 3-44 gives satisfactory result.

$$R = P - Q - PET \quad \text{Eq. 3-44}$$

where R, P, Q and PET are recharge, precipitation, surface runoff and potential evapotranspiration, respectively. Q was estimated as constant ratio of annual rainfall. Based on the work of Barry et al. (2005), a ratio of 0.085 was used for Bole and Wa, while a ratio of 0.108 was used for Navrongo.

Estimation of potential evapotranspiration (PET)

The PET can be estimated using several methods. However, the FAO- Penmann-Montieth method (Allen et al. 1998) has been found to estimate the PET more accurately. Therefore, it has been used as reference method in estimating PET (Walter et al. 2000; Droogers and Allen 2002). But, this method requires a lot of data that are not always available. To overcome this issue some methods have been proposed, among them is the Hargreaves method (Hargreaves et al. 1985) presented in Eq. 3-45.

$$ET_0 = 0.0022RA \times (TC + 17.8) \times TD^{0.5} \quad \text{Eq. 3-45}$$

where RA = extraterrestrial radiation in the same units (mm), TC = mean temperature in degrees Celsius, and TD = mean maximum minus mean minimum temperature in degrees Celsius.

$$RA = \frac{24(60)}{\pi} G_{sc} d_r [\omega_s \sin \varphi \sin \delta + \cos \varphi + \cos \delta \sin \omega_s] \quad \text{Eq. 3-46}$$

Ra extraterrestrial radiation [$\text{MJ m}^{-2} \text{ day}^{-1}$], G_{sc} solar constant = $0.0820 \text{ MJ m}^{-2} \text{ min}^{-1}$, d_r inverse relative distance Earth-Sun (Eq. 3-47), ω_s sunset hour angle [rad] (Eq. 3-49), φ latitude [rad], δ solar declination (Eq. 3-48) [rad]. The inverse relative distance Earth-Sun, d_r , and the solar declination, δ , are given by:

$$d_r = 1 + 0.033 \cos\left(\frac{2\pi}{365}J\right) \quad \text{Eq. 3-47}$$

$$\delta = 0.409 \sin\left(\frac{2\pi}{365}J - 1.39\right) \quad \text{Eq. 3-48}$$

where J is the number of the day in the year between 1 (1 January) and 365 or 366 (31 December). The sunset hour angle, ω_s , is given by:

$$\omega_s = \arccos[-\tan \varphi \tan \delta] \quad \text{Eq. 3-49}$$

A modified form of the Hargreaves method (MHG) that takes into account precipitation was suggested by Droogers and Allen (2002) presented by Eq. 3-50:

$$ET_0 = 0.408 \times 0.0013(T_{mean} + 17) \times (T_{max} - T_{min} - 0.0123P)^{0.76} \times Ra \quad \text{Eq. 3-50}$$

where T_{mean} , T_{max} and T_{min} are mean, maximum and minimum temperature, respectively, and P (mm) precipitation in per month. As the purpose of this work is to estimate the impact of climate change on groundwater, estimation of PET for the future is required. The original Hargreaves (HG) and the Modified Hargreaves were used in this study to estimate the PET as

data required for using the Penman-Montieth method for the future climate were not readily available. . As data required for the use of PM were available for the present climate the PET was estimated for the present climate using the three methods and a choice was made between the HG and MHG, depending on which one gave a better results compared to the results from the PM method.

3.4.7. Study of the impact of climate change

3.4.7.1. Statistical downscaling

Downscaling is the transformation from a large-scale feature to a small-scale one, either from grid to grid or from grid to point. There are two main downscaling methods, namely, dynamical and statistical downscaling. Dynamical downscaling uses RCM driven by boundary conditions from a GCM to derive smaller-scale information (Giorgi et al. 2001), whereas statistical downscaling approaches are based on empirical relationships between large-scale atmospheric variables (i.e predictors) and local variables (i.e. predictands) such as precipitation and temperature (Zorita and von Storch 1999). This approach is based on the assumption that the regional climate is conditioned by the large-scale circulation (LSC) and small-scale features like land-use, topography, land-sea contrast. The LSC is well resolved by the GCM, while the small-scale parameters are not well captured in the models. The relationship linking the large-scale information and local variable is assumed to remain the same in the future (Busuioc et al. 1999). Several previous studies have made a comparative analysis of the two downscaling methods (e.g., Haylock et al. 2006; Boé et al. 2007; Schmidli et al. 2007; Trzaska and Schnarr 2014; Ayar et al. 2016). The statistical downscaling approach is widely used in climate impact-related research work because, compared to the dynamical approach, it has the well-known advantage of lower computational requirement (Li et al. 2010). This has led to the development of several statistical based methods during the last decades and some inter-comparison studies of several statistical downscaling methods have been done by authors such as Goodess et al. (2007) and Gutmann et al. (2014). For instance, in evaluating the performance of four statistical downscaling methods, Gutmann et al. (2014) found that the daily disaggregated-to-daily Bias Corrected Spatial Disaggregation and the Bias Corrected Constructed Analog methods overestimate wet day fraction, while they underestimate extreme events. They also stressed that the Asynchronous Regression method reproduces extreme events and wet day fraction well at the

grid-cell scale, but does well estimates them at aggregated scales. Regarding the monthly disaggregated-to-daily Bias Corrected Spatial Disaggregation, the only limitation is its incapability to rescale the observed weather patterns. Although consisted of heterogeneous groups of methods, statistical downscaling methods can be classified into three categories, namely, linear method, weather classifications and weather generators. Linear methods find linear relationships between predictor(s) and predictand and weather classifications methods determine the local variable (predictand) based on large-scale atmospheric “states.” Compared with the linear methods, the weather classification methods have the advantage of performing well with a non-normal distributed variable such as daily rainfall. However, they require a huge amount of data leading a high computational demand. As for the weather generators, they are very useful for temporal downscaling (Trzaska and Schnarr 2014).

The quantile-quantile (qq-plot) method, also called quantile mapping or quantile matching used in this current study belongs to the non-linear downscaling group. It has the advantage of accounting for GCM biases in all statistical moments. As stated earlier, it is assumed that biases relative to historic observations will be the same during the projections (Thrasher et al. 2012). This downscaling method consists of matching the statistical distribution of a given climate variable to the statistical distribution of the observed variable on the historical period. The transformation for a given month and a given variable, as described by Angelina et al. (2015), follows these steps : First of all the historical dataset is divided into two dataset having the same length and corresponding to calibration period and a validation period. The calibration and validation periods for a given month are obtained by using data of that month during all the years in the observation, starting from the first year. For instance, in a 30-days month, 15 days are used for calibration and 15 days for validation. Basically, data for values date 1, 3, 5 etc. of the month are used for calibration; while date 2, 4, 6, etc. are used for validation. The daily time series of the month are extracted from both observations and RCM simulations based on the corresponding periods (calibration and validation). Then two empirical cumulative distribution functions FOBS and FRCM are developed using the observations and the RCM outputs, respectively, on the calibration period. The data simulated by the RCM is corrected for both validation period and future periods following Eq. 3-51.

$$X_{CORR} = F_{OBS}^{-1}(F_{RCM}(X_{RCM})) \quad \text{Eq. 3-51}$$

where X_{RCM} is the value of variable provided by the raw RCM simulations and X_{CORR} is the variable obtained after correction. Finally, the Q-Q transformation is applied to future RCM simulations.

Assessment of future climate change impacts are done based on scenarios. The new generation of IPCC climate scenarios called the Representative Concentration Pathways (RCPs) were used in this study. There are four RCPs, namely, RCP2.6, RCP4.5, RCP6 and RCP8.5. These RCPs were defined by scientific community based on existing literature. The number in the RCP' name refers to radiative forcing that will be reached in 2100. For instance, RCP4.5 means that this scenario results in a radioactive forcing of 4.5W/m² in 2100. The RCP2.6 represents the mitigation scenario, while and RCP8.5 is defined to be the very high baseline emission scenario. As for RCP4.5 and RCP6, they represent the medium stabilization scenarios. Even though technically feasible, several works have stressed that RCP2.6 is unrealistic as achievement of this target requires the full participation of countries and sectors in the greenhouse gases reduction efforts, which is impossible to have (e.g. van Vuuren et al. 2011).

Therefore RCP2.6 was eliminated from the analysis. As RCP6 is an intermediate scenario of RCP4.5 and RCP8.5, it was decided to choose RCP4.5 and RCP8.5 for this work. Therefore, two RCMs (RCA4 and CCLM) driven by three GCMs (ICHEC-EC-EARTH, MPI-M-MPI-ESM and CNRM-CERFACS-CNRM) under RCP4.5 and RCP8.5 scenarios were downscaled, resulting in twelve (12) different scenarios. The skills of the models were evaluated on the monthly basis because the computation of recharge is also done at this time scale.

3.4.7.2. Impact of climate change on groundwater recharge

In this study, the period 1976-2005 was chosen as baseline and periods 2011-2040, 2041-2070 and 2071-2100 were used as short, medium and long term future periods, respectively. For the assessment of climate change impact on recharge, we assumed that land-use and land-cover will not change and that only rainfall and temperature will change. The impact of climate change was based on the present-day recharge estimated using a simple water balance method (Anayah et al. 2013) because the WetSpass model (Abdollahi et al. 2017) did not perform well. As “the use of an ensemble of models helps limit the influence of any bias present in any one model” (Stanturf et al. 2011), ensemble approach based on the twelve scenarios was adopted.

3.5. Conclusion

During this work, issues of data availability and accessibility were faced. The methods were chosen based on the available data. As limited data can affect the results, considerable effort was made to collect as much as possible needed and available data. When possible, primary data was collected in addition to secondary data. Various methods were used, in order to get appreciable results in this limited data availability condition. After presentation of the data set and methods used during this thesis let us move to the next the first results chapter.

Chapter 4 HYDROGEOCHEMISTRY AND GROUNDWATER RECHARGE PROCESS

Chapter 4 is largely based on the published paper by Koffi et al. (2017) entitled Hydrochemical characteristics of groundwater and surface water for domestic and irrigation purposes in Veacatchment, Northern Ghana.

4.1.Introduction

Water is the basis of human life and all economic developments. Like most of Africa's semi-arid regions, Northern Ghana is characterized by a prolonged dry season (7 months of very little rainfall) leading to the drying up of many rivers and streams and a high variability of rainfall in space and time. Therefore, surface water is unreliable and insufficient to meet the increasing water demands for domestic and agricultural uses. An alternative solution to this issue is to build dams for surface water storage. The challenge here is that large plots of land are immersed resulting in reduction of the area that is available for agricultural use. Also, with high rate of evapotranspiration in the area, a large amount of the stored water would be lost by evaporation, calling for re-thinking of water storage in large surface dams. This makes the availability of surface water a big challenge in arid areas and mostly in developing countries where storage infrastructures are insufficient because of lack of finance and good water management policies. In addition, in areas with scattered settlements, like rural areas in northern Ghana, groundwater is the most appropriate source of water supply because, compared to surface water, it can be accessed at the vicinity and it is less exposed to pollution and evaporation. It also has a relatively constant temperature and its response to demand over time varies only slightly (Tsur and Graham-Tomasi 1991; Zektser and Everett 2004).

In the Veacatchment (study area), some small dams were built for irrigation and cattle breeding. The biggest among them is the Vea dam constructed for the irrigation of 1,400 hectares of land in the catchment and water supply of 4.5 million litres per day to the capital city of the Upper East Region of Ghana – Bolgatanga and its environs, which are outside of the Veacatchment. Generally, demand on water resource in the Veacatchment outstrips supply for two main reasons. Firstly, there is increasing demand for domestic water supply due to population growth in the basin areas as well as in Bolgatanga and its environs and the size of the Vea dam is not sufficient to meet the water demand, leading to shortage of water for domestic supply and

irrigation. Secondly, due to an annual siltation rate of $1000 \text{ m}^3/\text{km}^2/\text{year}$ in the Veia dam reservoir, its storage has been drastically reduced (Adongo et al. 2014). Climate change may worsen the situation as research findings suggest an increase in temperature and a decrease in rainfall in the area (Asante and Amuakwa-Mensah 2014) leading to less inflow to the dam and exacerbation of evaporation. The afore-mentioned challenges with surface water make groundwater the most preferred alternative source of water to compliment surface water sources for meeting the water demand in the area. But the use of groundwater in the study area is negated by the poor quality of the resource in some locations in Bongo and Bolgatanga where groundwaters with high fluoride concentrations have been found. High fluoride concentrations above WHO limit of 1.5 mg/L are related to health implications of mottled teeth, dental and skeletal fluorosis. This high content of fluoride has been found to be associated with microcline-rich granitoids (Smedley et al. 1995; Apambire et al. 1997; Firempong et al. 2013). Furthermore, in the rural areas, groundwater and surface water are used in domestic water supply without any proper treatment. Therefore, a study of water quality in the Veia area is of crucial importance. Some studies related to groundwater quality have been carried out in the Northern Ghana (e.g. Smedley et al. 1995; Anku et al. 2009; Loh et al. 2012; Tay 2012). However, Loh et al. (2012) focused on water quality of groundwater at the bigger scale in the crystalline basement aquifer of Northern Ghana, which encompasses the Veia catchment and did not take into account the quality of water for domestic use. Apambire et al. (1997), on the other hand, focused mostly on the genesis of elevated fluoride concentrations in groundwater.

To address the gap, this study aimed at determining the hydrogeochemical characteristics of groundwater and surface water for domestic and irrigation purposes, recharge process and origin in the area with high resolution data. Specifically, the study focused on determining (i) the processes influencing quality of groundwater, (ii) the water type and the influence of geological formations on the water resources, (iii) the usability of both groundwater and surface water for irrigation and domestic water supply, and finally (iv) groundwater recharge process and origin will be study using stable isotopes analysis.

As aquifer material and groundwater quality are often closely related, knowing the geological characteristics of a study area is a prerequisite for a meaningful groundwater chemistry investigation. Studies done to date have suggested the land area of Ghana is underlain by three

major geological terrains. The first terrain is comprised of Paleoproterozoic rocks (quartzites, phyllites, grits, conglomerates, schists, tuffs, greywackes, metamorphosed lavas and pyroclastic rocks) predominant in the southwestern and northwestern part of the country, whereas gneisses and supracrustal rocks of mostly Neoproterozoic age are found in the southeast and east of the country. The second geological terrain consists of flat-lying shelf/marine sediments of very late Precambrian to Paleozoic age, which are found in the central and northeastern part of the country; while the third sequence, the mostly Cenozoic sediments, occupies a small strip along the coast (Schlüter and Trauth 2008). In Veá catchment, bedrock is mainly comprised of granites, hornblende-biotite granodiorites (Hornblende B Granodiorite), biotite gneisses, basaltic and andesitic volcanics and intrusives and migmatites. Basically, granite contains at least 10% and up to 40% free quartz, together with feldspar and mica. Both alkali (K and Na rich, orthoclase, microcline) and plagioclase (Na and Ca rich, albite, oligoclase, andesine, etc.) feldspars are present in most granites (U.S. Bureau of Mines 1996). Pelig-Ba (2012) conducted a physical analysis of granite, hornblende-granodiorite and biotite-granodiorite samples taken from the study area and found that the granites and hornblende-granodiorites were composed of K-feldspar, hornblende and quartz while the Biotite-granodiorites were composed of biotite, hornblende and quartz. In addition, the granites and biotite-granodiorites were coarse-grained while the hornblende-granodiorites were medium size grains. Based on chemical analysis of these samples the same authors found that silica (SiO_2) with a weight percent ranging from 46.37 to 62.98 is the major geochemical component and it is followed by Al_2O_3 with weight percent ranging from 12.05 to 14.37. The coarse-grained granite of the study area comprise mainly of Bongo granite suite that was described by Murray (1960) as a pink rock composed of well-developed euhedral to subhedral microcline phenocrysts up to 1 cm in length, euhedral amphibole crystals, granular interstitial quartz, plagioclase, minor biotite, and trace accessory fluorite.

The ion balances of the samples range from 0 to 5 %, thus the laboratory analysis results of all the samples are acceptable. The distribution of these samples based on the geological setting of the area where the sampled boreholes are located is provided by Table 4-1, while range of all the parameters for groundwater samples is summarized in Table 4-2.

Table 4-1 Geological units, number of samples and predominant hydrochemical facies in the Veia catchment

Geological units	Number of groundwater samples	Facies
Granite	37	Ca-Mg-HCO ₃
Hornblende biotite granodiorite	11	Ca-Mg-HCO ₃ / Ca-Mg-Cl-SO ₄
Biotite gneiss	6	Ca-Mg-HCO ₃
Upper birimian	4	Ca-Mg-HCO ₃
Migmatite and undifferentiated granite	3	Ca-Mg-HCO ₃

Table 4-2 Statistics of physico-chemical and hydrochemical parameters of groundwater sampled in Veia Catchment, Northeast Ghana

Parameter	Unit	Min	Max	Mean	σ	Acceptable limits (GSA/WHO)
n= 61						
electrical conductivity (EC)	$\mu\text{S/cm}$	81.0	1291	26	187	-
Total dissolved solids (TDS)	mg/L	53.0	839	276	122	1000
pH	-	6.60	8.50	7.31	0.31	6,5-8,5
dissolved oxygen (DO)	mg/L	2.32	6.32	4.55	0.92	-
Temperature	$^{\circ}\text{C}$	28.9	32.4	31.1	0.69	-
Salinity	ppt	0.03	0.61	0.15	0.09	-
Total alkalinity (TA)	mg/L	48.2	312	126	46.8	-
Total Hardness (TH)	mg/L	50.8	272	115	47.3	500
Color	Hz	2.50	20.0	4.55	2.83	-
Turbidity	NTU	<1.00	13.0	1.20	1.96	-
total suspended solids TSS	mg/L	<1.00	28.0	1.96	4.90	-
Ca ²⁺	mg/L	12.3	76.2	24.8	11.4	-
Na ⁺	mg/L	7.50	52.0	20.1	8.93	-
Mg ²⁺	mg/L	2.50	37.9	12.8	6.66	-
Mn _{tot}	mg/L	<0.005	0.06	0.01	0.01	0.40
K ⁺	mg/L	1.10	43.5	3.99	5.34	-
NH ₄ ⁺	mg/L	<0.001	2.58	0.15	0.35	-
Fe _{tot}	mg/L	<0.01	1.28	0.17	0.26	0.30
HCO ₃ ⁻	mg/L	58.8	381	157	56.7	-
Cl ⁻	mg/L	2.00	93.3	14.4	15.0	250
SO ₄ ²⁻	mg/L	<1.00	93.8	7.32	14.8	250
PO ₄ ³⁻	mg/L	0.01	0.47	0.12	0.09	-
NO ₃ -N	mg/L	<0.001	0.07	0.02	0.02	50.0
NO ₂ -N	mg/L	<0.001	0.01	0.01	0.01	3.00

4.2. General Hydrogeochemistry

4.2.1. Chloro-Alkaline Indices

In this study, the chloro-alkaline indices were analyzed only for groundwater samples. The CAI-I ranged from -10.99 to 0.545, whereas CAI-II ranged from -0.49 to 0.25. For both indices, 93.4% of the samples are negative and only 6.6% are positive (Eq. 3-2). Thus, for the vast majority of the groundwater samples taken, the Ca^{2+} and Mg^{2+} of the water are replaced by Na^+ and K^+ of the rocks. Hence, cation exchange is the main ion exchange process and can also be one of the mechanisms controlling the chemical composition of the groundwater in the studied area. This result is similar to the findings of other works in Ghana such as Yidana and Yidana (2010) and Kaka et al. (2011), who analyzed 161 groundwater samples from the Voltaian sedimentary formation and 33 water samples (25 groundwater, 3 streams and 5 from the Volta Lake) from Manya Krobo area mainly underlain by rocks of the Voltaian Super-group, respectively.

Among the four sampled waters having positive chloro-alkaline indices, three are from an area underlain by granite and only one from an area underlain by hornblende granodiorite. Within the University of Lagos in Nigeria, Odukoya et al. (2013) observed that reverse ion exchange was the dominant process in the groundwater (52 %), whereas normal ion exchange was noticed in 48 % of the water samples. In their study, CAI values ranged between -0.86 to 5.5. In India, in an area characterised by crystalline rocks like this work, Jagadeshan et al. (2015) obtain results similar to this current research. In fact, they found that CAI 1 and CAI 2 vary with respect to time, but reverse ion exchange was the dominant process in the groundwater, even though normal ion exchange was also identified in very few sampled wells.

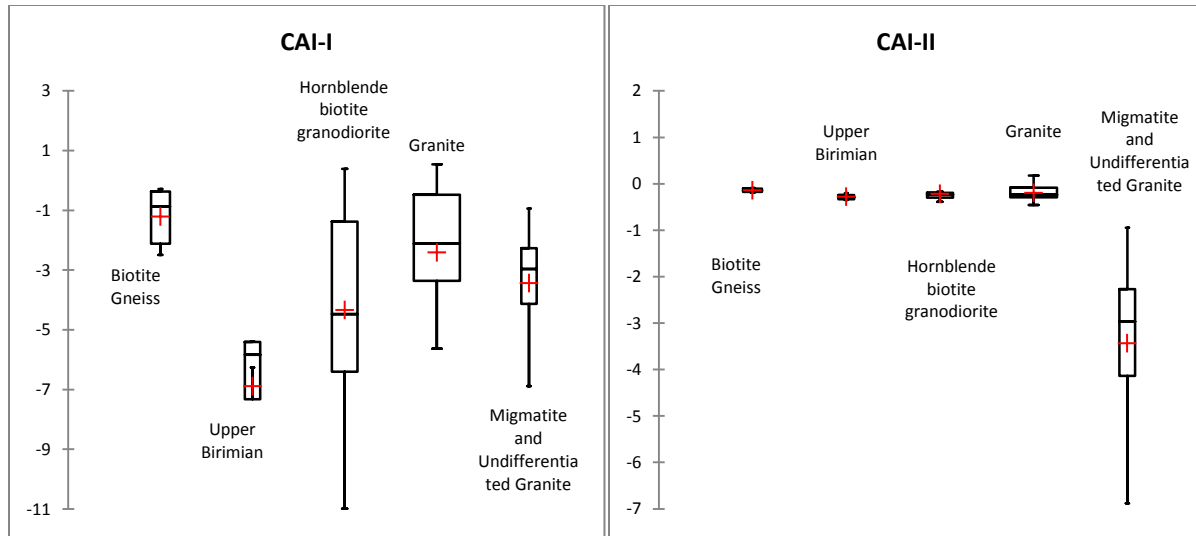


Figure 4-1: Box-plots of the chloro-alkaline indices of groundwater samples from different lithologies (Figure 3-5) in the study area. The red crosses indicate average values; black horizontal line indicates median values.

4.2.2. Weathering process

Figure 4-2 shows that most of the groundwater samples in this study plot below and along the $y = x$ line due to excess of bicarbonate as only six (five of them are from granite rock aquifers) representing 10% were found to be above the equiline. Thus compared to reverse ion exchange, ion exchange is the dominant process in the study area. It also indicates that silicate weathering is the main source of sodium and bicarbonate and it exerts major control on groundwater in this area (Lakshmanan et al. 2003; Rajmohan and Elango 2004). This result is in agreement with the findings of Loh *et al.* (2012) for the entire basement aquifer of Northern Ghana, and Tay (2012) whose study area, the Savelugu-Nanton District, is situated at about 140 km from the current study area. It is also supported by the plot of Na^+ versus Cl^- (Figure 4-3) showing that most of the groundwater samples fall above the 1:1 trend line. In fact, Meybeck (1987) stated that Na^+/Cl^- ratio greater than one is due to Na released from a silicate weathering reaction whereas a ratio approximately equal to one denotes a release of sodium from halite dissolution. According to Stallard and Edmond (1983), the excess of Na^+ can be attributed to silicate weathering from feldspars or due to anthropogenic activities like the seepage of waste water. Rogers (1989) found that if silicate weathering is a probable source of sodium, HCO_3^- would be the most abundant anion as it is in this study. The result is consistent with the TDS values as they are all lower than 500 mg/L except for one sample. In fact, Hounslow (1995) stressed that the weathering process

taking place in waters with TDS < 500 mg/L is silicate weathering. Figure 4-4 also shows that all the groundwater samples are in equilibrium with kaolinite supporting this aforementioned idea as silicate weathering produces kaolinite (Eq. 3-4). This result, in agreement with the work of Tay (2012), is in contrast with findings of Loh *et al.* (2012) who stressed that their sampled waters were in equilibrium with smectite. Like this work, their study areas are located in Northern Ghana. In India, precisely in the Kancheepuram district, characterized by both alluvium and weathered crystalline charnockite aquifer, Lakshmanan *et al.* (2003) observed that carbonate weathering was the dominant process by using the scatter plot $Ca^{2+}+Mg^{2+}$ versus $SO_4^{2-}+HCO_3^-$.

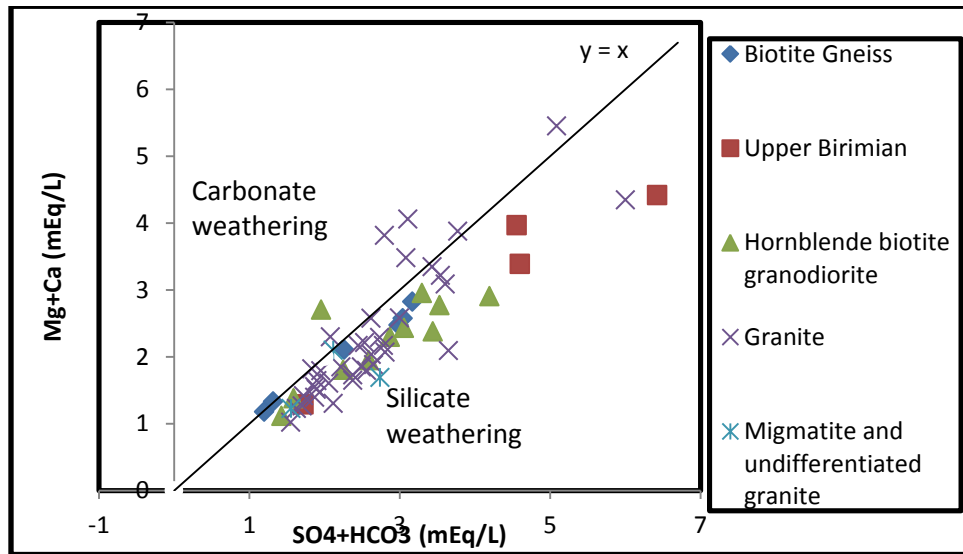


Figure 4-2: Relation between Ca+Mg and SO4+HCO3

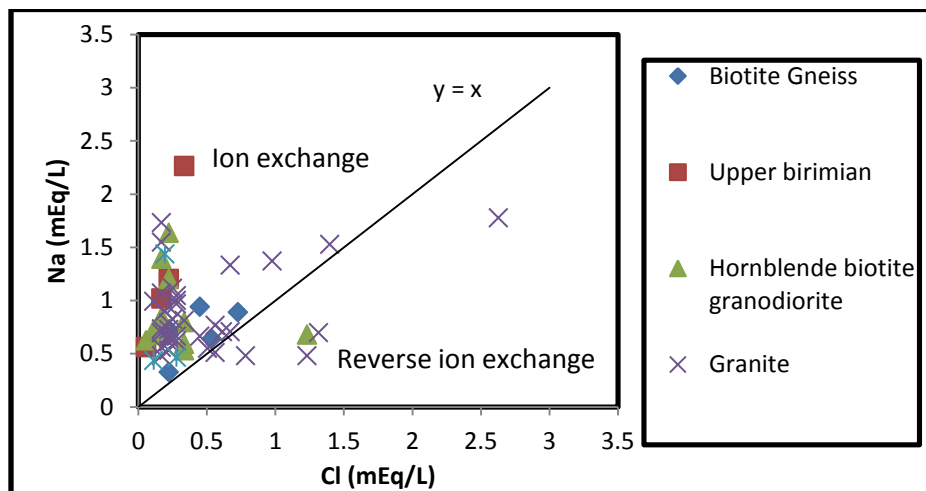


Figure 4-3: Plot of Sodium versus chloride

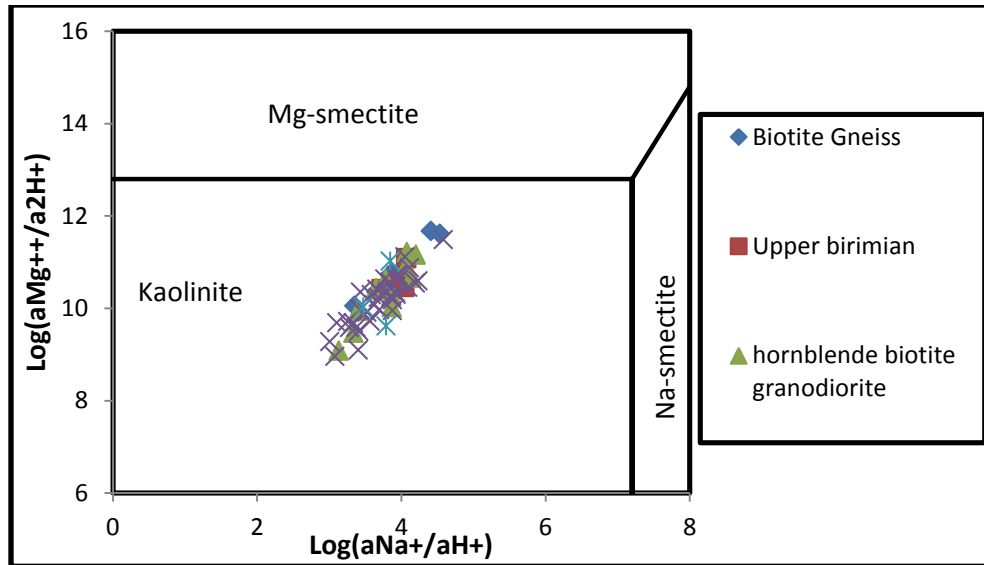


Figure 4-4: Stability field diagrams of the partial system $\text{MgO–Na}_2\text{O–Al}_2\text{O}_3\text{–SiO}_2\text{–H}_2\text{O}$ of the chemical composition of groundwater samples.

The plot of $\text{Na}^+\text{–Cl}^-$ versus $\text{Ca}^{2+}\text{+Mg}^{2+}\text{–SO}_4^{2-}\text{–HCO}_3^-$ (Figure 4-5) shows that all groundwater samples define a straight line ($R^2 = 0.9207$) with a slope of -1.003 . The trend line of the scatter plot nearly passes through the origin ($y = -0.0513$), revealing that essentially all Na^+ , Ca^{2+} and Mg^{2+} participate in the ion exchange reaction. It also implies that ion exchange is a significant process controlling the water composition. In fact, $\text{Na}^+\text{–Cl}^-$ refers to the amount of Na gained or lost relative to that provided by halite dissolution, whereas $\text{Ca}^{2+}\text{+Mg}^{2+}\text{–SO}_4^{2-}\text{–HCO}_3^-$ accounts for the amount of Ca^{2+} and Mg^{2+} gained or lost relative to that provided by gypsum, calcite, and dolomite dissolution (Fisher and Mullican 1997). Thus, silicate weathering and ion exchange are probably the processes explaining the deficit of calcium (Ca^{2+}) plus magnesium (Mg^{2+}) compared with bicarbonate (HCO_3^-) and they are responsible for the groundwater chemistry of the study area. A similar result was found by Anku et al. (2009) as well as Yidana and Yidana (2010). Using a plot of HCO_3^- against $(\text{Na}^+\text{+K}^+\text{+Ca}^{2+}\text{+Mg}^{2+})\text{–Cl}^-$, Yidana and Yidana (2010) also suggested that silicate mineral weathering does take place in their study area. In the Ga West Municipal area in Ghana underlain by the Cape Coast granite complex and rocks of the Togo formation, using the scatter plot $\text{Na}^+\text{–Cl}^-$ versus $(\text{Ca}^{2+}\text{+Mg}^{2+}\text{–SO}_4^{2-}\text{–HCO}_3^-)$, Saka et al. (2013) obtain similar result like in this work and concluded that concentrations in groundwater are derived from interaction with aquifer materials.

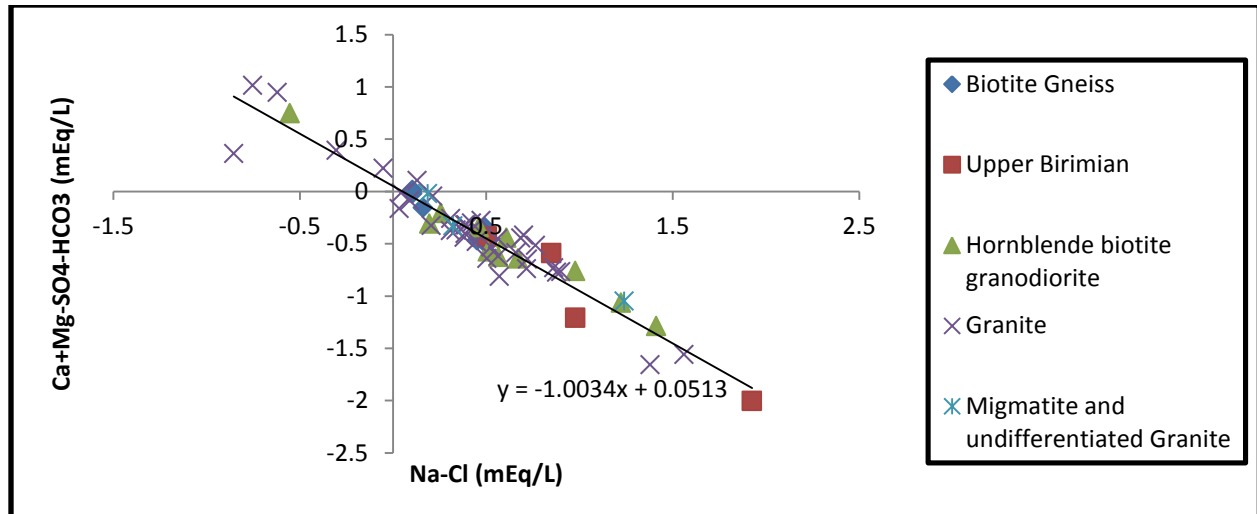


Figure 4-5: Relation between Ca+Mg-SO₄-HCO₃ and Na-Cl

The Gibbs' diagram for cations and anions (Figure 4-6) shows that all the samples plot in the rock–water–interaction dominance field in this area (Gibbs 1970), confirming that the chemistry of groundwater in the study area is dominated by the interaction between water and aquifer material. This result corroborates the cation exchange and silicate weathering found as dominant processes controlling the chemical composition of the groundwater. In Ghana, using the Gibbs diagram, Banoeng-Yakubo et al. (2009); Yidana (2009); Ganyaglo et al. (2011); Kaka et al. (2011); Yidana et al. (2012); Salifu et al. (2013) and Boateng et al. (2016) concluded that rock-water interactions are the most important processes that control the hydrochemistry of groundwater in different areas underlain by various geological formation such as the Birimian Supergroup, the Voltaian Super Group, the Togo, the Cape Coast granite complex, the Lower Birimian and the Buem. Therefore, results of these works are all in agreement with this present study. In Nigeria, a similar result was obtained by Talabi and Tijani (2013) and Okiongbo and Douglas (2015) who concluded that the waters of their study areas located in the Pre-Cambrian Basement Complex of Southwestern Nigeria and Yenagoa city in the Niger Delta alluvial plain in Southern Nigeria, respectively, have their chemistry controlled by the weathered materials derived from the underlying bedrocks. In India, studies in a similar geological environment suggest similar results (Lakshmanan et al. 2003; Rajmohan and Elango 2004).

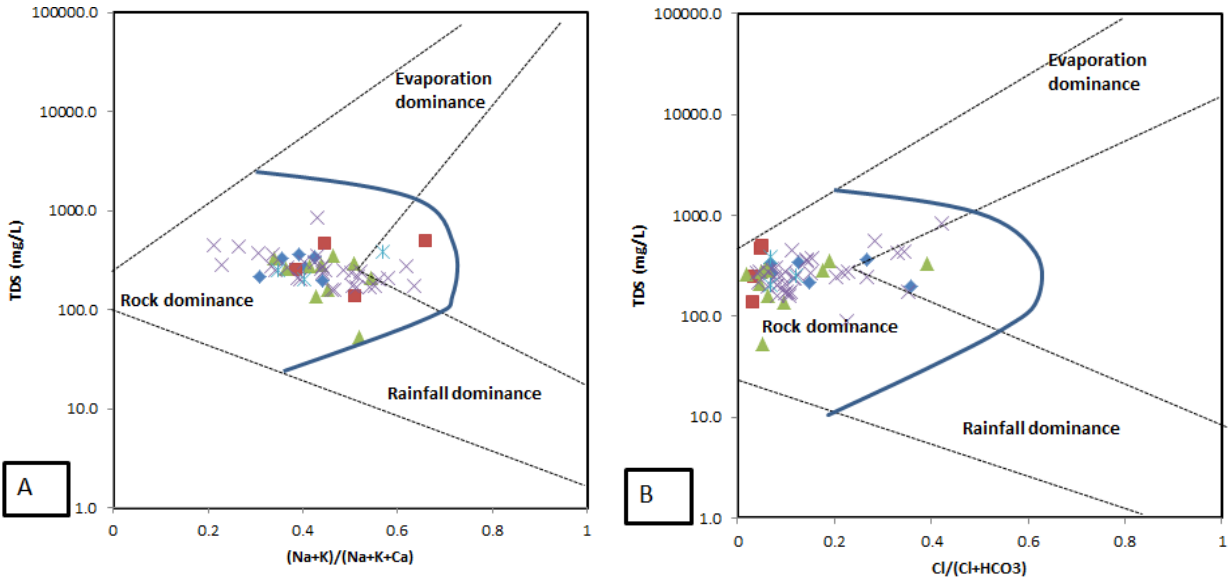


Figure 4-6: Gibbs' diagrams for cations (A) and anions (B) indicating rock-water interaction

4.2.3. Saturation index

Table 4-3 summarizing the saturation indices analysis shows that the groundwater samples analysed in this study are undersaturated with respect to gypsum and anhydrite. For aragonite, dolomite and calcite, only a few samples show oversaturation. Concerning aragonite, three samples show a clear saturation and about 41 % have an index greater than -0.5, thus around saturation. This suggests that the analysed groundwater generally has a low residence time in aquifers in the study area. The SI of dolomite and calcite differ from the findings of (Yidana et al. 2008; Banoeng-Yakubo et al. 2009a; Nartey et al. 2012), while SI of Gypsum is in agreement with those obtained by (Banoeng-Yakubo et al. 2009a). Nartey et al. (2012) suggested that the majority of their samples from East Gonja in Northern Ghana were saturated with respect to dolomite and calcite; while using an inverse modelling approach, Yidana et al. (2008) showed that groundwater from the Afram Plains area was supersaturated with respect to calcite, aragonite and dolomite. The findings of Fianko et al. (2010) in the Accra plains mostly underlain by Dahomeyan formation, are similar to the results of this work, as all their samples were undersaturated with respect to gypsum and anhydrite; and the majority of them were undersaturated with respect to dolomite, calcite and aragonite. In the Ankobra Basin mainly

consisting of lower Proterozoic rocks divided into Birimian and Tarkwaian systems, Kortatsi (2007) found that all the groundwater samples were undersaturated with respect to all the carbonate minerals considered in this current study. The results of this work and previous works regarding gypsum corroborate findings of Kesse (1985), who highlighted the scarcity of gypsum deposits in Ghana. The plotting of the dolomite saturation index against calcite saturation index (Figure 4-7) shows three groups of groundwater in the study area regarding to their flow rate and the residence time. Groundwater of group A, which contains water saturated and oversaturated with respect to dolomite and calcite, have higher residence times with low flow velocity that characterises aquifers with a low permeability, whereas group C has the lowest residence time with the highest flow velocity characterising mostly unconfined aquifers. Group B is an intermediary group between the two aforementioned groups. The Ca^{2+}/Mg^{2+} plotted in Figure 4-8 shows that many of the groundwater samples had more dissolved calcite than dolomite.

Values of the MGI were only able to be calculated for 48 of the 61 samples because SO_4^{2-} concentration should not be equal to zeros (0). MGI of 10 samples was found to be lower than 1, meaning 16 % of the 61 samples belong to deep meteoric water aquifers whereas only 84 % are from shallow meteoric water aquifers.

Table 4-3: Summary of mineral saturation indices of the sampled water

	Min SI	Max SI	Mean SI	Number of samples with SI<0	Number of samples with SI>0
Dolomite	-3.66	1.66	-1.31	88.5	11.5
Calcite	-1.42	1.07	-0.45	91.8	8.2
Aragonite	-1.56	0.92	-0.59	96.7	3.3
Anhydrite	-4.24	-1.66	-3.32	100	0
Gypsum	-4.04	-1.47	-3.13	100	0

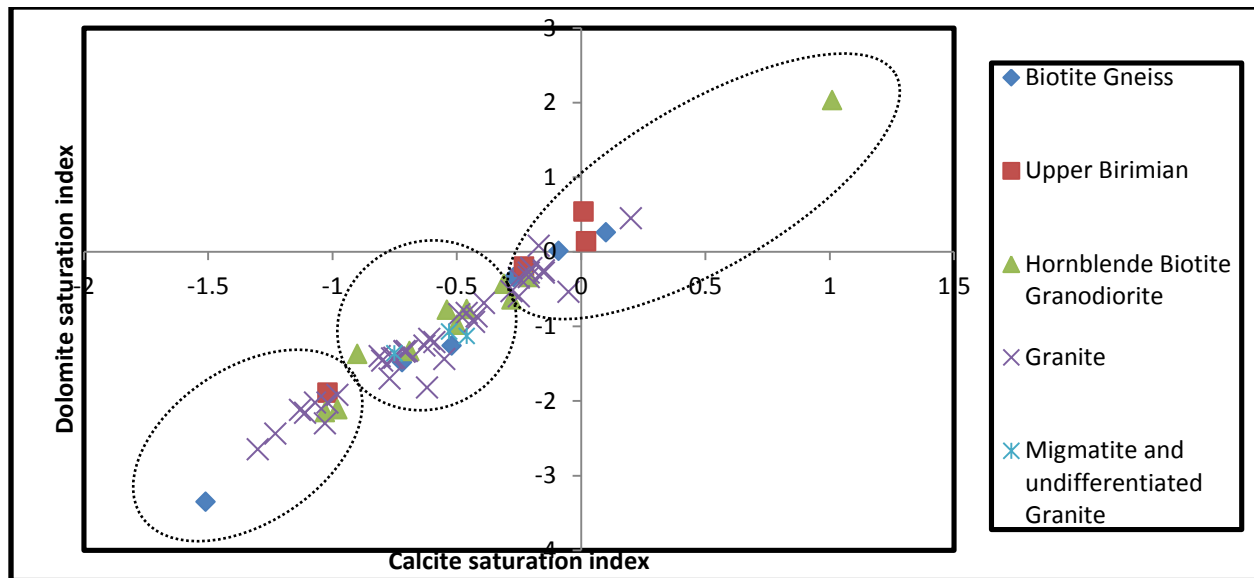


Figure 4-7: DSI/CSI of Groundwater in Veia Catchment, Northeast Ghana

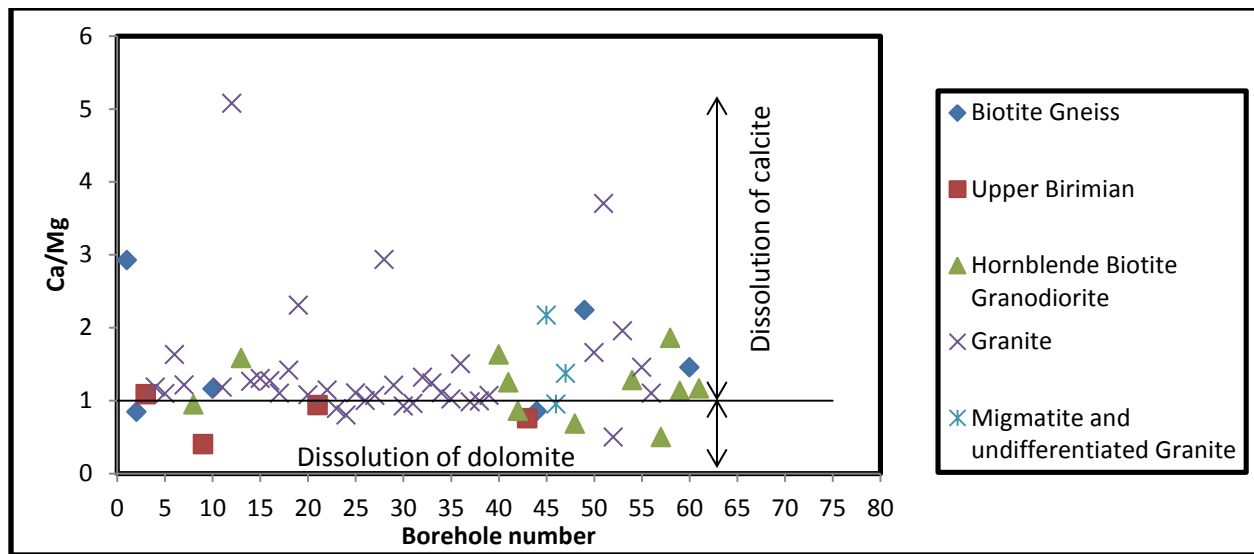


Figure 4-8: Ca/Mg ratio rock dissolution of groundwater in the Veia area, Northeast Ghana

4.3. Drinking water quality

The range of all the parameters for groundwater samples is summarized in Table 4-2. Only results regarding to TDS, turbidity, pH, Total Hardness, major ions will be discussed in detail.

4.3.1. Total Dissolved Solids (TDS) and turbidity

The study results showed that TDS in the groundwater samples varied from 53 mg/L to 839 mg/L, with average of 276 mg/L. This means that all the sampled groundwater are fresh (TDS<1000) according to the TDS classification by Freeze and Cherry (1979). Based on the WHO/GSA guideline value, 60 out of 61 samples (98%) met the drinking water quality standard with regards to TDS. The variations in the TDS values may be due to differences in the solubility of minerals (WHO 2011). As a low-TDS depicts either slow decomposition of rocks or short residence time of the groundwater, this result corroborates the short residence time, mostly characterising the shallow aquifer as earlier suggested by the saturation index study. The TDS contents are in agreement with those obtained by Anku et al. (2009) and Nartey et al. (2012) in areas underlain by the crystalline basement rock and Voltaian rocks (sandstone, shale, mudstone, sand), respectively, in Northern Ghana. These results are very low compared to TDS values between 62 and 11,900 mg/L found in the Savelugu–Nanton District area, in Northern Ghana, with average and median values of 942 and 405, respectively (Tay 2012).

Regarding the turbidity, values ranged from 0 NTU to 13 NTU, with two samples exceeding 5 NTU. This may make the water unsuitable for potable use even though there is no health-based guideline value for turbidity in the WHO guidelines. Also 19 out of 61 samples (31%) may be difficult to disinfect in case of need of disinfection. In fact, the WHO guidelines suggest that, ideally, water should have turbidity lower than 0.1 NTU for an effective disinfection.

4.3.2. Total Hardness

In this study, total hardness as calcium carbonate ranged from 50.8 mg/L to 272 mg/L, with mean value of 115 mg/L. The classification of groundwater based on total hardness shown in Table 4-4 indicates that the groundwater in the Veve area is mostly moderately hard, with about 60.6 % of the samples falling in that category. About 19.7 % of the samples can be described as soft water while the other 19.7 % can be described as hard water. Globally, total alkalinity is higher than total hardness, suggesting that hardness of water is derived mainly from carbonate sources as stressed by Cobbina et al. (2012) who obtain total hardness ranging from 54.0 mg/L to 642 mg/L with a mean value of 178 in Sawla-Tuna-Kalba district in Northern Ghana. This result is similar to the findings of Anku et al. (2009) who obtain hardness ranging from 20.43 mg/L to 495.11 mg/L with 52 % of the samples falling in the moderately hard class. In an area underlain

by crystalline Basement Complex rocks in Nigeria, thus similar to this work, Ifabiyi (2008) obtained a mean value of total hardness of 236.04 mg/L, while Alagbe (2002) reports very low hardness ranging from 0.4 to 42.2 mg/L with an average value of 5.7 mg/L. In the crystalline basement aquifer of Côte d'Ivoire, Lasm et al. (2011) obtained total hardness ranging from 20 mg/L to 500 mg/L with a mean value of 116 mg/L. In Kara region located in Northern Togo underlain by crystalline basement rock, Zoulgami et al. (2015) obtained total hardness ranging from 10 mg/L to 340 mg/L with a mean value of 147 mg/L, which is greater than the one of this study. Regarding the surface water, all the samples analysed fall in the soft water class, with an average hardness of 38.8 mg/L. Thus, 19.7 % of the groundwater and all of the surface water appears to potentially have corrosive effect on the pipes or distribution system.

Table 4-4: Total hardness as CaCO₃ for groundwater in the Veia area, Northeast Ghana

Total hardness as CaCO ₃ (mg/L)	Water class	Number of study samples in each class
0-75	Soft	12 (19.7%)
75-150	Moderately hard	37 (60.6%)
150-300	Hard	12 (19.7%)

4.3.3. Major Ions

The range of the major ions concentrations in groundwater samples is reported in Table 4-2. The mean concentration values of the cations are in the order Ca²⁺>Mg²⁺>Na⁺>K⁺, whereas that for anions is HCO₃⁻>Cl⁻>SO₄²⁻>NO₃⁻. This result is similar to the findings of Anku et al. (2009); Yidana and Yidana (2010) and Boateng et al. (2016), thus it may suggest that this water type is one of the predominant water types in the crystalline basement aquifer in Ghana and especially in Northern Ghana in general. Tay (2012) obtained similar results in Savelugu–Nanton District in Northern Ghana and stressed that the high bicarbonate contents support the idea of occurrence of silicate weathering process in the area. HCO₃⁻ is found to be the dominant ion in the majority of works done up to now in the different geological formations in Ghana (Anku et al. 2009; Yidana and Yidana 2010; Fianko et al. 2010; Ganyaglo et al. 2011; Boateng et al. 2016). However, the order of classification of cations with respect to their contents varies from an area to another (e.g. Apambire et al. 1997). The hydrochemical water type of groundwater and surface water samples is represented in the Piper diagram (Figure 4-9). The diagram shows that bicarbonate is the

dominant anion. For the cations there is no dominant element for all the samples except one in which calcium is dominant. Except one sample with Ca-Mg-Cl-SO₄ water type, the chemical composition of water (groundwater and surface) in the study area is mainly Ca-Mg- HCO₃ water type, regardless of the geology. Chloride concentrations show an outlier (93.3 mg/L) for borehole “Bongo 3” situated in Bongo town which may come from anthropogenic sources. However, this value is below the standard limit which is 250 mg/L.

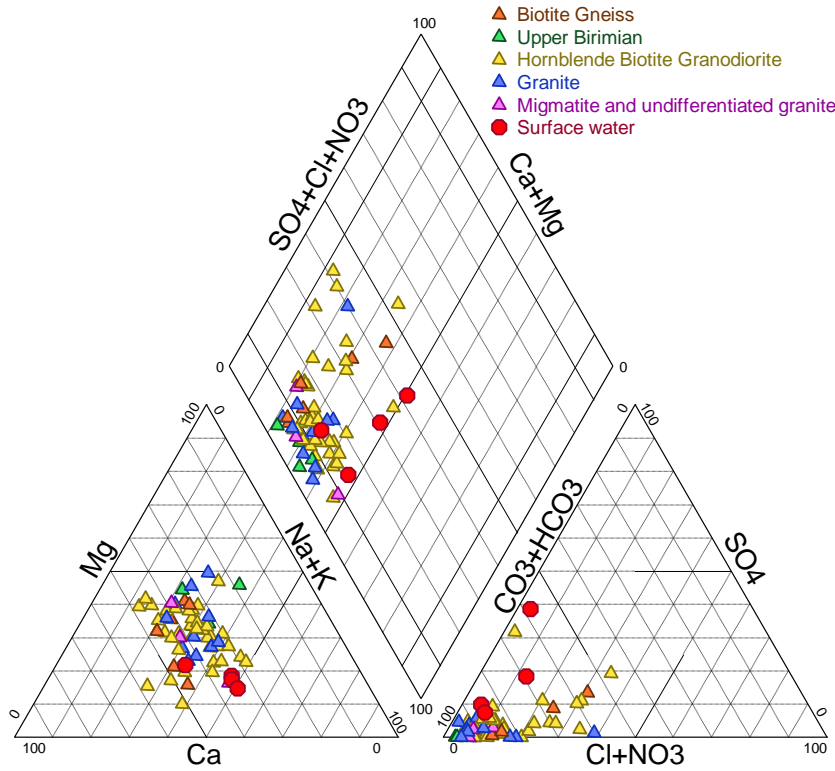


Figure 4-9: Piper diagram of the analysed groundwater samples (triangle) with respect to Geological formation and surface water samples

All the parameters analyzed are within the range of the GSA/WHO water quality guidelines and therefore can be said to be suitable for drinking. This can be explained by the fact that in the area and elsewhere in Ghana, groundwater accessed via boreholes are first analysed for drinking water quality before they are equipped with pumps for use. For that matter, only boreholes with good quality water are in use.

4.4. Usability of the water for irrigation

4.4.1. Sodium Absorption Ratio (SAR)

The plot of conductivity versus SAR in the Wilcox Log diagram shows one group with respect to the SAR and three groups to the conductivity (Figure 4-10). In this study, all the samples have low SAR values, ranging from 0.346 to 1.693 meq/L, and therefore are suitable for irrigation. In regards to EC, with the exception of two samples that belong to class C3, all the samples belong to Class C1 and C2. This means that the electrical conductivity in the study area is lower than 750 $\mu\text{S}/\text{cm}$ and the salinity ranges from low to medium salinity. Based on EC and SAR, three classes of irrigation water were found. Namely, C1-S1, C2-S1 and C3-S1 where the majority of samples belong to the second class (C2-S1). The results show an increase of electrical conductivity in surface water as you move from upstream to downstream, which implies there is a successive mineralisation of surface water along the flow path.

All the samples are classified as “excellent” as the SAR values are less than 10 meq/L. In fact, water with SAR value up to 10 meq/L, from 10 to 18 meq/L, from 18 to 26 meq/L and greater than 26 meq/L is classified as excellent, good, fair and poor, respectively (Raju 2006; Sadashivaiah et al. 2008). The result is in agreement with findings of Salifu et al. (2015). Analysis based on groundwater and surface water samples from the Birimian and Cape Coast Granitoid Complex formations in the Densu River Basin of Ghana shows that samples from Birimian and surface water are similar to samples of this current work as all of them plot in the excellent water category. However, the SAR values, ranging from 2.62 to 6.7 meq/L, are higher than those found in this current work, whose SAR values range from 0.346 to 1.693 meq/L. Regarding samples from the Cape Coast granitoid, only 73 % fall in the excellent category while 20 and 7 % fall in the good and doubtful category, respectively (Gibrilla et al. 2010). Regarding the Birimian formation, findings of Yidana et al. (2012) corroborate results of Gibrilla et al. (2010) and those of this current work. Although results of this current work are globally similar to the findings of Ganyaglo et al. (2011), whose study area is underlain by four main geological formations (the Upper Voltaian, the Togo, the Cape Coast granite complex and Lower Birimian), some differences should be highlighted. Two of their samples fell in classes C3-S2 and C3-S2; and C1-S1 and C3-S1 irrigation water classes were well represented while they are negligible in this current study. Using the Wilcox Log diagram, Yidana (2009) found that more than 90 % of

their surface water from different basins plots within the low sodicity and low to medium salinity fields. Similarly, the four surface water samples of this current work fall within this two classes.

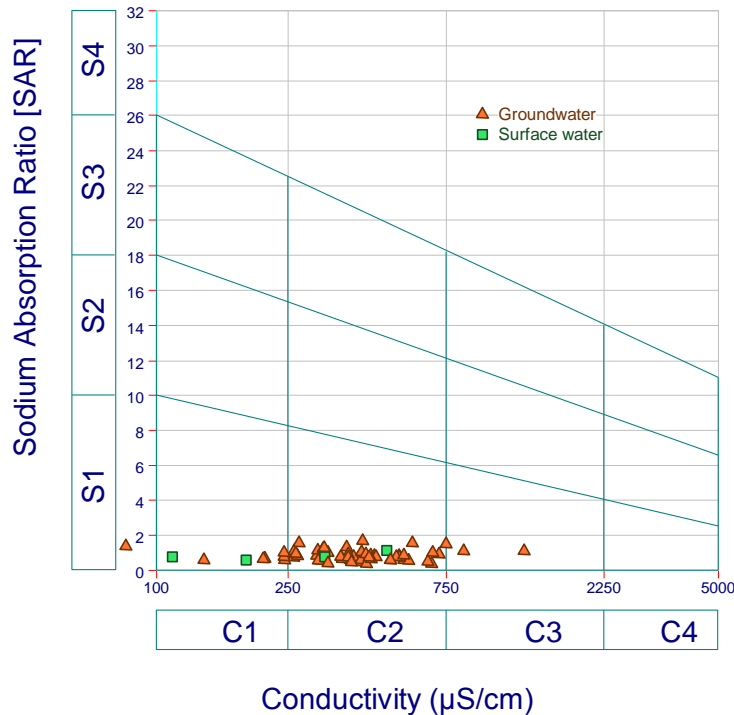


Figure 4-10: Wilcox Log diagram of groundwater in the Veia area, Northeast Ghana

4.4.2. Sodium percentage

The percentage of sodium in water in the study area ranges from 12.8 % to 49.0 %, with an average of 30.3 % for groundwater and from 33.6 % to 50.7 %, with an average of 44.8 % for surface water. The plot of sodium percentage with respect to EC in the Wilcox diagram (Figure 4-11) has revealed that out of 61 samples, 59 fall under excellent irrigation water quality class and the remaining two samples fall in the good irrigation water class. Based only on the sodium percentage (Wilcox 1955), 82 % of the samples are classified in the good water category, while 6.6 % and 11.4 % fall in the excellent and permissible category, respectively. Using the same classification, Ma (2016) found that 40 % of the samples belong to the excellent category, with 31 %, 25 % and 4 % belonging to the good, permissible and doubtful categories, respectively. Using the Wilcox diagram (Wilcox 1955) for irrigation water classification, he observed that about 62.5 % of the groundwater samples plotted in the excellent to good irrigation water category, with 31.25 % of the groundwater samples falling in the good to permissible water

classes and 3 % of the samples were classified as unsuitable for irrigation. Classification of water samples from Densu River Basin of Ghana suggested that 100 % of the surface water and 83 % of the Birimian were excellent to good while 16 % of the Birimian samples fell in the permissible to doubtful group. Regarding the Cape Coast granitoid, it showed a wide variation in the Wilcox diagram as 53 % of the samples fell in the excellent to good field, while 33 % plotted in the field permissible to doubtful and 13 % were doubtful to unsuitable (Gibrilla et al. 2010). His results deviate from the findings of this current work. The work done by Edjah et al. (2015) in the Ellebelle district in Ghana mainly underlain by Birimian rocks, showed that 38.46 % of the hand-dug wells and 60 % of the boreholes fell in the field of excellent to good while the permissible to doubtful category was represented by 30.77 % of the hand-dug wells and 34.44 % of the boreholes. 30.77 % of the hand-dug wells and 5.56 % of the boreholes plotted on the boundary between excellent to good and permissible to doubtful.

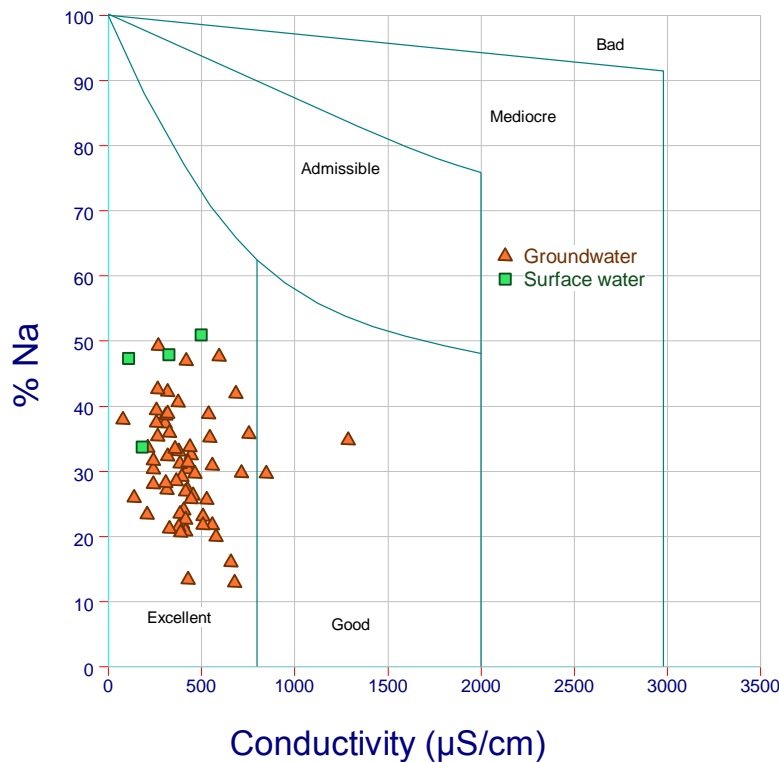


Figure 4-11: Rating of groundwater samples based on electrical conductivity and percent sodium in Vea area, Northeast Ghana

4.4.3. Residual Sodium Carbonate (RSC)

The values of RSC of all the samples analyzed in this study ranged from -1.84 meq/L to 1.83 meq/L and only two of them have values higher than 1.25 meq/L. Thus, they are suitable for irrigation. Anku et al. (2009), whose study area encompasses this study area, found that 68% of their samples had RSC values below 1.25 meq/L; 27 % in the marginal range of 1.25 meq/L –2.5 meq/L; and the remaining 5 % was not suitable for irrigation. Analysis of water from some Voltaian and Birimian aquifers in Northern Ghana revealed that 34 % of the samples have RSC values higher than 2.50 meq/L suggesting that they are not suitable for irrigation, while 42 % were excellent as their RSC values were lower than 1.25 meq/L. 24 % of the samples were classified in the intermediate group (Yidana et al. 2012). Based on the RSC, Kaka et al. (2011) found that 44 % of the samples were doubtful, while 32 % having RSC values above 2.50 mg/L were not suitable for irrigation and only 24 % were good as their RSC values were less than 1.25 meq/L. As for Salifu et al. (2015), they concluded that 56 % of the samples were safe for irrigation, while 34.78 % were marginal and the remaining 8.7 % were unsuitable for irrigation purpose. Thus, regarding the RSC these aforementioned works show quite different results compared with the current study.

4.4.4. Magnesium Hazard (MH)

Generally, Ca^{2+} and Mg^{2+} maintain a state of equilibrium in most waters, although in soil systems, Ca^{2+} and Mg^{2+} do not behave equally and Mg^{2+} deteriorates soil structure particularly when waters are sodium dominated and highly saline (Ravikumar et al. 2011). According to Batayneh et al. (2012), water with calcium and magnesium concentration of higher than 100 mg/L and 50 mg/L, respectively, is not suitable for irrigation purposes. In the study area, the calcium contents range from 12.3 mg/L to 76.2 mg/L, whereas magnesium contents range from 2.5 mg/L to 37.9 mg/L. Thus, considering this criterion, all the samples from the study area are suitable for irrigation.

As for the MH, values obtained in this study ranges from 16.46 % to 71.45 % and 17 out of the 61 groundwater samples analyzed (representing 27.9 %) have MH greater than 50 %, which makes them inappropriate for irrigation (Raihan and Alam 2008). Salifu et al. (2015) found in Upper West region of Ghana that the MH of all the samples analysed in their study were well

below 50 %. In the Manya Krobo area, Kaka et al. (2011) reported that the MH values of 56 % of the samples were below 50 %, while 44 % of the samples was found to be unsuitable with MH above 50 %.

4.4.5. Permeability index (PI)

In the study area, 7 out of the 61 samples (11.5 %) fall in class III and the remaining 88.5 % fall in class I and II (Figure 4-12). It means that based on this indicator, 11.5 % of the samples are not suitable for irrigation, whereas the remaining 88.5 % are suitable. Based on Doneen's chart and the USSL diagram, Salifu et al. (2015) found PI varying from 65.09 to 99.39 and 96.65 % of the samples fell in Class I while only one sample representing 4.35 % was categorized in Class II. Kaka et al. (2011) mentioned that PI of samples collected from the Manya Krobo area during the post monsoon season of September 2009 ranged from 17.15 % to 77.14 %. Additionally, they suggested that all the samples fell under classes I and II of Doneen's chart. Results of this current work slightly deviate from those of Kaka et al. (2011) and Salifu et al. (2015) but are close to those of Gibrilla et al. (2010) regarding samples from the Cape Coast granitoid formation. In fact, Gibrilla et al. (2010) mentioned that 87.5 % of the Cape Coast granitoid belongs to Class I while the remaining 12.5 % belong to Class II group; all the samples from Birimian formation and surface water fell in Class I.

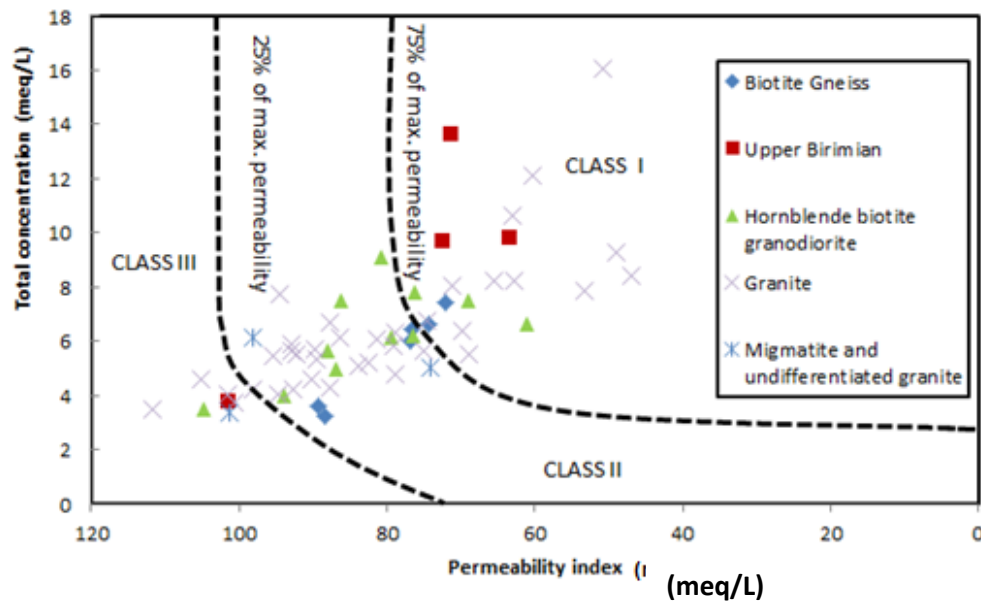


Figure 4-12: Classification of irrigation water in Veua (northeast Ghana), based on permeability index

4.5. Statistical analyses

The normality test as summarized in Table 4-5 showed that all the parameters, except pH, do not follow a normal distribution. So these parameters were log-transformed and normalized prior to the KMO and Bartlett's sphericity tests and subsequently for use in the PCA and HCA.

Table 4-5: Normality test of the variables based on 4 methods

Variable\Test	Shapiro-Wilk	Anderson-Darling	Lilliefors	Jarque-Bera
pH	0,592	0,570	0,257	0,456
EC	0,005	0,010	0,016	0,013
DO	0,043	0,069	0,070	0,207
Col	< 0.0001	< 0.0001	< 0.0001	< 0.0001
Ca	< 0.0001	0,000	0,001	< 0.0001
Mg	0,000	0,004	0,055	< 0.0001
HCO ₃ ⁻	0,001	0,010	0,035	< 0.0001
Cl ⁻	< 0.0001	< 0.0001	< 0.0001	< 0.0001
Na ⁺	< 0.0001	< 0.0001	0,000	< 0.0001
K ⁺	0,000	0,007	0,012	< 0.0001
NO ₃ ⁻	0,008	0,048	0,151	0,193
PO ₄	0,001	0,001	0,003	0,011
Fe	< 0.0001	< 0.0001	< 0.0001	< 0.0001

For the Bartlett's sphericity test, summarized in Table 4-6, two hypotheses are made:

- H₀: There is no correlation significantly different from 0 between the variables.
- H_a: At least one of the correlations between the variables is significantly different from 0.

As the computed p-value is lower than the significance level $\alpha=0.05$, one should reject the null hypothesis H₀, and accept the alternative hypothesis H_a. The risk to reject the null hypothesis H₀ while it is true is lower than 0.01%. Meaning that there are correlations between

parameters that need to be explored. Regarding to the KMO, it was found to be equal to 0.681, showing that it is adequate to use Principal Component analysis to find correlation in the dataset (Mustapha and Aris 2012).

Table 4-6: Bartlett's sphericity test

Chi-square (Observed value)	1130,719
Chi-square (Critical value)	129,918
DF	105
p-value	< 0.0001
alpha	0,05

4.5.1. Principal Component Analysis (PCA)

4.5.2. Correlation between parameters

The correlation matrix (Table 4-7) describing the interrelationship between variables (Mor et al. 2009), shows that with a significance level $\alpha=0.05$ there are: a high positive correlation between Ca^{2+} with EC (0.85), Ca^{2+} -salinity (0.828), Mg^{2+} - HCO_3^- (0.801), HCO_3^- with EC and TDS (0.719); positive moderate correlation between Mg^{2+} with EC and TDS (0.656), Mg^{2+} -salinity (0.639), Mg^{2+} - Ca^{2+} (0.563), Ca^{2+} - HCO_3^- (0.656), Na^+ - HCO_3^- (0.687); and a negative moderate correlation between DO - HCO_3^- . The very high correlation between Mg^{2+} and HCO_3^- reveals that they are from the same source. Thus they may form from magnesite which, according to Worrall (2013) as shown in Table 4-8, is formed from the weathering step of biotite, hornblende present in the study area (Yao and Robb 1998; Pelig-Ba 2012). The correlations from moderate to high between these EC with Ca^{2+} , HCO_3^- and Mg^{2+} suggest that they are controlled by these ions (Sundaray 2010). The moderate correlation (close to high correlation) shed light on the silicate weathering process analyses in section 4.2.2. This moderate correlation may also confirm the presence of other process in controlling water quality in the area as suggest earlier. Regarding to the moderate correlation of Ca^{2+} with HCO_3^- it suggests that the water samples originate from fresh recharge (Lakshmanan et al. 2003).

Table 4-7: Correlation matrix of the hydrochemical parameters.

Variables	EC	DO	Col	Ca	Mg	HCO ₃ ⁻	Cl ⁻	Na ⁺	K ⁺	PO ₄	Fe	pH	NO ₃ -N
EC	1												
DO	-0.329	1											
Col	-0.100	0.172	1										
Ca	0.850	-0.275	-0.084	1									
Mg	0.656	-0.293	-0.270	0.563	1								
HCO ₃ ⁻	0.719	-0.553	-0.187	0.656	0.801	1							
Cl ⁻	0.409	0.399	-0.001	0.376	0.255	-0.021	1						
Na ⁺	0.402	-0.387	0.036	0.347	0.329	0.688	0.017	1					
K ⁺	0.187	-0.048	0.115	-0.002	0.102	0.215	0.079	0.231	1				
PO ₄	-0.150	0.109	-0.127	-0.194	-0.119	-0.182	-0.012	-0.027	-0.171	1			
Fe	-0.036	0.025	0.041	0.065	-0.049	-0.064	0.050	-0.052	-0.049	-0.171	1		
pH	0.255	-0.422	-0.126	0.381	0.228	0.432	-0.205	0.245	-0.127	-0.114	0.116	1	
NO ₃ -N	0.081	0.067	0.218	0.112	0.011	-0.037	0.130	-0.190	-0.078	-0.099	-0.022	-0.081	1

Values in bold are different from 0 with a significance level alpha=0.05

Table 4-8: Composition of Igneous Rocks and their Breakdown (Worrall 2013)

Mineral	Approximate formula	Approximate % present		Probable decomposition products
		Granite	Basalt	
Orthoclase	$KAlSi_3O_8$	} 70	} 10	Kaolinite, colloidal silica, K_2CO_3
Anorthite	$CaAl_2Si_2O_8$			Kaolinite, colloidal silica, $CaCO_3$
Quartz	SiO_2	25	-	Unchanged
Hornblende	$((Na,K)_2(Fe^{2+},Mg)(Fe^{3+},Al)_4Al_2Si_6O_{22}(OH)_2$	-	} 90	Kaolinite or montmorillonite, limonite, haematite, $CaCO_3$, $MgCO_3$, colloidal silica
Pyroxene	$(Mg,Fe)SiO_3$	-		Colloidal silica, limonite, haematite, $MgCO_3$
Olivine	$(Mg,Fe)_2SiO_4$	-		As for pyroxene
Muscovite	$KAl_3Si_3O_{10}(OH)_2$	} 5	-	Probably unchanged
Biotite	$K(Mg,Fe)_3Si_3AlO_{10}(OH)_2$		-	Kaolinite or montmorillonite, iron oxides, colloidal silica, $MgCO_3$, K_2CO_3

4.5.3. Extraction of Components

PCA was applied to the 13 physiochemical parameters in Table 4-7 and it yielded factors or principal components. There are several criteria to identify the number of factors to be retained in order to understand the underlying data structure (Joreskog et al. 1976; Jackson 1991; Reyment and Jvreskog 1996). Here, PCs having an eigenvalue greater than 1 were retained so a five significant factors or principal components explaining 73.58% of the variance (i.e. information) of the original data set were retained (Table 4-9 and Figure 4-13). The two first factors, namely F1 and F2 explain 31.11% and 13.98% of the variance, respectively. Thus, they account for the majority of the variance in the original dataset. The factor loadings after varimax rotation presented in Table 4-10, show that F1 is mainly contributed by EC, Ca, Mg, HCO₃, and Na. Therefore, the variance can be initially assigned to 'natural mineralization' processes originating from water-rocks interaction. In this study these mineralization processes are mainly silicate weathering and ion exchange. F2 is contributed by Cl⁻ and DO. The contribution of F3 is linked to col and PO₄ and can be defined by "color factor". F4 is mainly contributed by K⁺ while F5 is contributed by NO₃⁻ and Fe. As NO₃⁻ is an indicator of pollution and it is negatively correlated with the factor, the latter can be defined as "safety to pollution". Because of the positive correlation of NO₃⁻ with Fe, it can be concluded that the more groundwater is protected from pollution, the more it contains Fe. Figure 4-14 summarizes the correlation between parameters and factors on the one hand and between parameters on the other hand on two plans.

Table 4-9: Eigenvalue, variability and cumulative (%) of each of the extracted components.

	Eigenvalue	Variability (%)	Cumulative %
F1	4.045	31.112	31.112
F2	1.817	13.978	45.091
F3	1.341	10.314	55.404
F4	1.295	9.963	65.367
F5	1.067	8.208	73.575
F6	0.876	6.737	80.313
F7	0.672	5.173	85.486
F8	0.562	4.325	89.810
F9	0.466	3.588	93.399
F10	0.443	3.405	96.803
F11	0.284	2.186	98.989
F12	0.105	0.811	99.801
F13	0.026	0.199	100.000

Components in bold are considered to be the most significant.

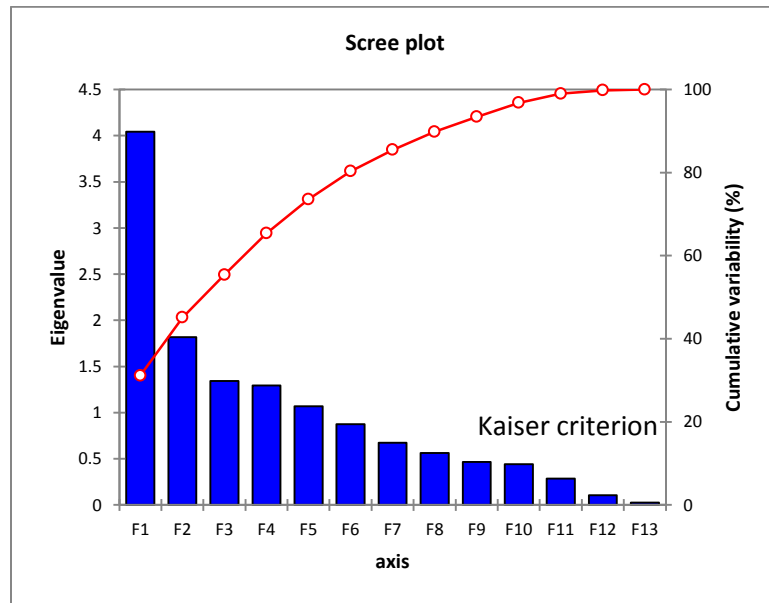


Figure 4-13 Screen plot of principal components showing change on slope after

Table 4-10: Factor loadings after varimax rotation

	F1	F2	F3	F4	F5
EC	0.860	0.337	-0.062	-0.005	-0.042
DO	-0.563	0.593	-0.143	0.053	0.180
Col	-0.209	0.242	0.672	0.126	-0.264
Ca	0.815	0.311	-0.037	-0.248	-0.024
Mg	0.792	0.155	-0.219	0.014	0.003
HCO ₃ ⁻	0.942	-0.140	0.027	0.114	-0.063
Cl ⁻	0.177	0.843	-0.237	0.022	0.203
Na ⁺	0.633	-0.200	0.131	0.393	0.038
K ⁺	0.192	0.133	0.385	0.689	0.210
PO ₄	-0.227	-0.121	-0.645	0.182	-0.189
Fe	-0.012	0.050	0.322	-0.489	0.648
pH	0.494	-0.434	0.084	-0.432	0.013
NO ₃ -N	-0.026	0.422	0.259	-0.337	-0.644
Eigenvalue	4.045	1.817	1.341	1.295	1.067
Variability (%)	31.112	13.978	10.314	9.963	8.208
Cumulative %	31.112	45.091	55.404	65.367	73.575

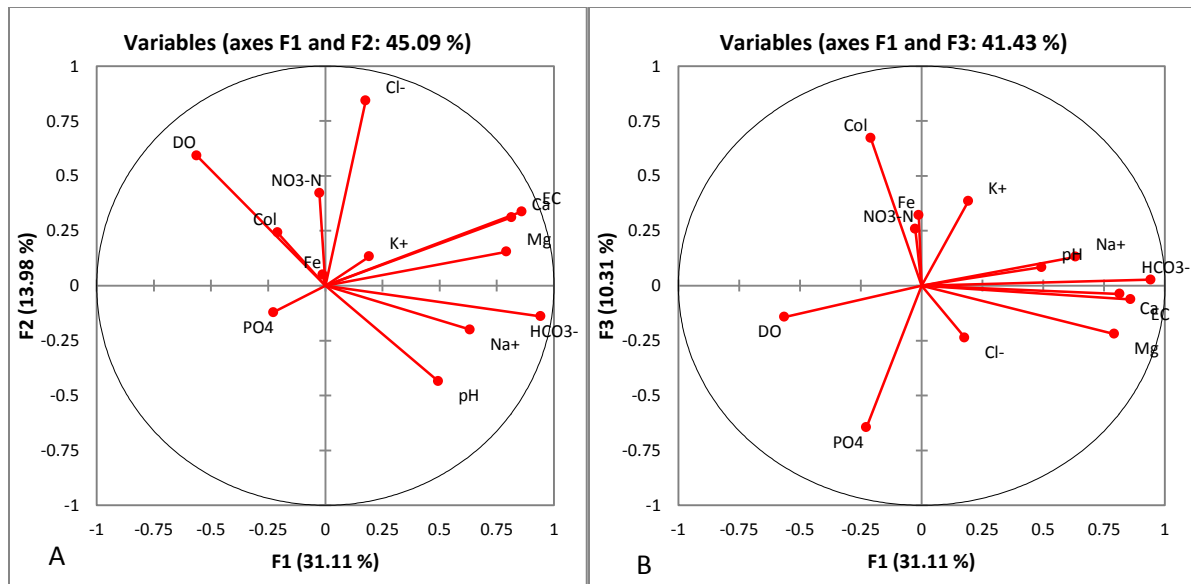


Figure 4-14: Plot of the variables on the plan F1-F2 (A) and plan F1-F3 (B) summarising correlation between variables and factors in the one hand and between parameters in the other hand.

4.5.4. Agglomerative hierarchical clustering (AHC)

The HCA classified the samples into 3 clusters (Figure 4-15). C1, C2 and C3 are composed of 12, 19 and 29 samples, respectively. Among these groups, samples of C2 and C3 have more similarity compared to those of C1. C2 and C3 are linked at a dissimilarity level of about 80 while they are different to those C1 at dissimilarity level of about 190. Figure 4-16 shows that the classification is not related to the geology even though samples falling in the hornblende biotite granodiorite formation are largely composed of C2 and C3 while the 4 samples falling in the birimian formation belong to C2 except for one which is from C1. The Stiff diagram in Figure 4-17 shows samples from C1, C2 and C3 are characterized by low, high and medium mineralisation, respectively.

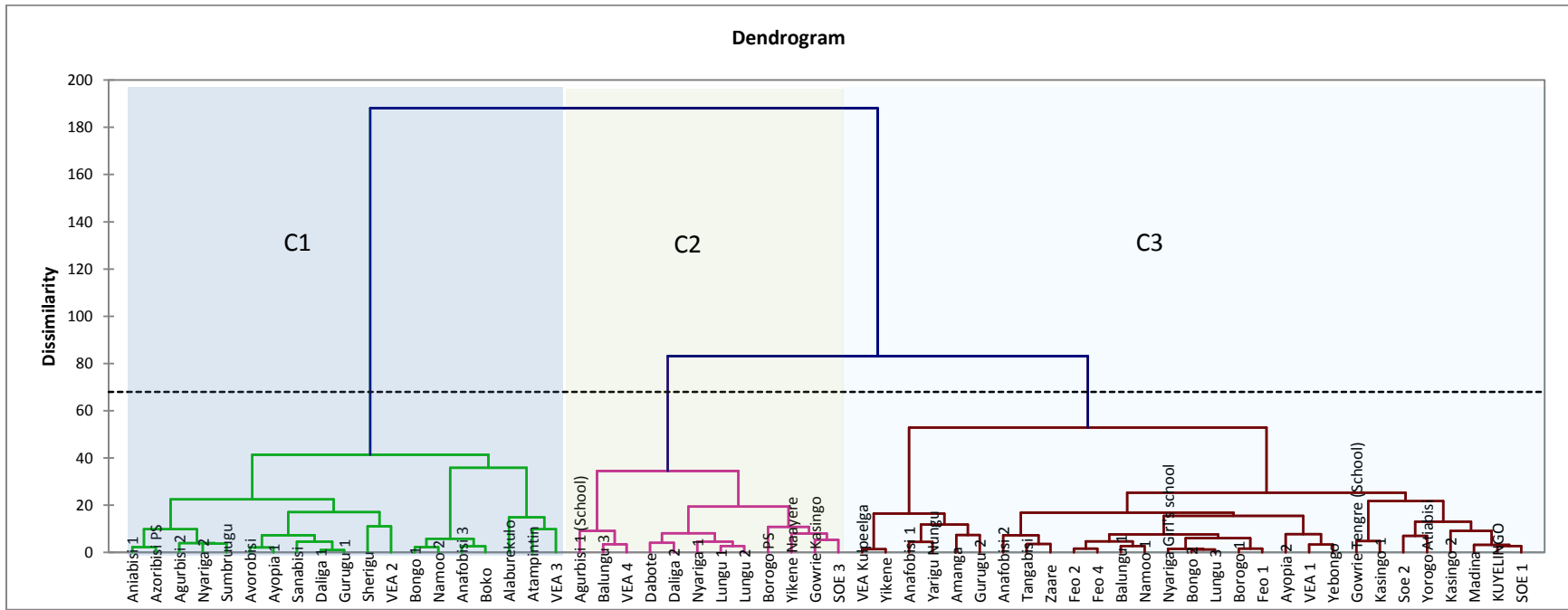


Figure 4-15: Dendrogram for the groundwater samples, showing the division into three clusters.

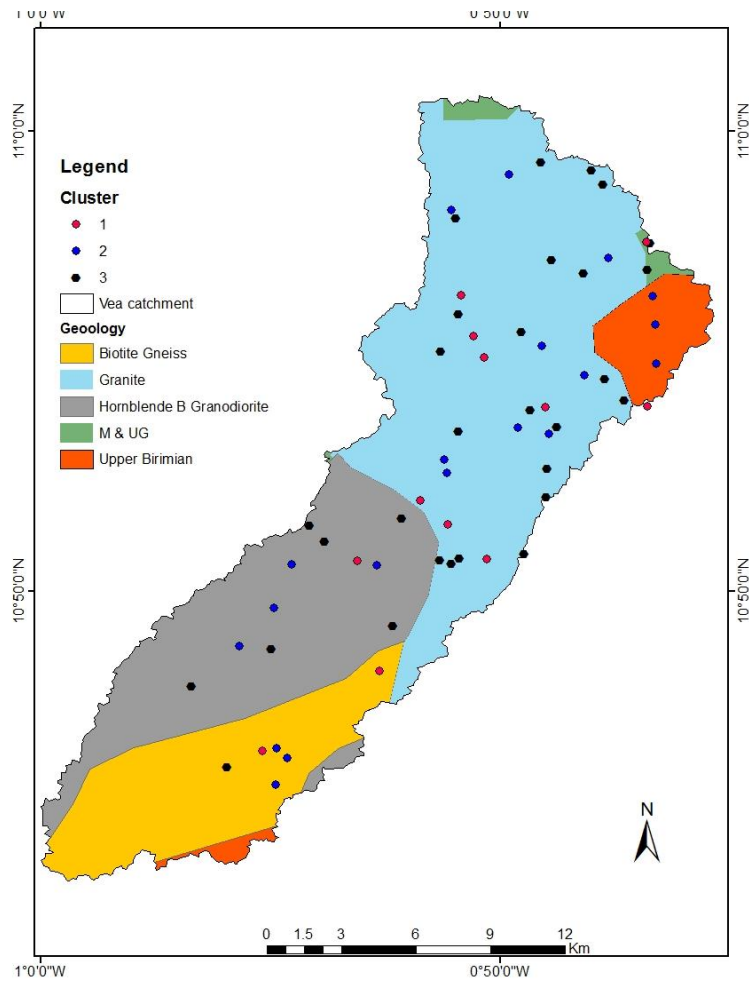


Figure 4-16: Distribution of the different clusters in the Veia catchment, Northern Ghana

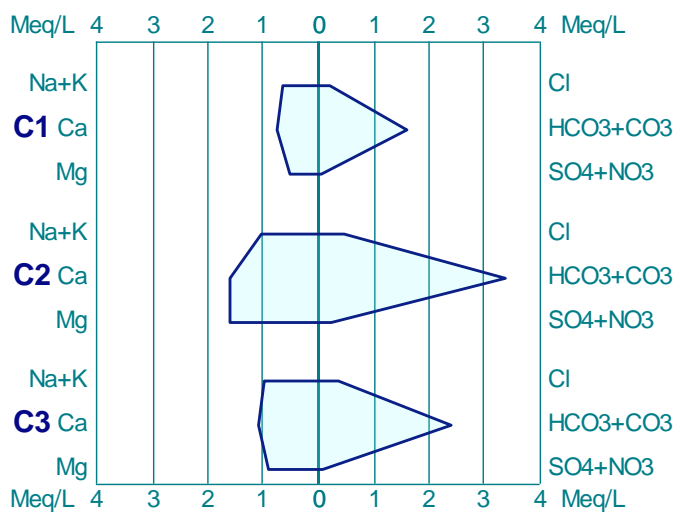


Figure 4-17: Stiff plot of major anions of the three clusters

4.6. Stable isotopes

Deuterium ratio of Groundwater varies from -24.602 to -15.245 while for surface water it varies from -12.307 to -5.600. Regarding ^{18}O ratio, it fluctuates between -4.262 and -2.758 for groundwater while it varies from -2.214 to -0.957 for surface water. The surface water samples lie on a regression line of equation $\delta^2\text{H}=5.2021 * \delta^{18}\text{O} - 0.5092$. Except for the sample from Avorobisi, all the samples have a deuterium excess lower than 9. This suggests that water recharging the aquifer undergone evaporation. This implies that the aquifer is recharged by flooded rain water. Thus focused recharge is the main recharge process in the area, supporting finding of many studies in semi-arid and arid regions (Wood and Sanford 1995; Gates et al. 2011). This idea is also supported by previous section of this work that highlighted that water in the area was fresh as suggested earlier by the statistical analysis (section 4.5.1). It is also observed that Deuterium excess of the sample of Gurugu dam is lower than the one of Vea dam, suggesting that Gurugu Dam is more affected by Evaporation than Vea dam. This could be explained by the sizes of these dams. In fact, Vea dam is far bigger than Gurugu dam thus the latter is faster affected by the fractionation process than the former. The sample “Avorobisi” plot on the GMWL suggesting that recharge source does not undergo evaporation. This implies that the aquifer is recharged from diffused source which is mainly rainfall. This site is quietly located at the border of the forest zone of the catchment. Thus recharge zone of this aquifer may be located in the forest. Forest may promote diffuse recharge as forest is known to promote more infiltration than runoff. Figure 4-18 shows that there are quite some differences between isotopes ratio in groundwater and surface water, suggesting that there is a little/no link between surface and groundwater in the catchment. Groundwater is more depleted in both ^{18}O and ^2H than the surface water. This result is similar to findings of many studies in Ghana (e.g., Acheampong and Hess 2000; Jørgensen and Banoeng-Yakubo 2001; Kortatsi et al. 2009). A similar result was also found by Ray et al. (2017) in a Precambrian sedimentary terrain in Central India. Although the relation between altitude and isotope ratio of groundwater is not strong, the distribution of the scatter on and around the regression lines of the two groups show that higher altitudes samples are globally depleted than those of low altitude. Banoeng-Yakubo et al. (2009) found a similar result in Volta Region in Ghana underlain by three main geological terrains, namely, the Buem, the Togo and Voltaian formations.

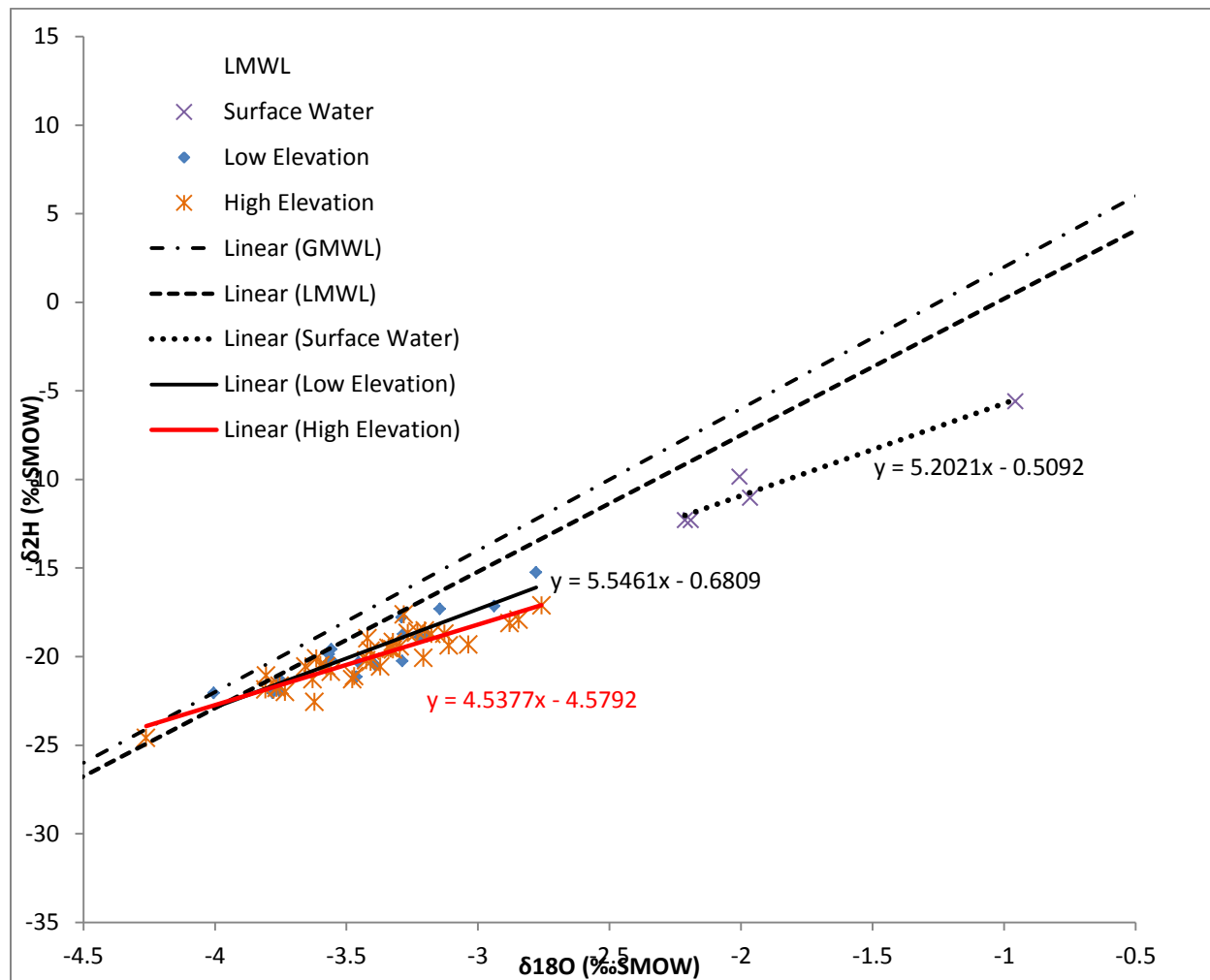


Figure 4-18: Plot of deuterium with respect to Oxygen 18

4.7. Conclusion

The aim of this work was to identify the geochemical processes influencing water quality and the suitability of surface and groundwater for agricultural and domestic uses in the area. The results show that cation exchange and silicate weathering are the dominant processes controlling the chemical composition of the groundwater in the studied area. The meteoric genesis index shows that the majority of samples belong to shallow meteoric water percolation. All the groundwater samples were found to be fresh based on the TDS values. The results obtained from the 65 water samples also show that water type in the study area is mainly Ca-Mg-HCO₃. According to the

observations and calculations conducted in this study, groundwater in the area is in large parts suitable for irrigation and agricultural purposes. No pollution due to anthropic activities was detected. Surface water is also found to be suitable for irrigation. PCA was found to be a useful tool as it yielded 5 significant factors from the original dataset of 15 parameters. The PCA also suggested that the groundwater samples originated from fresh recharge. The HCA classified the water samples into 3 classes that were found to be related to the level of mineralization of the samples but not to the geological formations. Samples of C1 have relatively lowest mineralization whilst C2 is composed of those of highest mineralisation and C3 is the transitional groups between them.

This is the first study to really address the hydrogeochemical processes influencing this area's water quality. Further study including heavy metals, other inorganic and organic trace substances as well as microbiological parameters is required to fully characterize groundwater hydrogeochemistry and usability, ideally also taking seasonal effects into account. Analyses based on stable isotope ratio of surface and groundwater suggest that focused recharge from flooded rain water dominates in the study area. Further, no link between surface and groundwater was found. In order to find whether the aquifer in area is recharged by heavy rains or light rains, or both, study taking into account $\delta^2\text{H}$ and $\delta^{18}\text{O}$ in rain is suggested.

Results of this chapter will help to really understand and discuss finding related to groundwater recharge that will presented in chapter 5.

Chapter 5 -ESTIMATION OF GROUNDWATER RECHARGE

5.1. Introduction

This chapter presents and discusses results of recharge estimated by four of the five methods used during this research work, namely the streamflow hydrograph analysis, the Water Table Fluctuation (WTF) method, the Chloride Mass Balance (CMB) method and the modelling method using WetSpa model. Results of the fifth method, namely the simple water balance method, are presented in Chapter 6 as the analysis of the impacts of climate change was based on recharge estimated by this method.

Regarding the streamflow hydrograph analysis, groundwater recharge was estimated using recession curve analysis and baseflow was estimated by four automated tools designed for hydrograph separations. These tools were: Web-based Hydrograph Analysis Tool (WHAT) (Lim et al. 2005), AdUKIH (Aksoy et al. 2008), EcoHydRology package of R (Fuka et al. 2013) and Aquapak (Nathan et al. 2007). The baseflow was estimated using three different options implemented in the WHAT tool whereas the three others use only one method. Hence six different methods were used to estimate baseflow. Prior to recharge estimation and the baseflow separation, hydrograph recession analyses was conducted and used for testing the performance of the baseflow filter models and recharge estimation.

The WTF and CMB was applied in the crystalline basement aquifer of Northern Ghana (Figure 2-5) which extends over parts of the three northern regions of Ghana, namely: the Upper East, Upper West and Northern regions, while the streamflow hydrograph analysis and the WetSpa model were applied in the Sissili basin with the outlet at Wiasi (Figure 3-1) which extends from Burkina-Faso to Northern Ghana.

Although groundwater recharge can result from other source than precipitation most the study related groundwater recharge to precipitation. Therefore in this work, groundwater recharge rate is either presented as water depth or converted from water depth to percentage of annual or seasonal rainfall.

5.2. Recharge estimation using streamflow hydrograph analysis

5.2.1. Recession analysis

An example of MRC is shown in Figure 5-1 while Table 5-1 presents the performance of the different regression models of the baseflow recession spreadsheet of Posavec et al. (2006) in fitting baseflow recession of the Sisili streamflow at Wiasi. The resulting coefficient of determination (R^2) values are all acceptable based on the work of Santhi et al. (2001) and Van Liew et al. (2003). The results also show that, except for the linear regression model, all the other models had good values for the coefficient of determination, meaning that they are able to fit baseflow recession in the watershed. The power regression is the model that best fitted baseflow recession of the Sisili river. It was followed by the exponential regression. In decreasing order of performance, the models are listed as: power regression, exponential regression, logarithmic regression and polynomial regression $y=f(x)$ having the same R^2 , polynomial regression $x=f(y)$ and linear regression. Thus the plausible baseflow recession in the area may be a power function.

Table 5-1: Performance evaluation of the different recession methods in the study area

Models	Equation	Coefficient of determination (R^2)
Linear regression	$y = -0.9848x + 73.717$	0.54
Power regression	$y = 435.31x^{-1.068}$	0.94
Exponential regression	$y = 55.911e^{-0.034x}$	0.86
Logarithmic regression	$y = -39.86\ln(x) + 162.14$	0.82
Polynomial regression $y = f(x)$	$y = 0.0606x^2 - 6.1083x + 149.86$	0.82
Polynomial regression $x = f(y)$	$y = 0.005x^2 - 1.1565x + 62.21$	0.70

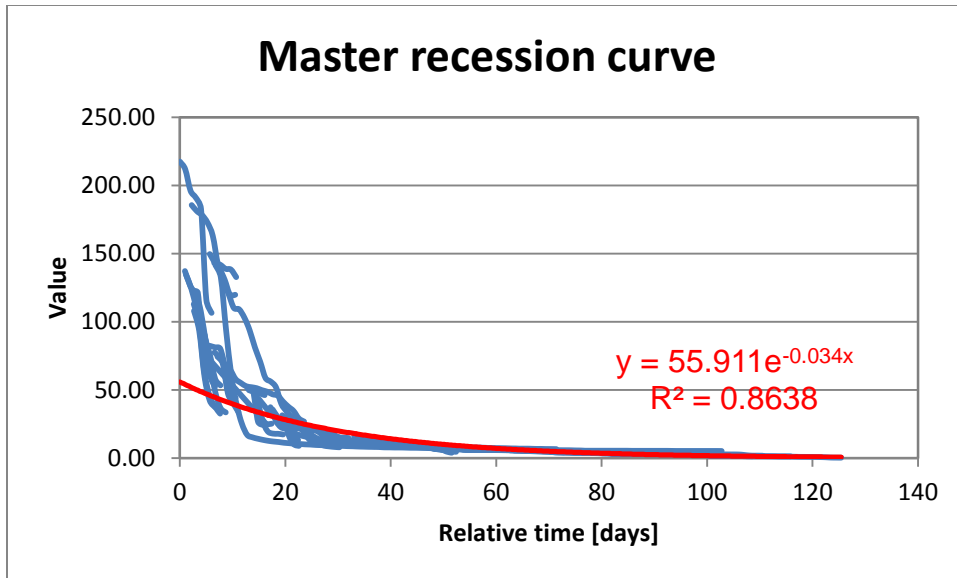


Figure 5-1: Power regression MRC of the Sisili river, tributary to the White Volta River, 2003-2007, Northern Ghana

5.2.2. Recharge estimated by recession analysis

Estimated annual recharge ranges from 27 mm in 2004 to 66 mm in 2008 (Figure 5-2). Although the smallest amount of rainfall occurred in 2005, recharge in this year was higher than what was estimated for 2007 where the highest rainfall during the study period occurred, suggesting that there is no linear correlation between groundwater recharge and rainfall amount in the study basin. This corroborate the fact that recharge does not always depend only on rainfall amount as indicated by several studies (e.g. Wu et al. 1996; Owor et al. 2009). Recharge also depends on rainfall patterns such as its temporal distribution and intensity as well as on the evapotranspiration. Owor et al. (2009) found that a better relationship between rainfall and recharge exist only when rainfalls exceeded a threshold of 10 mm/day in the Upper Nil basin. Results of this current work show that, the highest recharge was obtained in the year 2005. The estimated recharge ranged from 3% to 9% of the annual rainfall (Table 5-2), with an average of 5%. Results of this current work are similar to findings of several works done in similar geological formation around the study area. The average value is close to findings of Martin (2006) and Sandwidi (2007) who used chloride mass balance method in the Atankwidi catchment in Northern Ghana and in Kompienga Dam Basin in south-eastern Burkina Faso, respectively. The former obtain a long term recharge of 6% while the latter obtain 5.3%. In the crystalline rock aquifer of southwestern Ghana, Yidana et al. (2013) used a numerical

groundwater model (MODFLOW) to estimate groundwater recharge ranging from 0.25% to 9.13% of the annual rainfall. Using three methods, namely CMB, WTF and physically-based hydrological model (SWAT), Obuobie (2008) obtain average recharge ranging between 7% and 8% in the White Volta river basin.

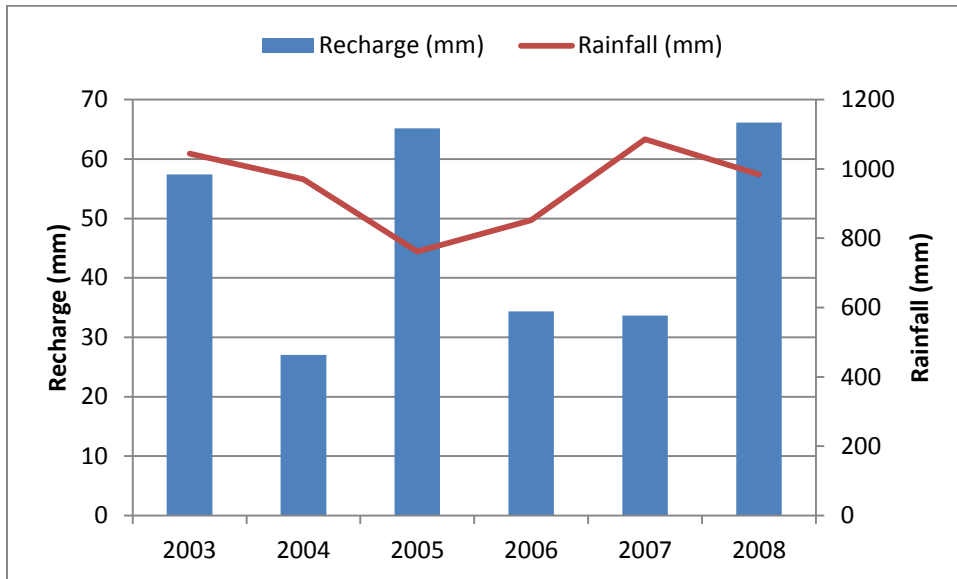


Figure 5-2: Annual recharge and rainfall amount

Table 5-2: Annual recharge in percentage

Years	Recharge (%)	Weighted average annual rainfall (mm)
2003	5	1044
2004	3	971
2005	9	761
2006	4	852
2007	3	1086
2008	7	984

5.2.3. Baseflow Separation

Before analysing baseflow, the quality of the flow data was first controlled in order to remove the flow yielded by other sources other than groundwater discharge and rainfall (Figure 5-3). It was observed that the highest flow during a given year (or the peak flow) occurred after the annual peak of rainfall and the low flow are obtained during the dry season. During the study period (2003-2008), the highest monthly rainfall occurred in August 2007 while the highest peak flow was obtained in September 2008. The different recession models discussed in section 5.2.1

identified all the dry seasons as recession period. These analyses suggested that the sources of streamflow in the dry season are mainly from groundwater discharge (baseflow) and rainfall. In other word, effect of dam (delay flow) and irrigation water within the watershed can be considered negligible. This therefore implies that, the baseflow component of the streamflow data can be equated to the groundwater discharge in the study area. The quality control analysis revealed a lag of about a month between the onset of rainfall and the end of recession or the rise of flow. This may be attributed to water losses owing to relatively high evapotranspiration and the high soil water deficit inherited from previous dry season (Pelig-Ba 2004) but also to the watershed characteristics (e.g. slope, soils and land use). As the size of river channel is big, water losses along the river channel during the period January-May might be considerable.

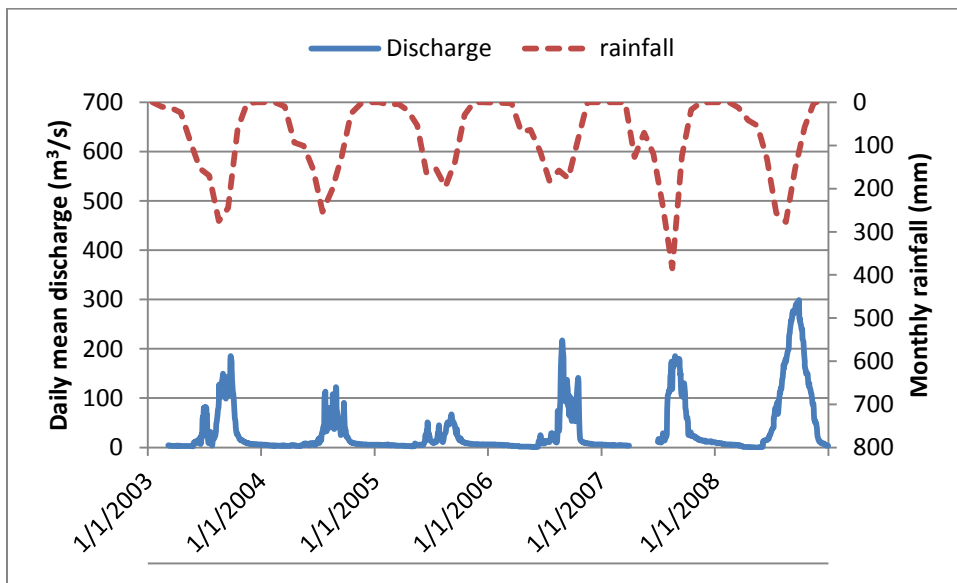


Figure 5-3: Comparison of discharge with rainfall for quality control

The highest flashiness index (FI) of the study period is 0.26 and was obtained in June 2005, while the smallest FI of about 0 was estimated in January 2006 (Figure 5-4). The highest values of FI are found at the beginning of the raining season in which low BFI are obtained and peak FI is obtained before the annual peak of rainfall. Figure 5-5 shows that the smaller the BFI the higher the FI. In fact, the rapidity of the rise and fall of the peak of streamflow (i.e. the flashiness) is controlled by quickflow while the baseflow sustains the flow during periods of no rains. The highest monthly average FI during the study period was 0.16 which was obtained in June although August is the month receiving the highest amount of rain as pointed out by many

studies (e.g. Obuobie 2008). The average monthly flashiness index during the study period is 0.06. Therefore, following the work by Baker et al. (2004) that classified the rivers by taking into account both the area of the watersheds and the flashiness index, the Sissili river at Wiasi is classified as stable river. On annual basis, FI ranges from 0.03 to 0.15 (Figure 5-8). It was also observed that when the BFI increases the FI decreases and vice versa, revealing the inverse relationship between these two parameters. This result is in agreement with finding of Deelstra et al. (2014) who compared FI and BFI from thirty catchments located in the Nordic-Baltic region and found a good coefficient of correlation ($R^2=0.6794$) with a linear correlation having a negative slope. Baseflow does not increase immediately at the beginning of the rainy season as notified by Lyne and Hollick (1979) who stressed that the baseflow takes days or weeks to respond while the streamflow responds more quickly and it is mostly a rise, resulting in high FI. Conversely, certain time after the rain season has begun, there is an increase of baseflow that acts as buffer against the drastic fall in flow during dry days, lowering the flashiness index. The high BFI obtained for the study basin as corroborated by the FI may be explained by the high evaporation that reduces surface flow in the study area. It may also confirm that regolith aquifer is the main source of water discharging as baseflow. The depth of the regolith layer in the study area can reach beyond 40 m and therefore the fractured zones are deep and do not discharge into the Sissili river. It is observed that the BLOW filter, the EcohydRology filter and the Aquapak filter using the same Lyne and Hollick (1979) method give different methods. This behaviour of baseflow filter was pointed out by Ladson et al. (2013).

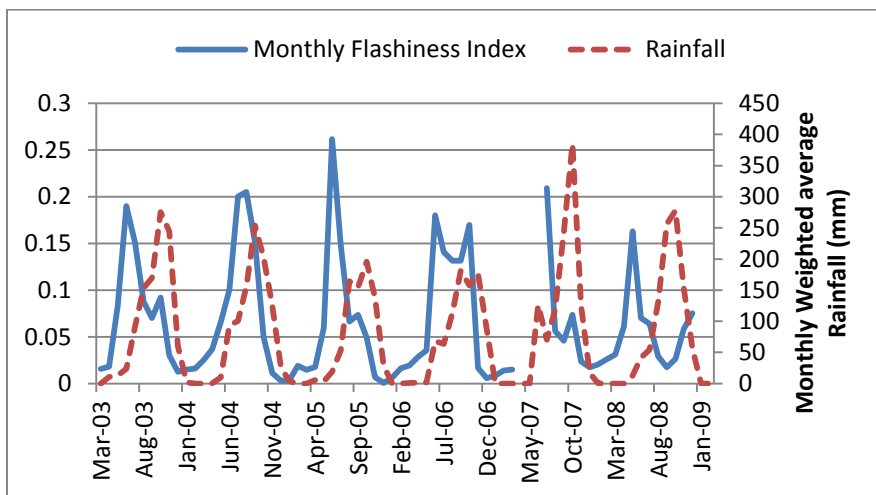


Figure 5-4: Comparison of monthly flashiness index and the monthly weighted average rainfall

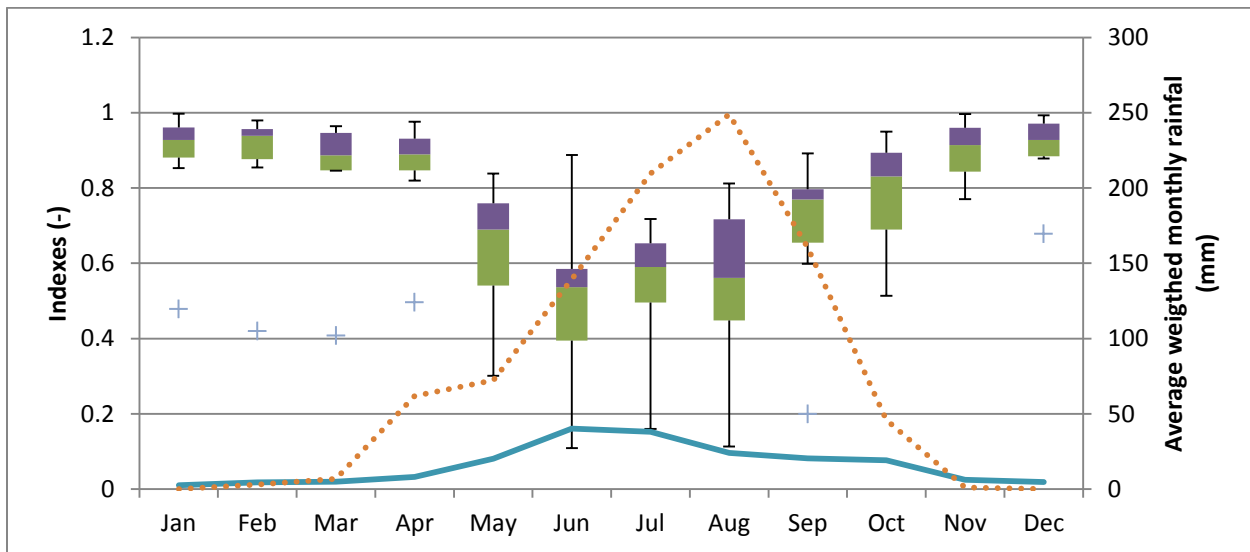


Figure 5-5: Variation of monthly average baseflow and flashiness indexes for the period 2003-2008. Box-plots represent the average monthly BFI, solid blue line represents FI, blue crosses represent outliers and discontinued red line represents monthly rainfall.

Figure 5-6 shows the range of BFI estimated with the different baseflow separation method. The Recursive Digital filter for Hard Rock aquifer (RD-HR) gave the least estimate of the BFI for the entire period of study. This was followed the EcohydRo and Aquapak tools, in an increasing order. The BFIs obtained with the recursive digital filters (RD-P and RD-HR) show low inter-annual variability as a result of the use of the BFI_{max} parameter for this method. With the WHAT system (Lim et al. 2005), the BFI_{max} is 0.8 and 0.25 for the RD-P and RD-HR, respectively. Generally, all the baseflow separation methods, gave the highest BFI values in 2008 except the Local Minimum and RD-HR which had the highest values of the BFI in 2007. Although the EcohydRo and the Aquapak use the Lyne and Hollick filter, their results are different. Similarly different results were obtained by Ladson et al. (2013) used different baseflow estimation tools using the Lyne and Hollick (1979) filter. For all the study years, the 'BFLOW method' is the only method that estimated BFI greater than 0.7, while the RD-HR method gave a BFI lower than 0.3 Figure 5-6 and Figure 5-7). Figure 5-8 shows that the highest BFI were obtained in 2008. BFI in 2005, year in which the smallest annual rainfall occurred, is higher than in some years (2003, 2004 and 2006) that received more rain. This may be explain by the fact that baseflow of a given year also depends on rainfall in the precedent year. In other word, baseflow contributing to flow does not come only from water that recharged the aquifer in that year.

Statistical analysis of the BFIs estimated by all the methods shows that BFI obtained with the RD-HR method is an outlier in 2003 and 2007. Compared to the results (BFI range of 0.033 - 0.33) obtained by Pelig-Ba (2004) who used the recession method proposed by Barnes (1939) to separate baseflow in five sub-catchment within the Volta basin, only the RD-HR method used in the current study had results within the range of that study.

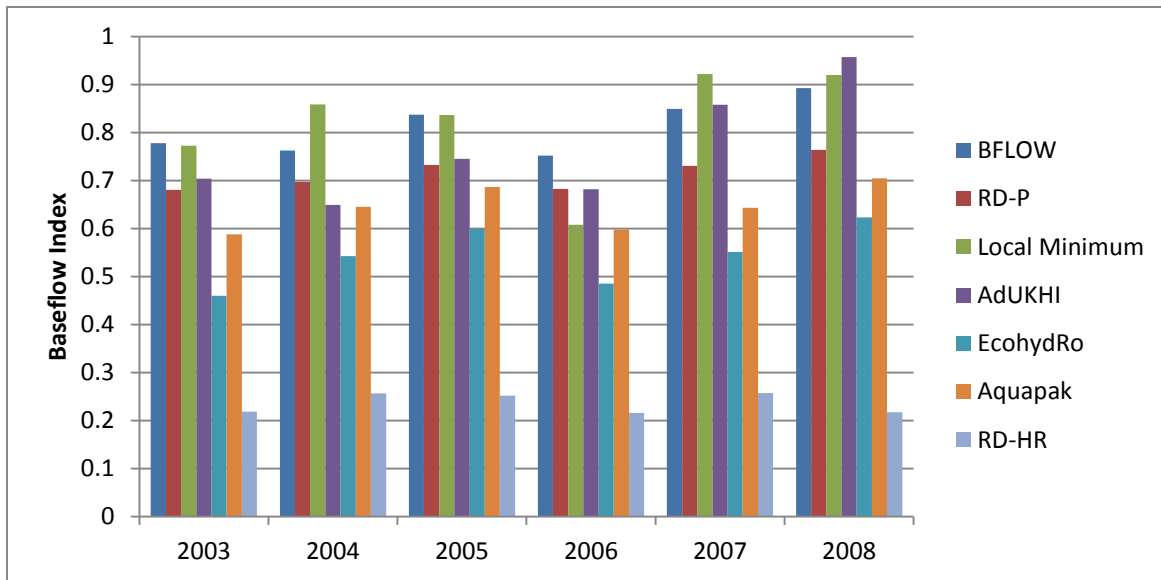


Figure 5-6: Range of annual Baseflow Index (BFI) estimated by the different methods

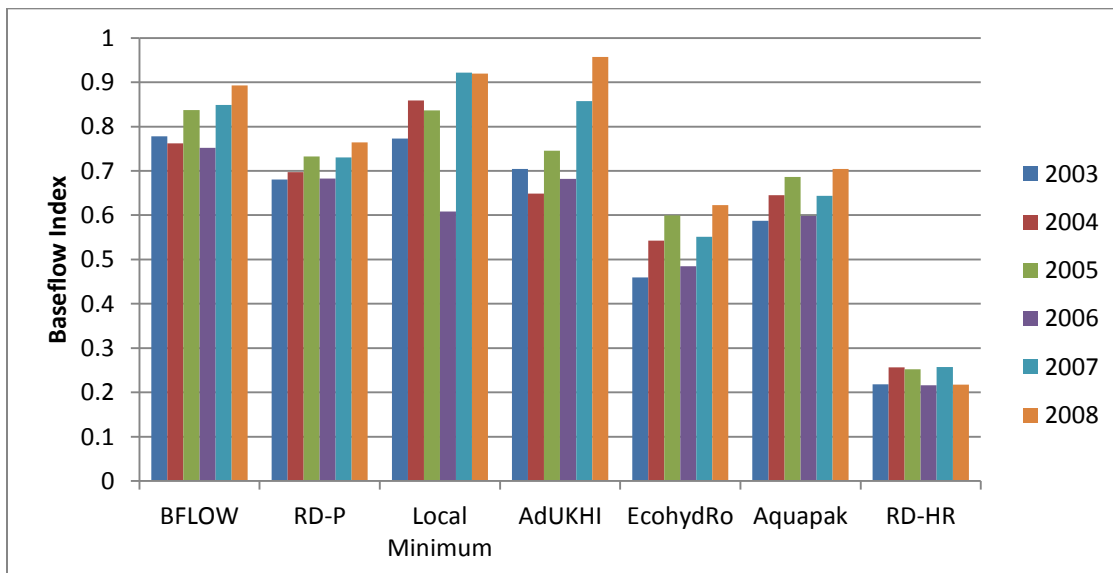


Figure 5-7: Variation annual Baseflow Index (BFI) with respect to the different filter methods

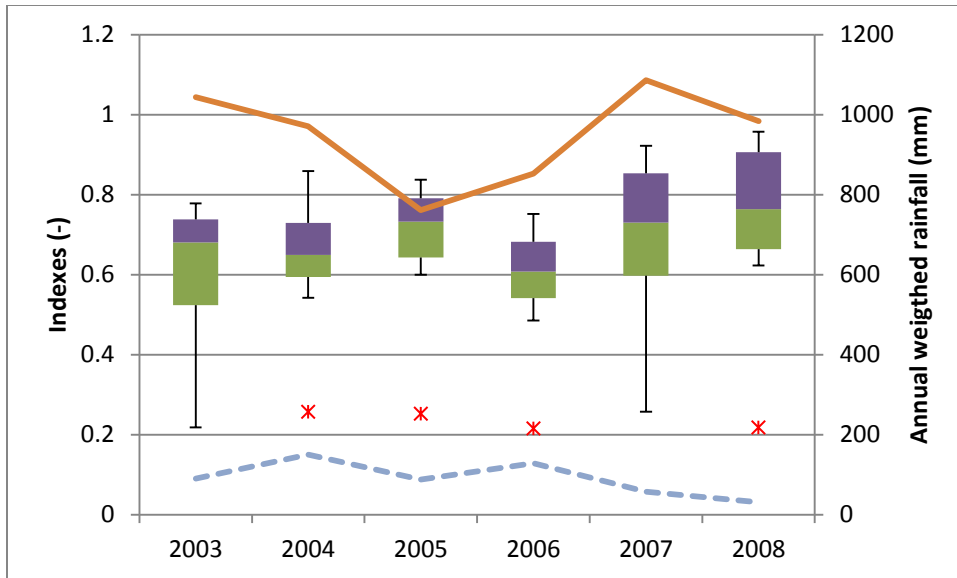


Figure 5-8: Interannual variability of baseflow index of the Sisili River at Wiasi, Northern Ghana. Box-plots represent the average monthly BFI, solid orange line represents annual rainfall, red asterisks represent outliers and discontinued blue line represents monthly FI.

There is an increase of baseflow from 2004 to 2008 (Figure 5-10). The combined analysis of rainfall and baseflow reveals the fact that the rainfall amount is not the only factor governing the baseflow. For instance, the annual rainfall in 2003 is higher than the one in 2008 but the baseflow for 2008 is higher than that for 2003. Relative to the median, the spread of the baseflow amount estimated by the different methods is wider with high baseflow estimates and narrower with low estimates. The estimated annual baseflow based on the different methods used in this study ranged from $2.4 \times 10^8 \text{ m}^3$ (19.07 mm) to $9 \times 10^8 \text{ m}^3$ (69.8 mm), representing 2% - 7% of the annual rainfall. The local minimum method gave the highest baseflow estimate for the whole study period, with the lowest was obtained with the RD-HR (Figure 5-9). These results are in line with findings of Pelig-Ba (2004) who obtained baseflow ranging from 2 mm to 42 mm in some sub-catchment of the White Volta and Black Volta rivers in Northern Ghana. Both baseflow and rainfall decrease from 2003 to 2004 while they increase from 2005 to 2007 showing the link between them although baseflow does not depend only on rainfall amount.

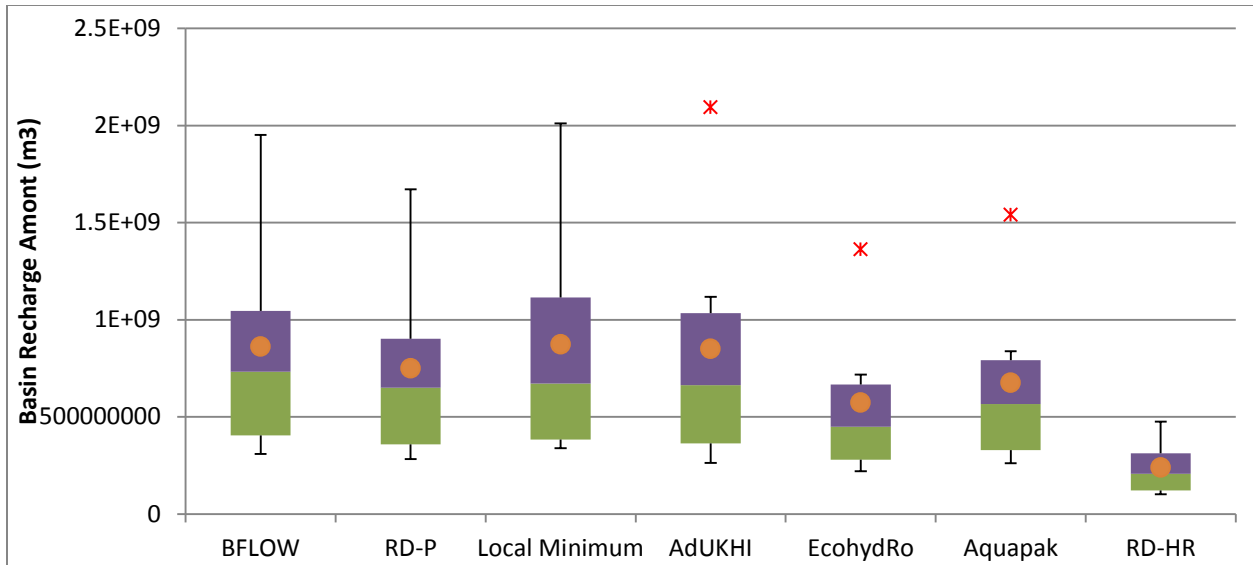


Figure 5-9: Range of baseflow estimated by baseflow tools for the period 2003-2008. The red asterisks and the dots represent outliers and mean values, respectively.

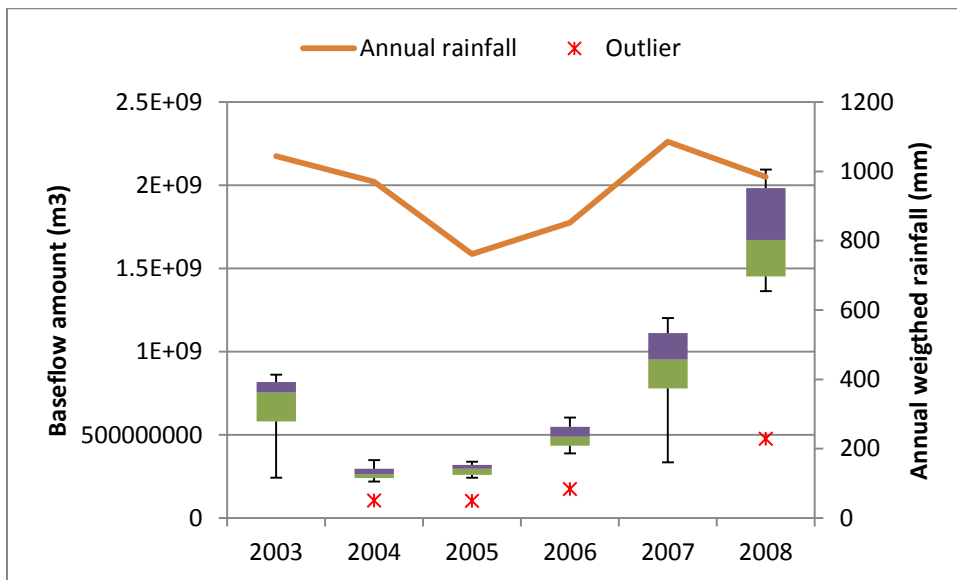


Figure 5-10: Comparison of baseflow and annual rainfall amount. Boxplots represent range baseflow estimated by the different methods, asterisks represent outliers and orange line represents annual rainfall.

Regarding the performance of the various baseflow separation methods used, the BFLOW digital filter out performed all the others giving the highest NSE during the entire dry season and the

recession period (Table 5-3). Conversely, the RD-HR method gave the worst performance, with the lowest NSE which suggests a poor ability to estimate baseflow in the dry season including the recession period.

Table 5-3: Performance of baseflow methods during dry and recession periods in the Sisili basin at Wiasi, Ghana

	BFLOW	RD-P	RD-HR	Local Minimum	AdUKHI	Eco-Hydro	aquapack
NSE in the recession periods	0.90	0.83	0.19	0.68	0.75	0.56	0.68
NSE in dry season flow	0.99	0.45	0.00	0.60	0.00	0.74	0.84

5.3. Recharge estimation using Water Table Fluctuation method

5.3.1. Groundwater level response to Rainfall

In the study area, the response of the groundwater level to rainfall varies spatially, owing to heterogeneity of aquifer properties that characterizes basement aquifers (Chandra et al. 2010). This can be illustrated by Figure 5-11 and Figure 5-12. A similar result was obtained by Leduc et al. (1997) by comparing groundwater hydrograph from several monitoring wells in Southern Niger. However, in most the cases, the peaks of groundwater level were in October. For the data considered in this study, the lowest (130 cm) and highest (770cm) annual variation in DH were obtained in Tumu and Bongo-Nayire, respectively. Lower water levels were mostly obtained in June except for the well at Gowrie located in the irrigated area of the Vea catchment (Figure 5-12). For this well the lowest water level was observed in December, which is the beginning of the dry season irrigation in the vea area. Contrary to the Gowrie well, the well at Bonia near Navrongodid not show recovery of the groundwater level during the dry season even though the well is located in an irrigated area (Figure 5-11). However the effect of the irrigated water can be detected as the slope of the recession change at the end of the dry season therefore the end of the irrigation. This is more pronounced in the 2008. In fact the irrigation reduces the falling of the water level and when it stops, a rapid falling is observed. Rapid rise and fall in water table at the

beginning and at the end of rainy season, respectively, are obvious in the shallow wells that access the shallow aquifer that infiltrated water reach easily. It obvious that the annual variation of the water level would not be constant but the inter-annual variation of the amplitude of fluctuation also varies from a well to another, as when there is a decrease of the amplitude of fluctuation from a year to another at a given well, an increase will be observed in another well. This may account for the spatial variability of rainfall, evapotranspiration and aquifer properties. At Atinyoro, the groundwater hydrograph show a depletion meaning that the annual abstraction of water from the aquifer accessed by the borehole is greater than the annual recharge. A similar case where found at the monitoring well of Wa North-East located at about 100 m from the pumping station of the Ghana Water Company that provide water to the town of Wa (Figure 5-13). Data of these aforementioned wells is therefore not suitable for estimating groundwater recharge by using the WTF method. Aquifer capture by piezometer with rise and rapid rise means that the aquifer captured by the well, recharge quickly and discharges quickly. Therefore the aquifer has a low storage capacity. The shallowest aquifer are mostly characterised by this kind of water level behaviour.

Table 5-4: Range of groundwater table fluctuation in the monitoring wells

Site	Well ID	Aquifer material	Depth (m)	Range DH (cm)
BONIA	WVB 4	Granite	72	230-360 (302.5)
DONIGA	HAP 22	Granite	153	430
Bongo-Nayire	WVB 6	Granite	35	515-770 (653.75)
TUMU	WVB 3	Granite	104	130-300 (238)
WA-Danko	WVB 1	Granite	104	208-220 (211)
GOWRIE	WVB 5	Granite	90	186-220 (202)
Yanyounyiri	HAP24	Granite	122	300
WAHABU	HAP23	Granite	122	300
Aniabisi	AN-M	Silty sand	7.1	290-300
Aniabisi	AN-D	Silty sand	5.4	320
Namoo	Namoo	Granite	-	320

Values in bracket are average values.

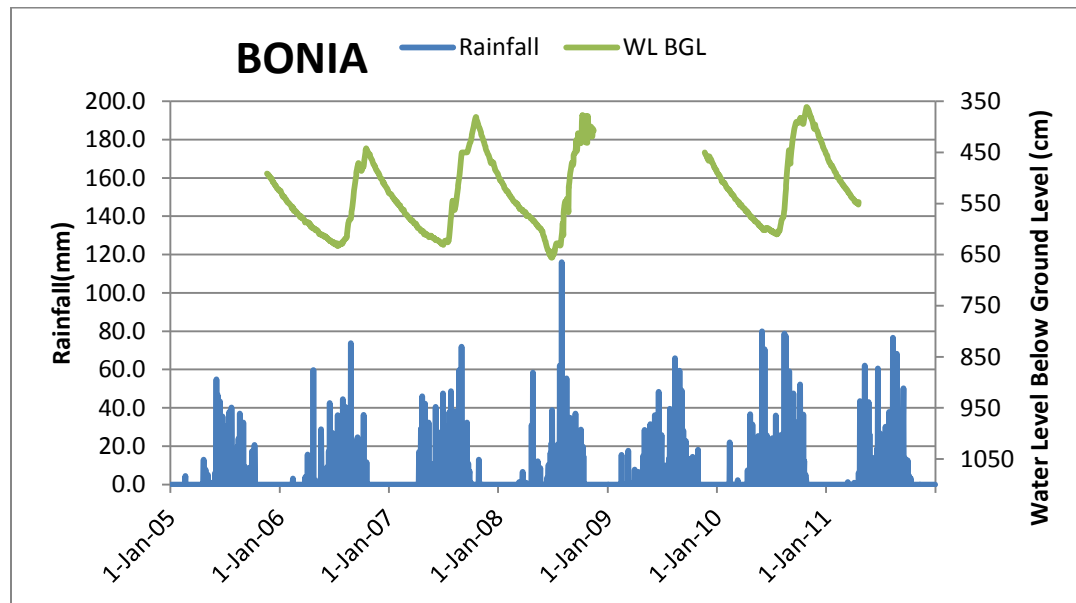


Figure 5-11: A plot of groundwater hydrograph and rainfall at Bonia (rainfall based on data from Navrongo station), showing seasonal variation of water level in response to the rainfall.

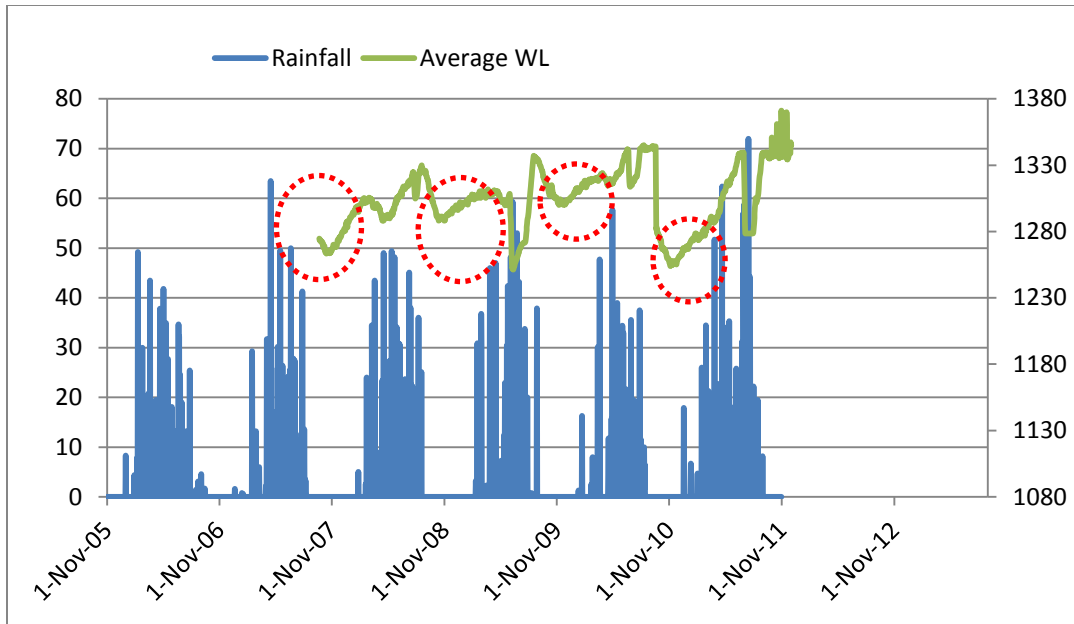


Figure 5-12: Variation of groundwater level at Gowrie in the rainy season (Apr - Sep). Encircled rises are attributed to recharge from irrigation water.

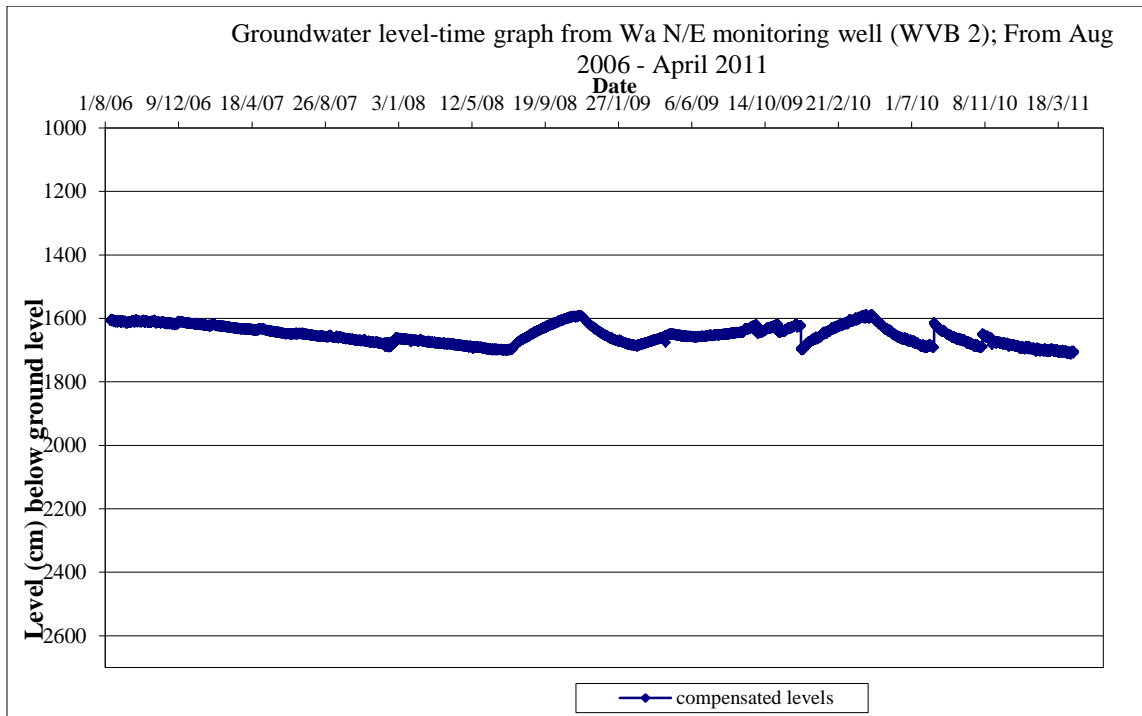


Figure 5-13: A plot of groundwater hydrograph for a well at Wa. The nature of decline of the groundwater levels is an indication of overexploitation of the resources.

5.3.2. Estimation of specific yield

Accurate estimation of recharge relies on good specific yield. The specific yield of the two monitoring wells at Aniabisi, estimated by the method of sample saturation and drainage, is 5%. This result is consistent with work by Johnson (1967) which suggested the same value for the same aquifer material. Aquifer materials of the others wells consist mainly of granite. Only single-well pumping test data are available. This does allow one to estimate a reliable specific yield as existing method requires a pumping test with observation well. A range of value has been suggested by many authors. A work by Heath (1983) suggests a specific yield of 0.09%, while Sinha and Sharma (1988) recommend values ranging from 2 to 4% for the same aquifer material. As aquifer in the area are not fully confined, the average value (i.e 3%) of the values suggested by the latter was used. Other studies in the Volta Basin used specific yield data from literature (e.g. Johnson 1967; Healy and Cook 2002) due to same difficulties in measuring the values as enumerated. However, some used the lower value in the range (e.g. Yidana et al. 2016) while others used the full range (e.g. Obuobie 2008; Martin 2006; Sandwidi 2007) to give indication of the minimum and maximum recharge expected.) . Table 5-5 presents the specific yield values used to estimate groundwater recharge at all the wells used in this study. The values were either 3% or 5%.

Table 5-5: Specific yield used in estimation of groundwater recharge in crystalline basement aquifers of northern Ghana.

Well ID	Range DH	Aquifer material	Depth (m)	Total aquifer thickness	Specific Yield
WVB 4	230-360	Granite	72	18	0.03
HAP 22	430	Granite	153	56	0.03
WVB 6	515-770	Granite	35	4	0.03
WVB 3	130-300	Granite	104	6	0.03
WVB 1	208-220	Granite	104	8	0.03
WVB 5	186-220	Granite	90	15	0.03
HAP24	300	Granite	122	104	0.03
HAP23	300	Granite	122	54	0.03
AN-M	290-300	Silty sand	7.1	-	*0.05
AN-D	320	Silty sand	5.4	-	*0.05
Namoo	320	Granite	-	-	0.03

NB:* Estimated based on laboratory analysis.

5.3.3. Groundwater recharge estimation

Recharge estimated with the WTF method ranged from 6% (68 mm) to 17% (163 mm) of the annual rainfall, with a mean value of 10%. These results were in the range of those obtained by other works in the vicinity of the study area in similar aquifer. As monitoring at Bonia and Gowrie are located in irrigated areas, recharge in these areas results from irrigation and rainfall. Therefore, in reality recharge from rainfall should be smaller than what is presented in Table 6-3. A comparison of the recharge estimated with the WTF to those estimated with the Chloride Mass Balance (CMB) method presented in section 5.4 showed that, the WTF-estimated recharge were generally higher than the CMB-estimated recharge, except for three wells. In Aniabisi where two of new monitoring wells are located, estimated recharge with WTF agrees with estimates from CMB. The results of the WTF from the middle slope and downslope wells are 14% and 15%, respectively, while the estimated recharge from the CMB was 14%. It should be highlighted that, specific yield of these two wells was estimated by the method of sample saturation and drainage. In Gowrie and Wahabu, recharge values estimated with the WTF method are lower than those estimated with the CMB. In the Kompienga dam basin in Burkina Faso, using the WTF method, Sandwidi (2007) obtained recharge ranging from 5.3% to 29.4% of the annual rainfall, with average value of 17% and he stressed that this wide range was due to the literature based specific yield that was used in calculating the recharge. In the Atankuidi basin in Northern Ghana, Martin (2006) reported recharge to range from 1.8% to 12.5% and 1.4% to 10.3% in 2003 and 2004, respectively. In Northern Ghana, using the WTF method, Yidana et al. (2016) estimated recharge in the range of 5.9 to 13.7% of the rainfall, with average value of 9.3%. All these results reflect the heterogeneity of aquifers in the area. Estimated recharge from wells WVB1, WVB3, WVB4, WVB5 and WVB6 are close to that obtained by Obuobie (2008) for 2005 and 2006. However, a difference of up to 1% of recharge was found for some wells when comparing average recharge during the period of the current work to result of Obuobie (2008). These differences may be attributed to the temporal variability of recharge.

Table 5-6: Estimated recharge by the Water Table Fluctuation method compared with recharge results from Chloride Mass Balance method.

Well ID	Range DH	Aquifer material	Specific Yield	Recharge (%Rainfall)	
				WTF	CMB
WVB 4	230-360	Granite	0.03	8	5
HAP 22	430	Granite	0.03	11	3
WVB 6	515-770	Granite	0.03	17	9
WVB 3	130-300	Granite	0.03	6	6
WVB 1	208-220	Granite	0.03	6	2
WVB 5	186-220	Granite	0.03	7	12
HAP24	300	Granite	0.03	10	-
HAP23	300	Granite	0.03	9	12
AN-M	290-300	Silty sand	0.05	14	14
AN-D	320	Silty sand	0.05	15	14
Namoo	320	Granite	0.03	11	4

5.4. Recharge estimation using the Chloride Mass Balance method

5.4.1. Chloride in Rain

Chloride concentrations obtained at the laboratory in Ghana were higher compared to those obtained in Germany and no correlation was found between both datasets. Also the chloride content of the 197 samples obtained by the analysis at the laboratory in Ghana was either 3.97 mg/L or 1.99 mg/L making this result unreliable. Therefore only results of the analysis done at RUB were used as chloride content in rain water for this study.

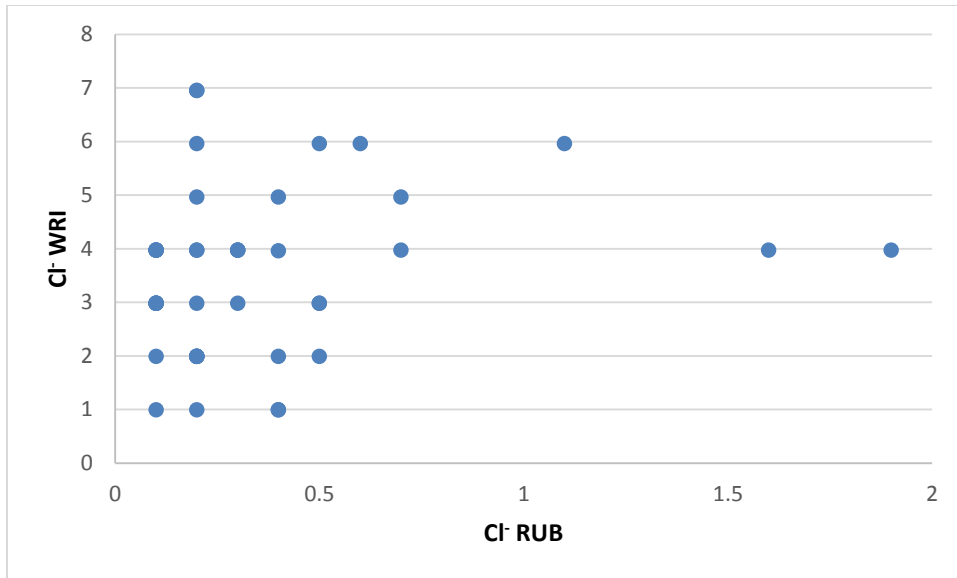


Figure 5-14: Comparison between chloride content obtained at the laboratories of WRI and RUB

The chloride content in rain ranges from 0.1 mg/L to 3.6 mg/L. As shown by Table 7-1, average chloride content obtained across the sampling site ranges from 0.17 mg/L to 1.62 mg/L. Using Thiessen polygon method of averaging rainfall over an area, the sampling sites were found to be located in areas covered by only two (Navrongo and Wa) of the five weather stations for which data were available for this study. Therefore, an average value of chloride content in rainwater for each of the two areas was calculated. The average chloride concentrations in rainwater in the areas covered by the Navrongo and Wa climate stations were 0.60 mg/L and 0.56 mg/L, respectively. These values are higher than the average values obtained by Martin (2006) for the rainy season of 2004 in the Atankwidi basin, which is encompassed by this study area but lower than findings of Obuobie (2008) whose study area (Northeastern Ghana) overlaps this study area and Sandwidi (2007) for the Compienga dam basin on the Burkina-Faso portion of the Volta Basin. Martin (2006) reported chloride values in the range of 0.1 - 3.7 mg/L, with average value of 0.2 mg/L while Obuobie (2008) obtained a range of 0.2 to 2.1 mg/L, with areal weighted average of 0.8 mg/L. And Sandwidi (2007) measured chloride content in rainfall as 0.87 mg/L and 0.88 mg/L for 2005 and 2006, respectively.

Table 5-7: Average Chloride content in rain for the rainy seasons of 2014 and 2015 in the study area

Station	Chloride content in rain (mg/L)
Bonia	0.50
Doniga	0.40
Kunchukor	0.43
Tumu	0.50
Pieng	0.56
Wahabu	0.17
Fian	0.33
Chepurie	0.37
Wa	0.82
Gowerie	0.27
Bongo	0.88
Sanabisi	0.37
Soe	0.27
Namoo	0.66
Tangabisi	1.62
Akuka	0.63
Paga	0.38
Manyoro	0.32
Aniabisi	0.95
Yebongo	0.55

5.4.2. Chloride in groundwater

Contrary to the results of chloride measured in rainwater, a very good correlation ($R^2=0.99$) was obtained between results of chloride analyses in groundwater done at the laboratories of WRI - Ghana and RUB –Germany. Consistently, the values obtained from the WRI laboratory were slightly higher than those determined in the RUB laboratory (Figure 5-15). A similarly good correlation was obtained by Sandwidi (2007) when he compared groundwater chloride analyses done in a laboratory in Burkina-Faso to that in Germany. The regression equation $y = 0.8188x - 0.1605$ was used to correct results obtained from the WRI-laboratory.

After correction, the chloride contents in groundwater sampled from the study area range from 1.48 mg/L to 76.23 mg/L. These results are consistent with those obtained by other authors whose study areas are located within or in the vicinity of the current one. Statistical analysis of the chloride contents in groundwater using a boxplot shows 4 values as outliers. Also, values

lower than 2 mg/L were discarded from the data as they may characterise very localized recharge zone that could not represent recharge zones of larger areas (Damtew 2015). High concentrations of chloride may have originated from sources other than precipitation. Three of the high chloride samples were from wells located in the granite formation in Bongo where high chloride contents were found to result from mineral dissolution (Martin 2006). High chloride concentrations were obtained from groundwater samples from Zaare, Kasingu, Vea and Bongo while samples with low chloride contents were collected from Borogo, Atinyoro and Kulyah. Finally, chloride contents ranging from 3.1 mg/L to 28.3 mg/L, with an average value of 10.1 mg/L were used for the analysis. Highest values were found in Wa, Pieng and Kunchurkor, while small value were found at Dabalansa, Azorbisi Primary school, Anafobisi and Soe.

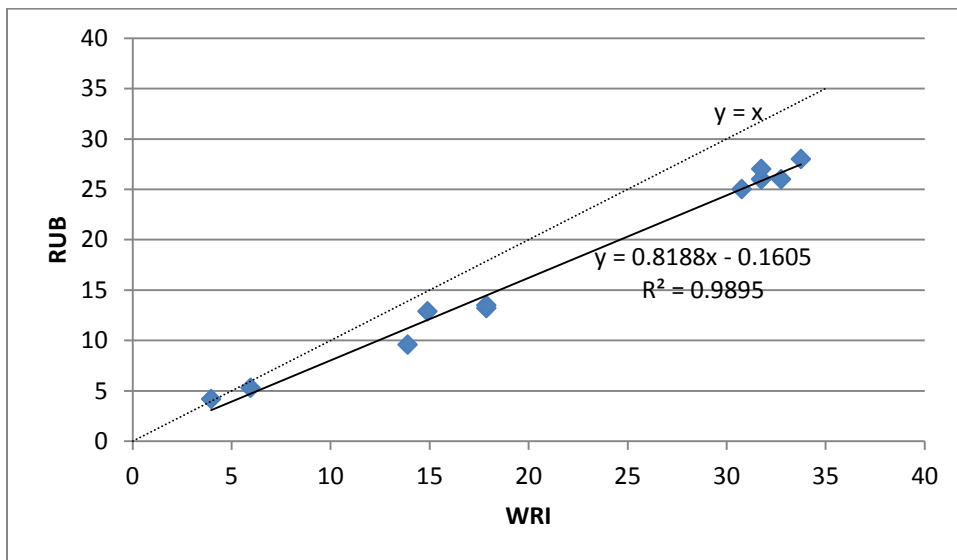


Figure 5-15: Comparison between chloride content in groundwater analysed at WRI and RUB laboratories

5.4.3. Recharge estimation

Estimated recharge for the study area ranges from 21 mm to 191 mm, representing 2.1% to 19.3% of the mean annual rainfall (994 mm). The areal average is 81 mm, representing 8.14% of the mean annual with a standard deviation of 4.26%. Results show high variability of recharge in the study area. This high spatial variability of recharge has been differently interpreted. In the Western Murray basin in Australia, Allison et al. (1990) found that this variability was mainly related to soil texture and differences in precipitation while Edmunds et al. (1988) attributed the large variability in recharge at Akrotiri peninsula in the island of Cyprus to the differences in

topography and vegetation cover. In this study, there was no a clear relationship between the large variability in recharge and the differences in geological formations. However, the migmatite and undifferentiated granite formation showed the highest variability of recharge, while the lowest variability was found in the upper birrimian as depicted by the low values of the coefficient of variation (

Table 5-9). This could be interpreted as aquifer properties are less variable in the former than in the latter. On average, migmatite and undifferentiated granite formation received the smallest recharge rate in the area, while the highest recharge was obtained in the hornblende biotite granodiorite formation. The average recharge obtained in this current work is consistent with results of other works that used CMB method to estimated groundwater recharge in and around the study area (Table 5-8). It is close to findings of Obuobie (2008) while it is higher than those obtained by Martin (2006), Sandwidi (2007) and Oteng-Mensah et al. (2014). It shows less variability compared to the findings of Yidana and Koffie (2014) and Oteng-Mensah et al. (2014). Average recharge of this current work is smaller than that obtained by Nyagwambo (2006) in a similar geological environment in Zimbabwe.

Table 5-8: Summary of recharge estimated using CMB method by previous works in the regions or in area with crystalline basement aquifer.

Authors	Country	Estimated recharge as % of rainfall
Oteng Mensah et al. (2014)	Ghana	0.9–21(5.5)
Yidana and Koffie (2014)	Ghana	1.8–32
Obuobie (2008)	Ghana	3.4 to 18.5 (8.3)
Sandwidi (2007)	Burkina-Faso	(5.3)
Martin (2006)	Ghana	3-6 (5.9)
Nyagwambo (2006)	Zimbawe	4.0-25.0 (12)
Bromley et al. (1997)	Niger	1.8-3.4

NB: Values in bracket represent average values.

Table 5-9: Estimated groundwater recharge with respect to geological formation

Geology	Recharge (%)	Standard deviation
Biotite Gneiss	7.32	2.36
Upper Birimian	8.10	1.36
Hornblende biotite granodiorite	10.17	5.36
Granite	8.34	3.85
Migmatite and Undifferentiated Granite	6.74	4.24

Base on the FAO soil type, the groundwater wells sampled are situated in eight soil types. The number of wells located in each soil is presented in

Table 5-10. As only two and one wells fall in the Lithic Leptosols and Dystric Leptosols soil types, respectively, these soil types were not considered in the statistical analysis conducted to understand how soil types may influence recharge rates in the study area. The analysis shows that the lowest recharge took place in the Calcic Vertisols while the highest was in the Eutric fluvisols. In an increasing order of recharge the soil types are listed as follows: Haplic Lixisols, Ferric Lixisols, Gleyic Lixisols and Eutric Leptosols. The highest recharge found in the Eutric fluvisols is obvious as this soil type is found mostly along river channels and commonly known as high groundwater potential zone. This result is consistent with the suggestions of Keller et al. (2013) who pointed out that the Eutric fluvisols soil type has a high potential for shallow groundwater. The low recharge found in the Calcic Vertisols is explained by the low saturated hydraulic conductivity of Vertisols owed to the presence of the 2:1 clay type and the relatively high clay content (Pathak et al. 2013). In India, comparing the saturated hydraulic conductivities of Vertisols and Alfisols at different depth, Pathak et al. (2013) found that the saturated hydraulic conductivities of the Alfisols ranging from 6.1 to 17.1 mm/h were far greater than those of the Vertisols that ranged from 0.21 to 0.6 mm/h and at given depth the hydraulic conductivity of the former was at least eighteen times greater than the one of the latter. As the groundwater recharge in the Eutric Leptosols and Gleyic Lixisols are close to the rate in the Eutric Fluvisols, these soils may probably have a similar texture. Conversely, The Lixisols may have soil particles finer than the aforementioned soil types (i.e. Eutric Leptosols, Gleyic Lixisols and Eutric Fluvisols). In this regards, soil type appears to be one the factors controlling groundwater recharge in the study

area. This result is consistent with findings of Cook et al. (1989) and Zhang et al. (1999). Oteng-Mensah et al. (2014) and Yidana and Koffie (2014), who worked in the White Volta basin in Northern Ghana, found that variation of groundwater recharge in their study areas was related to the nature of the unsaturated zone material.

Table 5-10: Groundwater recharge with respect to FAO soil types

Soil type	Number of wells sampled in soil type	Average annual recharge (%)	Standard deviation
Haplic Lixisols	5	6.88	2.35
Ferric Lixisols	22	7.28	3.60
Gleyic Lixisols	18	8.71	4.95
Eutric Leptosols	20	8.86	4.05
Lithic Leptosols	2	-	-
Dystric Leptosols	1	-	-
Eutric fluvisols	4	9.15	2.74
Calcic Vertisols	4	4.10	2.57

5.5. Recharge estimated by the WetSpass model

For purposes of calibration and validation of the WetSpass model, the modelled-total flow was compared to the observed total flow at Wiasi. Statistics of performance of the model for both the calibration and validation periods are summarised in Table 5-11. Based on the coefficient of determination (R^2) and the Nash-Sutcliffe Efficiency (NSE) coefficient, the performance of the model in simulating total runoff can be described as satisfactory as suggested by Moriasi et al. (2015). The values of R^2 and the Percentage Bias (PBIAS) suggest that the model overestimated total streamflow in the study area even though the simulated flow follows the same pattern as the observed as depicted in Figure 5-16.

The recharge estimated by the WetSpass model ranges from 519 mm to 756 mm, as reported in Table 8-2. Although, the performance criteria suggested that the model performance was acceptable, estimated recharge by WetSpass shows tremendous difference compared to previous works around the study area that used a model to estimate recharge (e.g., Obuobie 2008 and Abdollahi et al. 2017). For instance, Abdollahi et al. (2017) obtained recharge of about 13.9% of the annual rainfall during the period 1990-1993 by using the same model in the Black Volta

basin, while recharge estimated by this current work ranges from 55% to 70%. Obuobie (2008) using the SWAT model in the White Volta obtained mean groundwater recharge of 59.0 mm, representing 7 % of the mean annual rainfall during the period 1986-1999. Therefore, the WetSpa model setup for the Sisilli basin and calibrated at Wiasi in this study heavily over-estimated the recharge. As such, it was not used in the estimation of future groundwater recharge as originally envisaged. The poor performance of the WetSpa model in the study basin could be attributed to the model mechanism but also to the quality of the different input data as well as the observed streamflow data used to calibrate the model.

Table 5-11: Performance evaluation criteria of the model.

	Nash-Sutcliffe Efficiency	R ²	PBIAS (%)
Calibration	0.60	0.74	-129
Validation	0.52	0.65	-190

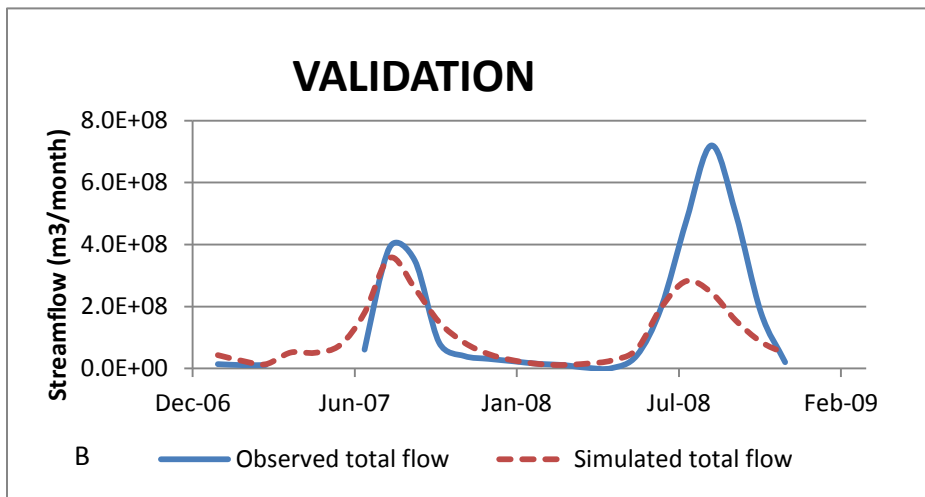
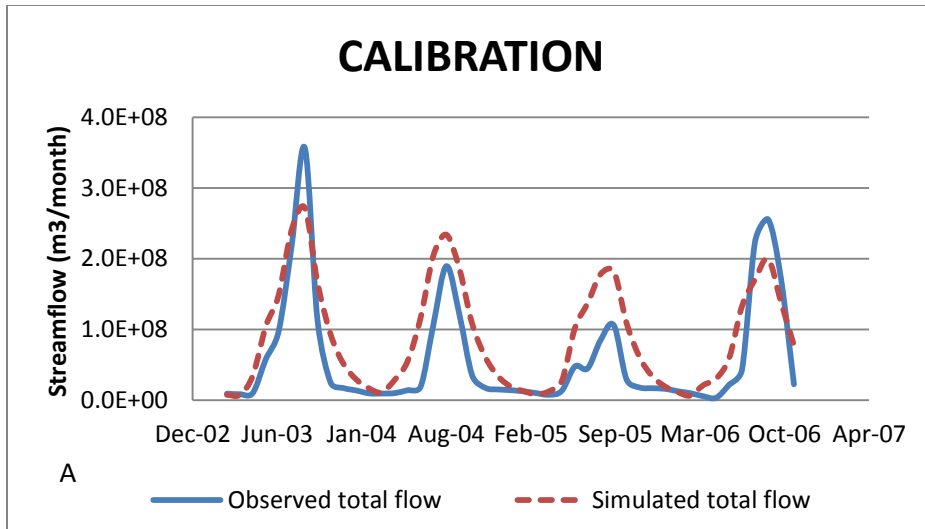


Figure 5-16: Comparison between simulated and observed total flow for the calibration (A) and validation (B) of the model.

Table 5-12: Estimated recharge by WetSpss in the study area

Year	Rainfall (mm)	recharge (mm)	Recharge (%)
2003	1044	620	59
2004	971	532	55
2005	761	519	68
2006	852	555	65
2007	1086	756	70
2008	984	642	65

5.6. Conclusion

The aim of this chapter was to discuss recharge estimated by the Water Table Fluctuation method, the Chloride Mass Balance method and the streamflow hydrograph analysis. Recharge and groundwater response to rainfall were found to be highly variable in time and space within the study area. These variabilities were attributed to the spatial and temporal variability of precipitation and the heterogeneity of aquifer properties. In contrast to geological formation, soil type appears to be one of the factors controlling groundwater recharge in the study area.

Recharge estimated by the recession curve analysis ranges from 29 mm (3%) to 68 mm (9%) of the annual rainfall, with average value of 49 mm (5%). The estimated annual baseflow based on the six different methods used in this study ranged from 19.07 mm to 69.8 mm or from 2% to 7% of the annual rainfall. Based on the modified Nash-Sutcliffe efficiency, the 'BFLOW' filter gave the best performance in estimating the baseflow in the period (2003-2008) analyzed. The average monthly flashiness index suggests that the Sisili river at Wiasi is a stable river.

Using the WTF method and based on groundwater hydrographs from 11 monitoring wells, recharge to the groundwater of the basement crystalline aquifers of northern Ghana has been estimated to range from 68 mm (6%) to 163 mm (17%) of the annual rainfall, with a mean recharge of 10%. Besides, recharge estimated from wells with specific yield estimated from laboratory analysis show good agreement with recharge estimated by the CMB method.

Estimated recharge by the chloride mass balance method ranges from 21 mm to 191 mm, representing 2.1% to 19.3% of the mean annual rainfall. The areal average recharge is 81 mm, representing 8.14% of the mean annual rainfall.

The recharge estimated by the WetSpa model, for the period lasting from 2003 to 2008, ranged from 519 mm to 756 mm. These values represent 68% and 70% of the annual rainfall during 2005 and 2007, respectively. This recharge rate was found to be very high compared to results of the other methods or findings other studies using this model around the study area.

After presentation and discussion of findings related to groundwater recharge in the study area, the impact of climate change on groundwater recharge is presented in the next chapter.

Chapter 6 - IMPACT OF CLIMATE CHANGE ON GROUNDWATER RECHARGE

This chapter presents the estimation of present recharge using a simplified water balance method. The impact of climate change on groundwater recharge in the study area is also analysed and discussed.

6.1. Introduction

The evidence of climate change has been proved by several studies (e.g. Thompson et al. 2003; Kaser et al. 2004; Hinzman et al. 2005; Dash et al. 2007). But the study of the impact of climate change is not straightforward. Firstly, a baseline period which is considered as a reference period has to be chosen. Secondly, outputs of models have to be compared with observed data such as rainfall, temperature, etc. Additionally, study of the impact of climate change for a future requires future climate data that are derived from Global Climate Model (GCM). The challenge is that, GCMs provide climate data at a coarse resolution (about 300 km) while for the impact analysis local or point scale data are needed (Dorji et al. 2017). The coarser GCM data resolution can be improved through statistical and dynamical downscaling methods. These methods have been discussed in this chapter. To achieve the objectives of this chapter, the present day recharge was first estimated with the WetSpass model (Abdollahi et al. 2017) and a simple water balance method (Anayah et al. 2013). This was followed by downscaling of climate data using a statistical method and finally analysis of climate change impact on the recharge.

The study area of the WetSpass model and the simple water balance method are the Sissili river with outlet at Wiasi and the crystalline basement aquifer of Northern Ghana presented in sections, respectively.

6.2. Recharge estimated using the simple water balance method

In this study, the original (HG) and modified Hargreaves (MHG) methods were compared with the Penman-Monteith (PM). Correlation coefficients of these methods and the Penman-Monteith method are compared at each station. The analyses show that the modified Hargreaves method has the highest correlation coefficient for all the stations, except for the station at Gaoua. An illustration is presented by Figure 6-1 and Table 6-1. PET estimated by this method is also the

closest to PM when compared to HG (Figure 6-2). During the rainy season, estimated PET by MHG is almost the same as estimated by PM. As groundwater recharge in the study area occurs mainly in the rainy season (Martin 2006; Sandwidi 2007; Obuobie 2008) the MHG is better for the estimation of the PET to be used in the water balance proposed by Anayah et al. (2013) for estimating the recharge. Although compared to MHG, the HG method is less good at reproducing the PET estimated with the PM, it was observed that that the dry season estimates of PET estimated by the HG method correlated better with the counterparts of the PM method than the dry season estimates. This observation is in agreement with work by Ghamarnia et al. (2011) and Patel et al. (2015) in Iran and India, respectively. Comparing HG and PM, Ghamarnia et al. (2011) found that estimations from the two methods were closer in warm months than in cold months. It is also seen that both MHG and HG underestimate PET in the dry season.

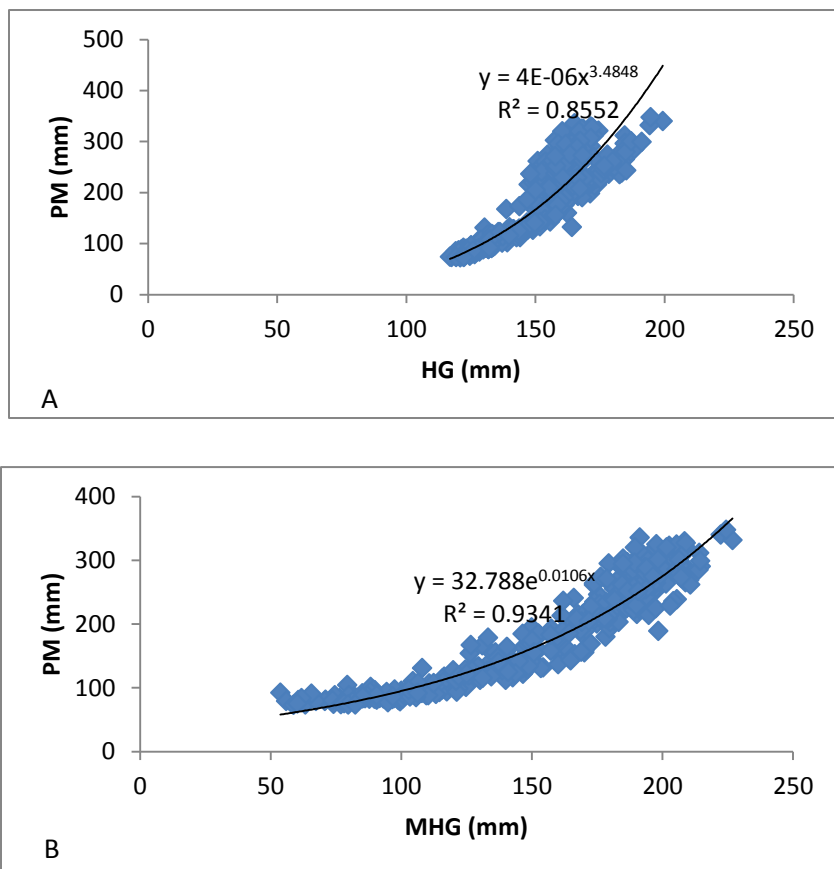


Figure 6-1: Monthly PET by the FAO Penman-Monteith versus: A) Hargreaves (HG) method, B) Modified Hargreaves (MDG) method, for the station of Tamale.

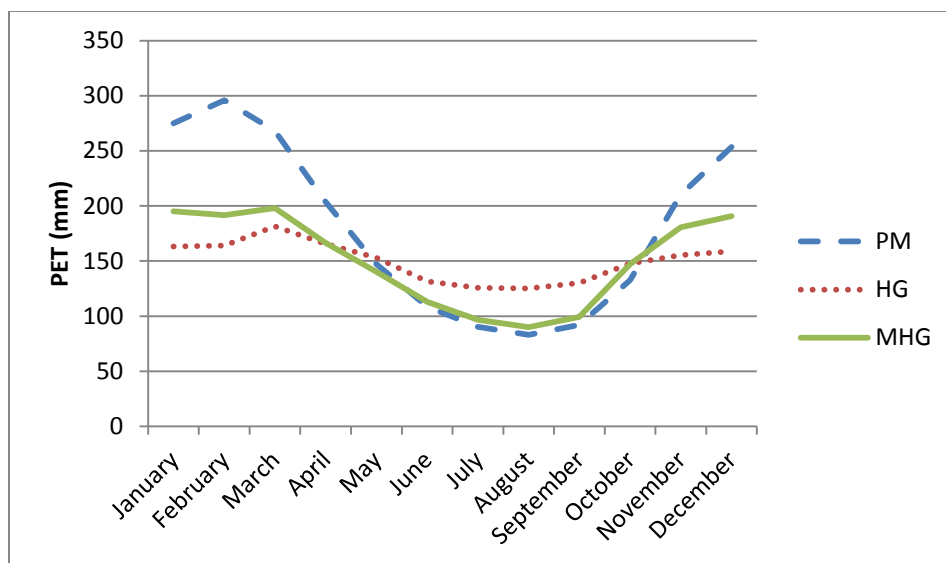


Figure 6-2: Average monthly potential evapotranspiration estimated by the FAO Penman-Monteith (PM), the Hargreaves (HG) method and the Modified Hargreaves (MDG) method for the period 1970-2009 for Tamale station.

Figure 6-2 shows a high correlation between the two versions of the Hargreaves method and the PM. For the MHG, this coefficient ranges from 0.53 to 0.93, while for the HG it varies between 0.57 and 0.87. The correlation coefficient decreases from south to north. As aridness in the study area increases from south to north, this may suggest that the correlation decrease with increasing aridity.

Table 6-1: Correlation between the FAO Penman-Monteith and two types of the Hargreaves methods.

	R-squared (R^2) between the FAO Penman-Monteith and :	
	Hargreaves (HG)	Modified Hargreaves (MHG)
Bole	0.87	0.93
Navrongo	0.7	0.89
Wa	0.74	0.91
Tamale	0.86	0.93
Gaoua	0.6	0.53
Ouaga	0.57	0.67
Yendi	0.76	0.89

Considering stations located within the study area, the estimated recharge are shown in Figure 6-3. The lowest recharge of 282 mm representing 26.3% of the annual rainfall is obtained in Wa and the highest of 330 mm (29.2%) was obtained in Bole while the recharge in Navrongo is 288 mm and it represents 28.5% of the annual rainfall. The average recharge of these three stations is 300 mm representing 28% of the annual rainfall. This result is close to findings of work by Anayah et al. (2013) who obtained recharge rate of 28%, 26% and 29% at Bole, Wa and Navrongo, respectively. Compared to work using other methods such as water table fluctuation method and chloride mass balance method in the study area, results of this current work are higher. This is due to the simplification of the simple water balance method which does not consider parameters like land use, soil properties, geology, etc. that influence groundwater recharge.

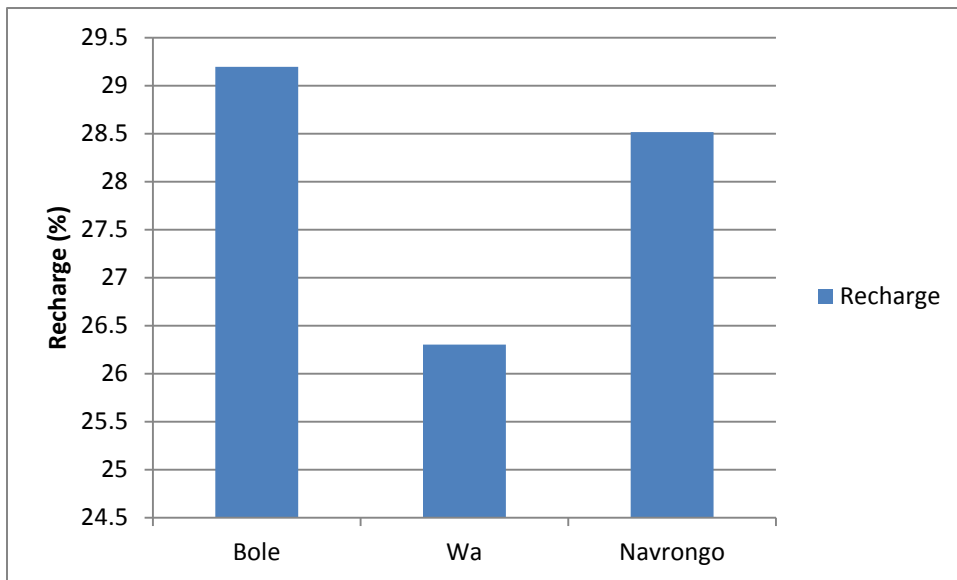


Figure 6-3: Mean annual recharge (%) during the baseline period (1976-2005)

6.3. Statistical downscaling

6.3.1. Comparison between models outputs and observation data

Table 6-2 presents statistics of uncorrected and corrected data of one model at the station of Navrongo. It shows how the bias correction method improves the quality of the downscaled climate variables. It is seen that corrected data for both rainfall and temperature shows lowest bias and RMSE compared to the uncorrected one. Further, the corrected data has the highest R-squared when compared to the uncorrected one.

Table 6-2: Comparison between uncorrected and corrected data showing the performance of the Bias Correction Method for the station of Navrongo

	Monthly Rainfall		Maximum temperature		Minimum temperature	
	Uncorrected	Corrected	Uncorrected	Corrected	Uncorrected	Corrected
RMSE	117.02	74.23	5.34	1.35	3.27	1.19
BIAS	-34.40	-5.42	4.28	0.08	1.99	0.05
R Squared	0.48	0.54	0.61	0.81	0.69	0.76

6.3.2. Future climate projection

6.3.2.1. Temperature

The estimated mean temperature by the different scenarios for the future and baseline periods is presented in Figure 6-4, while the range of projected change in mean temperature is summarized in

Table 6-3. All the models are consistent in predicting an increase in the future mean temperature regardless of scenario. By the middle of the century a clearer difference between ensemble means (of RCP4.5 and RCP8.5) is observed. Compared to the baseline (1976-2005) period, the mean temperature is projected to increase by 0.7 °C-1.2 °C in 2011-2040 for the medium forcing (i.e. RCP4.5) with an ensemble mean of 1.0 and by 0.7 °C-1.3 °C for the highest forcing (i.e., RCP8.5) with an ensemble mean of 1.1. For the period 2041-2070, the temperature is projected to increase by 1.1 °C- 2.0 °C with an ensemble mean of 1.7 °C and by 1.6 °C -2.5 °C with an ensemble mean of 2.2 °C for RCP4.5 and RCP8.5, respectively. For the period 2071-2100 the projected increase in mean temperature over the baseline ranges from 1.5 °C and 2.4 °C for the

medium scenario and from 2.5⁰C to 3.6⁰C for the highest scenario. The ensemble means are 2.1⁰C and 3.3⁰C for RCP4.5 and RCP8.5, respectively. The result of the trend analysis with the Mann-Kendall test is presented in Table 8-6. The test suggests a positive trend in observed mean temperature during the baseline period 1976-2005 and in projected ensemble mean temperature of RCP4.5 and RCP8.5 during the period 2006-2100. The slope represents the average increase in temperature per year. The results show that the projected ensemble temperature will increase by about 0.02⁰C per year and by 0.03⁰C -0.04⁰C per year for the ensemble of RCP4.5 and RCP8.5, respectively, while during the baseline period temperature increased by 0.02⁰C -0.03⁰C per year. The slopes of the ensemble mean temperature of RCP4.5 show a South-North gradient that increases from South to North. This means that mean temperature increases faster when going toward the north part of the study area. Results of this current work are consistent with findings of Stanturf et al. (2011) at Wallembele which is located within the area of the current work. Using 16 climate models based on scenarios A2, A1B and B1 their work suggested an increase in mean temperature of $1.92 \pm 0.52^{\circ}\text{C}$ and $2.10 \pm 0.71^{\circ}\text{C}$ by 2050 for wet and dry seasons, respectively. The same work suggested that by 2080 increase in temperature as compared to the baseline period 1961-1990 is projected to be $2.96 \pm 0.98^{\circ}\text{C}$ and $3.27 \pm 1.11^{\circ}\text{C}$ in the wet and dry seasons, respectively. This work was done by using climate data from Tamale station that was considered as representative of the area of this current work. As for the work of Margulis et al. (2010) it suggested that over the period 2010-2050 temperature will increase for about 2.2⁰C to 2.4⁰C. In the White Volta basin covering the biggest part of this current work, Kankam-Yeboah et al. (2013) found that the ensemble ECHAM4/CSIRO projected an increase in mean annual temperature of about 1.9% in the 2050s compared to the baseline period 1961–1990.

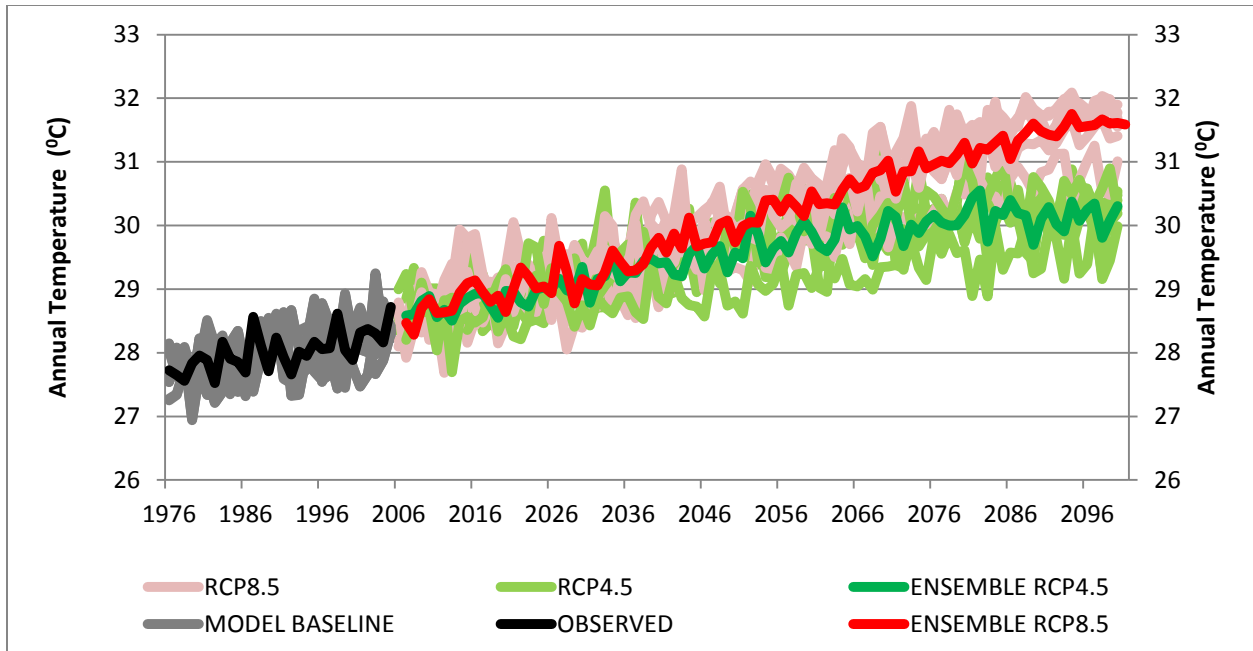


Figure 6-4: Estimated temperature by the twelve scenarios for the baseline and future periods in the study area

Table 6-3: Increase in future temperature compared to the observed mean temperature of the baseline period

	RCP4.5			RCP8.5		
	Min (°C)	Max (°C)	Ensemble (°C)	Min (°C)	Max (°C)	Ensemble (°C)
2011-2040	0.7	1.2	1.0	0.7	1.3	1.1
2041-2070	1.1	2.0	1.7	1.6	2.5	2.2
2071-2100	1.5	2.4	2.1	2.5	3.6	3.3

Table 6-4: Trend analysis of mean temperature in the baseline and the future periods across the study area.

		Bole		Wa		Navrongo	
		P-Value ^a	Slope	P-Value ^a	Slope	P-Value ^a	Slope
Baseline (1976-2005)	Observed	0.0018	0.0195	< 0.0001	0.0318	0.0020	0.0224
Projection 2006-2100	Ensemble RCP4.5	< 0.0001	0.0179	< 0.0001	0.0183	< 0.0001	0.0194
	Ensemble RCP8.5	< 0.0001	0.0349	< 0.0001	0.0344	< 0.0001	0.0377

a: the trend is significant for a P-value smaller than 0.05

6.3.2.2. Rainfall

Contrary to the temperature, there is no clear difference between ensembles regarding projected rainfall (Figure 6-5), but the range in projected rainfall becomes wider when going onward as presented in Table 6-5. As depicted in Table 8-8, trend analysis based on the Mann-Kendall test suggests no trend in past and projected ensemble mean annual rainfall in the study area except in the south-western (represented by Bole station) where a positive trend is obtained for the Ensemble of RCP8.5. However, the ensemble suggests an increase in future periods compared to the baseline as shown in Table 6-5. In the south-western of the study area, rainfall is projected to increase by 0.9 mm per year for the highest forcing. Rainfall is projected to change by -5% to 17% with ensemble mean of 6% in 2011-2040 for the medium forcing and by -10% to 14% with ensemble mean of 6% for the highest forcing in the same period. In the period 2041-2070 rainfall is projected to change by -16% to 19% and by -19% to 33% for the medium and the highest forcings, respectively. The ensemble mean changes are 6% and 8% for RCP4.5 and RCP8.5, respectively. In 2071-2100 the change in rainfall is projected to range by -20% to 32% with ensemble mean of 7% for RCP4.5 and by -29% to 46% with ensemble mean of 11% for RCP8.5. Results may suggest that higher is the forcing higher is the projected ensemble increase in future rainfall. Findings of this current work are consistent with those suggested by Stanturf et al. (2011) at Walembelle. Their work suggested change in projected rainfall ranging from -28% to 30% in wet season with an ensemble change of about -0.10 ± 9.63 and 0.69 ± 12.94 by 2050 and 2080, respectively. Obuobie (2008) stressed that projection generated by the stochastic weather

generator suggested that rainfall will increase by 6% in the period 2030-2039 compared to the baseline period 1991-2000. In this study the author found that projections by the Long Ashton Research Station Weather Generator (LARS-WG) were similar to those of MM5 forced by ECHAM4 based on the IS92a scenario. Findings of Padgham et al. (2015) corroborate the results of this current work as they suggest that rainfall will increase in the 2020s, 2030s and 2040s. They also stressed that there is no consistency in rainfall projections regarding the change direction in West-Africa as suggested by other authors like Roudier et al. (2014).

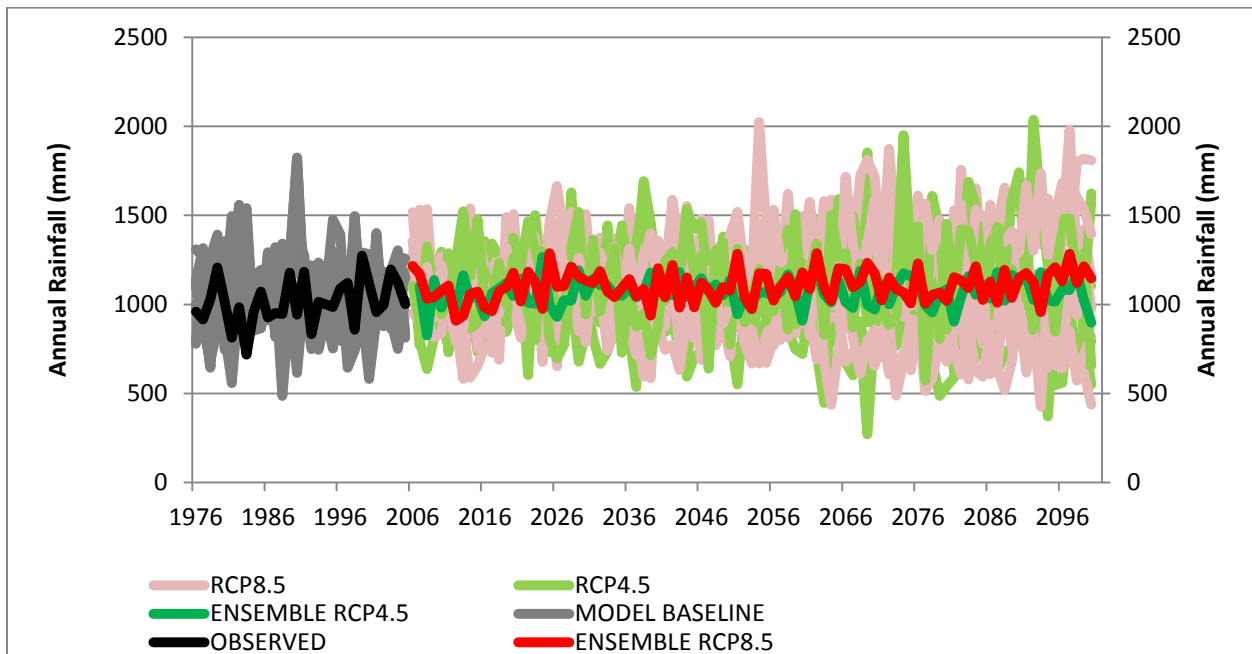


Figure 6-5: Estimated rainfall by the twelve scenarios for the baseline and future periods in the study area.

Table 6-5: Projected change in annual rainfall relative to the baseline (%).

Period	RCP4.5			RCP8.5		
	Min	Max	Ensemble	Min	Max	Ensemble
2011-2040	-5	17	6	-10	14	6
2041-2070	-16	19	6	-19	33	8
2071-2100	-20	32	7	-29	46	11

Table 6-6: Trend analysis of the annual rainfall in the baseline and future periods in the area.

		Bole		Wa		Navrongo	
		P-Value ^a	Slope	P-Value ^a	Slope	P-Value ^a	Slope
Baseline (1976-2005)	Observed	0.1261	6.9294	0.1091	6.8444	0.7238	1.2400
Projection 2006-2100	Ensemble RCP4.5	0.0946	0.7829	0.3380	0.3381	0.8219	0.0718
	Ensemble RCP8.5	0.0168	0.9332	0.2800	0.4583	0.0872	0.5813

a: the trend is significant for a P-value smaller than 0.05

6.4. Impact of climate change on groundwater recharge

During the baseline period the average groundwater estimated to be about 300 mm across the study area was. As presented by Table 6-7 and Figure 6-6, on average groundwater recharge is projected to increase in the study area. Compared to the baseline period, groundwater recharge is projected to increase by 6%-57% with ensemble mean of 34% for RCP4.5 during the period 2011-2040, while for RCP8.5 recharge is projected to change by about -5% to 62% with ensemble mean of 38% in the same period. In the period 2041-2070 groundwater recharge is projected to change by about -21% to 75% with ensemble mean of 33% for RCP4.5 and by -17% to 94% with ensemble mean 51% for RCP8.5. The change in recharge is projected to be about -25% to 91% with ensemble mean of 38% and -29% to 117% with ensemble mean of 51% for RCP4.5 and RCP8.5, respectively.

The results suggest a progressive increase in projected groundwater recharge from a period to the following for the ensemble mean of RCP4.5. While for the ensemble of RCP8.5 the projected change is the same for period 2041-20170 and 2071-2100. Lowest increase in future recharge is suggested to occur in the northern part of the study area (Navrongo area) while highest increase is suggested in the southern part (Bole area). The central part (Wa area) presents an intermediate condition to the two other areas. Therefore, the ensemble analysis suggests a south-north gradient that decreases from the south to the north.

Results of this current work corroborate findings of work by Obuobie (2008) that was done in the White Volta basin. Using future climate data provided by the run of the regional climate model MM5 forced by GCM ECHAM4 under the IS92a future climate scenario and the SWAT model, his work suggested that groundwater will increase by 29% in the period 2030-2039 compared to recharge in the ten-year baseline period lasting from 1991 to 2000. In other part of Africa, a similar result was obtained by Mileham et al. (2009) as their work projected an increase of 53% in groundwater in River Mitano catchment in Uganda during the period 2070-2100 compared to the forty-year baseline lasting from 1961 to 1990. This study was based on the regional climate model PRECIS under A2 emissions scenario. They also estimated groundwater recharge using a semi-distributed soil moisture balance model called SMBM which is different from the simple water balance method used in this current study. In Serral-Salinas aquifer located in South-Eastern part of Spain governed by a semi-arid climate, a work using several RCMs run under A1B and A2 scenarios suggests the ensemble projects a decrease in recharge in future (Pulido-Velazquez et al. 2015). The decreases projected by the ensemble are 14.0% and 57.7% for A2 and A1B, respectively. However, Pulido-Velazquez et al. (2015) stressed that some RCMs predict an increase in future recharge even when rainfall and temperature are projected to decrease and increase, respectively. In the grand river watershed in Ontario, Canada, Jyrkama and Sykes (2007) using eight scenarios based on the third assessment report of the IPCC (2001) found that climate change will increase groundwater recharge in the area. In their case they justified that the increase in recharge is due to the increase in future precipitation but also the increase in precipitation that will fall as rainfall in winter as result of increasing temperature. Their findings suggest increase in recharge ranging from 10% to 53%. In the Murray-Darling Basin (Crosbie et al. 2010) downscaled fifteen (15) GCMs under three climate scenarios and found that on average, climate change will increase the recharge by 5% around 2030 when compared to the baseline period. However, it should be stressed that, the impact of climate change varies widely from one model to another and spatially as suggested by the work done by Döll and Flörke (2005).

Table 6-7: Range of projected change in groundwater recharge relative to the baseline (%)

Period	RCP4.5			RCP8.5		
	Min	Max	Ensemble	Min	Max	Ensemble
2011-2040	6	57	34	-5	62	38
2041-2070	-21	75	33	-17	94	51
2071-2100	-25	91	38	-29	117	51

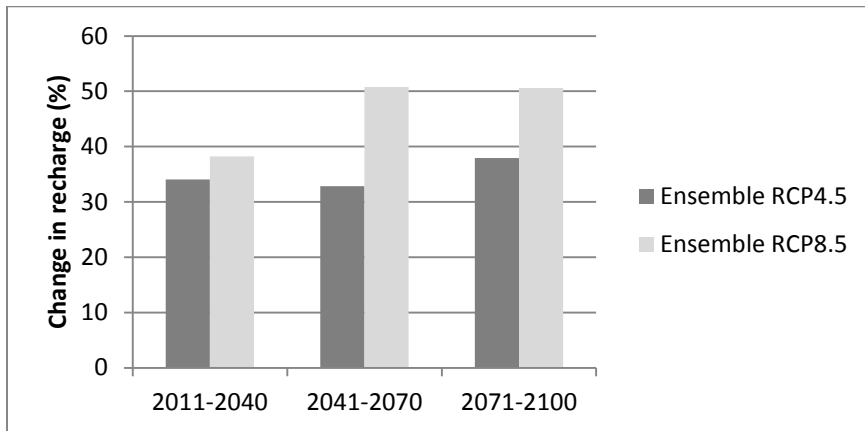


Figure 6-6: Projected change in groundwater recharge relative to the baseline period

6.5. Conclusion

The aim of this chapter was to estimate the impact of climate change on groundwater recharge in the crystalline basement aquifer of Northern Ghana. The ensemble analyse of the impact of climate change on groundwater recharge suggests an increase in recharge in the short-, medium- and long-term. Also, all the scenarios agree on the increase in future temperature and a positive trend was found for the temperature estimated by all the scenarios. Regarding rainfall, an increase was also suggested by eight of the twelve scenarios; the remainders suggested a decrease in future rainfall. Moreover, contrary to the temperature, trend in rainfall had mixed signal as the trend analysis suggests no trend for some scenarios, positive and negative trends for others. As the WetSpass model was calibrated using stream flow, the poor efficiency found may be due the quality of the streamflow data. Therefore, it is recommended a future study for which the calibrate procedure will be based on coupling the WetSpass model with a groundwater model such as MODFLOW.

Chapter 7 - GENERAL CONCLUSION AND PERSPECTIVES

7.1. Conclusion

This work was done to estimate the impact of climate change on groundwater recharge in the crystalline basement of Northern Ghana. Present day recharge estimated by the Baseflow analysis, Chloride Mass Balance method, Water Table Fluctuation method and a simple water balance method ranged from about 2% to 29%. Results of this current work were found to agree with previous works in and around the study area. Compared to recharge of about 300 mm during the baseline period, the recharge is likely to increase by 34% to 38%, by 33% to 51% and by 38% to 51% in the short-, medium- and long-term, respectively.

The aim of this hydrogeochemical investigation in this work was to identify the geochemical processes influencing water quality and the suitability of surface and groundwater for agricultural and domestic uses in the area. The results show that cation exchange and silicate weathering are the dominant processes controlling the chemical composition of the groundwater in the studied area, confirming the first hypothesis of the work. The meteoric genesis index shows that the majority of samples belong to shallow meteoric water percolation. All the groundwater samples were found to be fresh based on the TDS values. The results obtained from the 65 water samples also show that water type in the study area is mainly Ca-Mg-HCO₃. According to the observations and calculations conducted in this study, groundwater in the area is in large parts suitable for irrigation and agricultural purposes. No pollution due to anthropic activities was detected. Surface water is also found to be suitable for irrigation. PCA was found to be a useful tool as it yielded 5 significant factors from the original dataset of 15 parameters. The PCA also suggested that the groundwater samples originated from fresh recharge. The HCA classified the water samples into 3 classes that were found to be related to the level of mineralization of the samples but not to the geological formations. Samples of C1 have relatively lowest mineralization whilst C2 is composed of those of highest mineralisation and C3 is the transitional groups between them.

Analyses based on stable isotope ratio of surface and groundwater suggest that focused recharge from flooded rain water dominates in the study area. Further, no link between surface and groundwater was found.

Groundwater recharge and baseflow in the Sisili river basin (a sub catchment of the White Volta Basin) were estimated using recession curve analysis method and baseflow separation filters. An attempt was made to test the performance of the baseflow filters for the dry season and recession period. Findings suggest that the recharge ranges from 3% to 9% of the annual rainfall, with average value of 5%. The results also showed that the 'BFLOW' filter gave the best performance in estimating the baseflow in the period (2003-2008) analyzed. Recharge estimates based on recession and baseflow separation methods are considered potential recharge values and need to be validated with actual estimates from recharge methods such as tracers, water table fluctuation and chloride mass balance. The average monthly flashiness index suggests that the Sisili river at Wiasi is a stable river.

Using the WTF method and based on groundwater hydrographs from 11 monitoring wells, recharge to the groundwater of the basement crystalline aquifers of northern Ghana has been estimated to range from 6 to 17% of the annual rainfall, with a mean recharge of 10%. Spatial and temporal variability of the recharge and groundwater response to rainfall in the study area was attributed to the spatial and temporal variability of precipitation and the heterogeneity of aquifer properties within the study area. Besides, recharge estimated from wells with specific yield estimated from laboratory analysis show good agreement with recharge estimated by the CMB method.

Recharge estimated by the CMB method corroborates results of previous studies done in areas located within or in the vicinity of the area of the current work. Recharge was found to be highly variable within the study area. Estimated recharge by the chloride mass balance method ranges from 21 mm to 191 mm, representing 2.1% to 19.3% of the mean annual rainfall. The areal average recharge is 81 mm, representing 8.14% of the mean annual rainfall. In contrast to geological formation, soil type appears to be one of the factors controlling groundwater recharge in the study area.

The aim of the last chapter was to estimate the impact of climate change on groundwater recharge in the crystalline basement aquifer of Northern Ghana. As WetSpss poorly simulated groundwater recharge in the study area, the impact of climate change based on twelve climate scenarios was done by using a simple water balance approach. The ensemble analyse of the impact of climate change on groundwater recharge suggests an increase in recharge in the short-,

medium- and long-term, invalidating the second hypothesis of the current work. Also, all the scenarios agree on the increase in future temperature and a positive trend was found for the temperature estimated by all the scenarios. Regarding rainfall, an increase was also suggested by eight of the twelve scenarios; the remainders suggested a decrease in future rainfall. Moreover, contrary to the temperature, trend in rainfall had mixed signal as the trend analysis suggests no trend for some scenarios, positive and negative trends for others. As the WetSpass model was calibrated using stream flow, the poor efficiency found may be due the quality of the streamflow data. Therefore, it is recommended a future study for which the calibrate procedure will be based on coupling the WetSpass model with a groundwater model such as MODFLOW.

Since there is a good rate of recharge and this rate is projected to increase, it is recommended to increase groundwater developpement for irrigation and drinking water supply.

7.2. Perspectives

This is the first study to really address the hydrogeochemical processes influencing this area's water quality. Further study including heavy metals, other inorganic and organic trace substances as well as microbiological parameters is required to fully characterize groundwater hydrogeochemistry and usability, ideally also taking seasonal effects into account. In order to find whether the aquifer in area is recharged by heavy rains or light rains, or both, study taking into account $\delta^2\text{H}$ and $\delta^{18}\text{O}$ in rain is suggested. This work also suggests the use of high precision method such as ion chromatogram in determining chloride content in rain water.

It is suggested to estimate specific yield by using a laboratory analysis and/or combine it with long time pumping tests using observed well to improve the determination of the specific yield values and thereby the groundwater recharge estimated by the WTF method. The results of this study could be improved by increasing the number of wells monitored in the study area.

As it is not possible to relate the FAO soil class to soil texture, it is recommended to identify soil texture and saturated hydraulic conductivity of soil at the sites where the groundwater samples were collected in order to determine the extent to which soil texture controls groundwater recharge in the area. For chloride content analysis in rain, a high precision method such as ion chromatogram should is highly recommended.

As the WetSpass model was calibrated using stream flow, it is recommended a future study for which the calibration procedure will be based on coupling the WetSpass model with a groundwater model such as MODFLOW. In order to have a dense observation network of piezometers it is also suggested to equip new wells with automatic water level recorder. As a single well pumping test does not allow estimation of specific yield it is recommended to achieve long-term pumping test using observed well across the area. It is also suggested to densify the hydrometric network by installing new high precision stream gauges in order to collect that will enhance accuracy of water balance models in the area. The use of dynamical downscaling method is recommended in future work for a comparison purpose. In order to accurately estimate PET using a corrected Hargraves method, it is suggested to study the relation between Hargraves method and Penman Monteith on a monthly or at least on a seasonal basis. A long-term and continuous measurement of stable isotope in rainfall and groundwater will also help in elucidating groundwater recharge process in the area by checking whether the aquifer is a selective system regarding the type of rainfall (heavy or light) recharging the aquifer.

REFERENCES

- Abdollahi K, Bashir I, Verbeiren B, et al (2017) A distributed monthly water balance model: formulation and application on Black Volta Basin. *Environ Earth Sci* 76:198 . doi: 10.1007/s12665-017-6512-1
- Acheampong SY, Hess JW (2000) Origin of the shallow groundwater system in the southern Voltaian Sedimentary Basin of Ghana: an isotopic approach. *J Hydrol* 233:37–53 . doi: 10.1016/S0022-1694(00)00221-3
- Addai MO, Yidana SM, Chegbeleh L-P, et al (2015) Groundwater recharge processes in the Nasia sub-catchment of the White Volta Basin: Analysis of porewater characteristics in the unsaturated zone. *J Afr Earth Sci*
- Adongo TA, Kugbe JX, Gbedzi VD (2014) Siltation of the Reservoir of Veia Irrigation Dam in the Bongo District of the Upper East Region, Ghana. *Int J Sci Technol* 4:7
- Aghazadeh N, Mogaddam AA, others (2010) Assessment of groundwater quality and its suitability for drinking and agricultural uses in the Oshnavieh area, Northwest of Iran. *J Environ Prot* 1:30
- Aish AM, Batelaan O, De Smedt F (2010) Distributed recharge estimation for groundwater modeling using WetSpa model, case study—Gaza strip, Palestine. *Arab J Sci Eng* 35:155
- Aksoy H, Unal NE, Pektas AO (2008) Smoothed minima baseflow separation tool for perennial and intermittent streams. *Hydrol Process* 22:4467–4476
- Alagbe S (2002) Groundwater resources of river Kan Gimi Basin, north-central, Nigeria. *Environ Geol* 42:404–413 . doi: 10.1007/s00254-002-0544-9
- Alam F (2014) Evaluation of hydrogeochemical parameters of groundwater for suitability of domestic and irrigational purposes: a case study from central Ganga Plain, India. *Arab J Geosci* 7:4121–4131

- Alexander LV, Arblaster JM (2017) Historical and projected trends in temperature and precipitation extremes in Australia in observations and CMIP5. *Weather Clim Extrem* 15:34–56 . doi: 10.1016/j.wace.2017.02.001
- Allen RG, Pereira LS, Raes D, et al (1998) Crop evapotranspiration-Guidelines for computing crop water requirements-FAO Irrigation and drainage paper 56. FAO Rome 300:D05109
- Allison GB, Cook PG, Barnett SR, et al (1990) Land clearance and river salinisation in the western Murray Basin, Australia. *J Hydrol* 119:1–20
- Anayah FM, Kaluarachchi JJ, Pavelic P, Smakhtin V (2013) Predicting groundwater recharge in Ghana by estimating evapotranspiration. *Water Int* 38:408–432 . doi: 10.1080/02508060.2013.821642
- Angelina A, Gado Djibo A, Seidou O, et al (2015) Changes to flow regime on the Niger River at Koulikoro under a changing climate. *Hydrol Sci J* 60:1709–1723 . doi: 10.1080/02626667.2014.916407
- Anku YS, Banoeng-Yakubo B, Asiedu DK, Yidana SM (2009) Water quality analysis of groundwater in crystalline basement rocks, Northern Ghana. *Environ Geol* 58:989–997 . doi: 10.1007/s00254-008-1578-4
- Apambire WB, Boyle DR, Michel FA (1997) Geochemistry, genesis, and health implications of fluoriferous groundwaters in the upper regions of Ghana. *Environ Geol* 33:13–24
- Armanuos AM, Negm A, Yoshimura C, Valeriano OCS (2016) Application of WetSpas model to estimate groundwater recharge variability in the Nile Delta aquifer. *Arab J Geosci* 9:1–14
- Arnold JG, Allen PM (1999) Automated Methods for Estimating Baseflow and Ground Water Recharge from Streamflow Records1. *JAWRA J Am Water Resour Assoc* 35:411–424
- Arnold JG, Muttiah RS, Srinivasan R, Allen PM (2000) Regional estimation of base flow and groundwater recharge in the Upper Mississippi river basin. *J Hydrol* 227:21–40

- Asante FA, Amuakwa-Mensah F (2014) Climate change and variability in Ghana: Stocktaking. *Climate* 3:78–99 . doi: 10.3390/cli3010078
- Attoh K, Evans MJ, Bickford ME (2006) Geochemistry of an ultramafic-rodinigte rock association in the Paleoproterozoic Dixcove greenstone belt, southwestern Ghana. *J Afr Earth Sci* 45:333–346 . doi: 10.1016/j.jafrearsci.2006.03.010
- Ayar PV, Vrac M, Bastin S, et al (2016) Intercomparison of statistical and dynamical downscaling models under the EURO- and MED-CORDEX initiative framework: present climate evaluations. *Clim Dyn* 46:1301–1329 . doi: 10.1007/s00382-015-2647-5
- Bagamsah TT (2005) The impact of bushfire on carbon and nutrient stocks as well as albedo in the savanna of northern Ghana. Cuvillier Verlag
- Baker DB, Richards RP, Loftus TT, Kramer JW (2004) A new flashiness index: Characteristics and applications to midwestern rivers and streams¹
- Bannerman RR, Ayibotele NB (1984) Some critical issues with monitoring crystalline rock aquifers for groundwater management in rural areas. In: *Challenges in African Hydrology and Water Resources*. IAHS, Harare, Zimbabwe
- Banoeng-Yakubo B, Yidana SM, Anku Y, et al (2009a) Water quality characterization in some Birimian aquifers of the Birim Basin, Ghana. *KSCE J Civ Eng* 13:179–187 . doi: 10.1007/s12205-009-0179-4
- Banoeng-Yakubo B, Yidana SM, Nti E (2009b) An evaluation of the genesis and suitability of groundwater for irrigation in the Volta Region, Ghana. *Environ Geol* 57:1005–1010
- Barnes BS (1939) The structure of discharge-recession curves. *Eos Trans Am Geophys Union* 20:721–725
- Barry B, Obuobie E, Andreini M, et al (2005) Comprehensive assessment of water management in agriculture (comparative study of river basin development and management

- Barry RG, Chorley RJ (2004) *Atmosphere, Weather and Climate*, Routledge. Taylor & Francis e-Library, 11 New Fetter Lane, London EC4P 4EE
- Bart R, Hope A (2014) Inter-seasonal variability in baseflow recession rates: The role of aquifer antecedent storage in central California watersheds. *J Hydrol* 519:205–213
- Batayneh A, Laboun A, Qaisy S, et al (2012) Assessing groundwater quality of the shallow alluvial aquifer system in the Midyan Basin, northwestern Saudi Arabia. *Arab Gulf J Sci Res* 30:7–13
- Batelaan O, De Smedt F (2001) WetSpa: a flexible, GIS based, distributed recharge methodology for regional groundwater modelling. *IAHS Publ* 11–18
- Batelaan O, Wang Z-M, De Smedt F (1996) An adaptive GIS toolbox for hydrological modelling. *IAHS Publ-Ser Proc Rep-Intern Assoc Hydrol Sci* 235:3–10
- Batjes NH (2009) Harmonized soil profile data for applications at global and continental scales: updates to the WISE database. *Soil Use Manag* 25:124–127
- Belkhir L, Boudoukha A, Mouni L, Baouz T (2010) Application of multivariate statistical methods and inverse geochemical modeling for characterization of groundwater—A case study: Ain Azel plain (Algeria). *Geoderma* 159:390–398 . doi: 10.1016/j.geoderma.2010.08.016
- Berg G (1932) *Das Vorkommen der chemischen Elemente auf der Erde*. JA Barth
- Boateng TK, Opoku F, Acquah SO, Akoto O (2016) Groundwater quality assessment using statistical approach and water quality index in Ejisu-Juaben Municipality, Ghana. *Environ Earth Sci* 75:1–14 . doi: 10.1007/s12665-015-5105-0
- Boé J, Terray L, Habets F, Martin E (2007) Statistical and dynamical downscaling of the Seine basin climate for hydro-meteorological studies. *Int J Climatol* 27:1643–1655 . doi: 10.1002/joc.1602

- Bromley J, Edmunds WM, Fellman E, et al (1997) Estimation of rainfall inputs and direct recharge to the deep unsaturated zone of southern Niger using the chloride profile method. *J Hydrol* 188:139–154
- Brunner P, Bauer P, Eugster M, Kinzelbach W (2004) Using remote sensing to regionalize local precipitation recharge rates obtained from the chloride method. *J Hydrol* 294:241–250
- Burdon DJ, Mazloum S (1958) Some chemical types of groundwater from Syria. In: *Proceedings of the UNESCO Symposium, Teheran*. UNESCO, Paris. pp 73–90
- Burns DA (2002) Stormflow-hydrograph separation based on isotopes: the thrill is gone—what’s next? *Hydrol Process* 16:1515–1517
- Busuioc A, Von Storch H, Schnur R (1999) Verification of GCM-generated regional seasonal precipitation for current climate and of statistical downscaling estimates under changing climate conditions. *J Clim* 12:258–272
- Carrier M-A (2008) Synthèse hydrogéologique du Nord du Ghana. Master of Science, INRS-Eau, Terre et Environnement
- Cerling TE, Pederson BL, Von Damm KL (1989) Sodium-calcium ion exchange in the weathering of shales: Implications for global weathering budgets. *Geology* 17:552–554
- Chadha DK (1999) A proposed new diagram for geochemical classification of natural waters and interpretation of chemical data. *Hydrogeol J* 7:431–439
- Chandra S, Dewandel B, Dutta S, Ahmed S (2010) Geophysical model of geological discontinuities in a granitic aquifer: analyzing small scale variability of electrical resistivity for groundwater occurrences. *J Appl Geophys* 71:137–148
- Chapman DV (1996) *Water quality assessments: a guide to the use of biota, sediments and water in environmental monitoring*, 2nd edn. WHO, London
- Chaturvedi RK, Joshi J, Jayaraman M, et al (2012) Multi-model climate change projections for India under representative concentration pathways. *Curr Sci* 791–802

- Cherkauer DS (2004) Quantifying groundwater recharge at multiple scales using PRMS and GIS. *Ground Water* 42:97–110
- Cherkauer DS, Ansari SA (2005) Estimating ground water recharge from topography, hydrogeology, and land cover. *Groundwater* 43:102–112
- Childs EC (1960) The nonsteady state of the water table in drained land. *J Geophys Res* 65:780–782
- Clark I (2015) *Groundwater Geochemistry and Isotopes*. CRC Press, London
- Cloutier V, Lefebvre R, Therrien R, Savard MM (2008) Multivariate statistical analysis of geochemical data as indicative of the hydrogeochemical evolution of groundwater in a sedimentary rock aquifer system. *J Hydrol* 353:294–313
- Cobbina SJ, Nyame FK, Obiri S (2012) Groundwater Quality in the Sahelian Region of Northern Ghana, West Africa. *Res J Environ Earth Sci* 4:482–491
- Cook PG, Walker GR, Jolly ID (1989) Spatial variability of groundwater recharge in a semiarid region. *J Hydrol* 111:195–212
- Cooper DM, Wilkinson WB, Arnell NW (1995) The effects of climate changes on aquifer storage and river baseflow. *Hydrol Sci J* 40:615–631
- Craig H (1961) Standard for reporting concentrations of deuterium and oxygen-18 in natural waters. *Science* 133:1833–1834
- Crosbie RS, Binning P, Kalma JD (2005) A time series approach to inferring groundwater recharge using the water table fluctuation method. *Water Resour Res* 41:W01008 . doi: 10.1029/2004WR003077
- Crosbie RS, McCallum JL, Walker GR, Chiew FH (2010) Modelling climate-change impacts on groundwater recharge in the Murray-Darling Basin, Australia. *Hydrogeol J* 18:1639–1656

- Daintith J, Martin EA (2005) A dictionary of science. Oxford University Press, Oxford; New York
- Dakoure D (2003) ETUDE HYDROGEOLOGIQUE ET GEOCHIMIQUE DE LA BORDURE SUD-EST DU BASSIN SEDIMENTAIRE DE TAOUDENI (BURKINA FASO-MALI)-ESSAI DE MODELISATION. Université Pierre et Marie Curie-Paris VI
- Dams J, Woldeamlak ST, Batelaan O (2008) Predicting land-use change and its impact on the groundwater system of the Kleine Nete catchment, Belgium. *Hydrol Earth Syst Sci* 12:1369–1385
- Damtew AD (2015) Source, Mechanism, and Rate of Groundwater Recharge in the South-western Part of the Main Ethiopian Rift, East Africa. Univ., Selbstverl. Inst. für Geologie, Mineralogie und Geophysik
- Daniel III CC (1996) Ground-water recharge to the regolith-fractured crystalline rock aquifer system, Orange County, North Carolina
- Dansgaard W, Johnsen SJ, Clausen HB, et al (1993) Evidence for general instability of past climate from a 250-kyr. *Nature* 364:15
- Dash SK, Jenamani RK, Kalsi SR, Panda SK (2007) Some evidence of climate change in twentieth-century India. *Clim Change* 85:299–321
- Dassargues A (1991) Modeles Mathematiques en Hydrogeologie et parametrisation. In: *Annales de la Societe Geologique de Belgique*. Belgique, pp 217–229
- Datta PS, Tyagi SK (1996) Major ion chemistry of groundwater in Delhi area: chemical weathering processes and groundwater flow regime. *J-Geol Soc India* 47:179–188
- Davis JC (1986) *Statistics and data analysis in geology*. 1986. John Wiley & Sons, New York
- de Groen MM, Savenije HHG (2006) A monthly interception equation based on the statistical characteristics of daily rainfall. *Water Resour Res* 42:W12417 . doi: 10.1029/2006WR005013

- Deelstra J, Iital A, Povilaitis A, et al (2014) Reprint of “Hydrological pathways and nitrogen runoff in agricultural dominated catchments in Nordic and Baltic countries.” *Agric Ecosyst Environ* 198:65–73
- Demlie M, Wohnlich S, Gizaw B, Stichler W (2007) Groundwater recharge in the Akaki catchment, central Ethiopia: evidence from environmental isotopes ($\delta^{18}\text{O}$, $\delta^2\text{H}$ and ^3H) and chloride mass balance. *Hydrol Process* 21:807–818
- Deutsch WJ, Siegel R (1997) *Groundwater geochemistry: fundamentals and applications to contamination*. CRC press, Boca Raton
- Diouf OC, Faye SC, Diedhiou M, et al (2013) Combined uses of water-table fluctuation (WTF), chloride mass balance (CMB) and environmental isotopes methods to investigate groundwater recharge in the Thiaroye sandy aquifer (Dakar, Senegal). *Afr J Environ Sci Technol* 6:425–437
- Döll P, Flörke M (2005) Global-Scale Estimation of Diffuse Groundwater Recharge : Model Tuning to Local Data for Semi-Arid and Arid Regions and Assessment of Climate Change Impact
- Doneen LD (1964) *Water quality for agriculture*
- Dorji S, Herath S, Mishra BK (2017) Future Climate of Colombo Downscaled with SDSM-Neural Network. *Climate* 5:24
- Dow CL (2007) Assessing regional land-use/cover influences on New Jersey Pinelands streamflow through hydrograph analysis. *Hydrol Process* 21:185–197
- Droogers P, Allen RG (2002) Estimating reference evapotranspiration under inaccurate data conditions. *Irrig Drain Syst* 16:33–45
- Durov SA (1948) Natural waters and graphic representation of their composition. In: *Dokl Akad Nauk SSSR*. pp 87–90

- Eaton FM, others (1935) Boron in soils and irrigation waters and its effect on plants, with particular reference to the San Joaquin Valley of California. United States Department of Agriculture, Economic Research Service
- Eckhardt K (2005) How to construct recursive digital filters for baseflow separation. *Hydrological Process* 19:507–515
- Edjah AKM, Akiti TT, Osae S, et al (2015) Hydrogeochemistry and isotope hydrology of surface water and groundwater systems in the Ellembele district, Ghana, West Africa. *Applied Water Science* 1–15 . doi: 10.1007/s13201-015-0273-3
- Edmunds W, Fellman E, Goni I, Prudhomme C (2002) Spatial and temporal distribution of groundwater recharge in northern Nigeria. *Hydrogeology Journal* 10:205–215
- Edmunds WM, Darling WG, Kinniburgh DG (1988) Solute profile techniques for recharge estimation in semi-arid and arid terrain. In: *Estimation of natural groundwater recharge*. Springer, pp 139–157
- Edwards TW (1993) Interpreting past climate from stable isotopes in continental organic matter. *Climatic Change and Isotope Records* 333–341
- Eriksson E, Khunakasem V (1969) Chloride concentration in groundwater, recharge rate and rate of deposition of chloride in the Israel Coastal Plain. *Journal of Hydrology* 7:178–197
- Fan X, Cui B, Zhao H, et al (2010) Assessment of river water quality in Pearl River Delta using multivariate statistical techniques. *Water Science and Technology* 2:1220–1234 . doi: 10.1016/j.proenv.2010.10.133
- Ferket BV, Samain B, Pauwels VR (2010) Internal validation of conceptual rainfall–runoff models using baseflow separation. *Journal of Hydrology* 381:158–173
- Fianko JR, Nartey VK, Donkor A (2010) The hydrochemistry of groundwater in rural communities within the Tema District, Ghana. *Environmental Monitoring and Assessment* 168:441–449 . doi: 10.1007/s10661-009-1125-0

- Firempong CK, Nsiah K, Awunyo-Vitor D, Dongsogo J (2013) Soluble fluoride levels in drinking water-a major risk factor of dental fluorosis among children in Bongo community of Ghana. *Ghana Med J* 47:16–23
- Fisher RS, William F. Mullican III (1997) Hydrochemical Evolution of Sodium-Sulfate and Sodium-Chloride Groundwater Beneath the Northern Chihuahuan Desert, Trans-Pecos, Texas, USA. *Hydrogeol J* 2:4–16
- Forkuor G, Pavelic P, Asare E, Obuobie E (2013) Modelling potential areas of groundwater development for agriculture in northern Ghana using GIS/RS. *Hydrol Sci J* 58:437–451 . doi: 10.1080/02626667.2012.754101
- Freeze RA, Cherry JA (1979) *Groundwater*. Prentice-Hall Inc., New Jersey
- Fuka DR, Walter MT, Archibald JA, Easton ZM (2013) *EcoHydrology: A Community Modeling Foundation for Eco-Hydrology*. R Package Version 0.4. 5
- Furey PR, Gupta VK (2001) A physically based filter for separating base flow from streamflow time series. *Water Resour Res* 37:2709–2722 . doi: 10.1029/2001WR000243
- Ganyaglo SY, Banoeng-Yakubo B, Osae S, et al (2011) Water quality assessment of groundwater in some rock types in parts of the eastern region of Ghana. *Environ Earth Sci* 62:1055–1069 . doi: DOI 10.1007/s12665-010-0594-3
- Gates JB, Scanlon BR, Mu X, Zhang L (2011) Impacts of soil conservation on groundwater recharge in the semi-arid Loess Plateau, China. *Hydrogeol J* 19:865
- Gaye CB, Edmunds WM (1996) Groundwater recharge estimation using chloride, stable isotopes and tritium profiles in the sands of northwestern Senegal. *Environ Geol* 27:246–241
- Gebere SB, Alamirew T, Merkel BJ, Melesse AM (2016) Land Use and Land Cover Change Impact on Groundwater Recharge: The Case of Lake Haramaya Watershed, Ethiopia. In: *Landscape Dynamics, Soils and Hydrological Processes in Varied Climates*. Springer, Cham, pp 93–110

- Gebert WA, Radloff MJ, Considine EJ, Kennedy JL (2007) Use of Streamflow Data to Estimate Base Flow/Ground-Water Recharge For Wisconsin. *JAWRA J Am Water Resour Assoc* 43:220–236 . doi: 10.1111/j.1752-1688.2007.00018.x
- Ghamarnia H, Rezvani V, Khodaei E, Mirzaei H (2011) Calibration of Hargreaves equation for estimating monthly reference evapotranspiration in the west of Iran. In: RESEARCHES of THE FIRST INTERNATIONAL CONFERENCE on AGRICULTURE and NATURAL RESOURCES (BABYLON AND RAZI UNIVERSITIES)
- Ghana Standards Authority (GSA) (2013) Water Quality- Specification for drinking water, 4th edn. Ghana Standards Authority, Accra
- Ghana Statistical Service (2012) 2010 Population and Housing Census
- Gibbs RJ (1970) Mechanisms controlling world water chemistry. *Science* 170:1088–1090
- Gibrilla A, Osaе S, Akiti TT, et al (2010) Hydrogeochemical and Groundwater Quality Studies in the Northern Part of the Densu River Basin of Ghana. *J Water Resour Prot* 02:1071–1081 . doi: 10.4236/jwarp.2010.212126
- Giorgi F, Hewitson B, Christensen J, et al (2001) Regional climate information—evaluation and projections
- Girman J, Gun J van der, Haie N, et al (2007) Groundwater Resources Sustainability Indicators, Jaroslav Vrba and Annukka Lipponen. UNESCO, 7, Place de Fontenoy, 75352 Paris 07 SP (France)
- Gonfiantini R (1978) Standards for stable isotope measurements in natural compounds. *Nature* 271:534–536
- Gonzales AL, Nonner J, Heijkers J, Uhlenbrook S (2009) Comparison of different base flow separation methods in a lowland catchment. *Hydrol Earth Syst Sci* 13:2055–2068

- Goodess CM, Anagnostopoulou C, Bárdossy A, et al (2007) An intercomparison of statistical downscaling methods for Europe and European regions—assessing their performance with respect to extreme temperature and precipitation events. *Clim Change*
- Graszkievicz ZM, Murphy RE, Hill PI, et al (2011) Review of techniques for estimating the contribution of baseflow to flood hydrographs. In: *Proceedings of the 34th World Congress of the International Association for Hydro-Environment Research and Engineering: 33rd Hydrology and Water Resources Symposium and 10th Conference on Hydraulics in Water Engineering*. Engineers Australia, p 138
- Guilford JP (1942) *Fundamental statistics in psychology and education*.
- Güler C, Thyne GD (2004) Hydrologic and geologic factors controlling surface and groundwater chemistry in Indian Wells-Owens Valley area, southeastern California, USA. *J Hydrol* 285:177–198
- Gutmann E, Pruitt T, Clark MP, et al (2014) An intercomparison of statistical downscaling methods used for water resource assessments in the United States. *Water Resour Res* 50:7167–7186 . doi: 10.1002/2014WR015559
- Gyau-Boakye P (2001) Sources of Rural Water Supply in Ghana. *Water Int* 26:96–104 . doi: 10.1080/02508060108686890
- Hall DW, Risser DW (1993) EFFECTS OF AGRICULTURAL NUTRIENT MANAGEMENT ON NITROGEN FATE AND TRANSPORT IN LANCASTER COUNTY PENNSYLVANIA1. *JAWRA J Am Water Resour Assoc* 29:55–76
- Hall FR (1968) Base-Flow Recessions—A Review. *Water Resour Res* 4:973–983
- Hargreaves GL, Hargreaves GH, Riley JP (1985) Irrigation water requirements for Senegal River basin. *J Irrig Drain Eng* 111:265–275
- Haylock MR, Cawley GC, Harpham C, et al (2006) Downscaling heavy precipitation over the United Kingdom: a comparison of dynamical and statistical methods and their future scenarios. *Int J Climatol* 26:1397–1415

- Healy RW (2010) Estimating groundwater recharge. Cambridge University Press, Cambridge ; New York
- Healy RW, Cook PG (2002) Using groundwater levels to estimate recharge. *Hydrogeol J* 10:91–109
- Heath RC (1983) Basic ground-water hydrology: US Geological Survey Water-Supply Paper 2220, 84 p. 1984. Ground-Water Reg U S US Geol Surv Water-Supply Pap 2242:78
- Helena B, Pardo R, Vega M, et al (2000) Temporal evolution of groundwater composition in an alluvial aquifer (Pisuerga River, Spain) by principal component analysis. *Water Res* 34:807–816
- Helsel DR, Hirsch RM (1992) Statistical methods in water resources. Elsevier, Amsterdam
- Hill RA (1940) Geochemical patterns in Coachella Valley. *Trans Am Geophys Union* 21:46 .
doi: 10.1029/TR021i001p00046
- Hinzman LD, Bettez ND, Bolton WR, et al (2005) Evidence and implications of recent climate change in northern Alaska and other arctic regions. *Clim Change* 72:251–298
- Hirdes W, Konan KG, N'Da D, et al (2007) Geology of the Northern Portion of the Oboisso Area, Côte d'Ivoire. Sheets 4A B 4:
- Hoefs J (2009) Stable isotope geochemistry, Sixth edition. Springer, Berlin
- Holtzschlag DJ (1997) A generalized estimate of ground-water-recharge rates in the Lower Peninsula of Michigan. US Geol Surv Water-Supply Pap 1–37
- Hounslow A (1995) Water quality data: analysis and interpretation. Lewis Publishers, Boca Raton
- Ifabiyi IP (2008) Depth of hand dug wells and water chemistry: Example from Ibadan Northeast Local Government Area (LGA), Oyo-state, Nigeria. *J Soc Sci* 17:261–266
- Institute of Hydrology (1980) Low Flow Studies. Wallingford, Oxon

- Intergovernmental Panel on Climate Change (ed) (2001) Climate change 2001: the scientific basis: contribution of Working Group I to the third assessment report of the Intergovernmental Panel on Climate Change. Cambridge University Press, Cambridge ; New York
- IPCC (2014) Climate Change 2014: Impacts, Adaptation, and Vulnerability. Part B: regional aspects-Contribution of Working Group II to the Fifth Assessment Report of the Intergovernmental Panel on Climate Change, Cambridge University Press. United Kingdom and New York, , NY, USA
- IPCC (2013) Climate change 2013: the physical science basis ; summary for policymakers, a report of Working Group I of the IPCC, technical summary, a report accepted by Working Group I of the IPCC but not approved in detail and frequently asked questions ; part of the Working Group I contribution to the fifth assessment report of the Intergovernmental Panel on Climate Change. Intergovernmental Panel on Climate Change, New York
- IPCC (2007) Summary for Policymakers. In: Climate Change 2007: Impacts, Adaptation and Vulnerability. Contribution of Working Group II to the Fourth Assessment Report of the Intergovernmental Panel on Climate Change, M.L. Parry, O.F. Canziani, J.P. Palutikof, P.J. van der Linden and C.E. Hanson, Eds. Cambridge University Press, Cambridge, UK, pp 7–22
- Ishaku I, Ahmed A, Abubakar M (2011) Assessment of groundwater quality using chemical indices and GIS mapping in Jada area, Northwestern Nigeria. J Earth Sci Geotech Eng 1:35–60
- Jackson JE (1991) A user's guide to principal components
- Jagadeshan G, Kalpana L, Elango L (2015) Hydrogeochemistry of high fluoride groundwater in hard rock aquifer in a part of Dharmapuri district, Tamil Nadu, India. Geochem Int 53:554–564 . doi: 10.1134/S0016702915060038

- Johnson AI (1967) Specific yield: compilation of specific yields for various materials. US Government Printing Office
- Joreskog KG, Klovan JE, Reymont RA (1976) Geological factor analysis. Elsevier Scientific Pub. Co.
- Jørgensen N, Banoeng-Yakubo B (2001) Environmental isotopes (^{18}O , ^2H , and $^{87}\text{Sr}/^{86}\text{Sr}$) as a tool in groundwater investigations in the Keta Basin, Ghana. *Hydrogeol J* 2:190–201 . doi: 10.1007/s100400000122
- Jyrkama MI, Sykes JF (2007) The impact of climate change on spatially varying groundwater recharge in the grand river watershed (Ontario). *J Hydrol* 338:237–250 . doi: 10.1016/j.jhydrol.2007.02.036
- Kaiser HF (1960) The application of electronic computers to factor analysis. *Educ Psychol Meas*
- Kaka EA, Akiti TT, Nartey VK, et al (2011) Hydrochemistry and evaluation of groundwater suitability for irrigation and drinking purposes in the southeastern Volta river basin: manyakrobo area, Ghana. *Elixir Agric* 39:4793–4807
- Kankam-Yeboah K, Obuobie E, Amisigo B, Opoku-Ankomah Y (2013) Impact of climate change on streamflow in selected river basins in Ghana. *Hydrol Sci J* 58:773–788 . doi: 10.1080/02626667.2013.782101
- Karantk KR (1987) Ground water assessment: development and management. Tata McGraw-Hill Education, New Delhi
- Kasei RA (2010) Modelling impacts of climate change on water resources in the Volta Basin, West Africa
- Kaser G, Hardy DR, Mölg T, et al (2004) Modern glacier retreat on Kilimanjaro as evidence of climate change: observations and facts. *Int J Climatol* 24:329–339

- Keller A, Weight E, Taylor S (2013) Rapid assessment of water availability and appropriate technologies for small-scale farming: guidelines for practitioners. International Water Management Institute (IWMI).
- Kesse GO (1985) The mineral and rock resources of Ghana. A.A. Balkema, Rotterdam
- Kim J-H, Kim R-H, Lee J, et al (2005) Multivariate statistical analysis to identify the major factors governing groundwater quality in the coastal area of Kimje, South Korea. *Hydrol Process* 19:1261–1276
- Koffi KV, Obuobie E, Banning A, Wohnlich S (2017) Hydrochemical characteristics of groundwater and surface water for domestic and irrigation purposes in Vea catchment, Northern Ghana. *Environ Earth Sci* 76:185 . doi: 10.1007/s12665-017-6490-3
- Kortatsi BK (1994) Groundwater utilization in Ghana. *IAHS Publ-Ser Proc Rep-Intern Assoc Hydrol Sci* 222:149–156
- Kortatsi BK (2006) Hydrochemical characterization of groundwater in the Accra plains of Ghana. *Environ Geol* 50:299–311 . doi: 10.1007/s00254-006-0206-4
- Kortatsi BK (2007) Hydrochemical framework of groundwater in the Ankobra Basin, Ghana. *Aquat Geochem* 13:41–74 . doi: 10.1007/s10498-006-9006-4
- Kortatsi BK, Anku YSA, Anornu GK (2009) Characterization and appraisal of facets influencing geochemistry of groundwater in the Kulpawn sub-basin of the White Volta Basin, Ghana. *Environ Geol* 58:1349–1359 . doi: 10.1007/s00254-008-1638-9
- Kresic N (2009) Groundwater resources sustainability, management, and restoration. McGraw-Hill, New York
- Kumar CP (2012) Climate Change and Its Impact on Groundwater Resources. *Research Inventory: International Journal of Engineering and Science*, ISSN

- Kumar PS, Jegathambal P, Nair S, James EJ (2015) Temperature and pH dependent geochemical modeling of fluoride mobilization in the groundwater of a crystalline aquifer in southern India. *J Geochem Explor* 156:1–9 . doi: 10.1016/j.gexplo.2015.04.008
- Kumar SK, Logeshkumaran A, Magesh NS, et al (2014) Hydro-geochemistry and application of water quality index (WQI) for groundwater quality assessment, Anna Nagar, part of Chennai City, Tamil Nadu, India. *Appl Water Sci* 5:335–343 . doi: 10.1007/s13201-014-0196-4
- Kura NU, Ramli MF, Sulaiman WNA, et al (2013) Evaluation of Factors Influencing the Groundwater Chemistry in a Small Tropical Island of Malaysia. *Int J Environ Res Public Health* 10:1861–1881 . doi: 10.3390/ijerph10051861
- Ladson AR, Brown R, Neal B, Nathan R (2013) A standard approach to baseflow separation using the Lyne and Hollick filter. *Aust J Water Resour* 17:25–34
- Lakshmanan E, Kannan R, Kumar MS (2003a) Major ion chemistry and identification of hydrogeochemical processes of ground water in a part of Kancheepuram district, Tamil Nadu, India. *Environ Geosci* 10:157–166
- Lakshmanan E, Kannan R, Kumar MS (2003b) Major ion chemistry and identification of hydrogeochemical processes of ground water in a part of Kancheepuram district , Tamil Nadu , India. 157–166
- Lasm T, De Lasme O, Oga M-S, et al (2011) Caractérisation hydrochimique des aquifères fissurés de la région de San-Pedro (Sud-Ouest de la Côte d’Ivoire). *Int J Biol Chem Sci* 5:
- Leduc C, Bromley J, Schroeter P (1997) Water table fluctuation and recharge in semi-arid climate: some results of the HAPEX-Sahel hydrodynamic survey (Niger). *J Hydrol* 188:123–138
- Lee C-H, Chen W-P, Lee R-H (2006) Estimation of groundwater recharge using water balance coupled with base-flow-record estimation and stable-base-flow analysis. *Environ Geol* 51:73–82

- Lee G, Shin Y, Jung Y (2014a) Development of Web-Based RECESS Model for Estimating Baseflow Using SWAT. *Sustainability* 6:2357–2378
- Lee JM, Park YS, Kum D, et al (2014b) Assessing the effect of watershed slopes on recharge/baseflow and soil erosion. *Paddy Water Environ* 12:169–183
- Leube A, Hirdes W, Mauer R, Kesse GO (1990) The early Proterozoic Birimian Supergroup of Ghana and some aspects of its associated gold mineralization. *Precambrian Res* 46:139–165
- Li H, Sheffield J, Wood EF (2010) Bias correction of monthly precipitation and temperature fields from Intergovernmental Panel on Climate Change AR4 models using equidistant quantile matching. *J Geophys Res* 115: . doi: 10.1029/2009JD012882
- Liang S, Xiao Z (2012) Global land surface products: Leaf area index product data collection (1985–2010). Beijing Norm Univ Doi 10: . doi: 10.6050/glass863.3004.db
- Lim KJ, Engel BA, Tang Z, et al (2005) Automated web gis based hydrograph analysis tool, WHAT1. Wiley Online Library
- Lim KJ, Park YS, Kim J, et al (2010) Development of genetic algorithm-based optimization module in WHAT system for hydrograph analysis and model application. *Comput Geosci* 36:936–944
- Linsley BK (1996) Oxygen-isotope record of sea level and climate variations in the Sulu Sea over the past 150,000 years. *Nature* 380:234
- Linsley RK, Kohler MA, Paulhus JL (1982) Hydrology for engineers. McGraw-Hill Book Company. Inc N Y NY
- Lloyd JW, Heathcote JAA (1985) Natural inorganic hydrochemistry in relation to ground water
- Loh YS, Banoeng-Yakubo B, Yidana SM, et al (2012) Hydrochemical Characterisation of Groundwater in Parts of the Volta Basin, Northern Ghana. *Ghana Min J* 13:24–32

- Lutz AF, ter Maat HW, Biemans H, et al (2016) Selecting representative climate models for climate change impact studies: an advanced envelope-based selection approach. *Int J Climatol* 36:3988–4005 . doi: 10.1002/joc.4608
- Lyne V, Hollick M (1979) Stochastic time-variable rainfall-runoff modelling. In: Institute of Engineers Australia National Conference. pp 89–93
- Ma H (2016) Major ion chemistry of groundwater in the Sangong River Watershed, Northwestern China. *Environ Earth Sci* 75:1–17 . doi: 10.1007/s12665-016-5321-2
- MacDonald AM, Bonsor HC, Dochartaigh B é ó, Taylor RG (2012) Quantitative maps of groundwater resources in Africa. *Environ Res Lett* 7:024009 . doi: 10.1088/1748-9326/7/2/024009
- MacDonald GM, Edwardsi TW (1993) past climate warming. *Nature* 361:21
- Margulis S, Hughes G, Schneider R, et al (2010) Economics of adaptation to climate change: Synthesis report
- Martin N (2006) Development of a water balance for the Atankwidi catchment, West Africa – A case study of groundwater recharge in a semi-arid climate, Paul L.G.Vlek, Manfred Denich, Christopher Martius, Charles Rodgers. *Ecology and Development*
- Martin N, Van De Giesen N (2005) Spatial Distribution of Groundwater Production and Development Potential in the Volta River basin of Ghana and Burkina Faso. *Water Int* 30:239–249
- McNamara JP (2005) An assessment of the potential for using water and chloride budgets to estimate groundwater recharge in granitic, mountain environments. Final Rep
- Meinzer OE (1923) The occurrence of ground water in the United States: With a discussion of principles. University of Chicago
- Merritt WS, Letcher RA, Jakeman AJ (2003) A review of erosion and sediment transport models. *Environ Model Softw* 18:761–799

- Meybeck M (1987) Global chemical weathering of surficial rocks estimated from river dissolved loads. *Am J Sci* 287:401–428
- Meyboom P (1961) Estimating ground-water recharge from stream hydrographs. *J Geophys Res* 66:1203–1214
- Middelburg JJ, van der Weijden CH, Woittiez JR (1988) Chemical processes affecting the mobility of major, minor and trace elements during weathering of granitic rocks. *Chem Geol* 68:253–273
- Mileham L, Taylor RG, Todd M, et al (2009) The impact of climate change on groundwater recharge and runoff in a humid, equatorial catchment: sensitivity of projections to rainfall intensity. *Hydrol Sci J* 54:727–738 . doi: 10.1623/hysj.54.4.727
- Mor S, Singh S, Yadav P, et al (2009) Appraisal of salinity and fluoride in a semi-arid region of India using statistical and multivariate techniques. *Environ Geochem Health* 31:643–655
- Moriasi DN, Arnold JG, Van Liew MW, et al (2007) Model evaluation guidelines for systematic quantification of accuracy in watershed simulations. *Trans ASABE* 50:885–900
- Moriasi DN, Gitau MW, Pai N, Daggupati P (2015) Hydrologic and water quality models: Performance measures and evaluation criteria. *Trans ASABE* 58:1763–1785
- Morris DA, Johnson AI (1967) Summary of hydrologic and physical properties of rock and soil materials, as analyzed by the hydrologic laboratory of the U.S. Geological Survey, 1948-60. U.S. Govt. Print. Off.,
- Msangi JP (2014) Combating Water Scarcity in Southern Africa Case Studies from Namibia
- Murray RJ (1960) The geology of the Zuanengu 1/2 field sheet. *Ghana Geol Surv Bull* 25:117
- Mustapha A, Aris AZ (2012) Multivariate statistical analysis and environmental modeling of heavy metals pollution by industries. *Pol J Env Stud* 21:1359–1367

- Namara RE, Awuni JA, Barry B, et al (2011) Smallholder shallow groundwater irrigation development in the upper east region of Ghana. International Water Management Institute
- Nartey VK, Bam EK, Mahamah M (2012) The Geochemistry of some Ground and Surface water Systems in the East Gonja District of Northern Ghana. *J Environ Earth Sci* 2:10–20
- Nash JE, Sutcliffe JV (1970) River flow forecasting through conceptual models part I — A discussion of principles. *J Hydrol* 10:282–290 . doi: 10.1016/0022-1694(70)90255-6
- Nathan R, Gordon N, MacMahon T, et al (2007) Aquapak
- Nathan RJ, McMahon TA (1990) Evaluation of automated techniques for base flow and recession analyses. *Water Resour Res* 26:1465–1473 . doi: 10.1029/WR026i007p01465
- Nazzal Y, Ahmed I, Al-Arifi NS, et al (2014) A pragmatic approach to study the groundwater quality suitability for domestic and agricultural usage, Saq aquifer, northwest of Saudi Arabia. *Environ Monit Assess* 186:4655–4667
- Nyagwambo NL (2006) Groundwater recharge estimation and water resources assessment in a tropical crystalline basement aquifer. TU Delft, Delft University of Technology
- Oberthür T, Vetter U, Davis DW, Amanor JA (1998) Age constraints on gold mineralization and Paleoproterozoic crustal evolution in the Ashanti belt of southern Ghana. *Precambrian Res* 89:129–143
- Obuobie E (2008a) Estimation of groundwater recharge in the context of future climate change in the White Volta River Basin, West Africa, Paul L.G.Vlek. ZEF, Bonn
- Obuobie E (2008b) Estimation of groundwater recharge in the context of future climate change in the White Volta River Basin, West Africa, Paul L.G.Vlek, Manfred Denich, Christopher Martius, Ahmad Manschadi, Nick van de Giesen. *Ecology and Development*

- Odukoya AM, Folorunso AF, Ayolabi EA, Adeniran EA (2013) Groundwater Quality and Identification of Hydrogeochemical Processes within University of Lagos, Nigeria. *J Water Resour Prot* 05:930–940 . doi: 10.4236/jwarp.2013.510096
- Ofosu-Addo D, Jianmei C, Dong S (2008) Groundwater Development and Evaluation of the White Volta Basin (Ghana) using numerical Simulation. *J Am Sci* 4:64–71
- Oguntunde PG, Abiodun BJ (2013) The impact of climate change on the Niger River Basin hydroclimatology, West Africa. *Clim Dyn* 40:81–94
- Oguntunde PG, Abiodun BJ, Lischeid G (2017) Impacts of climate change on hydro-meteorological drought over the Volta Basin, West Africa. *Glob Planet Change* 155:121–132 . doi: 10.1016/j.gloplacha.2017.07.003
- Okiongbo KS, Douglas RK (2015) Evaluation of major factors influencing the geochemistry of groundwater using graphical and multivariate statistical methods in Yenagoa city, Southern Nigeria. *Appl Water Sci* 5:27–37 . doi: 10.1007/s13201-014-0166-x
- Oteng Mensah F, Alo C, Yidana SM (2014) Evaluation of groundwater recharge estimates in a partially metamorphosed sedimentary basin in a tropical environment: application of natural tracers. *Sci World J* 2014:
- Owor M, Taylor RG, Tindimugaya C, Mwesigwa D (2009) Rainfall intensity and groundwater recharge: empirical evidence from the Upper Nile Basin. *Environ Res Lett* 4:035009 . doi: 10.1088/1748-9326/4/3/035009
- Padgham J, Abubakari A, Ayivor J, et al (2015) Vulnerability and adaptation to climate change in the semi-arid regions of West Africa. *Glob Dryland Initiat UNDP*
- Pan Y, Gong H, ZHou D, et al (2011) Impact of land use change on groundwater recharge in Guishui River Basin, China. *Chin Geogr Sci* 21:734–743
- Patel J, Patel H, Bhatt C (2015) Modified Hargreaves Equation for Accurate Estimation of Evapotranspiration of Diverse Climate Locations in India. *Proc Natl Acad Sci India Sect B Biol Sci* 85:161–166 . doi: 10.1007/s40011-014-0314-y

- Pathak P, Sudi R, Wani SP, Sahrawat KL (2013) Hydrological behavior of Alfisols and Vertisols in the semi-arid zone: Implications for soil and water management. *Agric Water Manag* 118:12–21
- Pelig-Ba KB (2012) Geochemistry of Crystalline Rocks from the East of the Upper East Region of Ghana. *Res J Environ Earth Sci* 4:534–545
- Pelig-Ba KB (2004) Estimation of water balance in the Northern Region of Ghana. *Ghana J Dev Stud* 1:118–141
- Piper AM (1944) A graphic procedure in the geochemical interpretation of water-analyses. *Eos Trans Am Geophys Union* 25:914–928 . doi: 10.1029/TR025i006p00914
- Pistocchi A, Bouraoui F, Bittelli M (2008) A simplified parameterization of the monthly topsoil water budget. *Water Resour Res* 44:W12440 . doi: 10.1029/2007WR006603
- Pitkänen P, Partamies S, Luukkonen A (2004) Hydrogeochemical interpretation of baseline groundwater conditions at the Olkiluoto site. Posiva Oy, Finland
- Plummer LN, Jones BF, Truesdell AH (1976) WATEQF; a FORTRAN IV version of WATEQ : a computer program for calculating chemical equilibrium of natural waters. Dept. of the Interior, Geological Survey, Water Resources Division, Washington, DC
- Poff NL, Allan JD, Bain MB, et al (1997) The natural flow regime. *BioScience* 47:769–784
- Posavec K, Bačani A, Nakić Z (2006) A visual basic spreadsheet macro for recession curve analysis. *Ground Water* 44:764–767
- Posavec K, Parlov J, Bačani A (2009) A Visual BAsic spreadsheet macro for estimating groundwater recharge. *Rud-Geol-Naft Zb* 21:19–23
- Price K (2011) Effects of watershed topography, soils, land use, and climate on baseflow hydrology in humid regions: A review. *Prog Phys Geogr* 35:465–492
- Pulido-Velazquez D, García-Aróstegui JL, Molina J-L, Pulido-Velazquez M (2015) Assessment of future groundwater recharge in semi-arid regions under climate change scenarios

- (Serral-Salinas aquifer, SE Spain). Could increased rainfall variability increase the recharge rate? *Hydrol Process* 29:828–844 . doi: 10.1002/hyp.10191
- Raihan F, Alam JB (2008) Assessment of groundwater quality in Sunamganj of Bangladesh. *Iran J Env Health Sci Eng* 5:155–166
- Rajmohan N, Elango L (2004) Identification and evolution of hydrogeochemical processes in the groundwater environment in an area of the Palar and Cheyyar River Basins, Southern India. *Environ Geol* 46:47–61 . doi: 10.1007/s00254-004-1012-5
- Raju NJ (2006) Hydrogeochemical parameters for assessment of groundwater quality in the upper Gunjanaeru River basin, Cuddapah District, Andhra Pradesh, South India. *Environ Geol* 52:1067–1074 . doi: 10.1007/s00254-006-0546-0
- Ravikumar P, Venkatesharaju K, Prakash KL, Somashekar RK (2011) Geochemistry of groundwater and groundwater prospects evaluation, Anekal Taluk, Bangalore urban district, Karnataka, India. *Environ Monit Assess* 179:93–112 . doi: 10.1007/s10661-010-1721-z
- Ray RK, Syed TH, Saha D, et al (2017) Recharge mechanism and processes controlling groundwater chemistry in a Precambrian sedimentary terrain: a case study from Central India. *Environ Earth Sci* 76:136
- Razowska-Jaworek L (2014) Calcium and Magnesium in Groundwater: Occurrence and Significance for Human Health. CRC Press
- Reyment R, Jvreskog KG (1996) Applied factor analysis in the natural sciences. Cambridge University Press
- Richards LA (1954) Diagnosis and improvement of saline and alkali soils. UNITED STATES DEPARTMENT OF AGRICULTURE, Washington, D.C.
- Risser DW, Gburek WJ, Folmar GJ (2005) Comparison of methods for estimating ground-water recharge and base flow at a small watershed underlain by fractured bedrock in the eastern United States. US Department of the Interior, US Geological Survey

- Rogers RJ (1989) Geochemical comparison of ground water in areas of New England, New York, and Pennsylvania. *Ground Water* 27:690–712
- Roudier P, Ducharne A, Feyen L (2014) Climate change impacts on runoff in West Africa: a review. *Hydrol Earth Syst Sci* 18:2789–2801
- Rusan MJM, Hinnawi S, Rousan L (2007) Long term effect of wastewater irrigation of forage crops on soil and plant quality parameters. *Desalination* 215:143–152 . doi: 10.1016/j.desal.2006.10.032
- Sadashivaiah C, Ramakrishnaiah CR, Ranganna G (2008) Hydrochemical analysis and evaluation of groundwater quality in Tumkur Taluk, Karnataka State, India. *Int J Environ Res Public Health* 5:158–164
- Saka D, Akiti TT, Osae S, et al (2013) Hydrogeochemistry and isotope studies of groundwater in the Ga West Municipal Area, Ghana. *Appl Water Sci* 3:577–588 . doi: 10.1007/s13201-013-0104-3
- Salifu M, Aidoo F, Hayford MS, et al (2015) Evaluating the suitability of groundwater for irrigational purposes in some selected districts of the Upper West region of Ghana. *Appl Water Sci* 1–10 . doi: 10.1007/s13201-015-0277-z
- Salifu M, Yidana SM, Osae S, Armah YS (2013) The Influence of the Unsaturated Zone on the High Fluoride Contents in Groundwater in the Middle Voltaian Aquifers-The Gushegu District, Northern Region of Ghana. *J Hydrogeol Hydrol Eng* 2: 2. of 7:0–45 . doi: <http://dx.doi.org/10.4172/2325-9647.1000107>
- Sandwidi WJP (2007) Groundwater potential to supply population demand within the Kompienga dam basin in Burkina Faso. *Ecology and Development*
- Sanford RF, Pierson CT, Crovelli RA (1993) An objective replacement method for censored geochemical data. *Math Geol* 25:59–80
- Santhi C, Arnold JG, Williams JR, et al (2001) validation of the swat model on a large RWER basin with point and nonpoint sources1. *J Am Water Resour Assoc* 37:

- Sawyer CN, McCarty PL (1967) *Chemistry for Sanitary Engineers*, 2nd edn. McGraw Hill, New York
- Scanlon BR, Healy RW, Cook PG (2002) Choosing appropriate techniques for quantifying groundwater recharge. *Hydrogeol J* 10:18–39
- Scanlon BR, Reedy RC, Stonestrom DA, et al (2005) Impact of land use and land cover change on groundwater recharge and quality in the southwestern US. *Glob Change Biol* 11:1577–1593 . doi: 10.1111/j.1365-2486.2005.01026.x
- Schlüter T, Trauth MH (2008) *Geological atlas of Africa: with notes on stratigraphy, tectonics, economic geology, geohazards, geosites. and geoscientific education of each country*, 2nd ed. four-coloured rev. and enlarged ed. Springer, Berlin
- Schmidli J, Goodess CM, Frei C, et al (2007) Statistical and dynamical downscaling of precipitation: An evaluation and comparison of scenarios for the European Alps. *J Geophys Res Atmospheres* 112:D04105 . doi: 10.1029/2005JD007026
- Schoeller H (1965) Qualitative evaluation of groundwater resources. *Methods Tech Groundw Investig Dev* 54–83
- Shrestha S, Bach TV, Pandey VP (2016) Climate change impacts on groundwater resources in Mekong Delta under representative concentration pathways (RCPs) scenarios. *Environ Sci Policy* 61:1–13
- Shrestha S, Kazama F (2007) Assessment of surface water quality using multivariate statistical techniques: A case study of the Fuji river basin, Japan. *Environ Model Softw* 22:464–475
- Simler R (2015) *Diagrammes computer program—Version 6.5*
- Sinclair KA, Pitz CF (1999) *Estimated baseflow characteristics of selected Washington rivers and streams*. Washington State Department of Ecology, Environmental Assessment Program

- Singaraja C, Chidambaram S, Anandhan P, et al (2014) Hydrochemistry of groundwater from Tuticorin District, Tamil Nadu, India. *EnviroGeoChimica Acta* 1:172–179
- Singh AK, Tewary BK, Sinha A (2011) Hydrochemistry and quality assessment of groundwater in part of NOIDA metropolitan city, Uttar Pradesh. *J Geol Soc India* 78:523–540
- Singh KP (1968) Some factors affecting baseflow. *Water Resour Res* 4:985–999
- Singh S, Srivastava P, Abebe A, Mitra S (2015) Baseflow response to climate variability induced droughts in the Apalachicola–Chattahoochee–Flint River Basin, U.S.A. *J Hydrol* 528:550–561 . doi: 10.1016/j.jhydrol.2015.06.068
- Sinha BPC, Sharma SK (1988) Natural Ground Water Recharge Estimation Methodologies in India. In: Simmers PDI (ed) *Estimation of Natural Groundwater Recharge*. Springer Netherlands, pp 301–311
- Smedley PL, Edmunds WM, West JM, et al (1995) Vulnerability of shallow groundwater quality due to natural geochemical environment. 2, health problems related to groundwater in the Obuasi and Bolgatanga areas, Ghana
- Soltan ME (1998) Characterisation, classification, and evaluation of some ground water samples in upper Egypt. *Chemosphere* 37:735–745
- Spudis PD (2005) *The geology of multi-ring impact basins: the moon and other planets*, 1st pbk. ed. Cambridge University Press, Cambridge [England] ; New York, NY
- Stallard RF, Edmond JM (1983) Geochemistry of the Amazon: 2. The influence of geology and weathering environment on the dissolved load. *J Geophys Res Oceans* 88:9671–9688
- Stanturf JA, Warren ML, Charnley Jr S, et al (2011) Ghana climate change vulnerability and adaptation assessment
- Stewart MK (2015) Promising new baseflow separation and recession analysis methods applied to streamflow at Glendhu Catchment, New Zealand. *Hydrol Earth Syst Sci* 19:2587–2603

- Su C-H, Peterson TJ, Costelloe JF, Western AW (2016) A synthetic study to evaluate the utility of hydrological signatures for calibrating a base flow separation filter. *Water Resour Res* 52:6526–6540 . doi: 10.1002/2015WR018177
- Sumioka SS, Bauer HH (2003) Estimating ground-water recharge from precipitation on Whidbey and Camano islands, Island County, Washington, water years 1998 and 1999. US Department of the Interior, US Geological Survey
- Sundaray SK (2010) Application of multivariate statistical techniques in hydrogeochemical studies—a case study: Brahmani–Koel River (India). *Environ Monit Assess* 164:297–310
- Sutanto SJ, Wenninger J, Coenders-Gerrits AMJ, Uhlenbrook S (2012) Partitioning of evaporation into transpiration, soil evaporation and interception: a comparison between isotope measurements and a HYDRUS-1D model. *Hydrol Earth Syst Sci* 16:2605–2616
- Szabolcs I, Darab C (1964) The influence of irrigation water of high sodium carbonate content of soils. In: *Proceedings of 8th international congress of ISSS, Trans, II*. pp 803–812
- Szilagyi J, Harvey FE, Ayers JF (2003) Regional Estimation of Base Recharge to Ground Water Using Water Balance and a Base-Flow Index. *Ground Water* 41:504–513
- Talabi AO, Tijani MN (2013) Hydrochemical and stable isotopic characterization of shallow groundwater system in the crystalline basement terrain of Ekiti area, southwestern Nigeria. *Appl Water Sci* 3:229–245 . doi: 10.1007/s13201-013-0076-3
- Tay CK (2012) Hydrochemistry of groundwater in the Savelugu–Nanton District, Northern Ghana. *Environ Earth Sci* 67:2077–2087 . doi: 10.1007/s12665-012-1647-6
- Teklebirhan A, Dessie N, Tesfamichael G (2012) Groundwater Recharge, Evapotranspiration and Surface Runoff Estimation Using WetSpa Modeling Method in Illala Catchment, Northern Ethiopia. *Momona Ethiop J Sci* 4:96–110
- Thomas BF, Vogel RM, Famiglietti JS (2015) Objective hydrograph baseflow recession analysis. *J Hydrol* 525:102–112

- Thompson LG, Mosley-Thompson E, Davis ME, et al (2003) Tropical glacier and ice core evidence of climate change on annual to millennial time scales. *Clim Change* 59:137–155
- Thrasher B, Maurer EP, McKellar C, Duffy PB (2012) Technical Note: Bias correcting climate model simulated daily temperature extremes with quantile mapping. *Hydrol Earth Syst Sci* 16:3309–3314
- Tomar V, Kamra SK, Kumar S, et al (2012) Hydro-chemical analysis and evaluation of groundwater quality for irrigation in Karnal district of Haryana state, India. *Int J Environ Sci* 3:756 . doi: doi:10.6088/ijes.2012030132002
- Trzaska S, Schnarr E (2014) A review of downscaling methods for climate change projections. *U S Agency Int Dev Tetra Tech ARD* 1–42
- Tsur Y, Graham-Tomasi T (1991) The buffer value of groundwater with stochastic surface water supplies. *J Environ Econ Manag* 21:201–224
- UNEP (2013) AFRICA ENVIRONMENT OUTLOOK : Summary for Policy Makers. Nairobi, Kenya
- UNEP U (2008) Vital water graphics: An overview of the state of the world’s fresh and Marine waters. United Nations Environment Programme, Nairobi, Kenya
- UNESCO (2011) THE IMPACT OF GLOBAL CHANGE ON WATER RESOURCES: THE RESPONSE OF UNESCO’S INTERNATIONAL HYDROLOGY PROGRAMME
- U.S. Bureau of Mines (1996) Dictionary of Mining, Mineral, and Related Terms, 2nd edn. U.S. Bureau of Mines, US
- USGS (2013) USGS GWRP: Comparison of Selected Methods for Estimating Ground-Water Recharge In Humid Regions. <http://water.usgs.gov/ogw/gwrp/methods/compare/>. Accessed 24 Jul 2013
- Van der Gun J (2012) Groundwater and global change trends, opportunities and challenges. UNESCO, Paris

- Van der Sommen JJ, Geirnaert W (1988) On the continuity of aquifer systems on the crystalline basement of Burkina Faso. In: Estimation of Natural Groundwater Recharge. Springer, pp 29–45
- Van Liew MW, Arnold JG, Garbrecht JD (2003) Hydrologic simulation on agricultural watersheds: Choosing between two models. *Trans ASAE* 46:1539
- van Vuuren DP, Stehfest E, den Elzen MG, et al (2011) RCP2. 6: exploring the possibility to keep global mean temperature increase below 2 C. *Clim Change* 109:95–116
- Versluys J (1916) Chemische werkingen in den ondergrond der duinen. Verslag Gewone Vergad. Wis-& Nat. afd. Kon. Acad. Wetensch. Amsterdam
- Versluys J (1931) Subterranean water conditions in the coastal regions of the Netherlands. *Econ Geol* 26:65–95
- Walter IA, Allen RG, Elliott R, et al (2000) ASCE's standardized reference evapotranspiration equation. In: *Watershed management and operations management 2000*. pp 1–11
- Wang Z-M, Batelaan O, De Smedt F (1996) A distributed model for water and energy transfer between soil, plants and atmosphere (WetSpa). *Phys Chem Earth* 21:189–193 . doi: 10.1016/S0079-1946(97)85583-8
- WHO (2011) Guidelines for drinking-water quality, fourth edition. In: WHO. http://www.who.int/water_sanitation_health/publications/dwq_guidelines/en/#. Accessed 30 Mar 2016
- WHO/UNICEF (2015) Progress on sanitation and drinking water- 2015 update and MDG assessment. WHO/UNICEF Joint Water Supply and Sanitation Monitoring Programme.
- WHO/UNICEF (2011) Drinking water equity, safety and sustainability thematic report on drinking water 2011. UNICEF ; World Health Organization, New York; Geneva
- Wilcox Lv (1955) Classification and use of irrigation waters. U S Dep Agric

- Wilcox LV, others (1948) The quality of water for irrigation use. United States Department of Agriculture, Economic Research Service
- Williamson DF, Parker RA, Kendrick JS (1989) The box plot: a simple visual method to interpret data. *Ann Intern Med* 110:916–921 . doi: 10.1059/0003-4819-110-11-916
- Wittenberg H (2006) Impacts of forestation and land use on water balance and low flows in Northwest Germany. In: BALWOIS Conference. pp 23–26
- Wood WW, Sanford WE (1995) Chemical and isotopic methods for quantifying ground-water recharge in a regional, semiarid environment. *Ground Water* 33:458–468
- World Water Assessment Programme (ed) (2009) *Water in a changing world*, 3rd ed. UNESCO Publishing ; Earthscan, Paris : London
- Worrall WE (2013) *Ceramic Raw Materials: Institute of Ceramics Textbook Series*. Elsevier
- Wu J, Zhang R, Yang J (1996) Analysis of rainfall-recharge relationships. *J Hydrol* 177:143–160
- Xu Y, Beekman HE (2003) *Groundwater recharge estimation in Southern Africa*. Unesco, Paris
- Yao Y, Robb LJ (1998) *The Birimian granitoids of Ghana: A review*. University of the Witwatersrand
- Yidana SM (2010) Groundwater classification using multivariate statistical methods: Southern Ghana. *J Afr Earth Sci* 57:455–469 . doi: 10.1016/j.jafrearsci.2009.12.002
- Yidana SM (2009) The hydrochemical framework of surface water basins in southern Ghana. *Environ Geol* 57:789–796 . doi: 10.1007/s00254-008-1357-2
- Yidana SM, Banoeng-Yakubo B, Aliou A-S, Akabzaa TM (2012) Groundwater quality in some Voltaian and Birimian aquifers in northern Ghana—application of multivariate statistical methods and geographic information systems. *Hydrol Sci J* 57:1168–1183 . doi: 10.1080/02626667.2012.693612

- Yidana SM, Fynn OF, Adomako D, et al (2016) Estimation of evapotranspiration losses in the vadose zone using stable isotopes and chloride mass balance method. *Environ Earth Sci* 75:1–18 . doi: 10.1007/s12665-015-4982-6
- Yidana SM, Fynn OF, Chegbeleh LP, et al (2013) Hydrogeological Conditions of a Crystalline Aquifer: Simulation of Optimal Abstraction Rates under Scenarios of Reduced Recharge. *Sci World J* 2013:
- Yidana SM, Koffie E (2014) The groundwater recharge regime of some slightly metamorphosed neoproterozoic sedimentary rocks: an application of natural environmental tracers. *Hydrol Process* 28:3104–3117
- Yidana SM, Ophori D, Banoeng-Yakubo B (2008) Hydrochemical evaluation of the Voltaian system—The Afram Plains area, Ghana. *J Environ Manage* 88:697–707 . doi: 10.1016/j.jenvman.2007.03.037
- Yidana SM, Yidana A (2010) Assessing water quality using water quality index and multivariate analysis. *Environ Earth Sci* 59:1461–1473 . doi: 10.1007/s12665-009-0132-3
- Younger PL (2007) *Groundwater in the environment: an introduction*. Blackwell Pub, Malden, MA ; Oxford
- Zaidi FK, Nazzal Y, Jafri MK, et al (2015) Reverse ion exchange as a major process controlling the groundwater chemistry in an arid environment: a case study from northwestern Saudi Arabia. *Environ Monit Assess* 187:1–18 . doi: 10.1007/s10661-015-4828-4
- Zektser IS, Everett LG (2004a) *Groundwater resources of the world and their use*. UNESCO, Paris
- Zektser IS, Everett LG (2004b) *Groundwater resources of the world and their use*. UNESCO, Paris
- Zhang L, Dawes WR, Hatton TJ, et al (1999) Estimation of soil moisture and groundwater recharge using the TOPOG_IRM model. *Water Resour Res* 35:149–161

Zorita E, von Storch H (1999) The Analog Method as a Simple Statistical Downscaling
Technique: Comparison with More Complicated Methods. *J Clim* 12:2474–2489 . doi:
10.1175/1520-0442(1999)012<2474:TAMAAS>2.0.CO;2

Zoulgami S, Gnazou MDT, Kodom T, et al (2015) Physico-chemical study of groundwater in the
Northeast of Kara region (Togo). *Int J Biol Chem Sci* 9:1711–1724 . doi:
10.4314/ijbcs.v9i3.49

APPENDICE

Appendix A: Published article and communication

Publication

Koffi KV, Obuobie E, Banning A, Wohnlich S (2017) Hydrochemical characteristics of groundwater and surface water for domestic and irrigation purposes in Veua catchment, Northern Ghana. *Environ Earth Sci* 76:185. doi: 10.1007/s12665-017-6490-3.

Conference

Koffi KV (2015) Impact of climate change on groundwater recharge in the crystalline basement rocks aquifer of Northern Ghana. AGU Fall meeting 2015, San Francisco/ USA. (Accepted for oral presentation). Link: <http://adsabs.harvard.edu/abs/2015AGUFMGC42A..04K>

Koffi KV, Obuobie E, Banning A, Wohnlich S (2016) Hydrogeological processes controlling water quality in the crystalline basement aquifer of the Veua Catchment in Northeast Ghana. AGU Fall meeting 2016, San Francisco/ USA. (Poster Presentation). Link: <http://adsabs.harvard.edu/abs/2016AGUFM.H13A1345K>

Appendix 2: Chemical analysis

Table I : Result of the chemical analysis

SAMPLE ID	EC	Salinity	TDS	DO	Col	Ca	Mg	HCO3-	Cl-	Na+	K+	PO4	Fe	pH	NO3-	SO4	T/H	T.ALK
Agurbisi 1 (School)	-0.85	-0.74	-0.85	0.69	2.02	-0.74	-2.19	-2.69	0.91	-0.57	-0.68	-0.26	-0.62	6.83	-0.22	1.12	-1.56	-2.57
Agurbisi 2	0.05	-0.11	0.06	-0.86	-1.11	0.02	0.70	0.62	-0.35	-0.24	-1.02	0.12	-1.17	7.50	0.75	-1.41	0.41	0.65
Alaburekulo	1.81	1.89	1.81	-2.06	0.45	1.35	1.07	1.82	-0.35	1.06	2.56	-1.73	2.33	7.45	0.60	0.47	1.30	1.81
Amanga	0.16	-0.11	0.16	0.81	0.45	0.02	0.05	1.12	-0.75	2.01	0.70	1.50	-2.31	7.55	-2.19	0.49	-0.02	1.13
Anafobisi 1	-0.59	-0.74	-0.59	0.16	-1.11	-0.41	-0.07	0.13	-1.34	0.57	-0.79	0.85	0.47	7.68	-2.19	0.63	-0.30	0.17
Anafobisi 2	-0.19	-0.30	-0.19	0.12	0.45	0.34	-0.36	0.24	1.24	1.33	-1.02	-1.36	0.24	7.35	-0.80	-1.41	-0.10	-0.76
Anafobisi 3	1.66	1.81	1.66	0.71	0.45	1.85	1.19	-0.07	2.12	-1.31	0.11	-0.52	-0.38	7.02	0.52	1.66	1.61	-0.01
Aniabisi 1	0.00	-0.11	0.00	-2.01	0.45	0.15	0.57	0.56	-2.34	-0.64	-0.90	0.83	-0.58	7.30	0.94	0.70	0.39	0.59
Atampintin	1.98	2.04	1.98	-1.28	-1.11	0.34	2.36	2.79	0.24	2.70	1.92	0.26	-0.12	7.46	-1.77	0.89	2.00	2.76
Avorobisi	0.76	1.04	0.77	-0.66	0.45	0.61	0.47	0.65	-0.35	-0.43	0.39	-0.92	-0.76	7.78	0.67	-0.81	0.54	0.67
Ayopia 1	1.04	1.25	1.04	-0.70	0.45	1.30	0.89	1.00	0.98	-0.10	1.08	-1.61	-1.21	7.74	1.09	0.74	1.15	1.03
Ayopia 2	0.94	1.25	0.94	-0.50	0.45	-0.19	-2.89	-1.08	-0.03	-0.48	1.36	0.32	-0.21	7.40	0.52	-0.50	-1.38	-1.00
Azoribisi PS	0.22	0.07	0.22	-1.17	0.45	-0.05	-0.55	-0.32	-1.34	-0.25	-0.68	1.10	-0.15	7.62	0.88	0.28	-0.41	-0.29
Balungu 1	-0.14	-0.30	-0.14	1.25	0.45	-0.36	-0.32	-0.80	1.24	-0.31	0.64	0.93	0.34	7.00	0.71	0.54	-0.44	-1.44
Balungu 3	-1.35	-1.27	-1.34	1.14	2.94	-1.45	-1.08	-1.33	-0.75	-0.92	1.92	0.87	0.34	7.01	0.09	0.38	-1.45	-1.25
Boko	1.15	1.35	1.15	1.00	0.45	1.52	0.89	1.00	1.11	-0.31	1.03	-0.70	-0.34	7.36	0.52	-0.38	1.25	1.03
Bongo 1	1.57	1.72	1.57	1.15	-1.11	1.90	1.41	0.28	2.21	-0.35	-0.13	0.55	1.13	7.19	0.65	1.68	1.78	0.03
Bongo 2	-0.11	-0.30	-0.11	0.39	0.45	0.42	-0.03	-0.17	-0.35	-0.69	-0.39	-0.26	-0.22	7.40	0.73	1.20	0.13	-0.11

Boroga 1	0.13	-0.11	0.13	1.34	-1.11	0.17	0.33	-0.50	0.98	-1.15	0.25	-0.52	-0.13	7.15	0.04	-0.23	0.25	-0.62
Borogo PS	-1.97	-1.59	-1.97	-0.74	0.45	-1.77	-0.65	-0.99	-2.34	-0.90	0.25	0.09	0.59	7.21	-2.19	-1.41	-1.33	-0.90
Dabote	-1.53	-1.27	-1.53	1.39	-1.11	-1.24	-0.70	-0.80	-0.35	-0.44	0.25	1.19	-2.31	7.36	0.52	-0.47	-1.11	-0.73
Daliga 1	0.19	-0.11	0.18	-0.02	0.45	0.22	0.74	0.51	-0.55	0.31	-0.58	-0.96	0.17	7.56	0.86	0.62	0.54	0.53
Daliga 2	-1.26	-1.27	-1.27	1.21	-1.11	-1.54	-0.20	-0.75	-0.35	-1.05	-0.79	1.75	0.04	7.02	1.14	-0.91	-0.89	-0.69
Feo 1	-0.04	-0.11	-0.04	0.80	-1.11	0.03	0.20	-0.02	0.24	0.04	0.03	-0.65	0.48	7.15	0.44	-0.10	0.08	0.03
Feo 2	-0.29	-0.30	-0.30	0.70	-1.11	-0.60	-0.02	-0.41	-0.03	-0.65	0.82	0.97	-0.73	7.20	0.79	0.56	-0.35	-0.32
Feo 4	-0.16	-0.30	-0.16	0.34	-1.11	-0.16	0.14	0.39	-0.35	0.43	-0.13	1.39	-0.60	7.06	0.75	-0.14	-0.04	0.43
Gowrie Kasingo	-1.34	-1.27	-1.34	-1.01	-1.11	0.18	-1.59	-0.70	-0.75	-0.22	-2.05	0.12	1.66	7.66	-0.51	0.79	-0.71	-0.61
Gowrie Tengre School	-0.72	-0.74	-0.72	1.00	0.45	-0.52	-0.34	-0.13	-0.03	0.59	0.87	-3.60	1.60	7.37	0.30	0.06	-0.53	-0.06
Gurugu 1	0.41	0.07	0.42	-0.43	0.45	0.82	1.05	1.18	-0.03	0.70	-1.02	-1.18	0.18	7.33	0.52	-1.41	1.04	1.19
Gurugu 2	-0.82	-0.74	-0.81	-0.75	0.45	-0.74	-0.03	0.13	-0.75	0.76	-1.02	0.92	-2.31	7.45	-0.31	-0.44	-0.43	0.17
Kasingo 1	-0.76	-0.74	-0.75	0.87	0.45	-0.56	-0.53	-0.70	-0.75	-1.31	1.18	-2.23	-0.13	7.39	0.69	-1.41	-0.67	-0.64
Kasingo 2	-1.23	-0.99	-1.23	0.93	0.45	-0.81	-0.58	-0.85	1.78	1.40	0.98	1.60	0.39	7.12	0.30	0.05	-0.82	-0.77
KUYELINGO	-0.70	-0.74	-0.71	1.11	0.45	-0.80	-0.34	-0.13	-0.18	0.87	0.11	-0.22	1.87	7.28	0.18	0.06	-0.67	-0.09
Lungu 1	-1.56	-1.27	-1.57	0.51	0.45	-1.82	-1.59	-1.41	-0.75	-0.35	-0.68	-1.23	-1.35	7.00	1.19	-1.41	-1.96	-1.32
Lungu 2	-1.29	-1.27	-1.28	0.31	0.45	-1.41	-0.51	-0.99	-0.35	-0.55	-0.39	0.11	-0.28	7.00	0.44	-0.02	-1.07	-0.92
Lungu 3	-0.31	-0.51	-0.31	0.90	0.45	-0.56	-0.03	0.09	-0.35	-0.24	-0.13	-0.73	-0.05	6.90	0.09	-1.41	-0.36	0.13
Madina	0.11	-0.11	0.11	0.35	0.45	0.18	0.30	0.17	-0.03	0.50	-0.30	1.40	1.79	7.58	0.18	0.20	0.23	0.22
Namoo 1	0.24	0.07	0.23	0.23	0.45	0.39	0.63	0.15	0.66	-0.48	0.11	1.28	-0.50	7.18	0.37	1.64	0.54	0.20
Namoo 2	0.96	1.25	0.96	0.92	-1.11	1.40	1.14	0.28	1.46	-1.31	-0.90	0.27	0.11	7.23	0.52	-1.41	1.36	-0.14
Nyariga 1	-1.56	-1.27	-1.57	0.72	-1.11	-1.45	-1.52	-1.54	0.24	-1.05	-0.21	-0.08	0.09	7.10	-0.51	1.07	-1.69	-1.45

Nyariga 2	0.33	0.07	0.33	-2.16	-1.11	0.93	0.54	0.93	-0.35	1.06	-0.13	1.07	-0.08	7.61	0.71	-1.41	0.75	0.96
Nyariga Girl's school	-0.15	-0.30	-0.16	-0.24	0.45	-0.68	0.23	0.21	-0.75	0.14	0.25	-0.70	-0.48	7.21	0.73	-1.41	-0.21	0.26
Sanabisi	0.88	1.15	0.88	-1.28	0.45	1.25	1.71	1.86	-0.75	0.64	-0.58	-1.27	-0.29	7.60	-0.31	-0.91	1.71	1.86
Sherigu	1.24	1.45	1.25	-0.90	0.45	0.43	0.95	0.78	0.66	0.43	-2.45	0.55	1.51	7.34	0.77	0.08	0.79	0.82
SOE 1	-0.10	-0.30	-0.09	-0.16	0.45	0.08	-1.08	0.30	-0.55	1.52	0.52	0.33	1.53	7.30	0.65	0.08	-0.58	0.35
Soe 2	-0.80	-0.74	-0.80	-0.91	-1.11	-0.29	0.27	-0.48	-0.03	-1.39	-0.05	-0.49	1.64	7.69	0.09	-1.41	-0.02	-0.43
SOE 3	-2.01	-1.59	-2.02	-0.05	0.45	-1.39	-1.14	-1.29	-1.34	-1.56	-1.55	0.09	1.02	7.19	0.04	0.40	-1.46	-1.20
Sumbruugu	1.04	1.25	1.04	-1.78	-1.11	0.18	1.22	0.82	0.24	0.00	0.46	-0.16	-0.60	7.31	1.00	1.22	0.90	0.85
Tangabisi	0.45	0.23	0.44	0.39	0.45	0.77	-0.70	-0.55	1.36	0.28	-1.14	0.81	-0.25	7.49	-0.08	0.83	0.01	-0.49
VEA 1	0.13	-0.11	0.13	-0.80	-1.11	0.55	-0.26	0.24	-0.35	-0.03	1.03	-0.08	-0.43	7.16	-0.22	2.91	0.08	0.31
VEA 2	2.36	2.32	2.36	-0.23	0.45	3.33	-0.02	1.52	-0.75	1.72	-1.27	-0.49	0.01	7.50	0.37	1.06	1.97	1.52
VEA 3	1.68	1.81	1.67	-0.55	0.45	0.40	1.97	1.14	2.30	1.68	0.25	-0.44	-0.81	7.27	0.37	0.54	1.64	1.16
VEA 4	-0.67	-0.74	-0.68	0.40	3.59	-0.80	-1.44	-0.55	-0.18	0.08	0.87	0.32	-0.28	7.19	0.88	0.38	-1.29	-0.49
VEA Kulpeelga	0.68	0.39	0.68	-2.03	-1.11	1.11	0.60	1.55	-0.35	1.86	1.03	-0.12	-0.18	7.44	-2.19	0.38	0.88	1.56
Yarigu Nungu	0.22	0.07	0.21	-0.19	-1.11	-1.16	0.96	0.46	-0.75	-0.41	0.87	0.37	-0.29	7.10	-2.19	0.89	0.23	0.49
Yebongo	0.34	0.07	0.34	-0.32	-1.11	-0.68	-1.27	-1.23	0.24	-0.77	0.82	0.12	-0.41	7.06	-1.00	-0.18	-1.14	-1.31
Yikene	0.30	0.07	0.30	-1.75	-1.11	0.34	0.35	1.04	-0.75	1.44	0.87	-0.68	-0.99	7.13	-2.19	-1.41	0.32	1.06
Yikene Naayere	-0.68	-0.74	-0.68	1.05	-1.11	-1.07	-1.05	-1.83	-0.35	-2.30	-2.45	0.41	0.21	7.46	-1.28	-1.41	-1.23	-1.92
Yorogo Atiabisi	-0.59	-0.51	-0.59	1.09	0.45	-0.13	-0.44	-0.96	0.83	-0.96	0.18	0.06	2.21	7.53	-2.19	-0.81	-0.39	-0.86
Zaare	0.76	1.04	0.76	1.54	0.45	0.77	0.57	-0.67	2.12	-0.41	-0.30	0.68	-0.40	7.16	-1.28	-0.38	0.69	-0.60

Appendix 3 : Specific yield in the literature

Table II : Specific yield of rock material (Morris and Johnson 1967)

Material	Specific Yield (%)
Gravel, coarse	21
Gravel, medium	24
Gravel, fine	28
Sand, coarse	30
Sand, medium	32
Sand, fine	33
Silt	20
Clay	6
Sandstone, fine grained	21
Sandstone, medium grained	27
Limestone	14
Dune sand	38
Loess	18
Peat	44
Schist	26
Siltstone	12
Till, predominantly silt	6
Till, predominantly sand	16
Till, predominantly gravel	16
Tuff	21

Table III : Specific yield of rock material (Heath 1983)

Material	Porosity (%)	Specific Yield (%)
Soil	55	40
Clay	50	2
Sand	25	22
Gravel	20	19
Limestone	20	18
Sandstone (unconsolidated)	11	6
Granite	0.1	0.09

Appendix 4: Climate projection

Table IV: Change in projected recharge compared to the baseline period (%)

	Bole			Wa			Navrongo		
	2011-2040	2041-2070	2071-2100	2011-2040	2041-2070	2071-2100	2011-2040	2041-2070	2071-
CNRM_CCLM4_RCP45	48	64	65	34	48	52	18	24	40
CNRM_CCLM4_RCP85	66	73	67	85	99	79	32	46	37
CNRM_RCA4_RCP45	35	62	46	34	44	38	37	48	59
CNRM_RCA4_RCP85	51	69	100	42	65	120	46	78	122
ICHEC_CCLM4_RCP45				45	10	29	-4	-31	-23
ICHEC_CCLM4_RCP85	39	3	-12	39	2	-17	-5	-25	-38
ICHEC_RCA4_RCP45	61	76	101	50	41	91	59	49	79
ICHEC_RCA4_RCP85	40	120	133	35	89	101	50	71	114
MPI_CCLM4_RCP45	13	-16	-22	20	-11	-15	-16	-37	-38
MPI_CCLM4_RCP85	-7	-23	-24	5	-6	-22	-15	-22	-40
MPI_RCA4_RCP45	69	88	79	52	87	61	28	49	30
MPI_RCA4_RCP85	68	94	79	85	107	74	24	64	30



Candidate biography

Mr. Kouakou Valentin KOFFI is a PhD candidate in the GRP/ Climate Change and Water Resources Program at University of Abomey-Calavi, Benin in the framework of the WASCAL project. He holds a Master of Science in Water and Environmental Engineering from the International Institute for Water and Environmental Engineering. He is also author of an article on “Environmental Earth Science Journal” and worked as junior consultant for some projects in Côte d’Ivoire.

Abstract : Northern Ghana is mostly underlain by a crystalline rock aquifer. Like in many arid and semi-arid areas, surface water is largely unavailable in the prolonged dry season. Therefore groundwater appears to be a good alternative source for domestic and agricultural water supply. However, crystalline basement rocks are characterised by a poor water storage and low water yield. The water quality is also usually poor due to elevated content in some minerals. Further, climate change may worsen the situation groundwater since recharge is fairly related to rainfall in the area. Therefore this work was done to provide decision support for the sustainable development and management of groundwater resources in Northern Ghana.

The current work first studied the water quality of both surface and groundwater in a part of the crystalline basement aquifer of Northern Ghana which covers 25000 km² and used five different methods to estimate present day recharge, namely the baseflow (BF) recession analysis, the Chloride Mass Balance (CMB) method, the Water Table Fluctuation (WTF) method, the model based method using the distributed WetSpass model and the simple water balance method.

The study revealed that groundwater chemistry is mainly controlled by cation exchange and silicate weathering processes and Ca-Mg-HCO₃ is the major water type, regardless of aquifer geology.

The recession curve analysis results in recharge ranging from 29 mm to 68 mm representing 3% and 9% of annual rainfall in 2004 and 2005, respectively; with average value of 49 mm (5%) for the period 2003-2008. The estimated annual baseflow based on the six methods ranged from 19.07 mm to 69.8 mm or from 2% to 7% of the annual rainfall.

Groundwater recharge estimated by the WTF and CMB methods ranges from 68 mm (6%) to 163 mm (17%) with a mean value of 10% and from 21 mm (2.1%) to 191 mm (19.3%) with average value of 81 mm (8.1%), respectively.

The recharge estimated by the WetSpass model, for the period lasting from 2003 to 2008, ranged from 519 mm to 756 mm, representing 68% and 70% of the annual rainfall during 2005 and 2007, respectively. The Average recharge estimated using the simple water balance method for the period 1976-2005 fell within the range of 283 mm (26.3%) to 330 mm (29.2%) with average of 300 mm (28%).

Compared to the recharge rate of 300 mm during the baseline period (1976-2005), the ensemble mean recharge is projected to increase in periods 2011-2040, 2041-2070 and 2071-2100 by a rate ranging from 23% to 44%, from 29% to 55% and from 33% to 55%, respectively.

This work suggested the use of dynamical downscaling methods for comparison purpose and the the coupling of the WetSpass model with groundwater flow model in order to improve the results.

Key words : hydrogeochemistry, crystalline basement, groundwater recharge, climate change, modeling, Northern Ghana.

PhD

**Kouakou
Valentin
KOFFI**

**Hydrogeochemistry and Impacts of Climate
Change on Groundwater Recharge: Case
Study of the Crystalline Basement Aquifer of
Northern Ghana**

GRP/CCWR/INE/WASCAL – UAC December, 2017